Progress toward the Total Synthesis of Lomaiviticins

Dissertation Advisor: Professor Matthew D. Shair Hong Geun Lee

Progress Toward the Total Synthesis of Lomaiviticins

Abstract

A synthetic plan for the dimeric diazobenzofluorene natural product lomaiviticin A and lomaiviticin B is presented. The route features a late-stage oxidative enolate dimerization of a monomeric oxanorbornanone, as well as a cyanophthalide-based anionic annulation.

In chapter 2, a synthetic route to enone **2.42** is described. Starting from the readily prepared intermediate **1.101**, enone **2.42** was prepared in seven steps. A key cyanophthalide annulation utilizing enone **2.42**, where the C1 and C5 ketones are differentiated, was successfully applied.

Chapter 3 describes an optimization study of the oxanorbornanone enolate dimerization. By using simple ketone **3.3** as a model, reaction conditions minimizing undesired side reactions were identified. These conditions were effectively applied to the dimerization of the fully elaborated tetracyclic precursor.

A synthesis of the full carbon skeleton of the lomaiviticin aglycone is illustrated in chapter 4. A tetracyclic intermediate **4.13**, prepared from enone **2.42**, underwent stereoselective dimerization under the optimized conditions to provide C_2-symmetric dimer **4.12**. During the dimerization study, a critical remote steric effect of C11 substituent was observed. A crystal structure of a dimeric intermediate helps lend support to our hypothesis regarding the remote steric effect.

Finally, synthetic efforts to accomplish a synthesis of the lomaiviticin aglycone *ent*-**1.3** is described in chapter 5. Although the C4 sulfone of dimer **4.12** was efficiently substituted with an oxygen atom, the key $C11_b$-O bond cleavage was not realized under a variety of strategies.

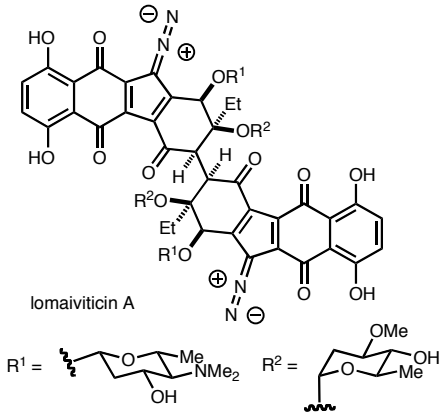

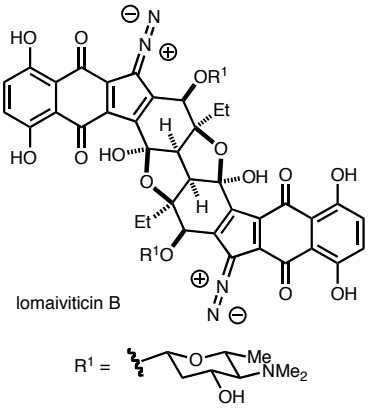

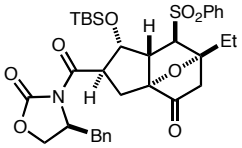

1.101

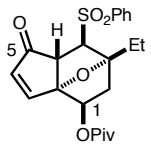

2.42

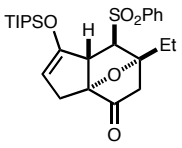

3.3

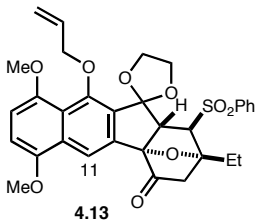

4.13

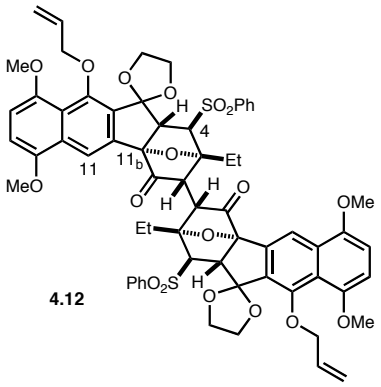

4.12

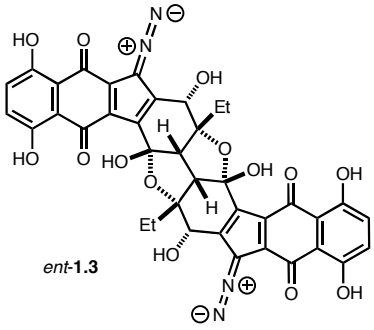

ent-**1.3**

Table of Contents

List of Abbreviations

Å	anstroom
Ac	acetyl
BOM	benzyloxymethyl
Bu	butyl
Calcd	calculated
Cp	cyclopentadienyl
DBU	1,8-diazabicyclo[5.4.0]undec-7ene
DDQ	2,3-dichloro-5,6-dicyano-1,4-benzoquinone
DIAD	diiopropyl azodicarboxylate
DIEA	N,N-diisopropylethylamine
DIBAL-H	diisobutylaluminium hydride
DMAP	4-(dimethylamino)pyridine
DMF	N,N-dimethylformamide
DMSO	dimethyl sulfoxide
dr	diastereomeric ratio
ESI	electrospray ionization
ent	enantiomeric
equiv	equivalent
Et	ethyl
gCOSY	gradient correlation spectroscopy
HMBC	heteronuclear multiple bond borrelation
HMPA	hexamethylphosphoramide
i	iso
IR	infrared
LDA	lithium diisopropylamide
LiHMDS	lithium bis(trimethylsilyl)amide

Me	methyl
MEM	(2-methoxyethoxy)methyl
MOM	methoxymethyl
Ms	methanesulfonyl
MS	molecular sieves
NBS	N-bromosuccinimide
NMO	N-methylmorpholine N-oxide
nOe	nuclear Overhauser effect
NMR	nuclear magnetic resonance
OTf	trifluoromethanesulfonate
Ph	phenyl
Piv	trimethylacetyl
py	pyridine
TBAF	tetrabutylammonium fluoride
TBAI	tetrabutylammonium iodide
TBHP	*t*-butyl hydroperoxide
TBS	*t*-butyldimethylsilyl
t	tertiary
Tf	trifluoromethanesulfonyl
TFA	trifluoroacetica cid
THF	tetrahydrofuran
TIPS	triisopropyl
TMS	trimethylsilyl
Tol	toluene
TPAP	tetrapropylammonium perruthenate
Ts	4-methylbenzenesulfonyl
UV	ultraviolet

Chapter 1

Lomaiviticins: New Diazobenzofluorene Natural Products

1. 1. Isolation and Structure Determination

In 2001, two new diazobenzofluorene glycosides were identified by He and coworkers during the investigation of the real producer of namenamicin related endieyne natural products. A potent antitumore agent, namenamicin was originally isolated from a marine ascidian *Polysyncraton lithostrotum* (Figure 1.1).[1]

Figure 1.1 Structure of namenamicin.

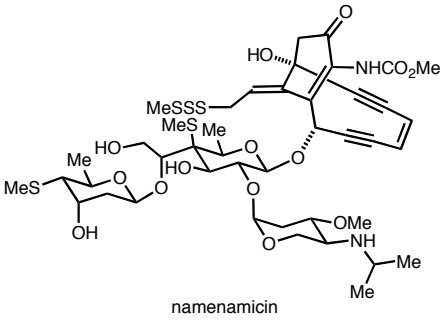

namenamicin

Early on it was suspected that one of the microbial symbionts was responsible for the production of the natural product, therefore several actinomycetes were isolated from the host and tested. The fermentation broth of *micromonospora lomaivitiensis*, one of the actinomycetes found in *Polysyncraton lithostrotum*, exhibited potent DNA-damaging activity and was found to be highly cytotoxic against a panel of cancer cell lines. Inspired by these observations, He and coworkers isolated two new compounds, lomaiviticin A

(1) McDonald, L. A.; Capson, T. L.; Krishnamurthy, G.; Ding, W.-D.; Ellestad, G. A.; Bernan, V. S.; Maiese, W. M.; Lassota, P.; Kramer, R. A.; Ireland, C. M., *J. Am. Chem. Soc.* **1996**, *118*, 10898-10899.

(**1.1**) and lomaiviticin B (**1.2**) by reverse phase HPLC purification of the acidic acetonitrile extract of *micromonospora lomaivitiensis* fermentation broth (Figure 1.2).[2]

Figure 1.2 Structure of lomaiviticin A, lomaiviticin B, and lomaiviticin aglycone.

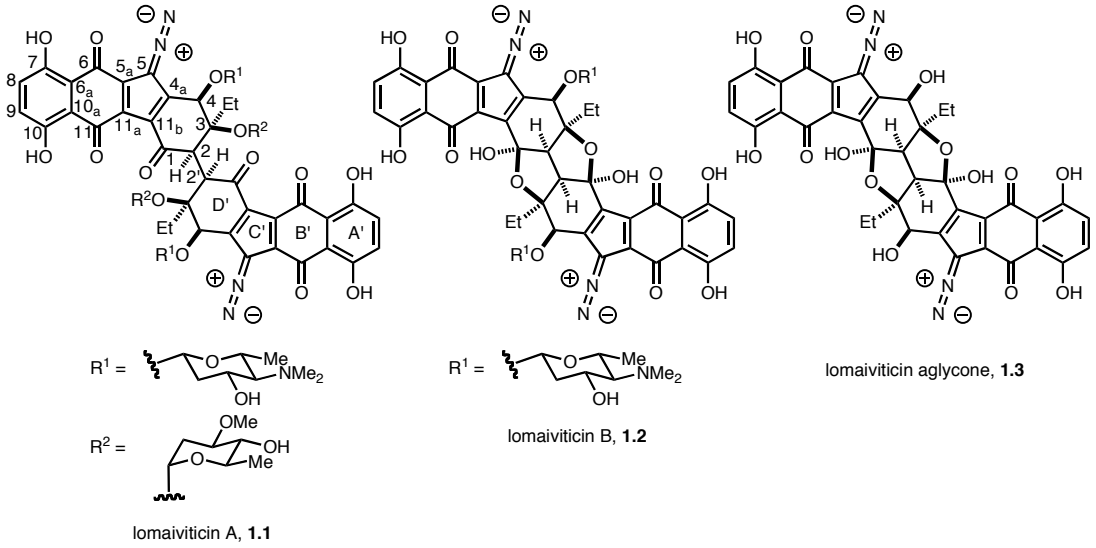

Lomaiviticin A and B were isolated as amorphous powders, precluding X-ray diffraction analysis. Their structural proposal was made primarily on extensive 1D and 2D NMR experiments together with high resolution mass spectroscopy. One of the striking features of their structures was found by comparing the number of ^{13}C signals from the NMR and the number of carbon atoms derived from the molecular formula. Since ^{13}C NMR spectra only accounted for half the number of carbon atoms determined by the mass spectroscopy, it was hypothesized that the lomaiviticins were symmetric dimers. The dimeric nature of the natural product is also revealed in the cross peak of H2 and C2'(or H2' and C2) in the HMBC spectrum. Since only the multiple bond correlation is displayed in HMBC, a linkage between C2 and C2' is suggested (Figure 1.3a). Other

(2) He, H.; Ding, W.-D.; Bernan, V. S.; Richardson, A. D.; Ireland, C. M.; Greenstein, M.; Ellestad, G. A.; Carter, G. T., *J. Am. Chem. Soc.* **2001**, *123*, 5362-5363.

substructures of the lomaiviticins were revealed by analysis of NMR spectral data. The presence of 5,8-dihydroxy-1,4-naphthoquinone and diazobenzofluorene unit, which were also detected by UV and IR absorption spectra, defines the tetracyclic backbone skeleton of the natural product (Figure 1.3b).[3] The two separate spin systems of the aliphatic region of the lomaiviticin A spectra were assigned to be originating from β-N,N-dimethylpyrrolosamine and α-oleandrose, which are attached at the C4 and C3 positions, respectively (Figure 1.3c). Lomaiviticin B, on the other hand, was decorated only with α-oleandrose at the C3 position. The orientation of the anomeric protons were determined by coupling constant analysis.

Figure 1.3 Substructures of lomaiviticins.

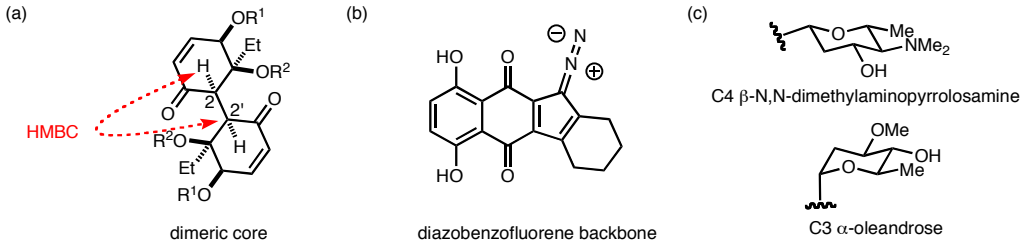

The relative stereochemistry of the cyclohexene D-ring region was determined based on the assumption that both natural products have the same relative configuration at C2, C3, and C4. First, the configuration of protons at the C2 and C4 positions were assigned to be identical in both natural products based on the w-coupling in the gCOSY spectrum (Figure 1.4a). Second, since lomaiviticin B exists as a bis-hemiketal, forming two furanol rings, the C2–C2' linkage and the C–O bond at the C2 position were thought to be placed on the identicall face of the cyclohexene ring (Figure 1.4b). This

(3) (a) Nawrat, C. C.; Moody, C. J., *Nat. Prod. Rep.* **2011**, *28*, 1426-1444. (b) Herzon, S. B.; Woo, C. M., *Nat. Prod. Rep.* **2012**, *29*, 87-118.

stereochemical assignment is reflected on the stereochemical assignment of lomaiviticin A, thereby suggesting the stereochemistry of the cyclohexene D-ring is as shown in Figure 1.2.

Figure 1.4 Relative stereochemistry of lomaiviticin D ring.

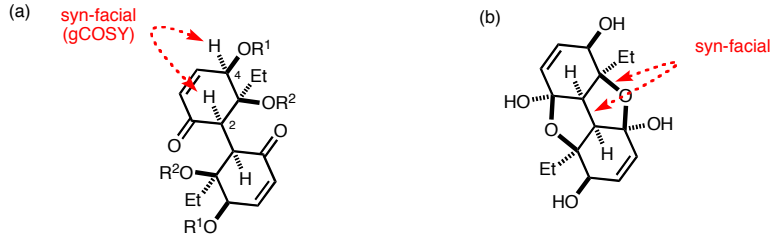

The absolute stereochemistry of the lomaiviticins, as well as the stereochemical correlation between the appended carbohydrate moieties and the aglycone were not elucidated. Given the structural similarities with the related diazobenzofluorene natural product kinamycins, however, it was deduced that both classes of the natural product have identical absolute configuration at the C3 and C4 positions (Figure 1.5).[4]

Figure 1.5 Structure of kinamycins.

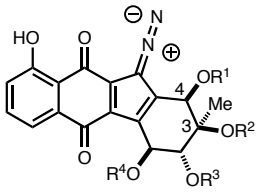

Kinamycin	R^1	R^2	R^3	R^4
A	H	Ac	Ac	Ac
B	H	H	Ac	H
C	Ac	Ac	H	Ac
D	H	Ac	H	Ac
F	H	H	H	H
J	Ac	Ac	Ac	Ac

(4) Gould, S. J., *Chem. Rev.* **1997**, *97*, 2499-2510.

On the other hand, the absolute stereochemistry of N,N-dimethylpyrrolosamine and oleandrose remain elusive, although they are found in other natural products such as β-pyrrolosporin[5] and avermectins[6] (Figure 1.6).

Figure 1.6 Lomaiviticin carbohydrates found in other natural products.

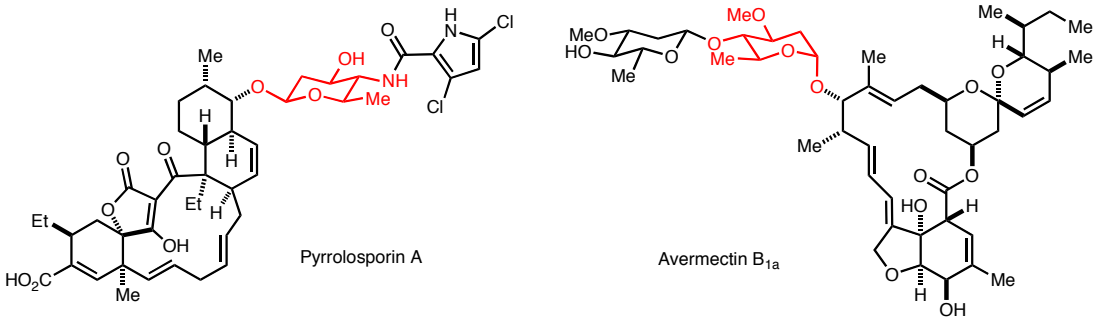

Given the limitations of spectroscopic methods described above, a complete structural elucidation of the natural products would be made possible only by a chemical synthesis of both the aglycone and the carbohydrate counterparts.

(5) Schroeder, D. R.; Colson, K. L.; Klohr, S. E.; Lee, M. S.; Matson, J. A.; Brinen, L. S.; Clardy, J., *J. Antibiot.* **1996**, *49*, 865-872.

(6) Davies, H. G.; Green, R. H., *Chem. Soc. Rev.* **1991**, *20*, 211-269.

1.2. Biosynthetic Hypothesis and Mechanism of Action

The exact biosynthetic pathway of the lomaiviticins has not been elucidated to date. However, the biosynthesis of the related natural product kinamycins has been comprehensively studied and reviewed in 1997.[4] In this section a brief survey of the kinamycin biosynthesis as well as possible dimerization pathways of the lomaiviticins are presented. In addition, proposed mechanisms of bioaction of the diazobenzofluorene compounds are discussed.

The kinamycin biosynthesis research was conducted by extensive feeding studies with isotopically labeled building blocks, such as sodium [1-^{13}C] acetate or [2-^{13}C] acetate, and isolation of biosynthetic intermediates which in turn were resubjected to the biosynthetic conditions (Figure 1.7).[7] The pathway commences with condensation of ten molecules of S-acetylcoenzyme A **1.4** to form a polyketide derived carbon skeleton of the natural product **1.5**, which in turn is converted to dehydrorabelomycin **1.6**.[8]

Figure 1.7 Biosynthesis of kinobscurinone.

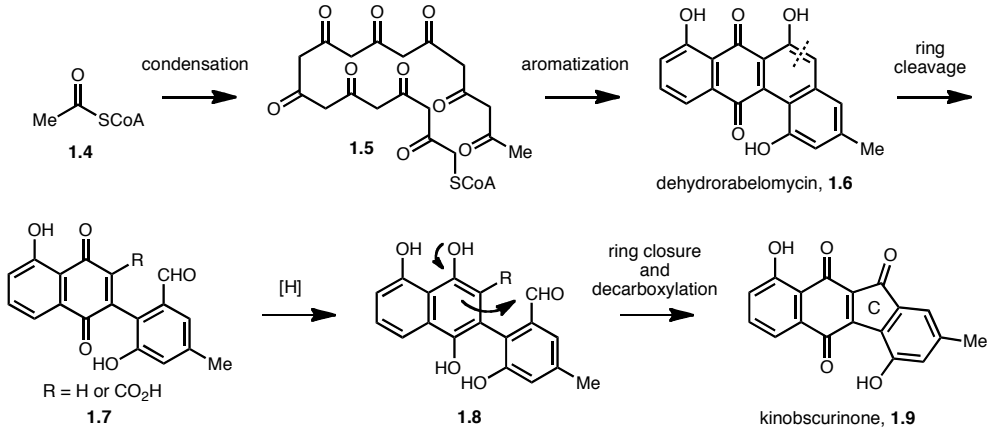

(7) Sato, Y.; Gould, S. J. *Tetrahedron Lett.* **1985**, *26*, 4023-6.

(8) (a) Seaton, P. J.; Gould, S. J., *J. Am. Chem. Soc.* **1987**, *109*, 5282-5284. (b) Seaton, P. J.; Gould, S. J. *J. Antibiot.* **1989**, *42*, 189-97.

Dehydrorabelomycin, the first co-metabolite of the kinamycin biosynthesis, undergoes an oxidative rearrangement to form the 5-membered C-ring over a three step sequence. First an oxidative C–C bond cleavage is believed to take place to provide intermediate **1.7**. Second, reduction of the B-ring triggers an intramolecular alkylation to form the five-membered C-ring of the natural product (**1.8**). Final decarboxylation concludes biosynthesis of kinobscurinone **1.9**, the earliest proven biosynthetic precursor possessing the five-membered C-ring.[9]

The next stage of the biosynthesis is the introduction of the diazo group, which is believed to take place in two separate events each providing one of the two nitrogens of the diazo moiety (Figure 1.8). The first nitrogen atom of kinamycin is introduced at the kinobscurinone stage by a reductive enamine formation to give another co-metabolite stealthin C **1.10**. This pathway was shown to be mediated by glutamine- or ammonia-dependent aminotransferase.[10] Oxidative introduction of the second nitrogen atom takes place with an unknown mechanism, which results in the formation of prekinamycin **1.11**.

Figure 1.8 Biosynthetic introduction of the diazo group in the kinamycins.

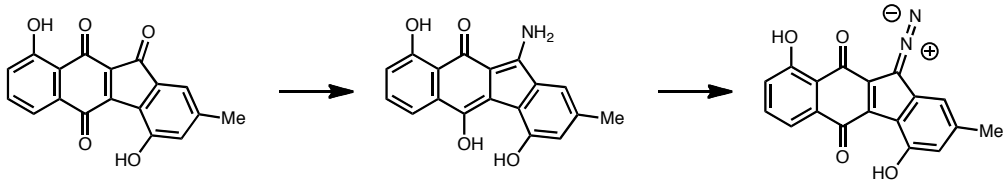

kinobscurinone, **1.9** strealthin C, **1.10** prekinamycin, **1.11**

(9) Gould, S. J.; Melville, C. R., *Bioor. Med. Chem. Lett.* **1995**, *5*, 51-54.

(10) Gould, S. J.; Melville, C. R.; Cone, M. C.; Chen, J.; Carney, J. R., *J. Org. Chem.* **1997**, *62*, 320-324.

Final decoration of the D-ring was proposed to involve multistep events consisting of oxidative transformations and acylations (Figure 1.9). First an oxidative dearomatization of the prekinamycin D-ring generates ketoanhydrokinamycin **1.12**.[8b] Then the D-ring oxidation state is adjusted through reduction of the carbonyl group together with epoxide opening to give kinamycin F **1.13**, a precursor to the other members of the natural product family. A multifunctional enzyme, kinamycin acetylstransferase I (KAT I), has been isolated, and it was shown that the acylation of kinamycin F takes place through the action of KAT I.[11] To date, only kinamycin D and E were isolated from the KAT I mediated acylation experiment, suggesting other KATs are yet to be identified.

Figure 1.9 Biosynthesis of kinamycin D-ring.

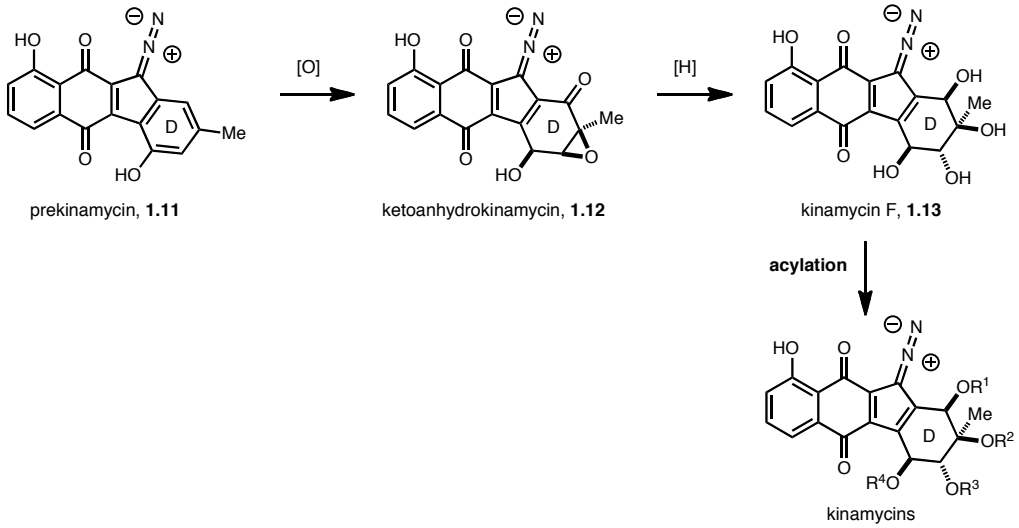

Based on the structural similarity, it is believed that the biosynthesis of the lomaiviticins follows a biosynthetic pathway similar to that of the kinamycins. One

(11) Gould, S. J.; O'Hare, T.; Seaton, P.; Soodsma, J.; Tang, Z., *Bioorg. Med. Chem.* **1996**, *4*, 987-994.

unanswered question is how and at which stage the dimeric structure is formed. The important step that forms the central C–C bond at the axis of symmetry is believed to occur through an oxidative phenolic coupling of **1.14**, an intermediate that resembles prekinamycin **1.11** of the kinamycin biosynthesis (Figure 1.10a). Oxidative phenolic coupling is a commonly observed reaction in the biosynthesis of other natural products.[12] After formation of the C2–C2' bond the intermediate may undergo a similar pathway as the kinamycins, except for the glycosylations. Another possibility is dimerization of an enolate species such as **1.16**, which could be generated from the corresponding epoxide **1.15** by two electron reduction. Epoxide **1.15** is an analogous intermediate to

Figure 1.10 Postulated dimerization pathways for the lomaiviticin biosynthesis.

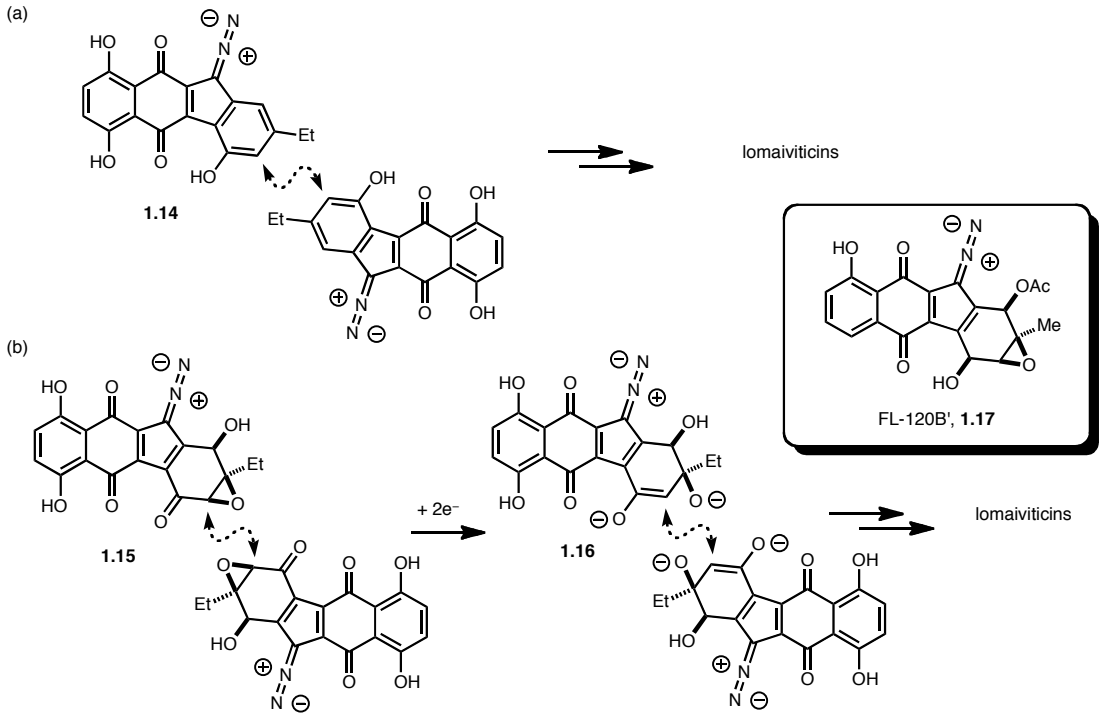

(12) (a) Hüttel, W.; Müller, M., *ChemBioChem* **2007**, *8*, 521-529. (b) Zhao, B.; Guengerich, F. P.; Bellamine, A.; Lamb, D. C.; Izumikawa, M.; Lei, L.; Podust, L. M.; Sundaramoorthy, M.; Kalaitzis, J. A.; Reddy, L. M.; Kelly, S. L.; Moore, B. S.; Stec, D.; Voehler, M.; Falck, J. R.; Shimada, T.; Waterman, M. R. *J. Biol. Chem.* **2005**, *280*, 11599-11607.

ketoanhydrokinamycin **1.12** in the kinamycin biosynthesis. This hypothesis was suggested in 2011 by Porco and coworkers in their synthetic work on FL-120B' **1.17**.[13]

The lomaiviticins are potent anticancer and antibacterial agents.[2] Lomaiviticin A is cytotoxic toward 24 cancer cell lines with IC_{50} values ranging from 0.007 to 72 nM. The lomaiviticins also inhibit the growth of gram positive bacteria *Staphylococcus aureus* and *Enterococcus faecium*, with MIC's ranging from 6 to 25 ng/spot in a plate assay. It is believed that these bioactivities stem from the ability of lomaiviticin A and B to cleave DNA *in vitro* under reducing conditions; however, no detailed mechanistic studies under physiologically relevant conditions havs been reported to date. It is only suggested that they possess a unique mode of action based on their unusual cytotoxicity profile.

Although little is known about the mechanism of action of the lomaiviticins, the related natural product kinamycins have been extensively studied with particular focus on the triggering pathway both *in vitro* and *in vivo*.[3] Findings made over the last three decades are summarized below.

The first experimental model system used to test a bioreactivity proposal on the kinamycin family was a simple diazofluorene ring system (Figure 1.11). In 1995 Jebaratnam and coworkers found that diazofluorene **1.18** in the presence of $Cu(OAc)_2$ or light cleaves single-stranded pBR322 DNA.[14] It was suggested that **1.18** is converted to a carbene (**1.19**) or a radical species (**1.20**), which is responsible for DNA cleaving activity.

---

(13) Scully, S. S.; Porco, J. A., *Angew. Chem. Int. Ed.* **2011**, *50*, 9722-9726.

(14) Arya, D. P.; Jebaratnam, D. J., *J. Org. Chem.* **1995**, *60*, 3268-3269.

Figure 1.11 Jebaratnam's proposed formation of reactive species.

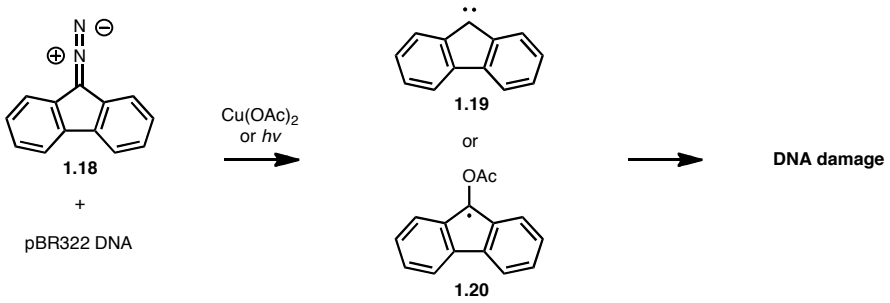

In 1977 Moore proposed a quinone methide intermediate as a reactive intermediate for the action of diazobenzofluorene natural products (Figure 1.12).[15] Reduction of the kinamycin B-ring to a hydroquinone such as **1.22** initiates expulsion of

Figure 1.12 Moore's hypothesis of quinone methide generation.

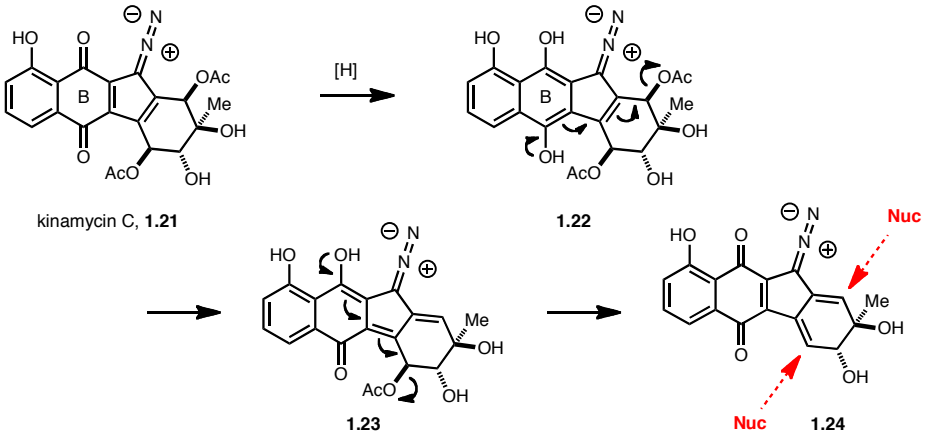

two acetates leading to a quinone methide species such as **1.23** or **1.24**. High nucleophilic susceptibility of these species was thought to be responsible for cell death via the attack of biological nucleophiles.

Moore's hypothesis was partially supported by the experimental work of Feldman and coworkers in 2006 (Figure 1.13).[16] Feldman showed that synthetic dimethyl

(15) Moore, H. W., *Science* **1977**, *197*, 527-532.

(16) Feldman, K. S.; Eastman, K. J., *J. Am. Chem. Soc.* **2006**, *128*, 12562-12573.

prekinamycin **1.25** undergoes quinone methide formation under reductive conditions and eventually leads to formation of thioether **1.26**–a thiol adduct to the quinone methide. It was proposed that the quinone methide is generated via the intermediacy of a vinyl radical species **1.29**, which upon reduction to quinone methide **1.30**, can trap a solvent molecule to form compound **1.26**. It was postulated that a DNA molecule may act as a bionucleophile to the quinone methide, providing an adduct such as **1.26**. Feldman's experiment not only validates the suggestion of a quinone methide or a vinyl radical as a reactive species, but also stresses the importance of the reductive conditions to initiate the pathway. One drawback of the experiment is that the employed condition is not mild enough to be extrapolated to biologically relevant circumstances.

Figure 1.13 Feldman's model DNA damaging experiment.

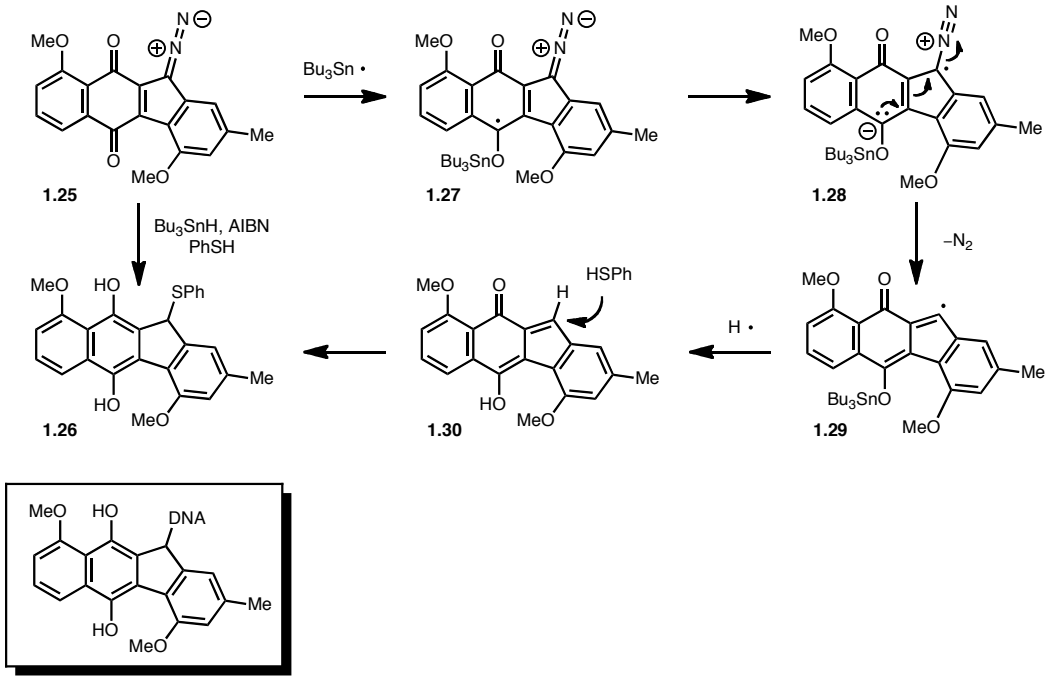

An orthogonal biological mechanism of action was proposed by Dmitrienko and coworkers in 2002 (Figure 1.14).[17] The authors proposed that direct attack of a protic nucleophile to the diazo group of **1.31** can lead to the formation of an azo compound such as **1.32**, which eventually decomposes to an aryl radical species **1.34** via loss of nitrogen. The hydrogen atom abstracted product of the aryl radical **1.35** was isolated as well as compound **1.36**–a direct adduct of the naphthol to intermediate **1.33**. The authors suggested that the kinamycins and the lomaiviticins may exhibit their cytotoxic activities by addition of biological nucleophiles to the diazo group or aryl vinyl radical formation via loss of nitrogen.

Figure 1.14 Dmitrienko's aryl radical proposal.

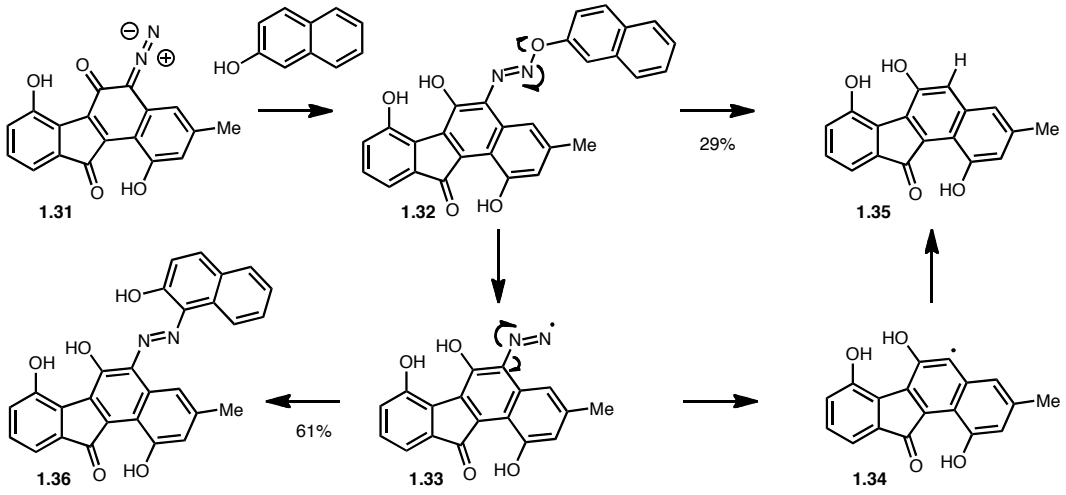

A biologically more relevant initiation condition was investigated by Melander and coworkers (Figure 1.15).[18] They found out that naturally occurring reducing agents such as dithiothreitol (DTT) or glutathione (GSH) with intracellularly relevant

(17) Laufer, R. S.; Dmitrienko, G. I., *J. Am. Chem. Soc.* **2002**, *124*, 1854-1855.

(18) (a) Ballard, T. E.; Melander, C., *Tetrahedron Lett.* **2008**, *49*, 3157-3161. (b) C. L. Heinecke, C. L.; Melander, C., *Tetrahedron Lett.* **2010**, *51*, 1455-1458.

concentrations are sufficient enough to trigger the decomposition of kinamycin D (**1.37**), eventually leading to double-stranded DNA cleavage. They speculated that this process is taking place through the intermediacy of quinone methide species **1.39** or radical species **1.41**. Formation of these intermediates are in accordance with the observations made by Feldman and Dmitrienko.

Figure 1.15 Melander's reductive initiation of the pathway.

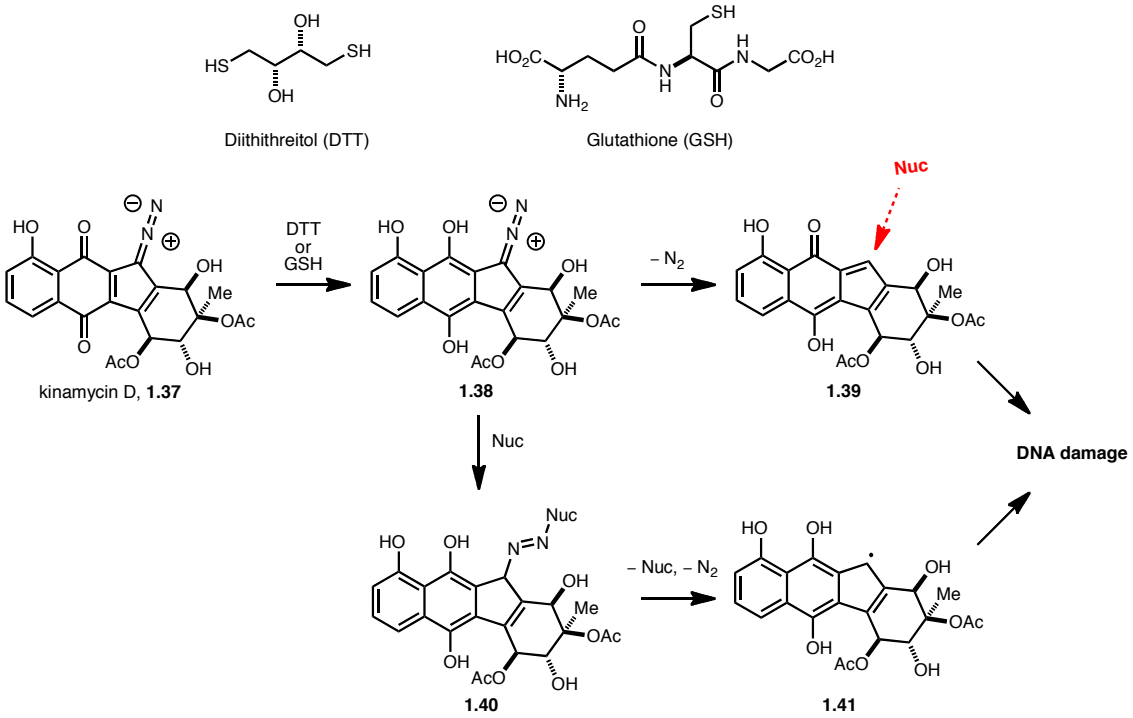

Given the structural similarities of the kinamycins and the lomaiviticins, it is believed that they share a common mechanism of action in the biosystem. However, it remains to be investigated why nature requires a dimeric structure for the lomaiviticins and what the roles of the carbohydrate moieties are. These questions offer further motivation for discovery of a totally synthetic approach to the supply of these potentially valuable natural products.

1.3. Other Synthesis Efforts

In the previous sections we discussed two reasons to synthesize the lomaiviticins: structure confirmation and biomedical research. As synthetic targets, lomaiviticins impose the highest level of complexity in several aspects (Figure 1.16).

Figure 1.16 Synthetic challenges associated with the lomaiviticin aglycone.

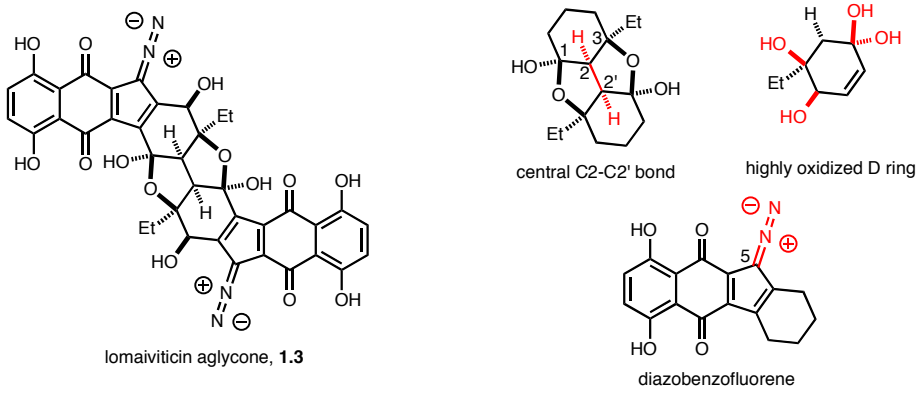

First and foremost, the axis of symmetry at the C2–C2’ bond imparts the greatest challenge. Generally, C_2-symmetric molecules are prepared either by two directional synthesis or late stage dimerization.[19] When the central bond exists between two sp^3 carbons, very few choices exist other than early stage formation of the bond and two directional expansion of the core. However, double processing of such a complex molecule might suffer from low yield and undesired reactivity. What makes the bond formation between C2 and C2’ more challenging is the fact that the bond formation, which is next to a quaternary center at C3, needs to be diastereoselective. Second, the highly reactive diazobenzofluorene ring should be prepared with the proper oxidation state of neighboring groups.[3] As is well documented in the literature, a diazo group is

(19) Vrettou, M.; Gray, A. A.; Brewer, A. R. E.; Barrett, A. G. M., *Tetrahedron* **2007**, *63*, 1487-1536.

highly reactive under acidic and nucleophilic conditions.[20] In order to prevent loss of the functionality, the diazo group at C5 has to be stabilized by neighboring electron-withdrawing groups such as the B-ring quinone or C1 ketone in the lomaiviticins. Although introduction of diazo groups in other molecules have been widely explored,[21] carrying this sensitive functional group through the synthesis can be problematic. Third, the D-ring of the natural product, with a net hydroquinone oxidation state, is highly oxidized. Furthermore, the oxygen substituents need to be introduced with proper stereochemistry and they cannot not be lost throughout the synthesis, since they are highly prone to aromatize by elimination of hydroxide or alkoxide.

As of April 2012, several efforts to overcome these challenges have been reported and reviewed.[3] Although a total synthesis of the lomaiviticins has not been accomplished to date, partial structures of the natural product, including the aglycone and the carbohydrate moieties of the natural product, have been prepared. In this section the published attempts to prepare the lomaiviticin natural products are presented. Synthesis and glycosylation studies of lomaiviticin carbohydrates are not discussed.[22]

---

(20) Regitz, M.; Maas, G., *Diazo Compounds-Properties and Synthesis*, Academic Press, Orlando, **1986**.

(21) For review, see: Maas, G., *Angew. Chem. Int. Ed.* **2009**, *48*, 8186-8195.

(22) (a) Morris, W. J.; Shair M. D., *Org. Lett.* **2008**, *11*, 9-12. (b) Gholap, S. L.; Woo, C. M.; Ravikumar, P. C.; Herzon S. B., *Org. Lett.* **2009**, *11*, 4322-4325. (c) Morris, W. J.; Shair M. D., *Tetrahedron Lett.* **2010**, *51*, 4310-4312.

In 2006, Nicolaou and coworkers have disclosed their synthesis of the D-D' dimeric core of lomaiviticin B (**1.42**) and lomaiviticin A (**1.43** or **1.44**).[23] The synthesis highlights two directional functionalization of simple symmetric dimer **1.47**, as is outlined in Figure 1.17.

Figure 1.17 Nicolaou's synthetic plan for the D-D' core of lomaiviticin A and B.

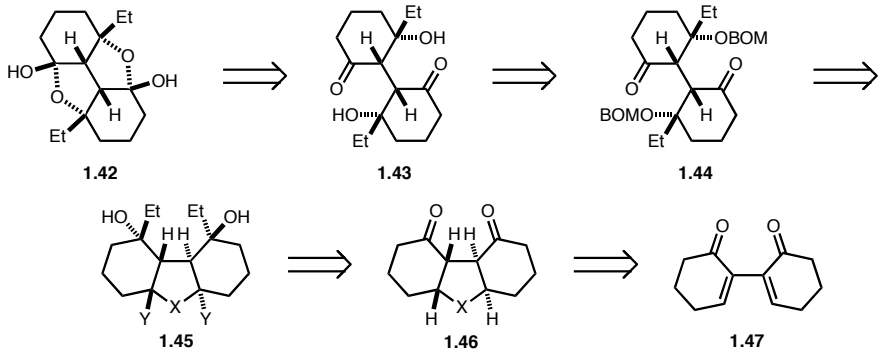

Starting from bisenone **1.47**, the C1 and C1' positions were masked with a C–C bond by double conjugate addition of dimethyl malonate to provide an unsymmetric dimer **1.48** (Scheme 1.1). The C3 ethyl group was introduced in a streoselective manner by addition to the carbonyl group at C3 to give diol **1.49**. Interestingly, one of the methyl esters was lost during the introduction of the ethyl group, presumably via a retro-aldol reaction. After protection of the resulting tertiary carbinol as BOM ether **1.50**, the central methine with a methyl ester was converted to ketone functionality (**1.52**) in six straightforward functional group manipulations through the intermediacy of olefin **1.51**. At this stage the oxidation state of C1 was increased to that of an alcohol by α oxidation of the ketone to provide a symmetric diol **1.53**. LAH reduction of the central carbonyl

(23) Nicolaou, K. C.; Denton, R. M.; Lenzen, A.; Edmonds, D. J.; Li, A.; Milburn, R. R.; Harrison, S. T., *Angew. Chem. Int. Ed.* **2006**, *45*, 2076-2081.

group of **1.53** gave triol **1.54** and set the stage for the exposure of the C1 ketone functionality.

Scheme 1.1 Nicolaou's synthesis of intermediate **1.54**.

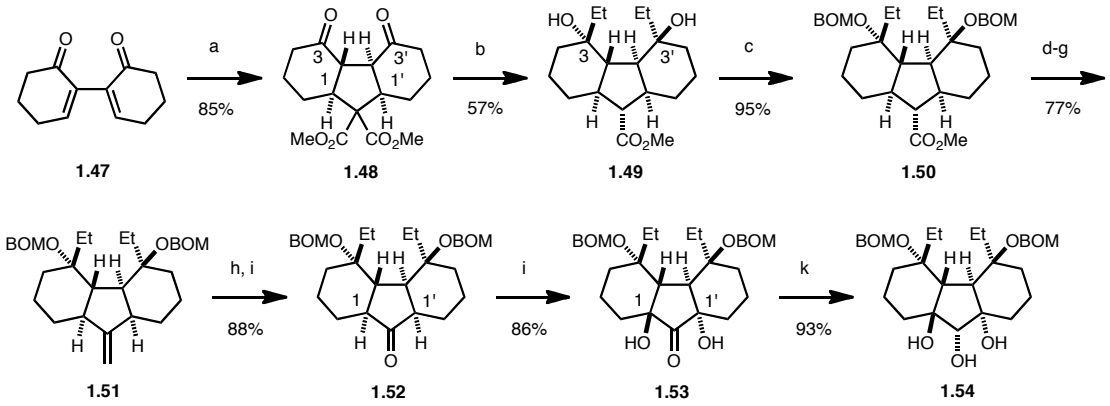

Reagents and conditions: (a) $CH_2(CO_2Me)_2$, NaOMe; (b) EtMgBr, $CeCl_3$; (c) BOMCl; (d) LAH; (e) I_2, PPh_3; (f) *o*-$NO_2C_6H_4SeCN$, $NaBH_4$; (g) *m*-CPBA; (h) K_2OsO_4, NMO; (i) $Pb(OAc)_4$; (j) KHMDS, O_2, $P(OEt)_3$; (k) LAH.

At this point the synthetic route has diverged to form either the core of lomaiviticin A or lomaiviticin B. For the synthesis of lomaiviticin A core, triol **1.54** was treated with $Pb(OAc)_4$ to induce oxidative C–C bond cleavage (Scheme 1.2). Interestingly, the initially formed α-hydroxy aldehyde **1.55** cyclizes on the C1 ketone of

Scheme 1.2 Nicolaou's synthesis of lomaiviticin A core.

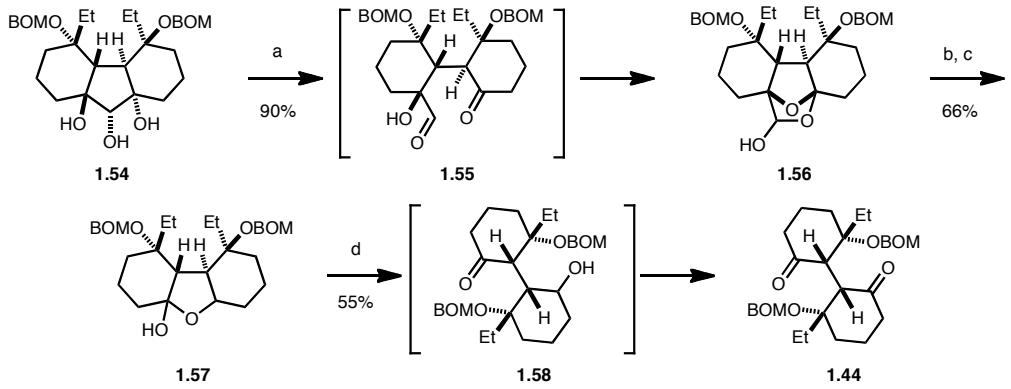

Reagents and conditions: (a) $Pb(OAc)_4$; (b) $LiBH_4$; (c) $Pb(OAc)_4$; (d) TPAP, NMO.

the other ring to give a cyclic hemiacetal **1.56**.[24] After reduction of the hemiacetal, the core was subjected to another round of oxidative C–C bond cleavage to give a cyclic ketal **1.57**. Upon exposure to Ley oxidation conditions, cyclic ketal **1.57** was converted to, through the intermediacy of hydroxy ketone **1.58**, the lomaiviticin A core, **1.44**.

Synthesis of the lomaiviticin B core commenced with the removal of the BOM protecting group at C3 of **1.54** to give intermediate **1.59** (Scheme 1.3). Under the oxidative C–C bond cleaving conditions, a mono formate **1.62** was isolated as the major product, presumably through formation of **1.60** and **1.61**. Deformylation in methanolic ammonia proceeded smoothly to give the core structure of lomaiviticin B **1.42** in a bishemiketal form.

Scheme 1.3 Nicolaou's synthesis of lomaiviticin B core.

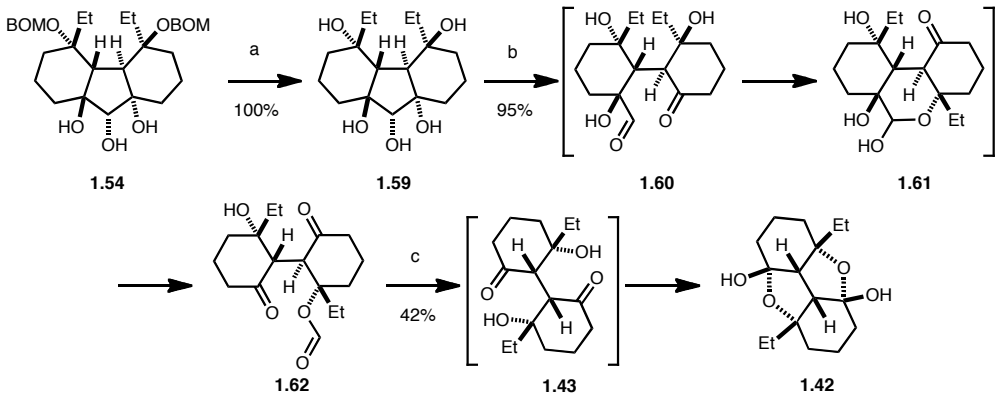

Reagents and conditions: (a) H_2, Pd/C; (b) $Pb(OAc)_4$; (c) NH_3, MeOH.

The Nicolaou group has also reported a synthesis of the monomeric half lomaiviticin aglycone **1.63** by adapting the route previously developed for the synthesis

(24) Similar phenomena have also been observed in our own research program. See section 1.4, 3.1, and 5.1 for details.

of kinamycin C, F, and J.[25] Retrosynthetically, they joined of building blocks of similar complexity, **1.64** and **1.65**, by a transition metal catalyzed coupling reaction and the benzoin condensation (Figure 1.18).[26]

Figure 1.18 Nicolaou's synthetic plan for the half lomaiviticin.

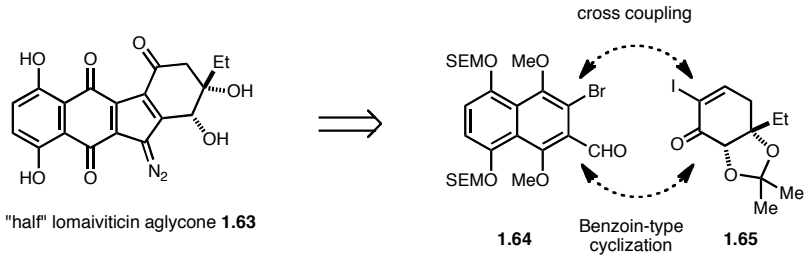

Naphthyl bromide **1.64** and iodoenone **1.65** were joined to give **1.66** in the presence of Pd catalyst and Cu (Scheme 1.4). The resulting keto aldehyde **1.66** was treated with catalyst **1.67**,[27] developed in the research group of Rovis, to form the five membered C-ring of the natural product (**1.68**). A novel allylic transposition reaction sequence installed the oxygen atom at C1 to give alcohol **1.69**. After introduction of the C5 hydrazone, Dess-Martin periodinane was used to oxidize both the C5 hydrazone and the C1 hydroxyl group to give the stabilized diazo compound **1.70**. All that separated them from the desired monomeric unit was a four-step sequence of oxidation state adjustment and removal of protecting groups.

---

(25) Nicolaou, K. C.; Li, H.; Nold, A. L.; Pappo, D.; Lenzen, A., *J. Am. Chem. Soc.* **2007**, *129*, 10356-10357.

(26) Nicolaou, K. C.; Nold, A. L.; Li, H., *Angew. Chem. Int. Ed.* **2009**, *48*, 5860-5863.

(27) (a) Kerr, M. S.; Read de Alaniz, J.; Rovis, T., *J. Am. Chem. Soc.* **2002**, *124*, 10298–10299. (b) Kerr, M. S.; Read de Alaniz, J.; Rovis, T., *J. Org. Chem.*, **2005**, *70*, 5725–5728.

Scheme 1.4 Nicolaou's synthesis of half lomaiviticin.

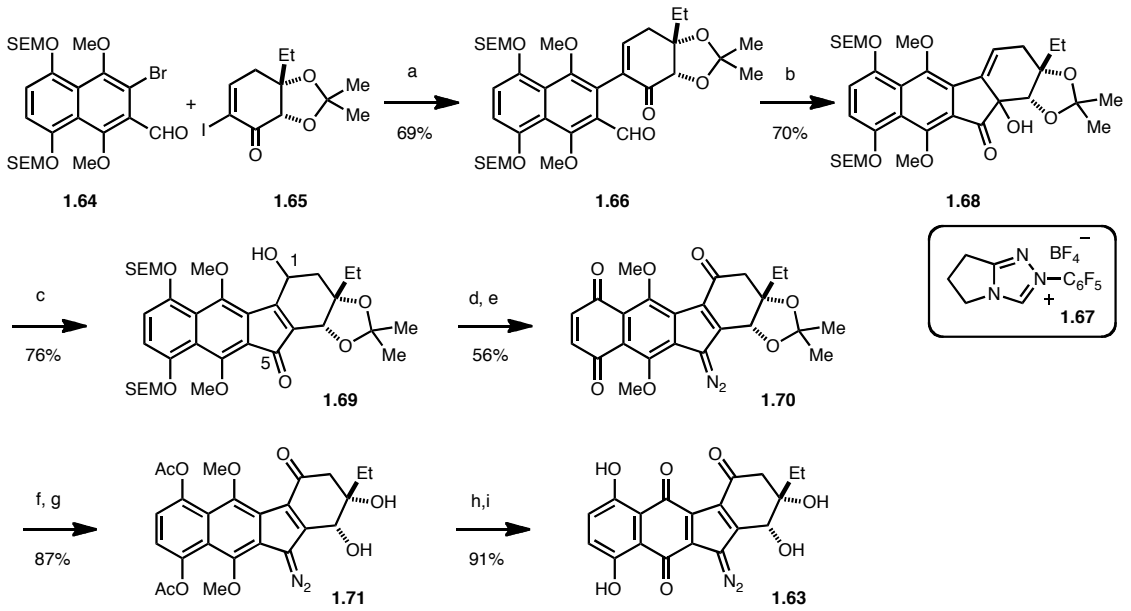

Reagents and conditions: (a) $Pd_2(dba)_3$, CuI, Cu; (b) **1.67**, Et_3N; (c) SmI_2, O_2; then $Na_2S_2O_3$; (d) $TsNHNH_2$; (e) DMP; (f) $Na_2S_2O_4$; then Ac_2O, Et_3N; (g) TMSOTf; (h) CAN; (i) KOH.

The Sulikowski group has also demonstrated the synthesis of the central D-D' core system, albeit in a form devoid of the C3 hydroxyl group.[28] As in Nicolaou's approach, it was prepared by two directional expansion (Scheme 1.5). Nickel-catalyzed reductive dimerization of iodoenone **1.72** provided bisenone **1.73**. Double conjugate addition of vinyl cuprate, followed by stereoselective protic quenching, established the desired stereochemistry at the C2 and C2' positions to give ketone **1.74**. Elimination of the acetonide functionality took place uneventfully in the presence of DBU; however, an epimerization of one of the C2 stereocenter occurred under these conditions to provide unsymmetric bisenone **1.75** in 56% yield. Interestingly, DBU mediated elimination of reduced product **1.76**, generated by catalytic hydrogenation of **1.74**, produced an entirely

(28) Zhang, W.; Baranczak, A.; Sulikowski, G. A., *Org. Lett.* **2008**, *10*, 1939-1941.

different product **1.77**. It is suspected that **1.77** is formed by base-mediated acetonide cleavage followed by capture of the carbonyl group on the other side by the diol.

Scheme 1.5 Sulikowski's attempted synthesis of lomaiviticin D-D' core.

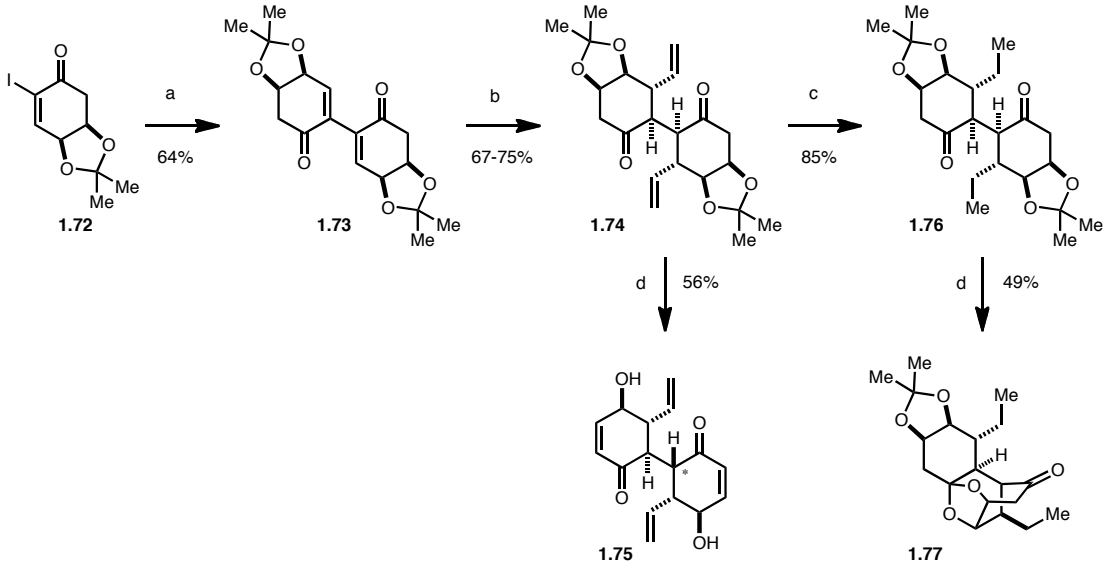

Reagents and conditions: (a) $NiCl_2(PPh_3)_2$, Zn, NaH; (b) $(C_2H_3)_2CuLi_2(CN)$; (c) H_2, Pd/C; (d) DBU.

To circumvent this unexpected reactivity, the Sulikowski group pursued an alternative strategy (Scheme 1.6). Enolsilane **1.78** was prepared by treating **1.73** with allyltributyltin in the presence of TBSOTf. In six straightforward functional group manipulations, the C3 ally group of **1.78** was converted to an ethyl group (**1.79**). Treatment of **1.79** with TBAF resulted in removal of the TBS groups as well as cleavage

Scheme 1.6 Sulikowski's synthesis of lomaiviticin D-D' core.

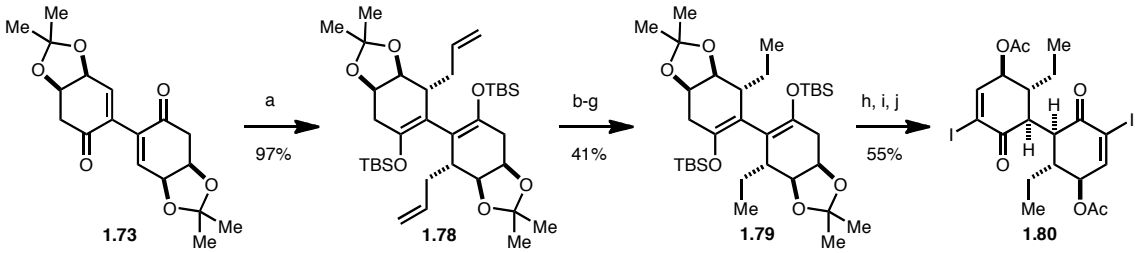

Reagents and conditions: (a) $AllylSnBu_3$, TBSOTf; (b) OsO_4; (c) $Pb(OAc)_4$; (d)$NaBH_4$; (e) MsCl, Et_3N; (f) NaI; (g) H_2, Pd/C; (h) TBAF; (i) Ac_2O, pyr; (j) I_2, pyr.

of the acetonide protecting groups to give an intermediate bisenone (not shown). The enone was acetylated and iodinated to give bis(α-iodoenone) **1.80**, which constitutes the C3/C3' dideoxy core of the lomaiviticins.

In 2011 a synthesis of the lomaiviticin aglycone was reported by the Herzon group.[29] Their synthesis closely resembles their own synthesis of kinamycin F, with the addition of the final dimerization strategy.[30] A highly functionalized intermediate such as **1.82** allowed rapid entry to the lomaiviticin aglycone after dimerization (Figure 1.19).

Figure 1.19 Herzon's synthesis plan for lomaiviticin aglycone

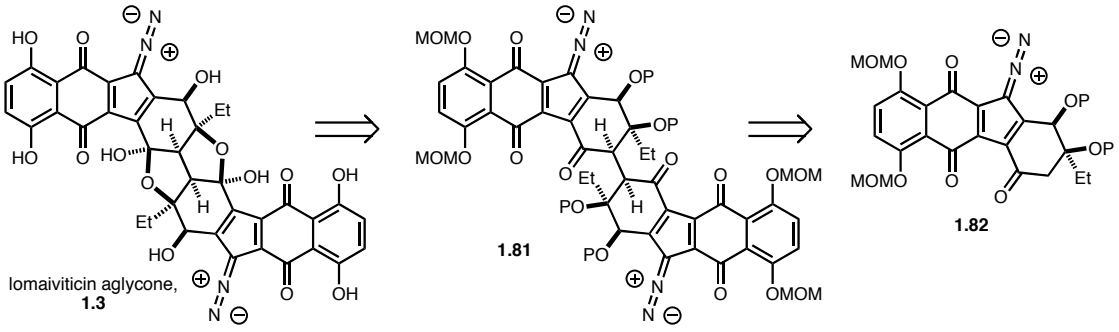

Preparation of the dimerization precursor is described in Scheme 1.7. The synthesis commences with Birch reduction of TIPS protected 3-ethylphenol, followed by Sharpless asymmetric dihydroxylation to install two hydroxyl groups at C3 and C4 (**1.84**). Diol **1.84** was subjected to a Saegusa oxidation to provide enone **1.85**, which was subsequently converted to a diastereomeric mixture of mesityl acetals **1.86**. Conjugate addition of (trimethylsilyl)methylmagnesium chloride, trapping of the resultant enolate as

(29) Herzon, S. B.; Lu, L.; Woo, C. M.; Gholap, S. L., *J. Am. Chem. Soc.* **2011**, *133*, 7260-7263.

(30) Woo, C. M.; Lu, L.; Gholap, S. L.; Smith, D. R., *J. Am. Chem. Soc.* **2010**, *132*, 2540-2541.

a TMS enol ether, followed by another round of Saegusa oxidation provided enone **1.87**. Enone **1.87** underwent addition-elimination reaction with dibromoquinone **1.88** in the presence of an anhydrous fluoride source to give coupling product **1.89**. Palladium-mediated cyclization reaction of **1.89** furnished hydroxyfulvene **1.90**, which contained the five-membered C-ring of the natural product. Compound **1.90** underwent Regitz diazo transfer reaction[31] in the presence of TfN_3 and DMAP, to establish the diazofluorene unit of the natural product. At this point, the two diastereomeric mesityl acetals were separated by silica gel chromatography to provide two different dimerization precursors, **1.91** and **1.92**.

Scheme 1.7 Herzon's syntheis of dimerization precursor.

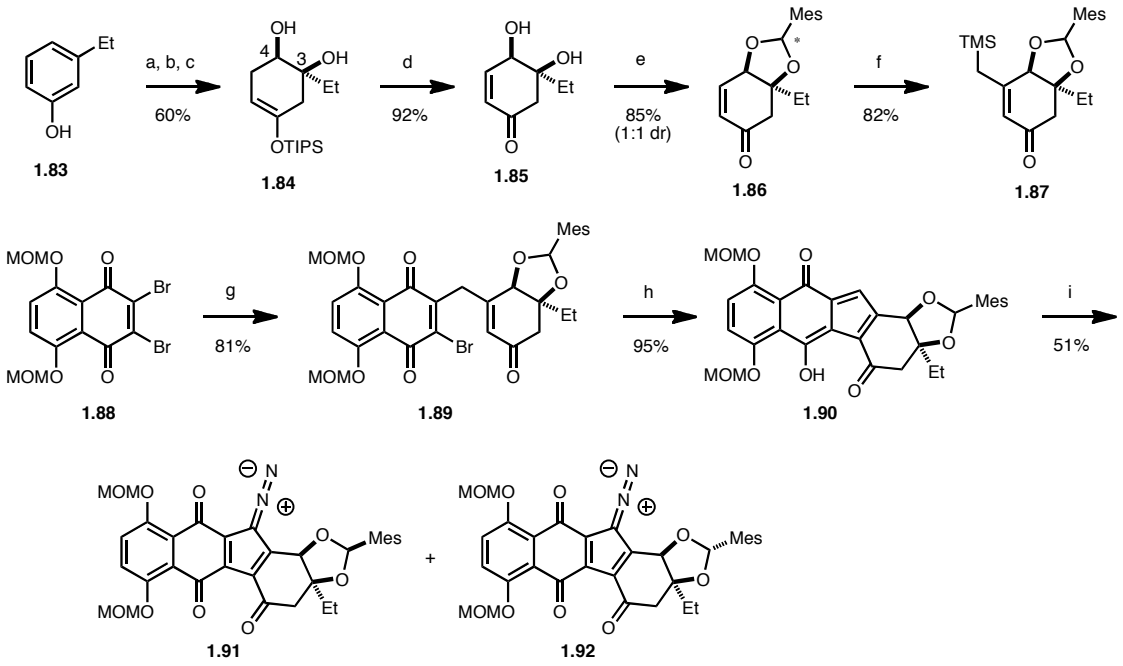

Reagents and conditions: (a) TIPSCl, imd; (b) Li, NH_3; (c) $(DHQD)_2PHAL$, K_2OsO4, $K_3Fe(CN)_6$; (d) $Pd(OAc)_2$; (e) $MesCH(OMe)_2$, PPTS; (f) $TMSCH_2MgCl$, CuI, TMSCl; then $Pd(OAc)_2$; (g) TASF, **1.87**; (h) $Pd(OAc)_2$; (i) TfN_3, DMAP.

(31) Regitz, M., *Angew. Chem. Int. Ed.* **1967**, *6*, 733.

While the precursor **1.91** was not effective towards the desired dimerization, compound **1.92** was successfully elaborated to the lomaiviticin aglycone (Scheme 1.8). The TMS enol ether of ketone **1.82** was treated with manganese tris(hexafluoroacetylacetonate) to mediate oxidative dimerization. It should be noted that a judicious choice of oxidant, which is non-Lewis acidic and does not have coordinating ligands, was crucial to the success of the reaction. Under the optimized conditions, the desired (2*R*, 2'*R*)-diastereomer **1.93**, along with the minor undesired (2*S*, 2'*S*)-diastereomer **1.94**, was isolated. The authors attributed the stereochemical outcome to the long distance steric influence of the C3, C4 mesityl acetal (see the figure in the box). It was proposed that the methyl group of the mesityl group gears the ethyl group at the C3

Scheme 1.8 Herzon's synthesis of lomaiviticin aglycone.

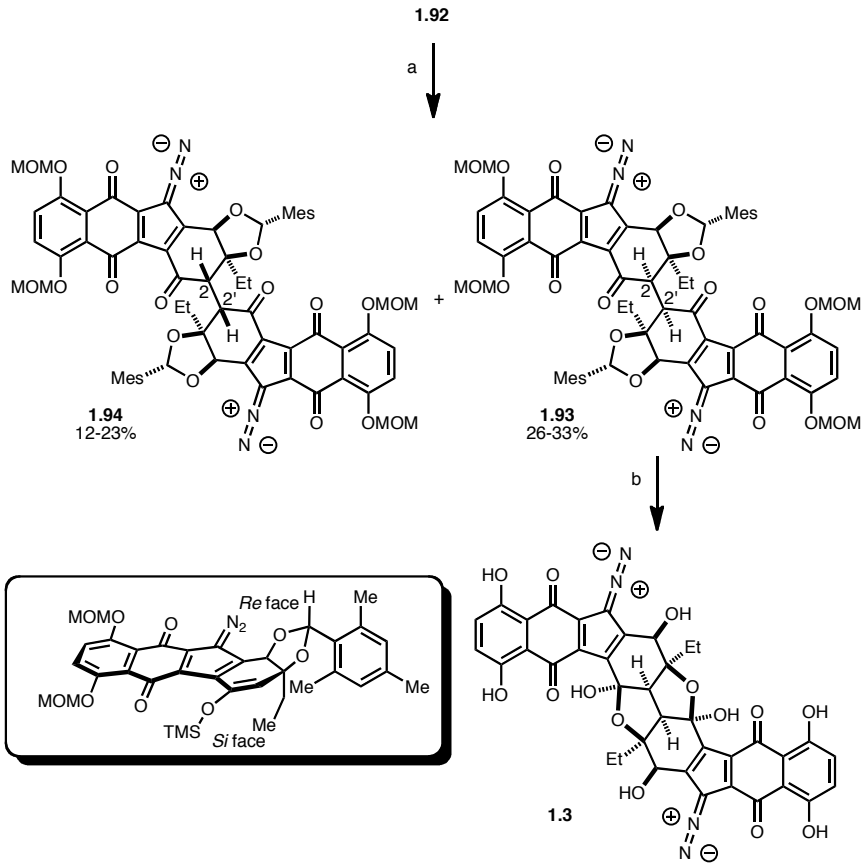

Reagents and conditions: (a) TMSOTf, Et_3N; then $Mn(hfacac)_3$; (b) TFA, TBHP.

position toward the *Si* face of the enolsilane, effectively blocking the undesirable face to dimerization. One step global deprotection of **1.94** provided the aglycone of the natural product. As was expected, the initially formed 1,4-diketone product spontaneously cyclized to the bisketal form of the product **1.3** upon standing in chloroform or upon chromatographic purification.

1.4. Shair Group Strategy

In the previous section, synthetic efforts towards the lomaiviticin natural products were reviewed. Parallel to these attempts, the Shair group has also been tackling the problem with our own strategies since 2004. In this section the synthetic strategies devised in the Shair group, as well as the plans to accomplish a synthesis of the lomaiviticins are presented.

As was discussed in Section 1.3, the biggest challenge of the synthesis is the formation of the central C2–C2' bond which connects two identical halves of the natural product. Due to convergency and efficiency issues, the best way to make a C_2-symmetric molecule is to unify two pieces of advanced intermediates at the latest stage possible.[19] To this end oxidative dimerization of the enolate of the cyclohexenone D-ring to form the C2–C2' bond was the pathway of choice (Figure 1.20).[32] It was envisioned that a dimerization precursor such as ketone **1.95** would undergo dimerization in the presence of base and oxidant.

Figure 1.20 Oxidative enolate coupling strategy for the synthesis of lomaiviticin aglycone

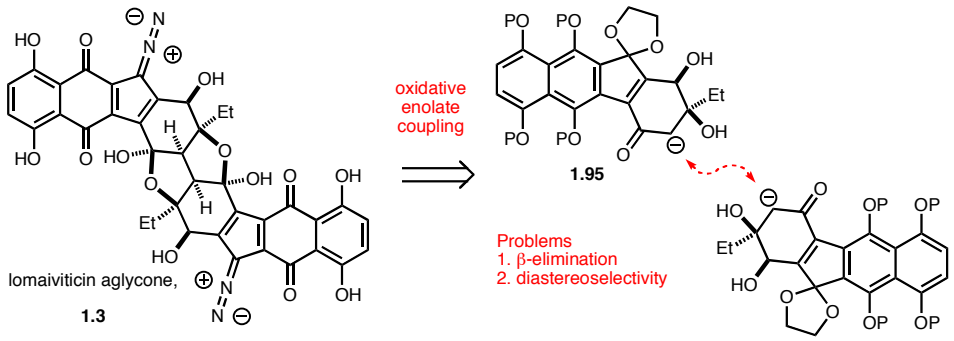

(32) Ito, Y.; Konoike, T.; Saegusa, T., *J. Am. Chem. Soc.* **1975**, *97*, 2912-2914.

This strategy, however, has two potential problems (Figure 1.21). First, the intermediate enolate is highly prone to expel oxygen substituent at the C3 position through β-elimination, thereby forming an aromatized compound such as **1.96** (path I). Second, there is no straightforward way to control the stereoselectivity of the dimerization event (path II). The size of the neighboring substituents at the C3 position, ethyl and hydroxyl groups, do not differ significantly. In addition, the orientation of the C4 substituent disfavors the desired dimerization, since it is directing the face of desired dimerization. In Herzon's synthesis of the lomaiviticin aglycone, the dimerization had low levels of stereocontrol due to the same reason.

Figure 1.21 Problems associated with oxidative dimerization strategy.

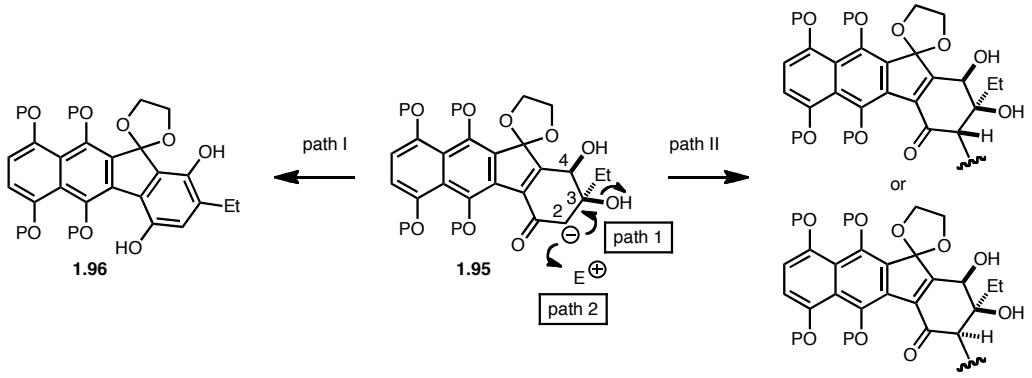

To circumvent these problems, Dr. Evan Krygowski formulated an ingenious solution (Figure 1.22).[33] By using a connective transform, cyclohexenol D-ring was retrosynthetically converted to an oxanorbornanone, which can be converted back to the cyclohexenol by base mediated elimination (Figure 1.22a). In the oxanorbornane system, the σ* orbital of C–O bond is not efficiently aligned with the π orbiral of the enolate

(33) Krygowski, E. S., Ph. D. Thesis, Harvard University, Cambridge, MA, 2008.

thereby obstructing efficient β-elimination of the C3 hydroxide (Figure 1.22b).[34] Use of the oxanorbornane solves the diastereoselectivity problem as well. As is well documented in the literature, the favored face of approach is the *exo* face–the same face of the oxygen bridge (Figure 1.22c).[35] Therefore by using a dimerization precursor such as **1.97**, it was anticipated that the β-elimination and diastereoselectivity problems would be resolved (Figure 1.22d).

Figure 1.22 Connective transformation of D ring to oxanorbornanone.

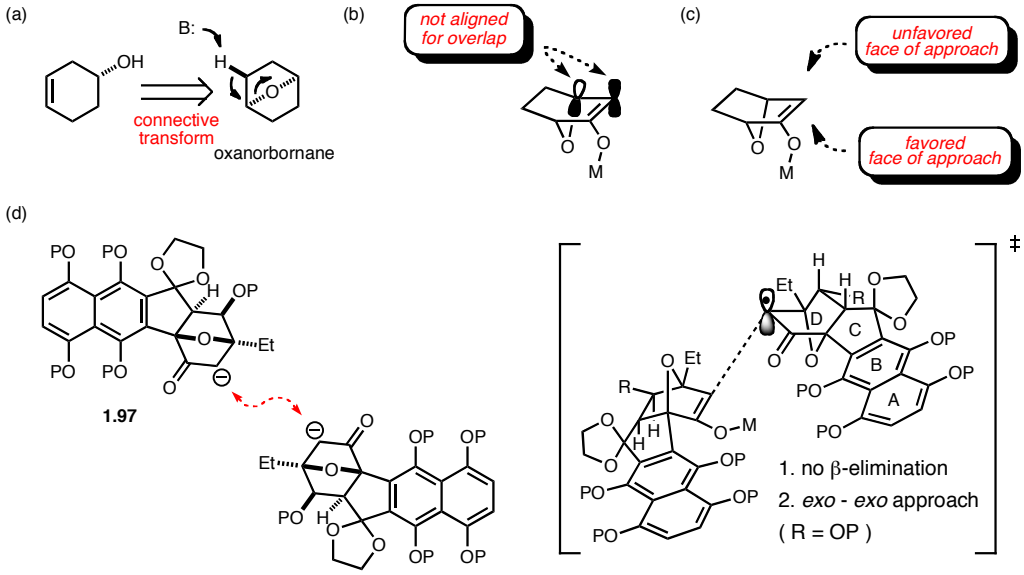

(34) (a) Jackson, S. R.; Johnson, M. G.; Mikami, M.; Shiokawa, S.; Carreira, E. M. *Angew. Chem., Int. Ed.* **2001**, *40*, 2694-2697. (b) Tojo, S.; Isobe, M. *Synthesis* **2005**, 1237-1244.

(35) (a) Marchionni, C.; Vogel, P.; Roversi, P., *Tetrahedron Lett.* **1996**, *37*, 4149-4152. (b) Mosimann, H.; Vogel, P.; Pinkerton, A. A.; Kirschbaum, K., *J. Org. Chem.* **1997**, *62*, 3002-3007. (c) Arjona, O.; Menchaca, R.; Plumet, J., *Org. Lett.* **2001**, *3*, 107-109.

In order to test the idea, a model study was initiated and the result was published in 2008 (Scheme 1.9).[36] The desired oxanorbornanone model D-ring was constructed from three simple building blocks, furanone **1.98**,[37] acrylate **1.99**,[38] and aldehyde **1.100**,[39] in six straightforward steps. The highlight of the synthesis includes conjugate addition of the furanone enolate to acrylate **1.99**, Evans' anti-selective aldol reaction,[40] and a diastereoselective furan Diels-Alder reaction.[41] It should be noted that this sequence of reactions was highly scalable, hence over 50 g of **1.101** could be easily prepared from a single batch in enantiopure form. Oxanorbornanone **1.101** was converted to the dimerization precursor **1.102** in four steps, which involves acid mediated removal of the oxazolidinone chiral auxiliary and Barton decarboxylation.[42] The model CD-ring system **1.102** was successfully dimerized. In the presence of an amide base, the corresponding enolate was formed without undergoing significant β-elimination and, by using an non-coordinating Fe(III) oxidant $[Cp_2Fe]PF_6$,[43] the enolate was dimerized in a

---

(36) Krygowski, E. S.; Murphy-Benenato, K.; Shair, M. D., *Angew. Chem. Int. Ed.* **2008**, *47*, 1680-1684.

(37) Stuart, J. G.; Nicholas, K. M. *Heterocycles* **1991**, *32*, 949-963.

(38) Ho, G.-J.; Mathre, D. J. *J. Org. Chem.* **1995**, *60*, 2271-2273.

(39) Danda, H.; Hansen, M. M.; Heathcock, C. H., *J. Org. Chem.* **1990,** *55*, 173-181.

(40) Evans, D. A.; Tedrow, J. S.; Shaw, J. T.; Downey, C. W., *J. Am. Chem. Soc.* **2001**, *124*, 392-393.

(41) For review see: Oliver Kappe, C.; Shaun Murphree, S.; Padwa, A., *Tetrahedron* **1997**, *53*, 14179-14233.

(42) Barton, D. H. R.; Crich, D.; Motherwell, W. B., *J. Chem. Soc. Chem. Commun.* **1983**, *17*, 939.

(43) (a) Jahn, U. *J. Org. Chem.* **1998**, *63*, 7130-7131. (b) Jahn, U.; Hartmann, P. *Chem. Commun.* **1998**, 209-210.

diastereoselective manner in 45% isolated yield. C_2-symmetric dimer **1.103** was isolated as a single diastereomer.

Scheme 1.9 Model oxidative enolate dimerization of oxanorbornanone.

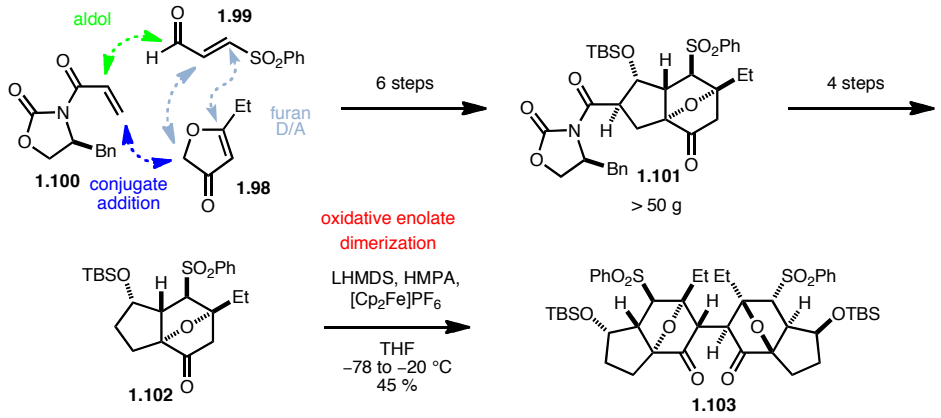

After a successful dimerization, model core **1.103** was moved forward to an intermediate that more closely resembles the natural product (Scheme 1.10). In two steps, C5 ketone was revealed by desilylation of the C5 TBS ether and oxidation. Interestingly, the central 1,4-diketone moiety of the dimer incorporated one molecule of water to form bishemiketal **1.104** as soon as a ketone oxidation state was set at the C5 position. This would become a universal observation made several other times in future investigations. With the C5 ketone in hand, the stage was set for the conversion of oxanorbornane to a cyclohexenol. By treating ketone **1.104** with K_2CO_3 in methanol, the desired cyclohexenol unit was obtained in high yield to provide cyclohexenol **1.105**. Under harsher conditions, the resulting allylic sulfone of **1.105** underwent displacement with methoxide, completing the CDD'C' system of the lomaiviticins in a hydrate form (**1.106**).

Scheme 1.10 Model synthesis of lomaiviticin CDD'C' core.

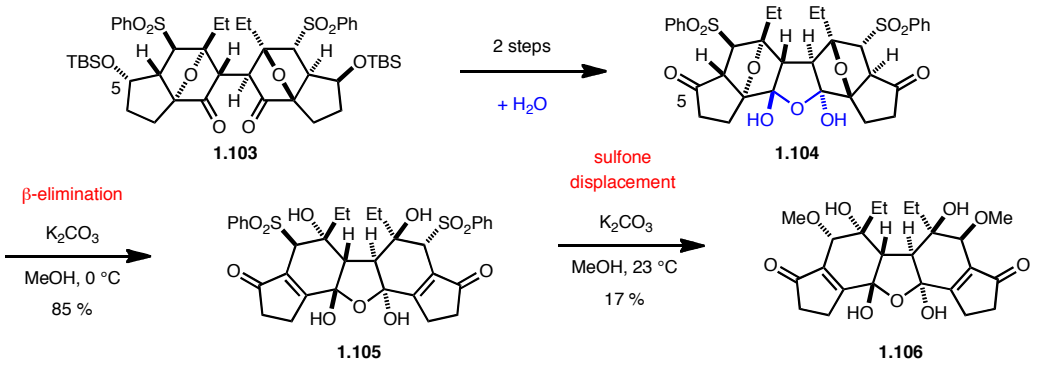

Based on these preliminary results, a strategy to prepare the entire carbon skeleton of the lomaiviticin aglycone was formulated (Figure 1.23). Due to the availability issue of the oxazolidinone chiral auxiliary, the enantiomeric form of lomaiviticin aglycone **1.3** was targeted. First, indeneone **1.107** was chosen to be the direct precursor to the lomaiviticin aglycone. Well-precedented diazo group introduction (*vide infra*) and B-ring oxidation, together with global deprotection, would generate the target compound. Indenone **1.107** would be generated from the oxanorbornanone **1.109** by the cascade fragmentation/displacement reaction discovered in the Krygowski's model study. The cascade is believed to take place with the intermediacy of allylic sulfone **1.108**. Metal hydroxide would be the choice of base to install protecting group free C4 hydroxyl group. 1,4-Diketone **1.109** is the dimerization product of ketone **1.110**. It was anticipated that the dimerization would occur in a diastreoselective manner if the result of the model dimerization was reflected in the real system. Dimerization precursor **1.110**, which has two extra rings compared to the model CD ring system **1.102**, would be prepared from an enone **1.111** and a phthalide derivative **1.112** by an anionic annulation reaction (*vide infra*). Finally it was anticipated that enone **1.105** could be accessed from previously prepared intermediate **1.101**.

Figure 1.23 Retrosynthetic analysis of lomaiviticin aglycone.

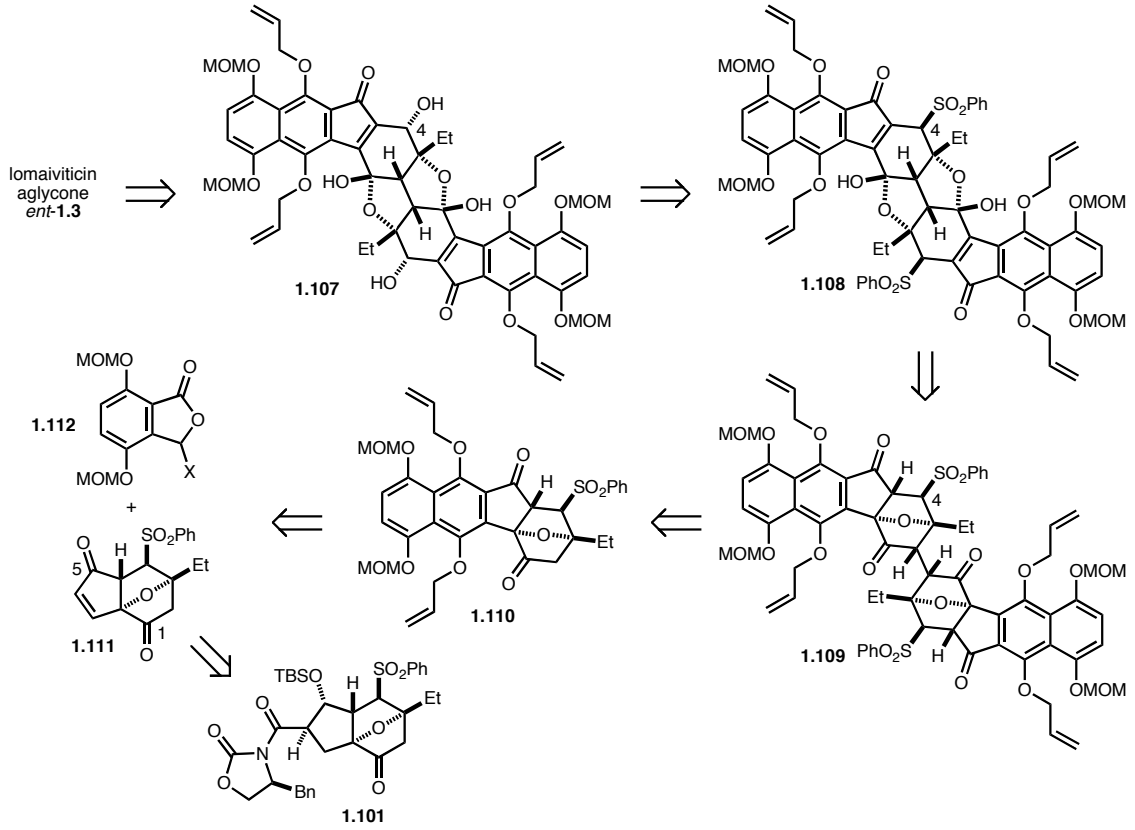

In addition to the global strategy, two specific transformations deserve further comment. First, the challenging diazo group introduction would be attempted on the C5 ketone of dimer **1.107**. Related conversions of ketones to the corresponding diazo groups through the intermediacy of hydrazones have been investigated by other groups (Figure 1.24). Porco and coworkers used a two-step sequence to introduce the diazo group of kinamycin C (Figure 1.24a).[44] Indenone **1.113** was converted to the corresponding TBS hydrazone (not shown) by a protocol previously reported by Myers and coworkers.[45] The resulting hydrazone was oxidized to afford kinamycin C **1.114** by the action of a

(44) Lei, X.; Porco, J. A., *J. Am. Chem. Soc.* **2006**, *128*, 14790-14791.

(45) Furrow, M. E.; Myers, A. G., *J. Am. Chem. Soc.* **2004**, *126*, 12222-12223.

hypervalent iodine oxidant. The Nicolaou group also used an analogous strategy in their synthesis of the kinamycins (Figure 1.24b).[25] Indenone **1.115** was converted to diazo compound **1.116** with the intermediacy of a tosyl hydrazone (not shown). In this case, the oxidation of the hydrazone was accompanied with the oxdation of the B-ring hydroquinone, to give stabilized diazo compound **1.116**.

Figure 1.24 Literature examples of diazo group introduction.

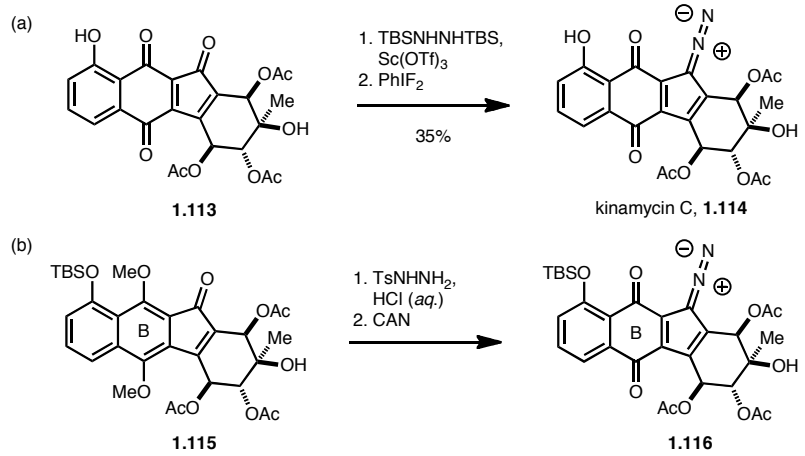

The other key reaction of the strategy is the anioninc annulation of phthalide derivatives (Figure 1.25).[46] In the annulation donor **1.117**, X is usually an electron withdrawing group which can be eliminated, such as a cyanide or a sulfone. It is generally believed that the reaction takes place through a Michael/Dieckmann reaction cascade of the anion of phthalide derivative **1.117** onto an enone (path I). However, a concerted cycloaddition mechanism cannot be completely excluded (path II). In both cases, elimination of substituent X, followed by aromatization, is operational to provide hydroquinone product **1.118**.

(46) For review see: (a) Mal, D.; Pahari, P., *Chem. Rev.* **2007**, *107*, 1892-1918. (b) Rathwell, K.; Brimble, M. A., *Synthesis* **2007**, 643-662.

Figure 1.25 Mechanism of phthalide derivative anion annulation.

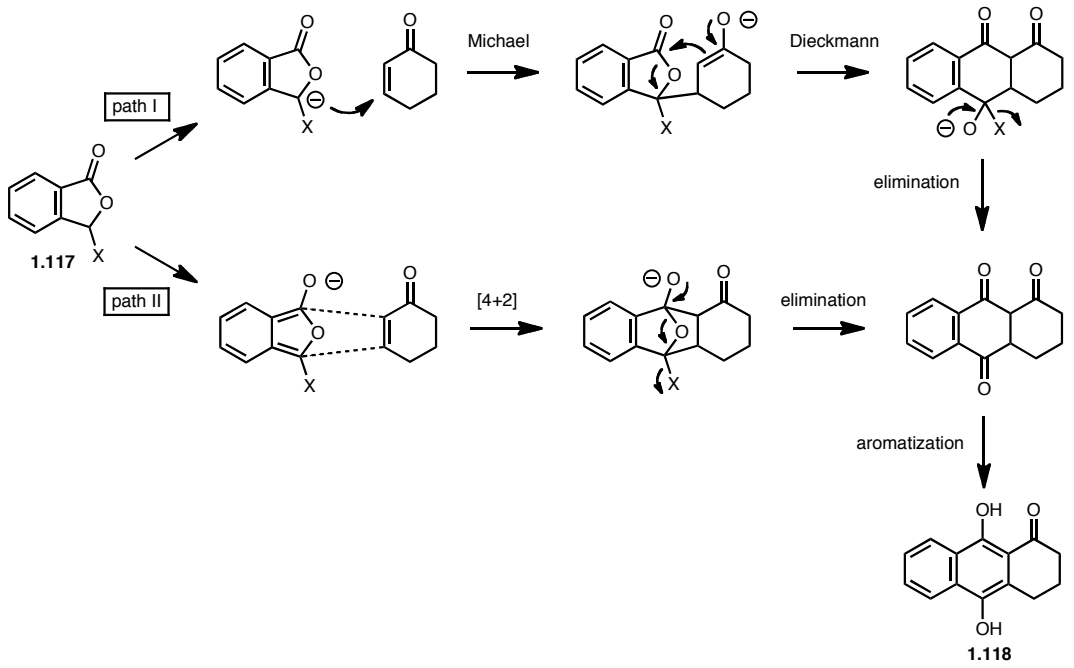

In addition to the original synthetic plan, a more conservative strategy was also conceived (Figure 1.26). Due to the anionic nature of the annulation and dimerization, C1 and C5 ketones may have to be protected in a base resistant form, as in dimerization

Figure 1.26 Alternative synthetic plan.

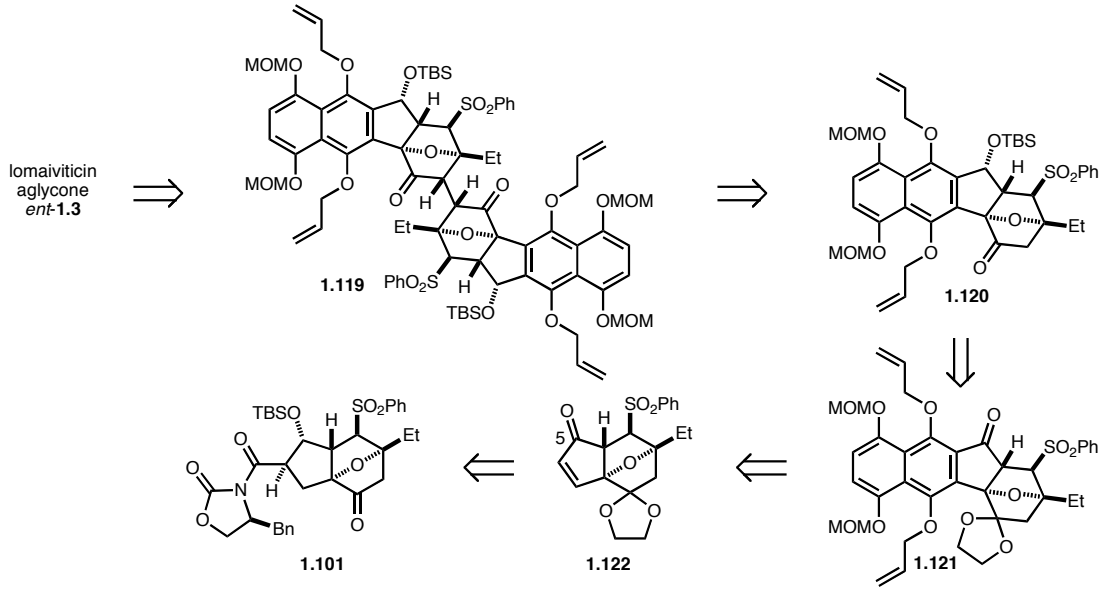

precursor **1.120** or annulation precursor **1.122**. This obviously is a secondary strategy of choice, since additional protection/deprotection manipulations are required at compound **1.119** or **1.121** stage.

In this chapter, background information of the diazobenzofluorene natural products lomaiviticin A and B has been described. For structure elucidation and further biomedical research, a completely synthetic supply of the natural product is required. Synthetic efforts to access these natural products, including our own approach, has been reviewed.

Chapter 2

Key Intermediate Synthesis and AB-Ring Annulation

2.1. First Generation Enone Synthesis

As was discussed in the previous section, enone **1.111** was chosen as the primary target to investigate the possibility of avoiding protective groups of the C1 or C5 carbonyl groups during the dimerization or annulation steps (Figure 2.1).[1] Intermediate **1.101** was chosen as a rational position to begin investigations on this possibility, since **1.101** is easily accessible in large quantities and in enantiopure form.

Figure 2.1 Synthetic aim.

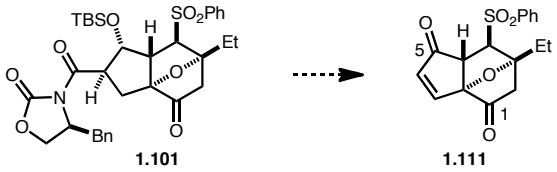

The synthetic strategy to transform **1.101** to **1.111** is outlined in Figure 2.2. The immediate precursor to enone **1.111** was expected to be TBS ether **2.1**. It was envisioned

Figure 2.2 Synthethsis plan for enone **1.111**.

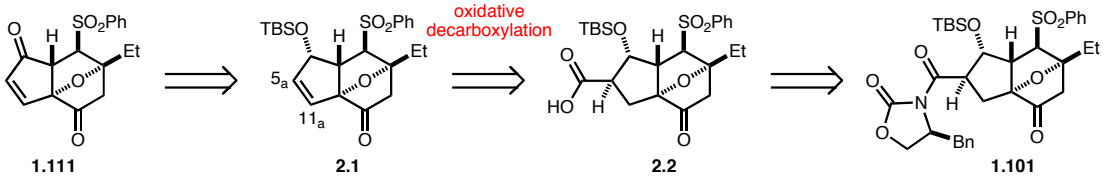

(1) For review of protecting group free synthesis: Young, I. S.; Baran, P. S., *Nature Chem.* **2009**, *1*, 193-205.

that the $C5_a$–$C11_a$ double bond could be installed through an oxidative decarboxylation reaction of acid **2.2**. Consequently, the synthetic problem of **1.111** was reduced to an efficient preparation of carboxylic acid **2.2** from oxanorbornanone **1.101**, a compound previously prepared by Dr. Evan Krygowski.[2]

Scheme 2.1 describes the forward synthesis of compound **1.111**. A global reduction of oxanorbornanone intermediate **1.101** provided diol **2.3** in 79% yield, with concomitant removal of oxazolidinone chiral auxiliary. It should be noted that the strength of the reducing agent had to be attenuated by forming a mixed boronate to maximize the yield.[3] Addition of 1.0 equiv of methanol to $LiBH_4$, prior to addition of the substrate, formed $LiBH_3OMe$. After a two-step oxidation sequence, carboxylic acid **2.2** was obtained. Oxidative decarboxylation of carboxylic acid **2.2**, upon treatment with $Pb(OAc)_4$ and $Cu(OAc)_2$ in refluxing benzene, provided the desired allylic TBS ether **2.1** in 19% yield.[4]

Scheme 2.1 Synthesis of intermediate **2.1**.

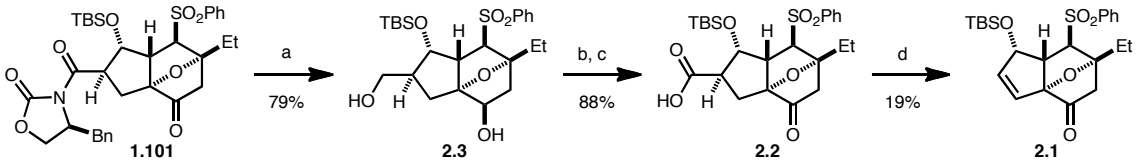

Reagents and conditions: (a) $LiBH_4$, MeOH, Et_2O, 0 °C; (b) $(COCl)_2$, DMSO, CH_2Cl_2; then Et_3N, −78 to 0 °C; (c) $NaClO_2$, NaH_2PO_4, 2-methyl-2-butene, *t*-BuOH, H_2O, 23 °C; (d) $Pb(OAc)_4$, $Cu(OAc)_2 \cdot H_2O$, pyr, benzene, 78 °C.

---

(2) Krygowski, E. S.; Murphy-Benenato, K.; Shair, M. D., *Angew. Chem. Int. Ed.* **2008**, *47*, 1680-1684.

(3) Beshore, D. C.; Smith, A. B., III, *J. Am. Chem. Soc.* **2007**, *129*, 4148-4149.

(4) Bird, C. W.; Butler, H. I.; Coffee, E. C. J.; James, L. M.; Schmidl, B. W. C., *Tetrahedron* **1989**, *45*, 5655-5666.

In an effort to improve the oxidative decarboxylation reaction, the mechanism of the reaction was analyzed. Figure 2.3 describes the generally accepted reaction. It is believed that the homolytic cleavage of Pb–O bond in intermediate **2.4** is the rate-limiting step. Accordingly, we tried to enhance the facility of this process by rendering the metal center more electropositive. We suspected that $Pb(OCOCF_3)_4$, which is in equilibrium with $Pb(OAc)_4$ in the presence of TFA, would participate preferentially in the reaction cycle to form an intermediate **2.7**, which might undergo a faster Pb–O bond cleavage than intermediate **2.4**.

Figure 2.3 Mechanism of oxidative decarboxylation reaction.

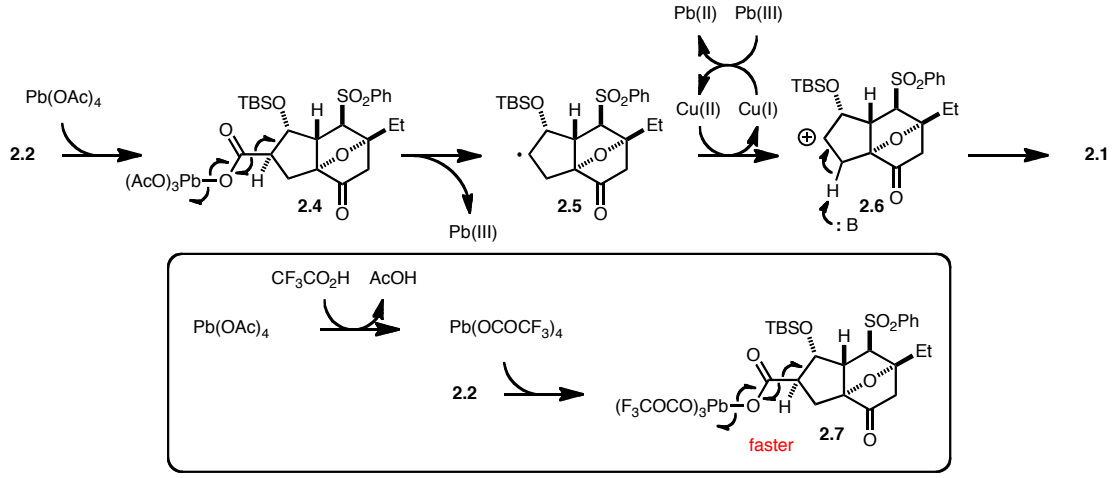

Simple exchange of the acetate ligand for trifluoroacetate improved the yield significantly to 42% yield, 63% yield based on recovered starting material (Scheme 2.2).

Scheme 2.2 Synthesis of enone **1.111**.

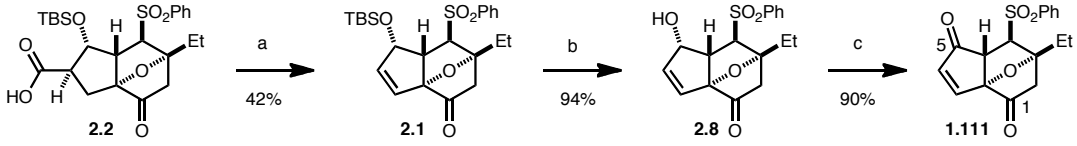

Reagents and conditions: (a) $Pb(OAc)_4$, $Cu(OAc)_2 \cdot H_2O$, TFA, benzene, 78 °C; (b) HF(*aq*), CH_3CN, 23 °C; (c) Dess–Martin periodinane, CH_2Cl_2, 23 °C.

Although this was not a satisfactory result, a sufficient amount of material was prepared to test the key annulation. TBS deprotection and DMP oxidation[5] of **2.1** took place uneventfully to provide enone **1.111** with 85% yield over two steps.

Enone **1.111** contains handles for two key reactions: the C1 ketone for enolate dimerization and the C5 enone for phthalide derivative annulation. First, enone **1.111** was treated with the anion of well-documented phthalide annulation donors such as cyanophthalide **2.10**[6] or sulfonylphthalide **2.11**[7] (Scheme 2.3a). To our disappointment, enone **1.111** underwent rapid decomposition even at −78 °C. A nonanionic annulation donor **2.12**[8] was also applied to the reaction, yet the starting material still decomposed.

Scheme 2.3 Attempted annulation and dimerization of enone **1.111**.

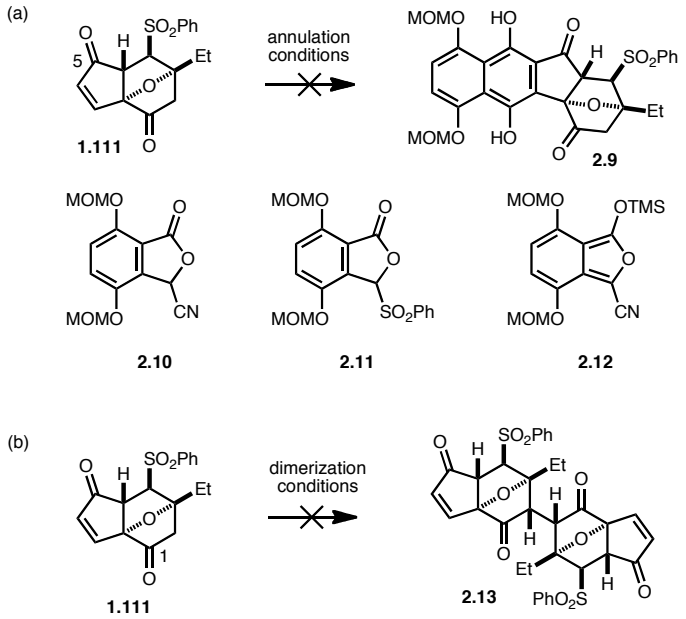

(5) Dess, D. B.; Martin, J. C., *J. Org. Chem.* **1983**, *48*, 4155-4156.

(6) Okazaki, K.; Nomura, K.; Yoshii, E., *Synth. Commun.* **1987**, *17*, 1021-1027.

(7) Hauser, F. M.; Rhee, R. P., *J. Org. Chem.* **1980**, *45*, 3061-3068.

(8) Myers, A. G.; Tom, N. J.; Fraley, M. E.; Cohen, S. B.; Madar, D. J., *J. Am. Chem. Soc.* **1997**, *119*, 6072-6094.

Dimerization of enone **1.111** was also attempted under Dr. Krygowski's optimized conditions, but gave only decomposed starting material (Scheme 2.3b). No dimeric product **2.13** was detected.

Based on these observations, it is evident that the ketone at C1 and the enone at C5 are not compatible under anionic annulation or dimerization conditions (Figure 2.4). This led us to devise an orthogonal protecting group strategy so that we can mask the C1 or C5 ketone selectively. According to the original plan, it was decided to protect the C1 ketone before attempting annulations on the C5 enone.

Figure 2.4 Incompatibility of C1 and C5 ketones.

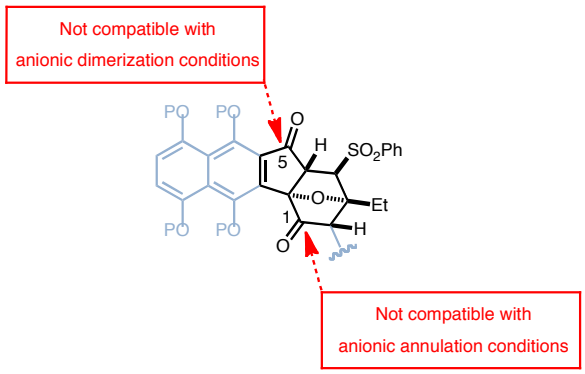

2.2. Second Generation Enone Synthesis

The next goal of the project was the preparation of a C5 enone annulation precursor, where the C1 carbonyl group is masked in a base insensitive form. Differentiation of the C1 and C5 carbonyl groups was realized after the oxidative decarboxylation described in section 2.1 (Scheme 2.4). The C1 ketone of allylic alcohol **2.8** was protected as a 5,5-dimethyl-1,3-dioxane by treatment of **2.8** with 2,2-dimethyl-1,3-propanediol in the presence of a catalytic amount of acid to give compound **2.14**.[9] The C5 ketone was generated in a two-step protocol described in the previous section. In this way, the desired annulation precursor **2.15**, where C1 the ketone is protected as its corresponding ketal, was prepared.

Scheme 2.4 Protection of C1 ketone.

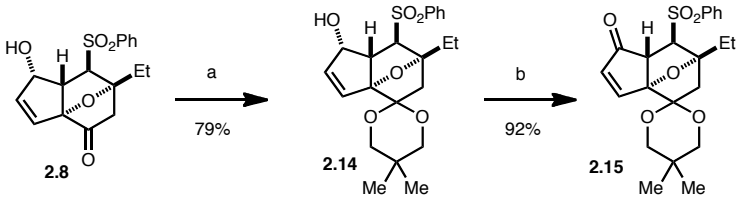

Reagents and conditions: (a) 2,2-Dimethylpropane-1,3-diol, *p*-TsOH·H_2O, benzene, 78 °C; (b) Dess–Martin periodinane, CH_2Cl_2, 23 °C.

Since this sequence of reactions is still hampered by the low yield of the Pb mediated oxidative decarboxylation described earlier, another more efficient and benign decarboxylation condition was sought. A protocol developed by Tsuji using catalytic Pd was determined to be the condition of choice (Figure 2.5).[10] In the proposed catalytic cycle of the reaction, Pd(0) first associates with the allyl ester **2.16**, followed by oxidative

(9) Williams, D. R.; McGill, J. M., *J. Org. Chem.* **1990**, *55*, 3457.

(10) Shimizu, I.; Tsuji, J., *J. Am. Chem. Soc.* **1982**, *104*, 5844-5846.

addition to give intermediate **2.17**. This Pd carboxylate readily undergoes decarboxylation to give a Pd π allyl complex **2.18**. **2.18** undergoes β-hydride elimination to form the desired enone **2.15**.

Figure 2.5 Tsuji's decarboxylative oxidation.

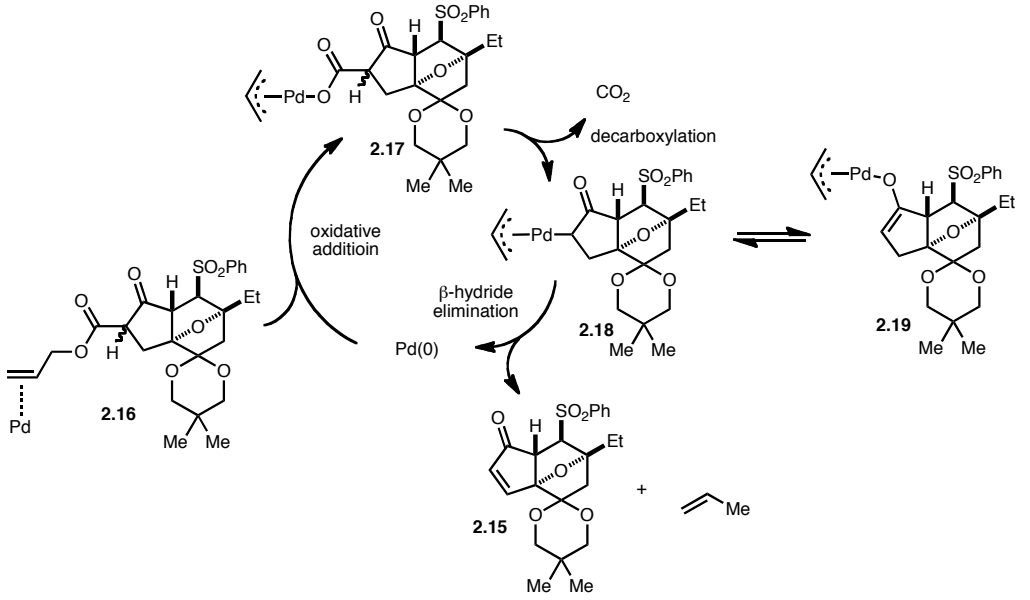

To prepare the requisite β-keto allyl ester **2.16**, carboxylic acid **2.2** was alkylated with allyl bromide to give allyl ester **2.20** in 91% yield (Scheme 2.5). At this stage, the

Scheme 2.5 Synthesis of β-keto ester **2.16**.

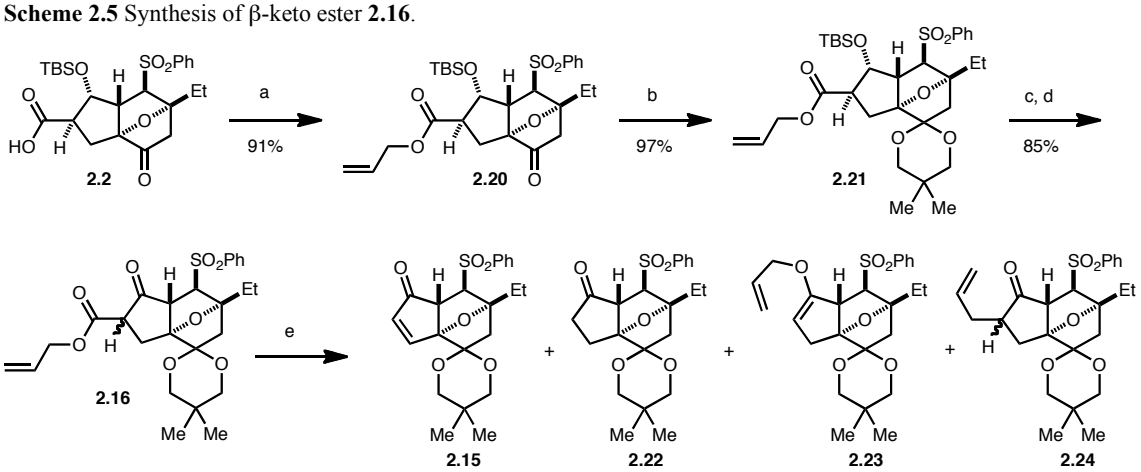

Reagents and conditions: (a) Allyl bromide, Cs_2CO_3, DMF, 23 °C; (b) 2,2-Dimethylpropane-1,3-diol, *p*-TsOH·H_2O, benzene, 78 °C; (c) TBAF, THF, 0 °C; (d) Dess–Martin periodinane, CH_2Cl_2, 23 °C; (e) "Pd" sources.

C5 ketone was protected in its corresponding ketal form in 97% yield (**2.21**). In two straightforward transformations involving TBS removal and oxidation, the desired β-keto allyl ester **2.16** was prepared, setting the stage to test the desired Pd catalyzed transformation discussed in Figure 2.5. The desired catalytic cycle, however, was severely impeded by undesired side reactions, such as proto depalladation, C–O reductive elimination, or C–C reductive elimination to give ketone **2.22**, allyl vinyl ether **2.23**, or allyl ketone **2.24**, respectively. Use of various Pd sources, such as $Pd(OAc)_2$, $Pd(PPh_3)_4$, $PdCl_2(PPh_3)_3$, or $Pd_2(dba)_3$, did not improve the selectivity.

The undesired reaction pathways are depicted in Figure 2.6. It was suspected that the π allyl complex **2.18** did not undergo competitive β-hydride elimination, due to the lack of an extra alkyl group at the α position, which sterically enforces β-hydride

Figure 2.6 Undesired reaction cycle.

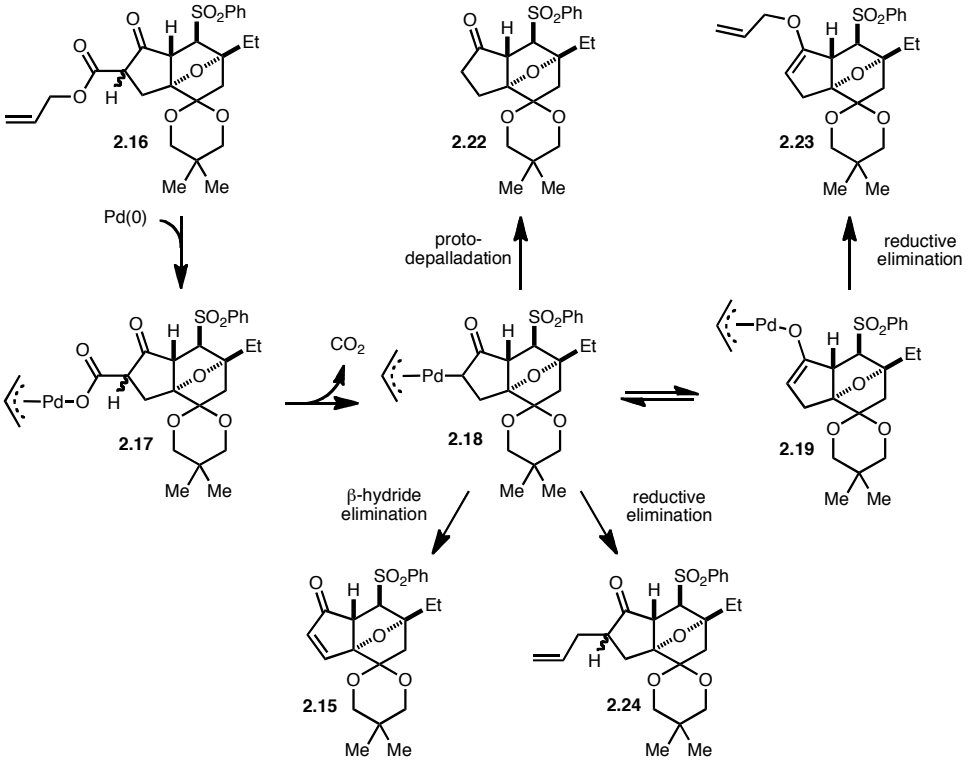

elimination. Thus, the Pd π allyl complex allows other side reactions to occur before the desired β-hydride elimination. Additionally, the side products were hard to separate from the desired product by silica gel chromatography.

Although we were not able to access the desired enone in one step, the reaction served as a reliable method to remove the ester functionality. We focused our attention on the selective formation of ketone **2.22** by using an alternative Tsuji's protocol,[11] and decided to oxidize the ketone at C5 to the corresponding enone in a separate step. The alternative reductive deallylation/decarboxylation protocol is described in Figure 2.7. The π allyl complex **2.18** undergoes transmetallation with a metal hydride such as Bu_3SnH, to give a metal carboxylate such as **2.25**. Upon heating, **2.25** loses one molecule of CO_2, to provide a metal enolate, which is protonated to yield ketone **2.22**.

Figure 2.7 Reductive deallylation/decarboxylation.

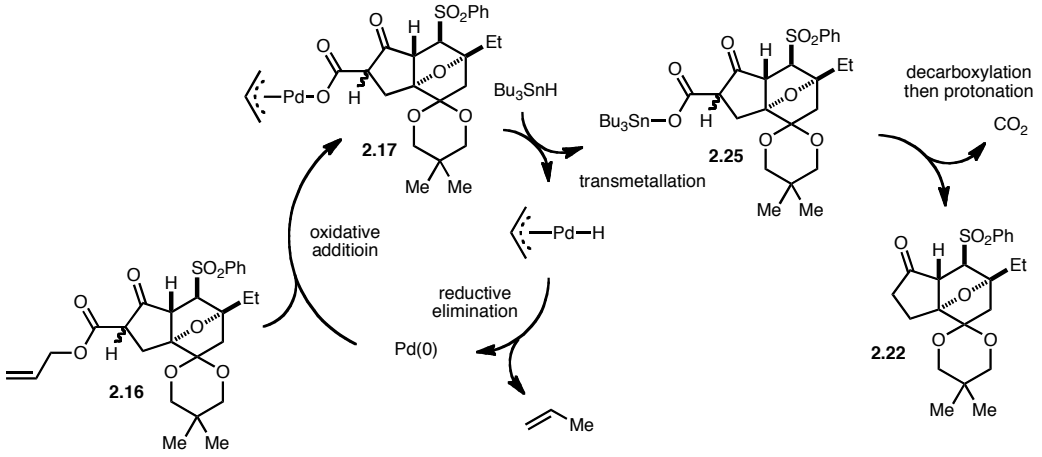

By adding Bu_3SnH as an external hydride source, ketone **2.22** was isolated as a single product in 89% yield (Scheme 2.6). Subsequent oxidation of **2.22** was achieved by

(11) Tsuji, J.; Nisar, M.; Shimizu, I., *J. Org. Chem.* **1985**, *50*, 3416-3417.

treatment with Barton's benzeneseleninic anhydride.[12] This oxidation reaction suffered a conversion issue, due to the lack of complete conversion to the desired enone 2.15. Additionally, a small amount of unreacted starting material **2.22** remaining in the reaction was hard to separate from the product enone **2.15**. This protocol, however, provided a sufficient amount of desired enone **2.15** to study the key annulation reaction until a better method was discovered.

Scheme 2.6 Synthesis of enone **2.15**.

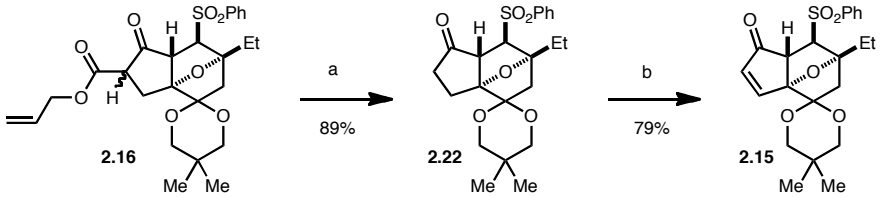

Reagents and conditions: (a) $PdCl_2(PPh_3)_2$, Bu_3SnH, toluene, 23 to 111 °C; (b) $(PhSeO)_2O$, $NaHCO_3$, toluene, 111 °C.

With the protected enone **2.15** in hand, the key annulation was attempted (Scheme 2.7). Treatment of enone **2.15** with the anion of Kraus annulation donor **2.10**[6] provided tetracyclic hydroquinone **2.26** in 41% yield.[13] To avoid isolating side product **2.28**, which is formed after initial conjugate addition, the reaction had to be stirred at an elevated temperature, a condition that drives the reaction to completion. The hydroxyl groups of the hydoquinone was protected as the corresponding allyl ether to give tetracyclic intermediate **2.27**.

(12) Barton, D. H. R.; Lester, D. J.; Ley, S. V., *J. Chem. Soc., Perkin Trans. 1* **1980**, 2209.

(13) Kraus, G. A.; Sugimoto, H., *Tetrahedron Lett.* **1978**, *19*, 2263-2266.

Scheme 2.7 Cyanophthalide annulation of enone **2.15**.

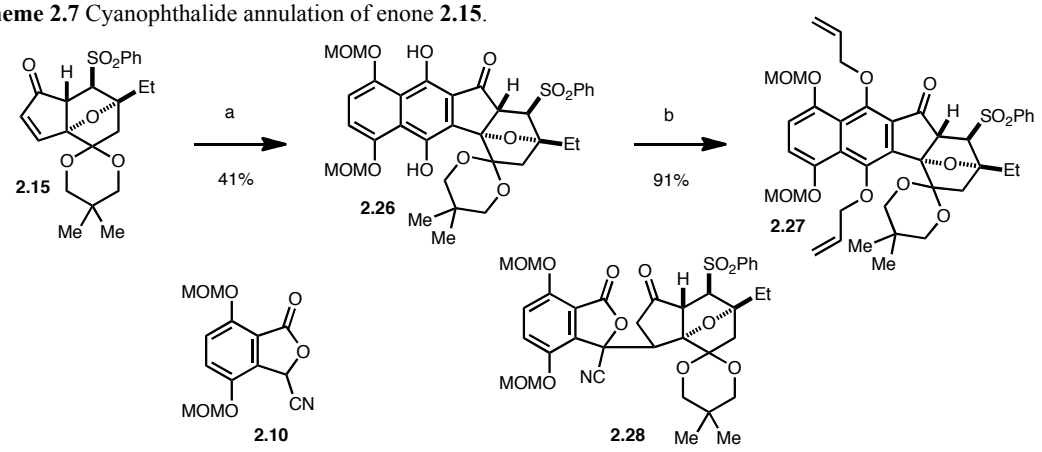

Reagents and conditions: (a) LiHMDS, HMPA, **2.10**, THF, −78 °C, then **2.15**, −78 to 50 °C; (b) Allyl bromide, Cs_2CO_3, TBAI, DMF 23, °C.

In order to investigate the oxidative enolate dimerization, we attempted to deprotect the ketal at the C1 position of **2.27** (Scheme 2.8). However, under a variety of Lewis and Bronsted acidic conditions, a clean deprotection was not realized (Scheme 2.8a). Under these conditions loss of the MOM ether was the first event to take place. Even after MOM deprotection, ketal deprotection did not occur before other undesired side reactions. A control experiment using **2.22** suggests that the hindered CD-ring system is problematic (Scheme 2.8b).

Scheme 2.8 Attempted C1 ketal deprotection.

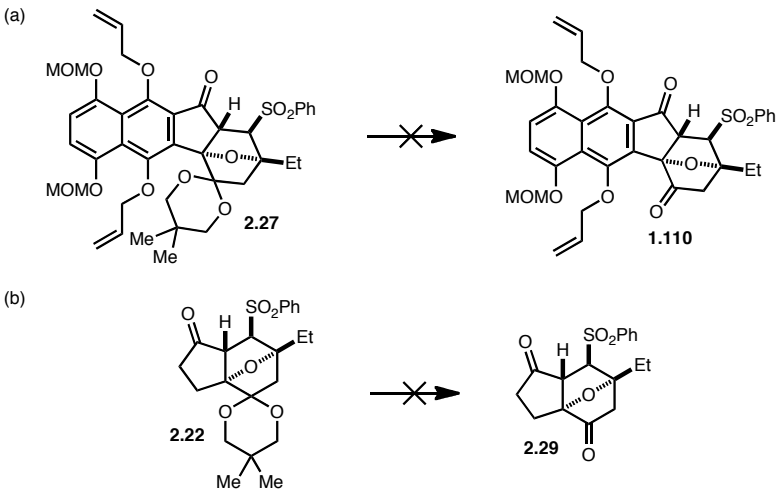

In summary, the desired oxidative enolate dimerization could not be attempted at this stage since the revelation of the C1 ketone was problematic. However, we have acquired useful knowledge regarding: 1) protection of the C1 ketone; 2) preparation of the enone functionality; and 3) execution of the cyanophthalide annulation, which provided the tetracyclic intermediate **2.26**.

2.3. Third Generation Enone Synthesis

After unsuccessful deprotection of the C1 ketal, a decision was made to change the protecting group strategy (Figure 2.7). Instead of protecting the C1 carbonyl group as the corresponding ketal, it was reduced and protected. To ultimately regenerate the C1 ketone, an additional oxidation step would be required.

Figure 2.8 Revised protecting group strategy.

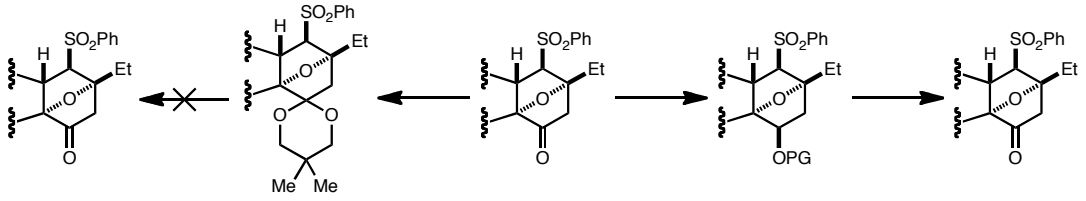

The first protecting group chosen was the MEM ether, which is known to be cleaved significantly faster than the MOM ether.[14] Fortunately, the C1 ketone of **1.102** could be stereoselectively reduced and the resulting hydroxyl group was protected as a MEM ether in 89% yield over two steps (**2.30**). After three identical transformations, enone **2.31**, with the C1 ketone protected as a MEM ether, was prepared. As expected, cyanophthalide annulation, as well as allyl ether formation, was realized uneventfully to

Scheme 2.9 Synthesis of MEM protected tetracycle **2.33**.

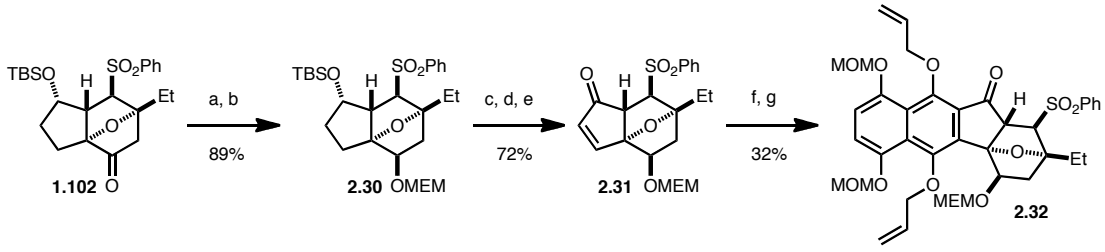

Reagents and conditions: (a) $NaBH_4$, MeOH, 0 °C; (b) MEMCl, DIEA, CH_2Cl_2, 40 °C; (c) TBAF, THF, 0 °C; (d) TPAP, NMO, 4 Å MS, CH_2Cl_2, 23 °C; (e) $(PhSeO)_2O$, $NaHCO_3$, toluene, 111 °C; (f) LiHMDS, HMPA, **2.10**, THF, –78 °C, then **2.32**, -78 to 50 °C; (g) Allyl bromide, Cs_2CO_3, TBAI, DMF 23 °C.

(14) Corey, E. J.; Gras, J.-L.; Ulrich, P., *Tetrahedron Lett.* **1976**, *17*, 809-812.

provide tetracycle **2.32**.

The MEM ether, however, was resistant to removal (Scheme 2.10). Under standard Lewis acidic conditions, MOM ether deprotection occurred first. It is suspected that the coordinative assistance of the allyl ether oxygen is responsible for the inverted deprotection selectivity (**2.34**). This finding led us to use another protecting group, that could be removed under non-acidic conditions.

Scheme 2.10 Attempted removal of MEM protecting group of tetracycle **2.33**.

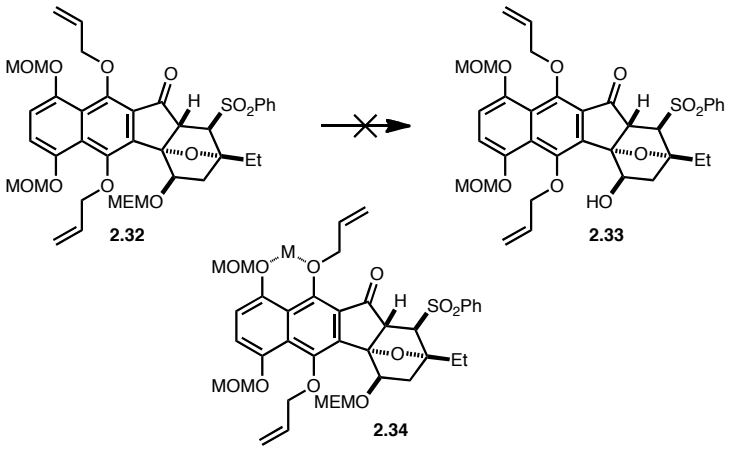

The next protecting group utilized was a pivalate ester, a functionality which can be deprotected under reductive conditions. Instead of using the reduction product of **1.102** (not shown) as a pivalate precursor, a slightly different class of intermediate was ultimately used. The route could be established due to a serendipitous finding that enabled both removal of oxazolidinone auxiliary and differentiation of the C1 and C5 carbonyls at the same time (*vide infra*).

During our continued effort to devise a more efficient route to the annulation acceptor, an interesting and potentially useful transesterification reaction was discovered (Scheme 2.11). Under a standard $NaBH_4$ reduction condition, global reduction of **1.101**

took place to give diol **2.3** as the major product (Scheme 2.11a). Interestingly, when the reaction mixture was quenched at a low temperature with acetone as a hydride scavenger, the oxazolidinone was exchanged with a solvent molecule to give methyl ester **2.35** (Scheme 2.11b). Inspired by this result, the solvent was changed to allyl alcohol and the identical reactivity was observed with similar efficiency (Scheme 2.11c). It is believed that a boronate species such as the structure in the box is responsible for the observed reactivity. This finding established an easy and efficient route to allyl ester **2.36**, where the C1 and the C5 hydroxyl groups are differentiated.

Scheme 2.11 Reduction/transesterification of **1.101**.

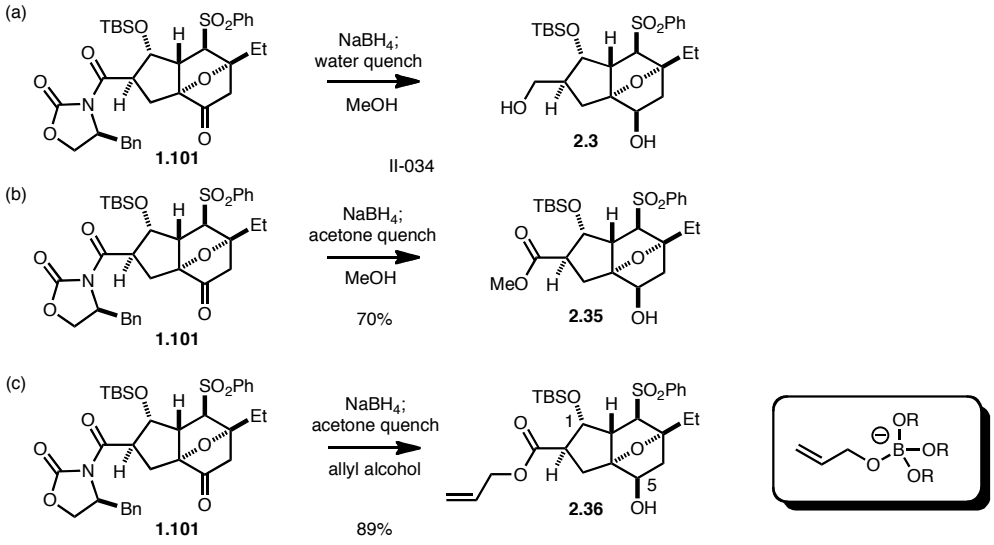

The newly discovered reactivity was applied to the prepration of a new annulation precursor **2.42** (Scheme 2.12). The C1 hydroxyl group of allyl ester **2.36** was protected as a pivalate ester. We anticipated that this ester could be selectively cleaved under reductive conditions, that do not affect other parts of the molecule during the preparation of the tetracyclic intermediate. Then the C5 TBS ether was exposed to TBAF to give hydroxy ester **2.37** in 91% yield over two steps. Subsequent Swern oxidation of **2.37** not

only oxidized the C5 hydroxyl group, but also oxidized the $C5_a$ carbon to give α-chloro β-keto ester **2.39** as the sole product. Similar reactivity has been witnessed by Smith and coworkers and is attributed to electrophilic chlorination of the enol tautomer of the first oxidation product **2.38**.[15] The α-chloride **2.39** was readily reduced in the presence of zinc,[16] then the resulting β-keto allyl ester **2.40** was subjected to the optimized decarboxylation reaction, discussed in the previous section, to provide ketone **2.41** in 82% yield over two steps. Finally ketone **2.41** was converted to enone **2.42** through a standard α-selenation/oxidation sequence in 73% yield.[17] The seven-step sequence from **1.101** to **2.42** was highly scalable and reproducibly provided over 10 g of enone **2.42** in a single batch. Therefore, this sequence has been utilized throughout the research program without further modifications.

Scheme 2.12 Synthesis of a new annualation precursor enone **2.42**.

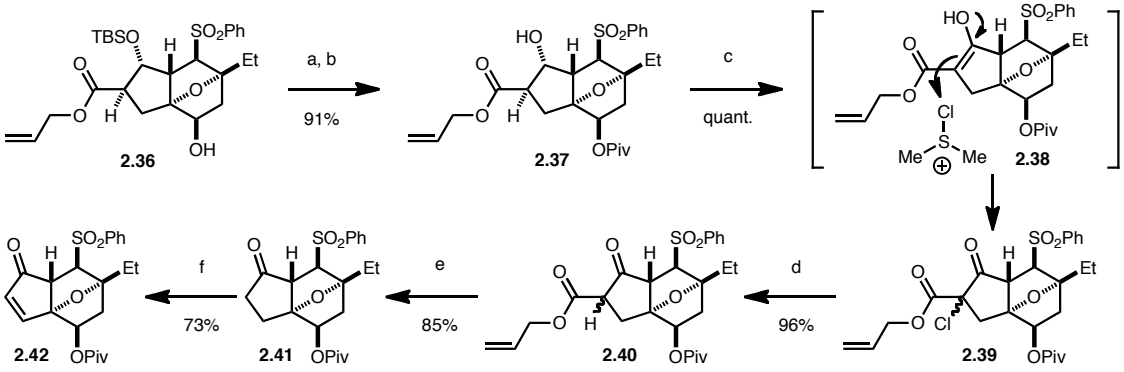

Reagents and conditions: (a) PivCl, pyr, CH_2Cl_2, 40 °C; (b) TBAF, THF, 23 °C; (c) $(COCl)_2$, DMSO, CH_2Cl_2, −78 °C; then Et_3N, 23 °C; (d) Zn dust, AcOH, 23 °C; (e) $PdCl_2(PPh_3)_2$, Bu_3SnH, AcOH, toluene, 0 °C; then 111 °C; (f) LiHMDS, THF, −78 °C; then PhSeBr, −78 °C; then H_2O_2, THF, CH_2Cl_2, 0 °C.

(15) Smith, A. B., III; Leenay, T. L.; Liu, H.-J.; Lloyd, A. K. N.; Ball, R. G., *Tetrahedron Lett.* **1988**, *29*, 49-52.

(16) Snider, B. B.; Patricia, J. J., *J. Org. Chem.* **1989**, *54*, 38-46.

(17) Reich, H. J.; Renga, J. M.; Reich, I. L., *J. Am. Chem. Soc.* **1975**, *97*, 5434-5447.

As anticipated, enone **2.42** underwent efficient Kraus annulation in 85% yield (Scheme 2.13). The allyl protecting group of the B-ring hydroquinone was introduced through a Mitsunobu reaction to give fully protected tetracyclic intermediate **2.44**.[18]

Scheme 2.13 Synthesis of tetracycle **2.44**.

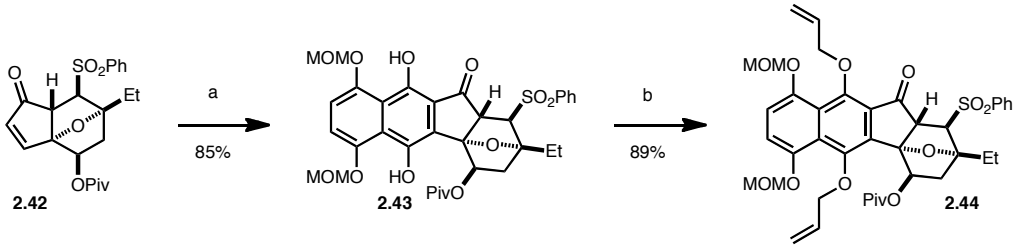

Reagents and conditions: (a) LiHMDS, HMPA, **2.10**, THF, −78 °C, then **2.42**, −78 to 50 °C; (b) Allyl alcohol, DIAD, PPh_3, THF, 50 °C.

The C1 hydroxyl group deprotection was tested under reductive conditions (Scheme 2.14). Exposure of **2.44** to DIBAL-H led to pivalate cleavage with concomitant nonstereoselective reduction of the C5 ketone.

Scheme 2.14 Deprotection of C1 hydroxyl group.

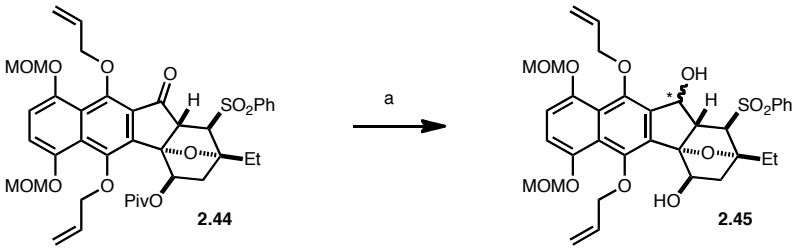

Reagents and conditions: (a) DIBAL-H, CH_2Cl_2, −78 °C.

In summary, a highly reliable procedure for the preparation of an annulation acceptor **2.42** was discovered. Enone **2.42** could be successfully advanced to a tetracyclic intermediate by cyanophthalide annulation. The C1 and C5 ketones could be strictly

(18) For review see: Kumara Swamy, K. C.; Bhuvan Kumar, N. N.; Balaraman, E.; Pavan Kumar, K. V. P., *Chem. Rev.* **2009**, *109*, 2551-2651.

differentiated by protecting the C1 hydroxyl group as a pivalate ester. Finally, the protecting group could be cleanly removed at a post-annulation stage under reductive conditions, albeit with undesired reduction of the C5 ketone.

2.4. Synthesis of Tetracyclic Dimerization Precursor

With scalable access to the tetracycle **2.44** available, we turned our focus to the preparation of an appropriate dimerization precursor. Initially, we attempted to remove the pivalate protecting group under nucleophilic conditions without affecting the C5 ketone (Scheme 2.15). However, a variety of nucleophilic conditions resulted in extensive decomposition of the starting material before removal of the pivalate protecting group at C1 was observed. This result was in accordance with the problems incurred during the ketal deprotection at the C1 position due to the steric hindrance around the D-ring oxanorbornane. The pivalate protecting group could only be cleaved by a hydride nucleophile. DIBAL-H reduction of **2.44** provided diol **2.45** in approximately 1:1 diastereoselectivity at C5. Global Swern oxidation of **2.45** generated a potential dimerization precursor **2.47** in 59% yield over two steps.

Scheme 2.15 Synthesis of dimerization precursor **2.47**.

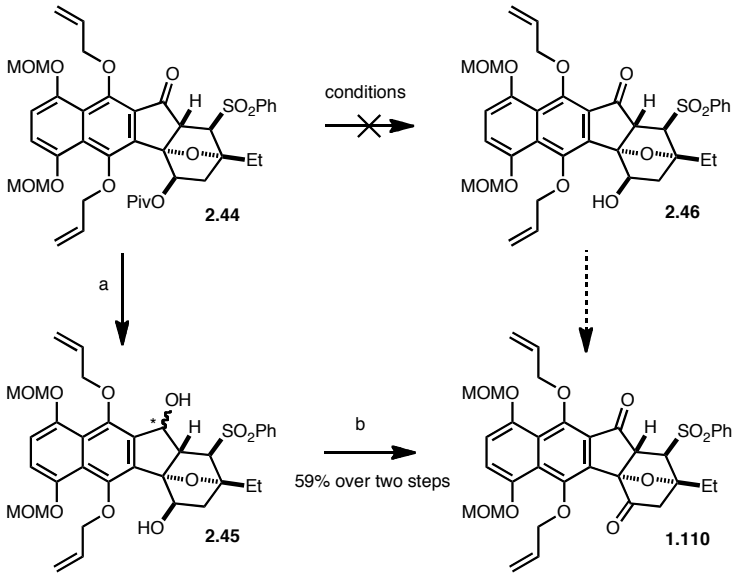

Reagents and conditions: (a) DIBAL-H, CH_2Cl_2, −78 °C; (b) $(COCl)_2$, DMSO, CH_2Cl_2; then Et_3N, −78 to 0 °C.

However, ketone **1.110** does not tolerate the basic enolization conditions required for the oxidative dimerization reaction just like compound **1.111** (Scheme 2.16). As soon as an amide base, either LDA or LiHMDS, was added to **1.110**, the starting material disappeared and multiple unidentified compounds were formed. We hypothesized that the C5 ketone is responsible for the decomposition pathway, hence it was decided that the C5 ketone should be protected in a base tolerant form.

Scheme 2.16 Attempted dimerization of oxanorbornanone **1.110**.

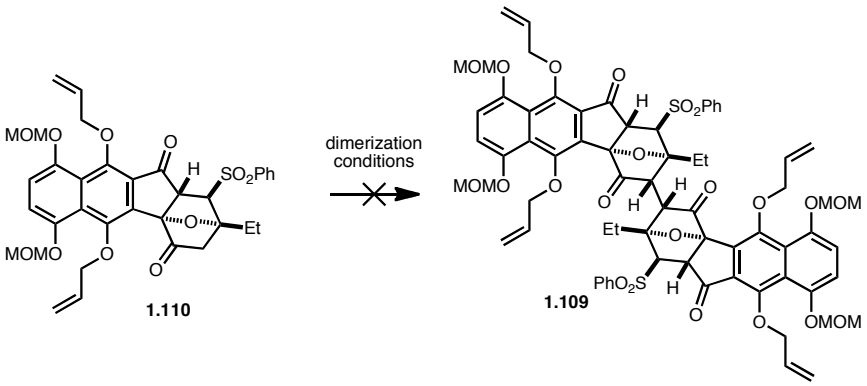

The investigation of a suitable C5 carbonyl group began with its reduction and protection as its corresponding TBS ether. (Scheme 2.17). A chemoselective C5 carbonyl group reduction was realized by exposing **2.44** to $NaBH_4$ at low temperature. As was observed in the global reduction to form **2.45** in Scheme 2.15, the diastereoselectivity of was low, ranging from 1:1 to 2:1. The mixture of diastereomers was treated with TBSOTf in the presence of Hunig's base to give TBS ether **2.47** in 31% yield over two steps. Two straightforward subsequent manipulations provided the C1 ketone in 71% yield over two steps. Although a dimerization precursor could be prepared through this method, the low yield and low stereoselectivity in the first step prevented us from preparing a sufficient amount of dimerization precursor to attempt oxidative dimerization.

Scheme 2.17 Protection of C5 ketone as a TBS ether.

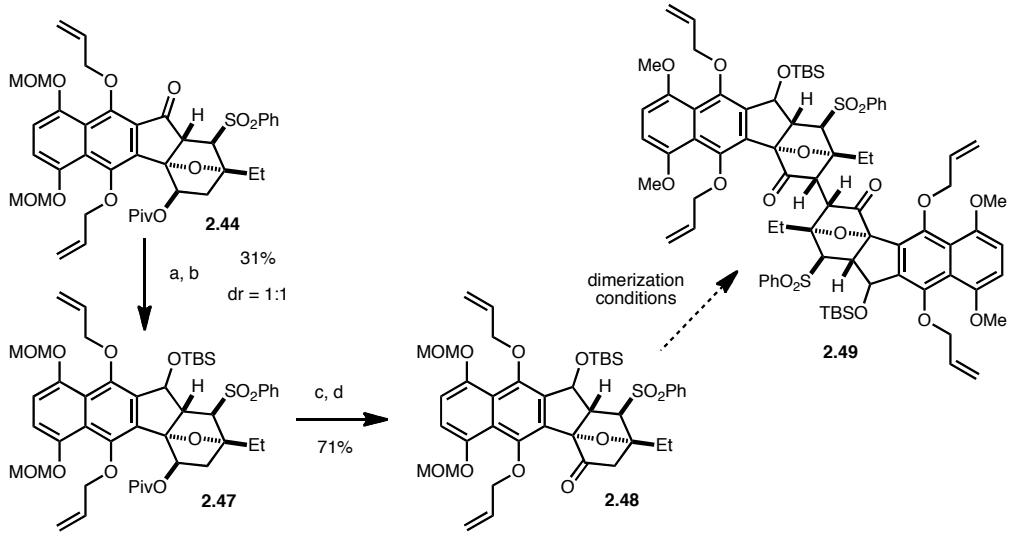

Reagents and conditions: (a) $NaBH_4$, MeOH, −20 °C; (b) TBSOTf, DIEA, CH_2Cl_2, 40 °C; (c) DIBAL-H, CH_2Cl_2, −78 °C; (d) $(COCl)_2$, DMSO, CH_2Cl_2; then Et_3N, −78 to 0 °C.

Additionally, protection strategies for the C5 ketone of **2.44** in a variety of forms were pursued (Figure 2.8). Targeted compounds included, but were not limited to, ketals (**2.50**, **2.51** or **2.52**), thioketal (**2.53**), olefin (**2.54**), hydrazones (**2.55**), silyl enol ethers (**2.56**), or

Figure 2.9 Structure of targeted C5 protected compounds.

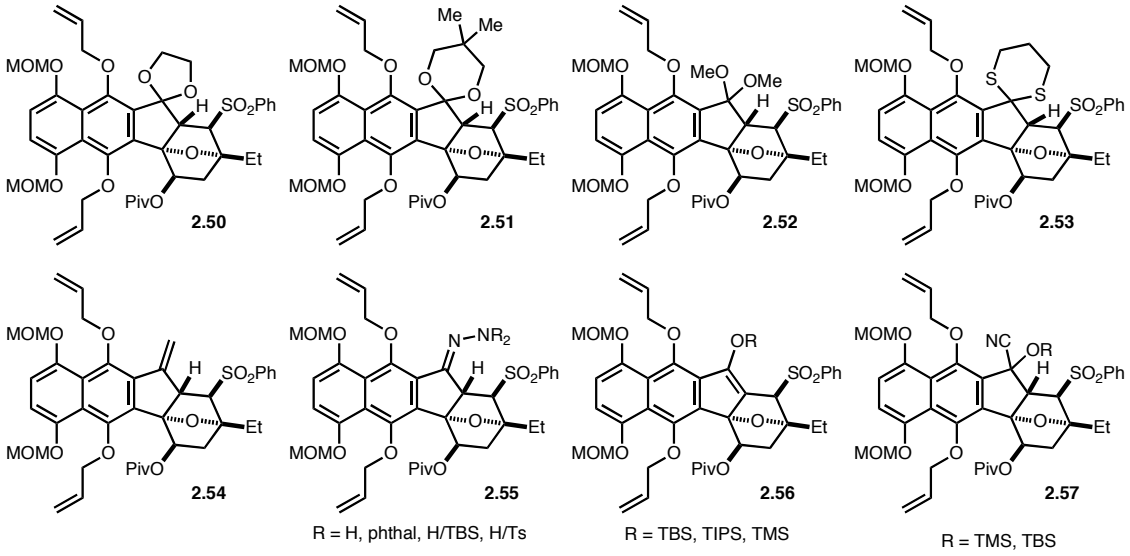

cyanohydrins (**2.57**). In all cases, sufficient conversion was not realized or the starting material did not react.

A breakthrough was made when the protecting group of the A-ring hydroquinone was changed from a MOM ether to a methyl ether, a functional group which is more stable under acidic conditions. Methyl protected cyanophthalide **2.58**[6] and enone **2.42** underwent efficient annulation to give tetracycle **2.59** in 85% yield. This compound was highly stable towards Lewis acidic conditions, thus tolerating the forcing reaction conditions required to install a C5 protecting group. In addition, the sequence of protecting group introduction had to be switched. Exposure of the annulated product **2.59** to Noyori's ketalization conditions provided dioxolane **2.60** in 76% yield.[19] When the allylated version of tetracycle **2.59** (not shown) was exposed to identical conditions, no ketalization was observed, suggesting the steric bulk of the allyl ether retarded ketalization of the C5 ketone.

Scheme 2.18 Protection of C5 ketone.

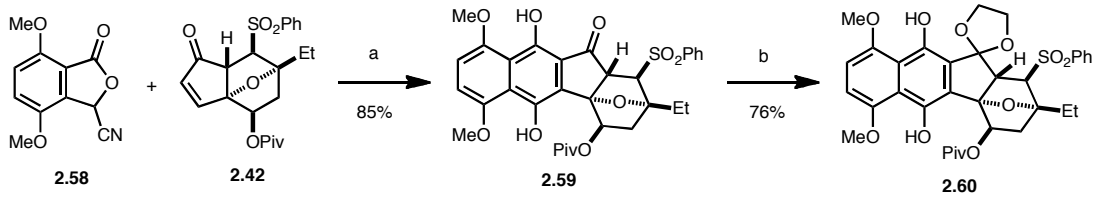

2.58 **2.42** **2.59** **2.60**

Reagents and conditions: (a) LiHMDS, HMPA, **2.58**, THF, −78 °C, then **2.42**, −78 to 50 °C; (b) 1,2-Bis(trimethylsilyloxy)ethane, TMSOTf, CH_2Cl_2, 23 °C.

After the C5 ketone was successfully masked, the B-ring hydroquinone was protected as a bisallyl ether under nucleophilic alkylation conditions to provide bisallyl ether **2.61** in 87% yield (Scheme 2.19). When Mitsunobu conditions were employed, a

(19) Tsunoda, T.; Suzuki, M.; Noyori, R., *Tetrahedron Lett.* **1980**, *21*, 1357-1358.

quinone **2.64** was isolated as a major product presumably through the assistance of DIAD (**2.63**). Finally, the C1 ketone was exposed under the optimized protocol, which involves $NaBHEt_3$ reduction and Ley oxidation to provide ketone **2.62**.

Scheme 2.19 Synthesis of tetracyclic dimerization precursor **2.62**.

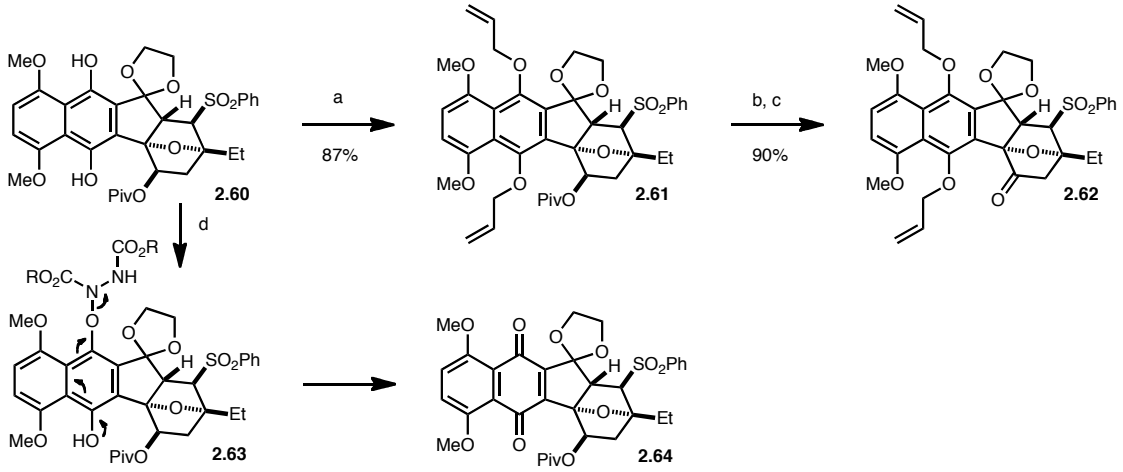

Reagents and conditions: (a) Allyl bromide, Cs_2CO_3, DMF, 23 °C; (b) $NaBHEt_3$, THF, 0 °C; (c) TPAP, NMO, 4 Å MS, CH_2Cl_2, 23 °C; (d) DIAD, PPh_3, THF, 23 °C..

In summary, a route to the targeted dimerization precursor **2.62** was established. Annulation precursor enone **2.42** was prepared in seven steps from the readily accessible compound **1.101**. Enone **2.42** was protected at the C1 position to avoid decomposition during the anionic annulation. It was elaborated to the dimerization precursor **2.62** in five additional steps. During the course of the investigation, judicious choice of protecting groups as well as appropriate stage of application of those protecting groups were crucial

Figure 2.10 Summary of chapter 2.

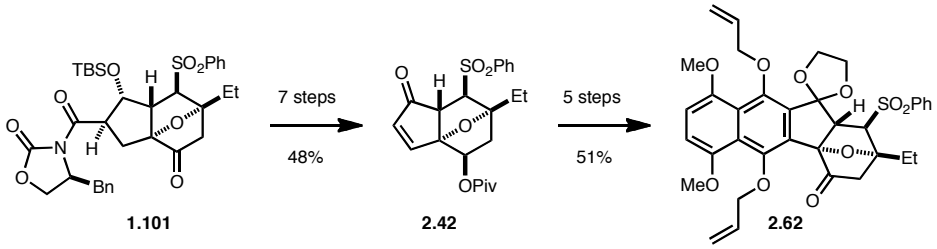

for the successful preparation of **2.62**.

Chapter 3

Two Directional Synthesis

Although the initial plan was to dimerize an advanced tetracyclic intermediate to minimize double processing, a strategy involving an early stage dimerization and expansion of the core was also investigated (Figure 3.1).[1] In this strategy, dimeric intermediate **1.109** would be generated from a dimeric enone such as **3.1** through the bidirectional annulation method discussed in chapter 2. Therefore, the first goal was the preparation of enone **3.1** from well established intermediate **2.41** by using an oxidative enolate dimerization. This strategy didn't successfully culminate with the formation of the advanced intermediate. However, a very important piece of information regarding dimerization of the oxanorbornanone enolate was discovered during the investigation. In

Figure 3.1 A strategy involving two directional synthesis.

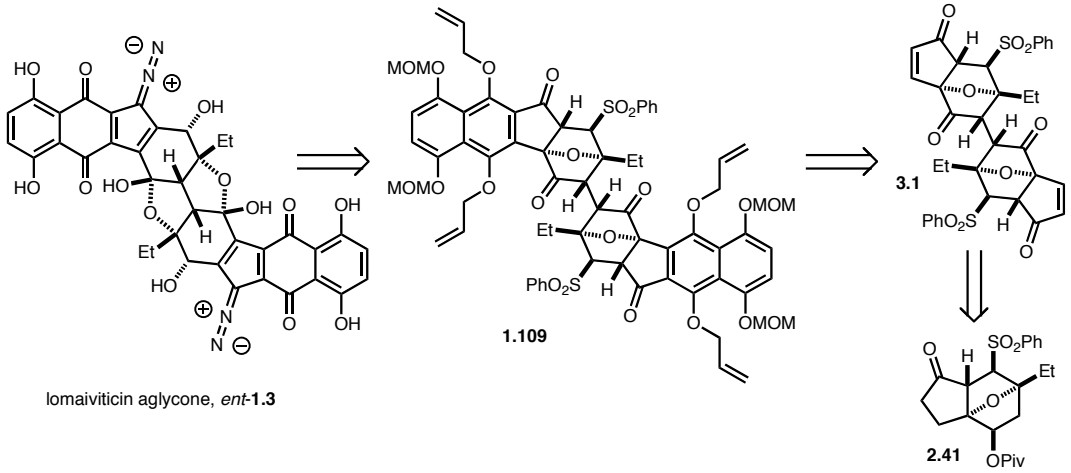

(1) Vrettou, M.; Gray, A. A.; Brewer, A. R. E.; Barrett, A. G. M., *Tetrahedron* **2007**, *63*, 1487-1536.

this chapter, the finding is described.

The starting point of this approach was intermediate **2.41** where the C1 and C5 ketones are fully differentiated. As a prelude to the dimerization, the C5 ketone was protected as a TIPS enol ether, a functionality which can be converted to an enone at a later stage to provide compound **3.1** (Scheme 3.1). The removal of the pivalate protecting group and subsequent oxidation to a ketone took place uneventfully to give ketone **3.3** in 94% yield over two steps. At this point, conversion of the TIPS enol ether to the corresponding enone was assured in the monomeric setting. Saegusa oxidation condition provided enone **1.111**, a compound previously prepared from a different route, in 71% yield.[2]

Scheme 3.1 Synthesis of dimerization precursor **3.3**.

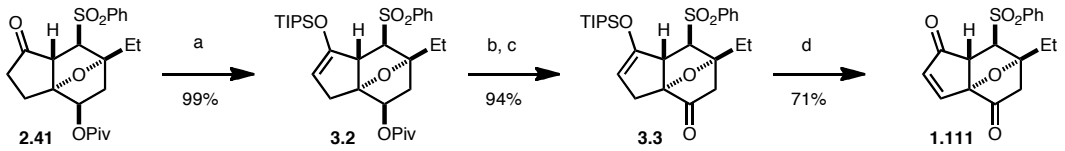

Reagents and conditions: (a) NaHMDS, TIPSOTf, THF, −78 to 23 °C; (b) $NaBHEt_3$, THF, 0 °C; (c) TPAP, NMO, 4 Å MS, CH_2Cl_2, 23 °C; (d) $Pd(OAc)_2$, O_2, DMSO, 100 °C.

In the previous model study, the yield of the dimerization was never greater than 51%.[3] To improve the conversion of the reaction, an optimization study was initiated. The primary goal was to minimize undesired β-elimination, which was often observed upon warming the reaction from −78 °C to −20 °C, a condition utilized in the model

(2) Ito, Y.; Hirao, T.; Saegusa, T., *J. Org. Chem.* **1978**, *43*, 1011-1013.

(3) Krygowski, E. S.; Murphy-Benenato, K.; Shair, M. D., *Angew. Chem. Int. Ed.* **2008**, *47*, 1680-1684.

study (Figure 3.2). By suppressing the side reaction at a low temperature, it was anticipated that the conversion to the desired product, dimer **3.5**, would be maximized.

Figure 3.2 Side reaction of the oxidative enolate dimerization.

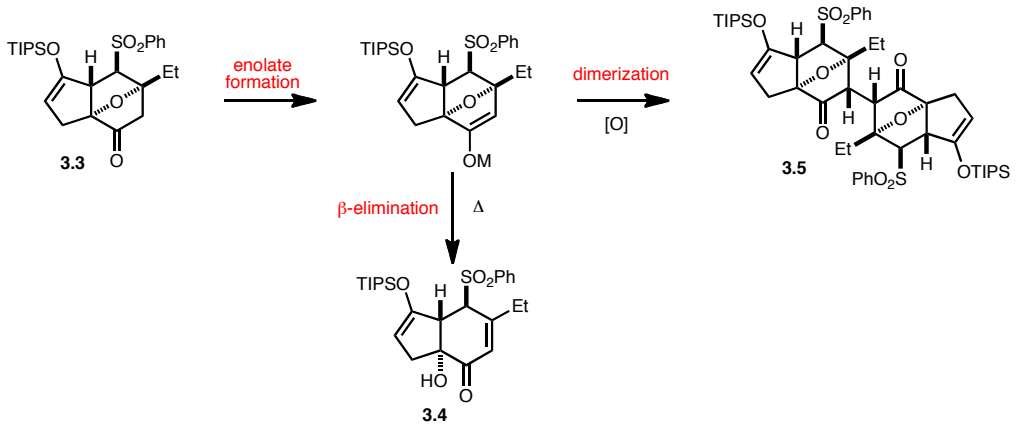

In order to find the optimal reaction temperature, ketone **3.3** was treated with an amide base for 1 hour at −78 °C to initiate enolate formation, then the mixture was warmed to a desired temperature and maintained for 3 hours. At the end of the reaction, the reaction mixture was quenched with TMSCl to trap the lithium enolate as a TMS enol ether. Usually, the enol ether product **3.6** was isolated together with the β-elimination product **3.4** as well as the unreacted starting material **3.3**. The ratio of these products are summarized in Scheme 3.2.

Scheme 3.2 Enolization experiment of ketone **3.3**.

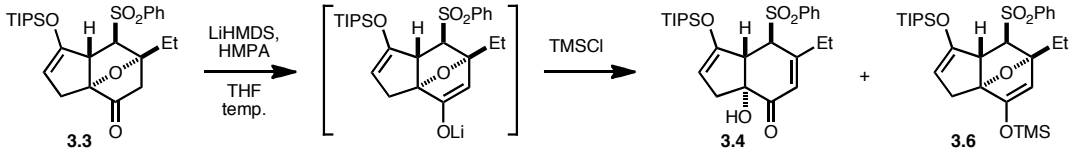

Temperature (°C)	3.3	3.4	3.6
−20	1	0.80	0
−40	1	0.67	0
−60	1	0.25	0.25
−78	1	0	0

At −20 °C, only starting material and the β-elimination byproduct were detected (entry 1). By lowering the temperature to −40 °C, the formation of byproduct was suppressed (entry 2). Eventually, the desired TMS enol ether was formed and detected at −60 °C, suggesting the enolate had a certain lifetime to be trapped after 3 hours of enolization (entry 3). At −78 °C, no product, other than the starting material was observed, suggesting that the enolization of hindered ketone **3.3** is slow at this temperature (entry 4).

Based on these observations, a scenario regarding the enolization of ketone **3.3** was made (Figure 3.3): 1) the enolate formation of the oxanorbornanone **3.3** is slow at or below −78 °C; 2) the undesired β-elimination is predominant at or above −40 °C; 3) at −60 °C both enolate formation and β-elimination take place. Since the oxidation of an enolate species to form enoxy radical **3.7**, an electron transfer reaction, should be fast enough to take place before undergoing undesired β-elimination, it was hypothesized that the lithium enolate, formed at −60 °C, would undergo oxidation to dimerize before forming **3.4**.

Figure 3.3 Postulated behavior of the oxanorbornanone lithium enolate.

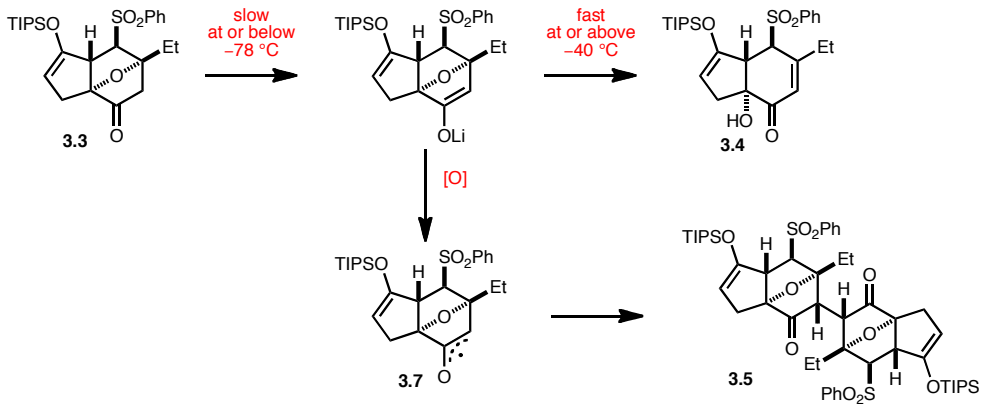

By utilizing the optimized temperature, the desired dimerization took place in 57% yield to provide symmetric dimer **3.5** (Scheme 3.3).[4] The reaction was highly reproducible up to 300 mg scale, and the only byproduct was unreacted starting material **3.3**. Dimer **3.5** was further advanced to attempt double annulation by introducing the enone functionality from the TIPS enol ether. Under Saegusa oxidation conditions, bisenone **3.8** was isolated in 59% yield in a cyclic hydrate form instead of a 1,4-diketone. As was observed in the model study of Dr. Krygowski, the initially formed bisenone **3.1** has gained one molecule of water to form a bishemiketal.

Scheme 3.3 Synthesis of dimeric enone **3.8**.

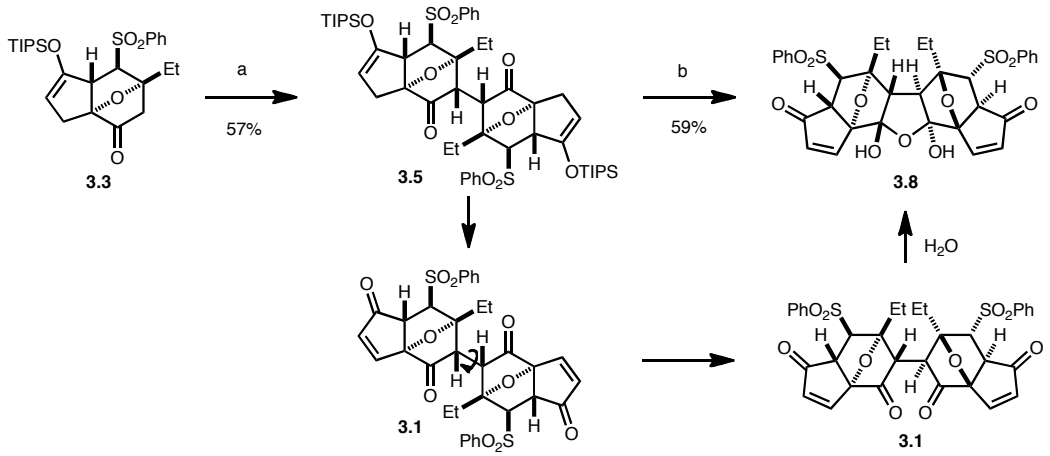

Reagents and conditions: (a) LiHMDS, HMPA, −78 °C; $[Cp_2Fe]PF_6$, −60 °C; (b) $Pd(OAc)_2$, O_2, DMSO, 100 °C.

With the dimeric enone in hand, the well-investigated Kraus annulation was applied to expand the core (Scheme 3.4).[5] To our disappointment, however, enone **3.8**

(4) Later in the investigation, it was found that longer reaction time was required to maximize the yield. See chapter 4.

(5) Kraus, G. A.; Sugimoto, H., *Tetrahedron Lett.* **1978**, *19*, 2263-2266.

underwent rapid decomposition upon treatment with the anion of cyanophthalide **2.10**[6] or silyloxyisobenzofuran **2.12**,[7] derived from **2.10**. It was suspected that the acidic protons of the central bishemiketal were responsible for the observed decomposition. Therefore, it was decided that the bishemiketal should be protected.

Scheme 3.4 Attempted annuulation of enone **3.8**.

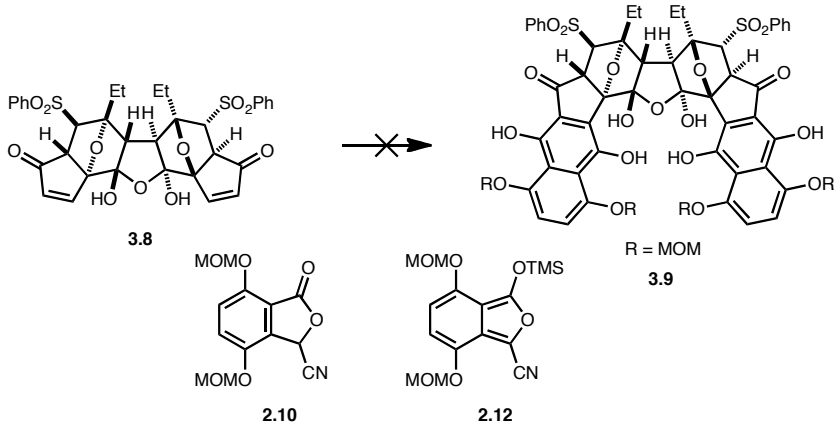

The protection of the hemiketal turned out to be highly challenging presumably due to the sterically hindered nature of the core structure. Standard silylating agents such as TMSCl or TMSOTf did not provide any silylated product. It was not until Corey's silylation condition was applied to the system that the bistrimethylsilyl ether of the

Scheme 3.5 Protection of cyclic hydrate.

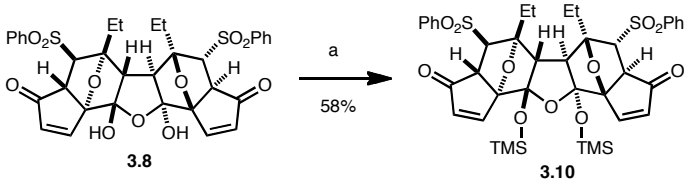

Reagents and conditions: (a) TMSCN, neat, 80 °C.

(6) Okazaki, K.; Nomura, K.; Yoshii, E., *Synth. Commun.* **1987**, *17*, 1021-1027.

(7) Myers, A. G.; Tom, N. J.; Fraley, M. E.; Cohen, S. B.; Madar, D. J., *J. Am. Chem. Soc.* **1997**, *119*, 6072-6094.

bishemiketal was isolated (Scheme 3.5).[8] In neat TMSCN at elevated temperatures, enone **3.8** underwent a smooth silylation to provided fully protected bisenone **3.10** in 58% yield, setting the stage for the anionic annulation.

The attempted annulations are summarized in Scheme 3.6. Unlike bisenone **3.8**, **3.10** turned out to be highly unreactive towards various annulation conditions. Under standard Kraus' conditions only conjugate adduct **3.11** was formed, suggesting that the final Dieckmann reaction did not occur (equation a). A more reactive annulation donor **3.12** increased the reactivity of conjugate addition. However, the desired Dieckmann condensation still did not occur until the end of the reaction (equation b). A less reactive annulation donor such as **2.12** or **3.14** did not react at all with enone **3.10** even at an elevated temperature (equation c).

(8) Corey, E. J.; Wu, Y. J., *J. Am. Chem. Soc.* **1993**, *115*, 8871-8872.

Scheme 3.6 Attempted annuulation of enone **3.10**.

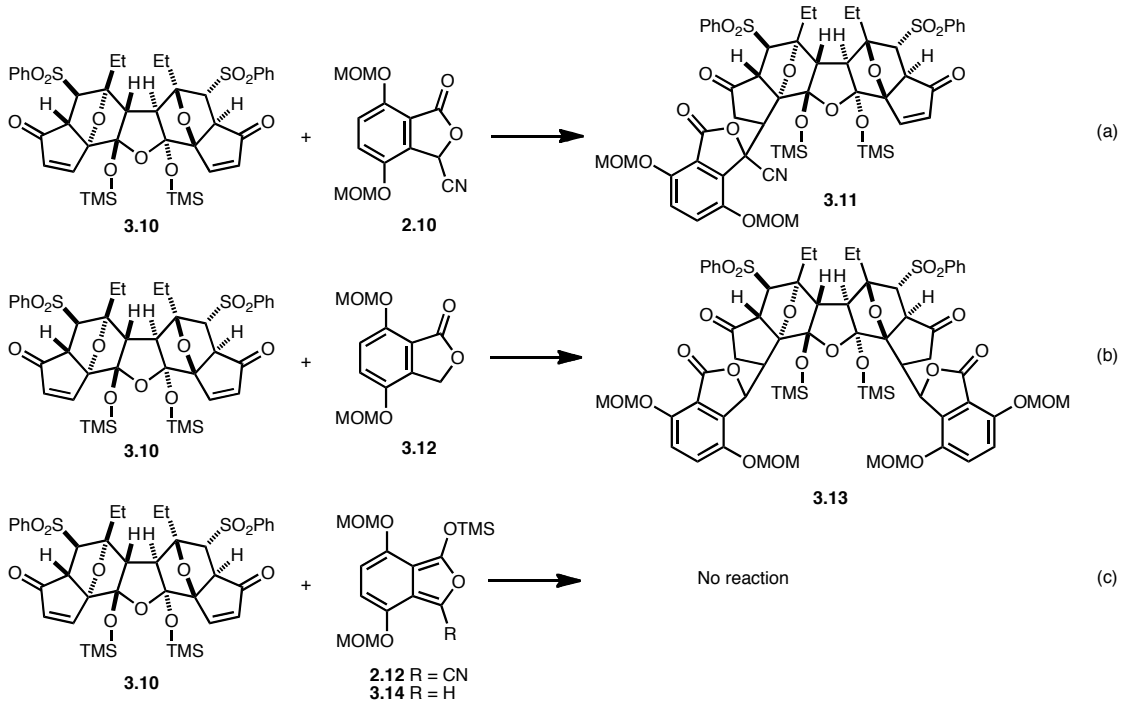

Since the stereochemical outcome of the Michael addition is not clear, it is hard to analyze the transition state of the Dieckmann condensation. However, such a hampered Dieckmann condensation in Kraus annulations under crowded settings are documented (Figure 3.4). Danishefsky[9] and Myers[7] have independently reported similar conjugate additions of a cyanophthalide anion in their synthesis of dynemicin A. In both cases a hindered electrophile did not allow for the final Dieckmann condensation.

(9) Shair, M. D.; Yoon, T. Y.; Mosny, K. K.; Chou, T. C.; Danishefsky, S. J., *J. Am. Chem. Soc.* **1996**, *118*, 9509-9525.

Figure 3.4 Conjugate addition of cyanophthalide anions in the literature.

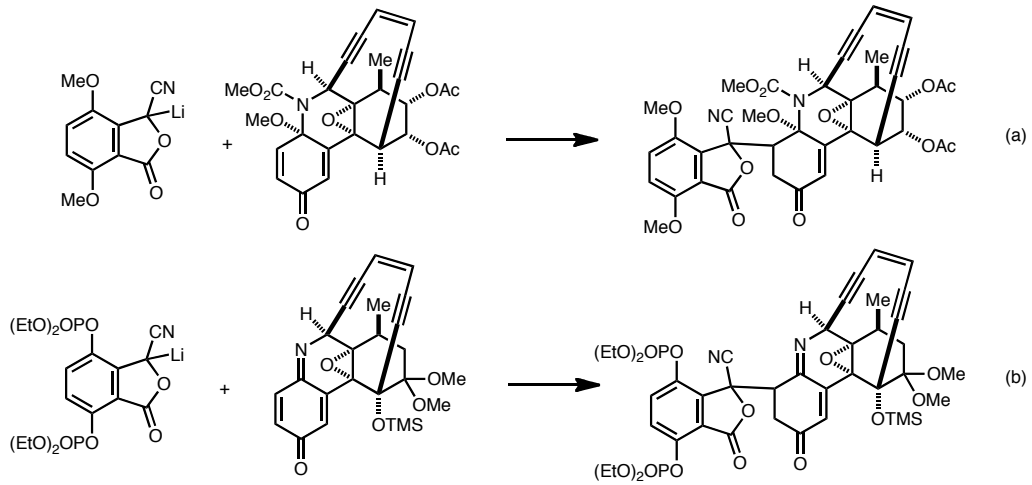

In conclusion, optimized dimerization conditions were found by utilizing ketone **3.3** as a model oxanorbornanone (Figure 3.5). The control of enolization temperature was critical for minimizing formation of β-elimination byproduct. This optimal temperature found in the model study was universally applicable to other dimerization precursors containing oxanorbornanone substructure (*vide infra*). The dimer thus formed was advanced to the annulation stage, which did not culminate into the desired product due to the steric congestion of the core structure. The dimerization condition used in the route was eventually used to prepared advanced intermediates in the future to prepare the entire carbon skeleton of the natural product.

Figure 3.5 Summary of chapter 3.

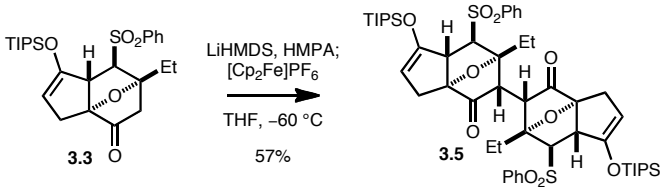

Chapter 4

Synthesis of the Full Carbon Skeleton of the Lomaiviticins

4.1. Remote Steric Effect of the C11 Substituent

In chapter 2 and 3, the synthesis of the dimerization precursor and optimization of the dimerization conditions were discussed, respectively. In the real dimerization event, however, additional insights were required than were disclosed in the previous chapters.

The dimerization precursor **2.62**, the synthesis of which was discussed in chapter 2, was subjected to the optimized dimerization conditions; LiHMDS, HMPA, and $[Cp_2Fe]PF_6$ in THF at −60 °C. To our disappointment, the compound did not undergo desired dimerization under these conditions (Scheme 4.1). Only starting material **2.62** was recovered with greater than 80% yield and none of dimer **4.1** was detected. At this point a variety of solvent/oxidant combinations was reexamined, still without yielding any dimeric product.

Scheme 4.1 Attempted dimerization of oxanorbornanone **2.62**.

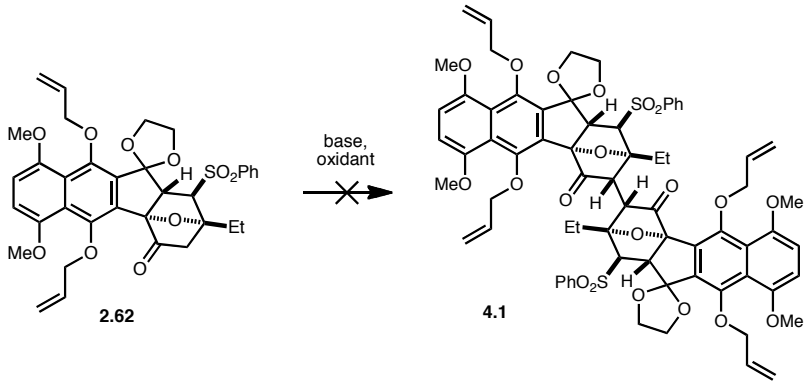

Compound **2.62** showed a similar enolization profile to the oxanorbornanone **3.3**, a compound used in the model study in chapter 3. LiHMDS-mediated enolization at −60 °C, followed by TMSCl quenching provided both desired silyl enol ether **4.2** and β-elimination product **4.3** (Scheme 4.2). The experimental result suggests that a post-enolization event, either oxidation to the enoxy radical or union of enoxy radical and enolate, is responsible for the unsuccessful dimerization of **2.62**.

Scheme 4.2 Enolization experiment of oxanorbornanone **2.62**.

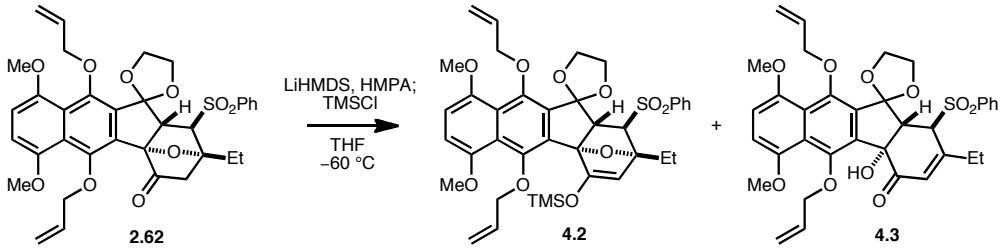

Later, critical insight was gained when a modified approach was attempted. In 2008, Thomson and coworkers reported a successful dimerization of simple cyclic ketones via the intermediacy of a silyl bis-enol ether such as **4.5** (Figure 4.1).[1] Since a similar enolization/silylation pathway was successfully applied to our own tetracyclic ketone system **2.62** (Scheme 4.2), it was anticipated that a similar oxidative condition

Figure 4.1 Thomson's oxidative dimerization of silyl bis-enol ether.

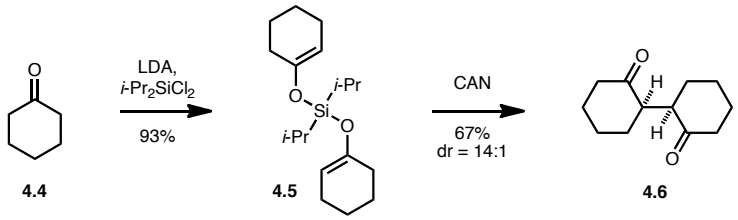

(1) Avetta, C. T.; Konkol, L. C.; Taylor, C. N.; Dugan, K. C.; Stern, C. L.; Thomson, R. J., *Org. Lett.* **2008**, *10*, 5621-5624.

could provide the desired dimeric structure, as in Thomson's approach.

However, ketone **2.62** did not undergo any silyl bis-enol ether formation under a variety of conditions attempted (Scheme 4.3). No dimeric enol ether **4.7** was detected under the reaction conditions employed. Instead, starting material was isolated presumably through the intermediacy of silyl mono-enol ether such as **4.8**, which undergoes hydrolytic regeneration of **2.62**. This hypothesis is supported by isolation of a small amount of amino silane **4.9**, which presumably was formed by reaction of **4.8** with the amide base. From this observation, it was speculated that certain steric interactions exist in the dimeric structure of ketone **2.62**, although their exact nature was elusive. The postulated interaction may be obstructing the approach of two molecules of **2.62**, even in the presence of a silicon linker.

Scheme 4.3 Attempted formation of silyl bis-enol ether.

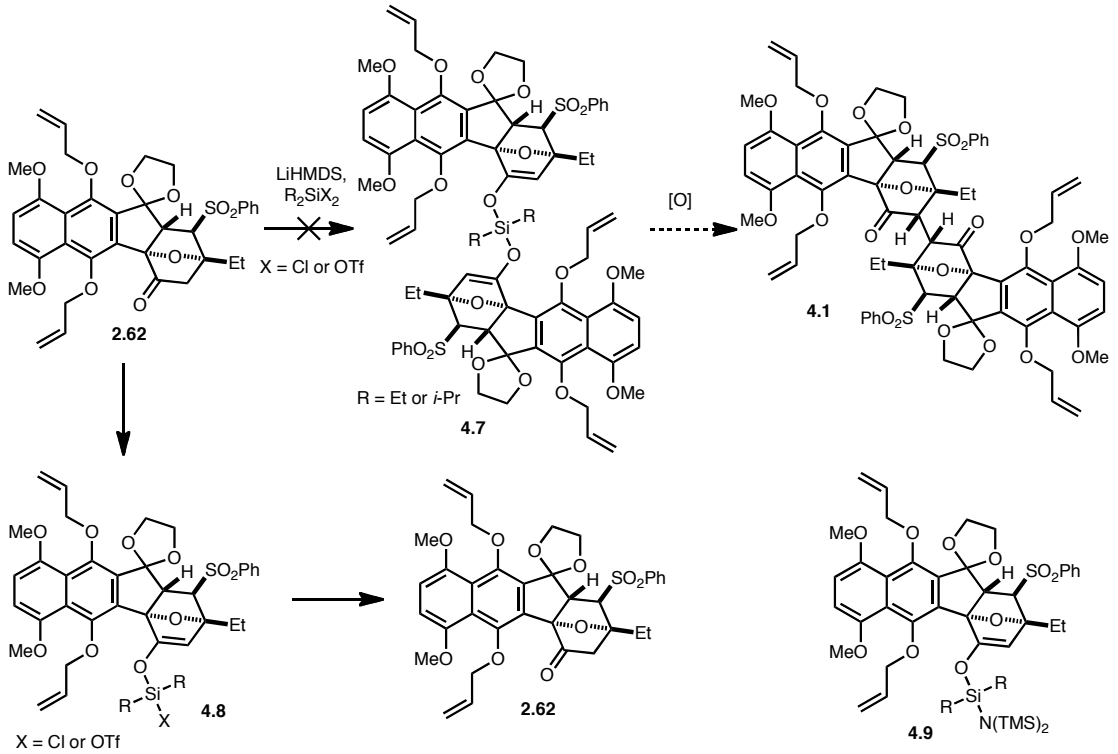

Since little is known about the exact mechanism of the dimerization, the destabilizing interactions developing during the dimerization cannot be analyzed. Instead, we tried to extrapolate the interactions in the potential products to the transition state (Figure 4.2).

Figure 4.2 Postulated destabilizing interactions in the transition state, reflected in the hypothetical product **4.1**.

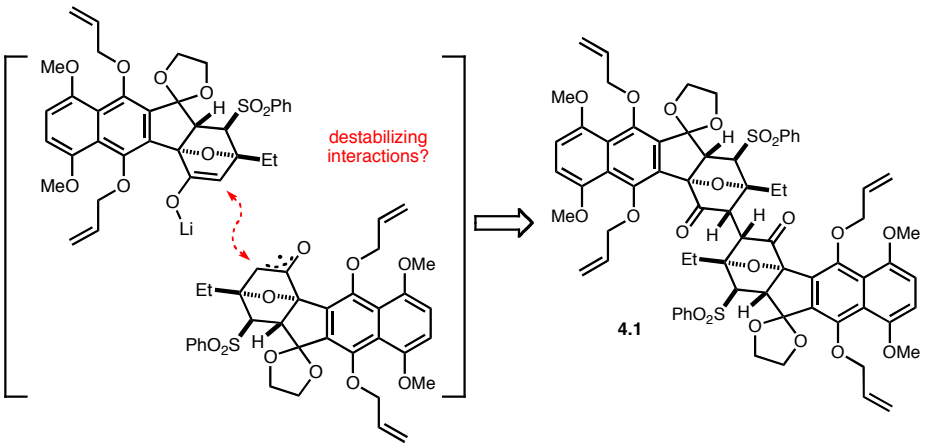

Potentially, three products, with one antiperiplanar and two gauche conformations regarding the H2C2C2'H2' dihedral angle, can be formed depending on the trajectory of the approaching reaction partners (Figure 4.3). In all cases unfavorable steric congestions were found.[2] The examined interactions are depicted as red arrows. In the case when the dihedral angle is 180 ° (antiperiplanar), a non-bonded interaction between the C3 ethyl group and the C3' ethyl group was observed (Entry 1). When the dihedral angle is 60 ° (gauche$^-$), interactions between the C11 allyloxy group and the C3' ethyl group, or between the C11' allyloxy and the C3 ethyl group, were observed (Entry 2). Finally the conformer with a −60 ° dihedral angle (gauche$^+$) suffered from severe steric repulsion between the C11 allyloxy group and the C11' allyloxy group (Entry 3).

---

(2) The analysis was made by simple hand-held plastic models.

Figure 4.3 Dihedral angle dependent steric congestions in the hypothetical dimerization product **4.1**.

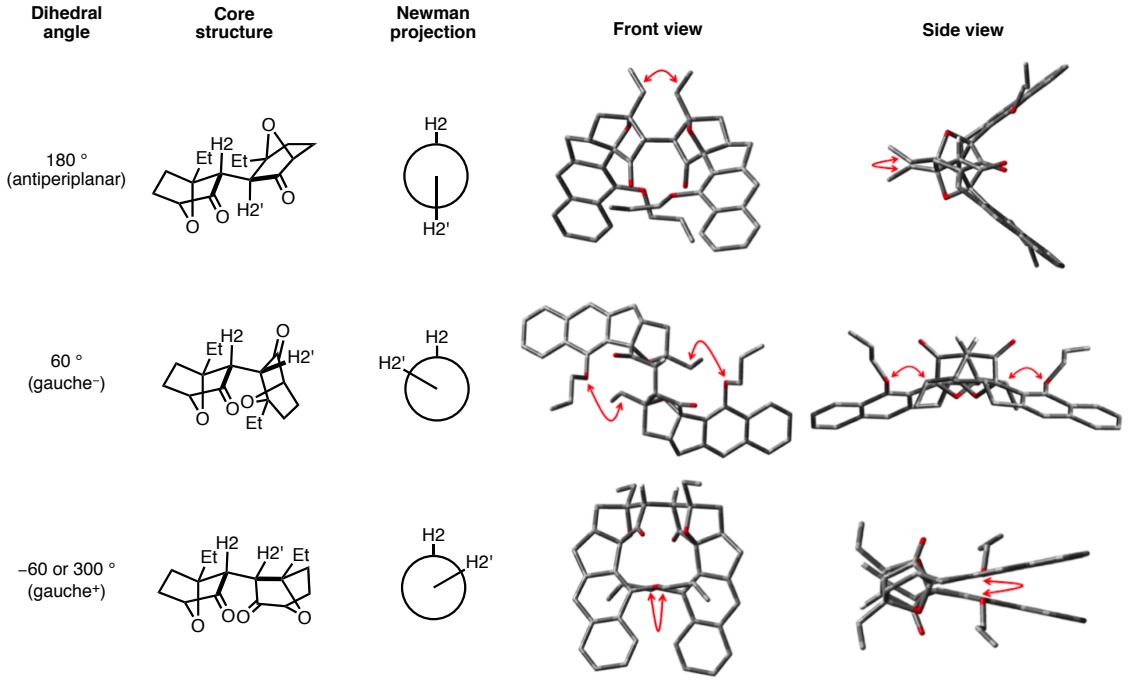

Based on these observations, it was concluded that the steric repulsion between the C3 ethyl group or the C11 allyloxy group with some other part of the other reaction partner is responsible for the unfavorable dimerization (Figure 4.4). Therefore, by reducing the size of the C11 substituent, the energy barrier to the dimerization would be lowered. Removing the C3 ethyl group was not a strategy of choice, since it is extremely hard to reintroduce at a later stage.

Figure 4.4 Steric congestions in the hypothetical dimerization product **4.1** arising from the C11 substituent.

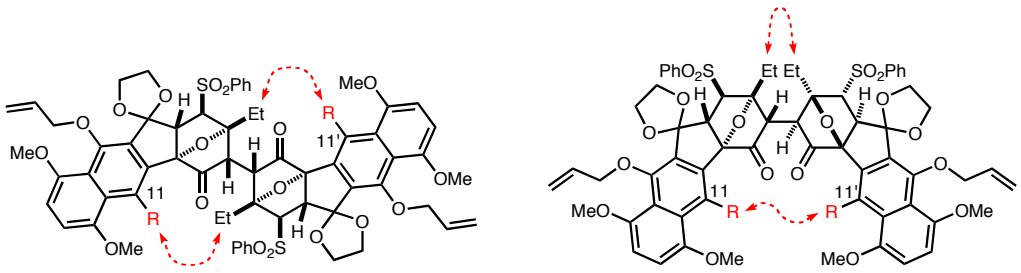

The hypothesis was quickly tested simply by changing the protecting group of the C11 hydroxyl group (Scheme 4.4). Previously prepared compound **2.60** was treated with NaHMDS in the presence of MeOTf to methylate both hydroxyl groups of the B-ring hydroquinone. Then the C1 ketone functionality was exposed by an established two-step sequence to give new dimerization precursor **4.10**. Ketone **4.10** was subjected to identical dimerization conditions. In contrast to the dimerization attempt of **2.62**, a small amount of quasi-stable product was isolated. Although clean magnetic resonance spectroscopic data was not acquirable due to rapid decomposition at room temperature, the compound had the correct molecular weight of the dimeric structure **4.11** based on high resolution mass spectroscopy.[3] The stark difference between the dimerization result of **2.62** (Scheme 4.1) and **4.10** (Scheme 4.4) suggested that the size of the C11 substituent indeed is related to the dimerization result, even though they are located remotely from the reacting center.

Scheme 4.4 Oxidative dimerization of ketone **4.10**.

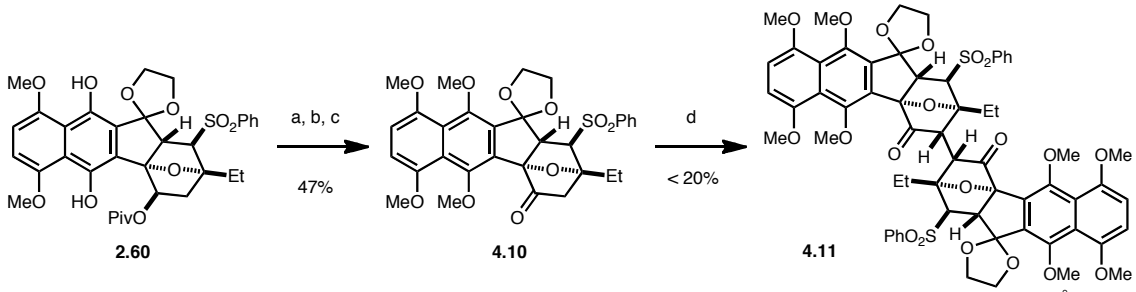

Reagents and conditions: (a) NaHMDS, MeOTf, THF, −78 °C; (b) $NaBHEt_3$, THF, 0 °C; (c) TPAP, NMO, 4 Å MS, CH_2Cl_2, 23 °C; (d) LiHMDS, HMPA, −78 °C; $[Cp_2Fe]PF_6$, −60 °C.

Although the desired dimerization was not realized with the previously established strategy, a new prerequisite for the reaction was suggested. Based on the

(3) Exact mass calculated for $C_{62}H_{62}NaO_{20}S_2$ $[(M+Na)^+]$: 1213.3168; found 1213.3160.

structural analysis of the potential products, non-bonded interactions of the C11 substituent were suspected to be the reason for inefficient dimerization. It was anticipated that by further reducing the size of the C11 substituent, we would be able to prepare the dimeric intermediate through oxidative enolate coupling.

4.2. Dimerization of Tetracyclic Precursor

Based on the findings discussed in the previous section, we decided to revise the synthetic plan (Figure 4.5). Most notably, it was decided to use tetracycle **4.13** as the new dimerization precursor. Compound **4.13** has a hydrogen atom, the smallest substituent possible, at the C11 position. Since the oxidation state of the B-ring is a phenol, an extra oxidation step would be required after dimerization in dimer **4.12**. Now the synthetic challenge is reduced to the preparation of the new dimerization precursor **4.13** from enone **2.42**.

Figure 4.5 Revised synthetic plan.

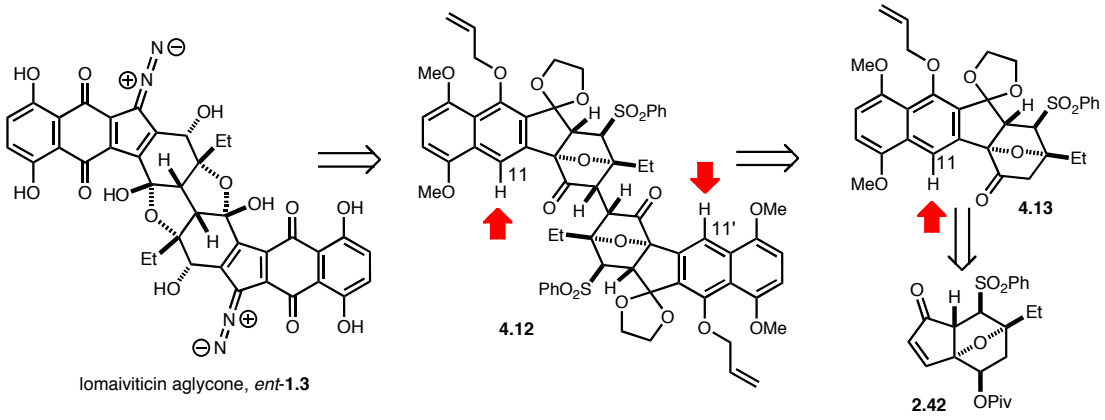

Among the various strategies available for this type of annulation, a protocol developed by Hauser was chosen (Figure 4.6).[4] In this reaction, the anion of sulfoxide **4.14** first undergoes conjugate addition to enone **4.15**, followed by Dieckmann condensation. After cyclization to form intermediate **4.17**, the cyclized product is heated to eliminate the sulfoxide and the newly formed ring tautomerizes to provide phenol **4.19**.

(4) Hauser, F. M.; Rhee, R. P., *J. Org. Chem.* **1978**, *43*, 178-180.

Figure 4.6 Hauser's sulfoxide annulation.

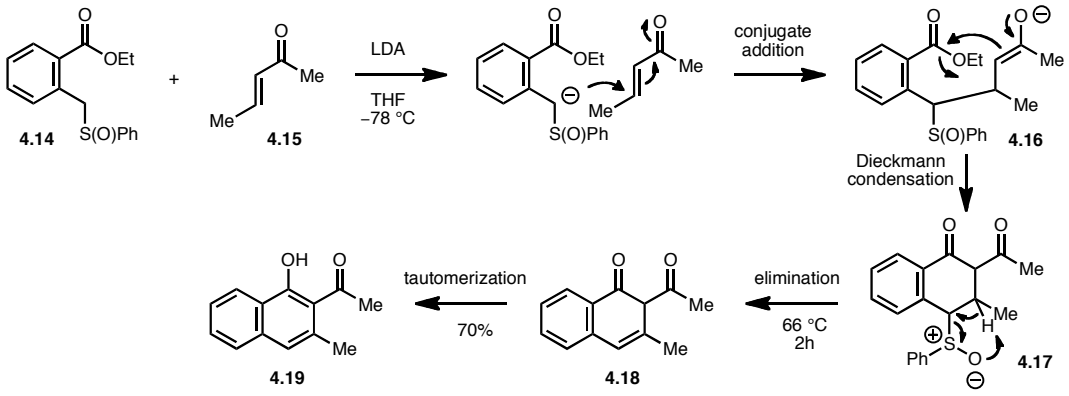

As a major modification to this strategy, we decided to use a phenyl ester instead of the conventionally used methyl or ethyl esters.[5] As is documented in the literature, the use of a phenyl ester greatly facilitates the Dieckmann condensation in a similar Michael/Dieckmann sequence (Figure 4.7).[6] The lower basicity of the phenoxide would make it a better leaving group. It was also expected that the phenoxide generated would not cause side reactions due to the lower nucleophilicity.

Figure 4.7 Myers' Michael/Dieckmann annulation using a phenyl ester.

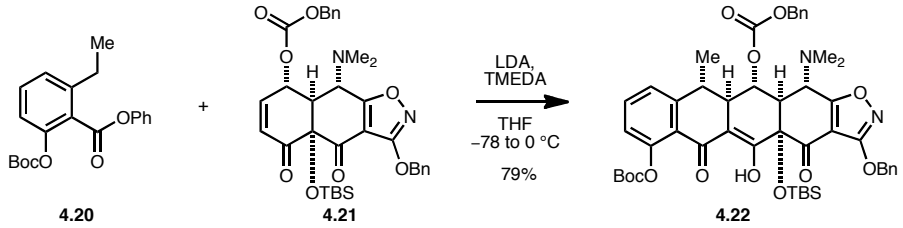

(5) White, J. D.; Nolen, E. G.; Miller, C. H., *J. Org. Chem.* **1986,** *51*, 1150-1152.

(6) For use of phenyl esters in related annulations, see: (a) Charest, M. G.; Lerner, C. D.; Brubaker, J. D.; Siegel, D. R.; Myers, A. G., *Science* **2005**, *308*, 395-398. (b) Sun, C.; Wang, Q.; Brubaker, J. D.; Wright, P. M.; Lerner, C. D.; Noson, K.; Charest, M.; Siegel, D. R.; Wang, Y.-M.; Myers, A. G., *J. Am. Chem. Soc.* **2008**, *130*, 17913-17927.

The desired sulfoxide annulation donor was prepared from commercially available 2,3-dimethyl hydroquinone (Scheme 4.5).[7] After protection of the acidic hydroxyl groups of the hydroquinone, one of the methyl groups was brominated under radical conditions. The resulting benzylic bromide was treated with $Ca(OH)_2$ in aqueous media to provide benzylic alcohol **4.24** in 61% yield over three steps. Alcohol **4.24** was oxidized to the corresponding acid **4.25** in a standard two-step protocol, then acid **4.25** was converted to the phenyl ester **4.26** through the intermediacy of an acid chloride. Another round of radical bromination provided another benzylic bromide. The bromide underwent a substitution reaction with NaSPh to provide a sulfide, which in turn was oxidized to the corresponding sulfoxide **4.27**. All procedures were amenable to scale, and up to 10 g of sulfoxide **4.27** was easily prepared from a single batch.

Scheme 4.5 Synthesis of sulfoxide **4.27**.

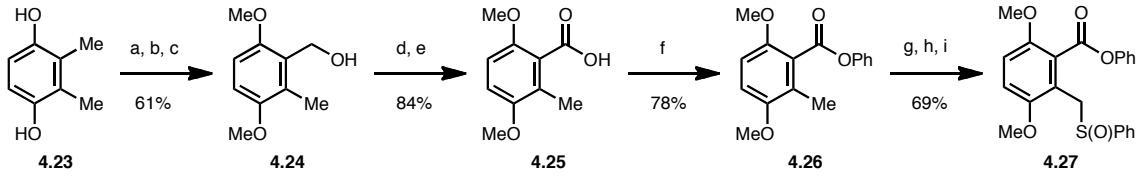

4.23 **4.24** **4.25** **4.26** **4.27**

Reagents and conditions: (a) Me_2SO_4, K_2CO_3, acetone, 57 °C; (b) NBS, AIBN, CCl_4, 77 °C; (c) $CaCO_3$, H_2O, dioxane, 50 °C; (d) TPAP, NMO, 4 Å MS, CH_2Cl_2, 23 °C; (e) $NaClO_2$, NaH_2PO_4, 2-methyl-2-butene, *t*-BuOH, H_2O, 23 °C; (f) $(COCl)_2$, DMF, benzene, 23 °C; then py, PhOH, CH_2Cl_2, 23 °C; (g) NBS, AIBN, CCl_4, 77 °C; (h) NaSPh, DMF, 0 °C; (i) $NaIO_4$, MeOH, H_2O, 23 °C.

The use of this annulation donor established a synthetic route to the desired tetracyclic intermediate **4.28**, which has the desired oxidation state in the B-ring (Scheme 4.6). Deprotonation of sulfoxide **4.27** with LiHMDS, followed by addtion of enone **2.42**, provided compound **4.28** in 90% yield.

---

(7) Mal, D.; Bandhyopadhyay, M.; Datta, K.; Murty, K. V. S. N., *Tetrahedron* **1998,** *54*, 7525-7538.

Scheme 4.6 Annulation of sulfoxide **4.27** and enone **2.42**.

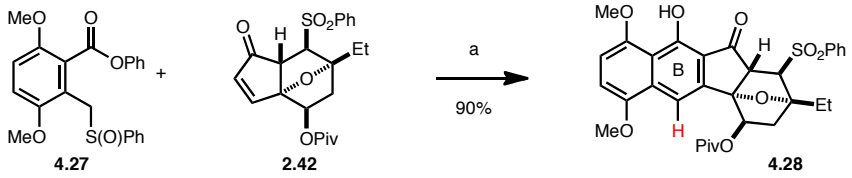

Reagents and conditions: (a) LiHMDS, **4.27**, THF, -60 °C; then **2.42**, −78 °C.

The optimization of the annulation reaction deserves further comment. First, full deprotonation of sulfoxide **4.27** was slow. Based on a deuterium quenching experiment, it takes no less than 6 hours at −60 °C to achieve greater than 95% deprotonation. Second, use of three equivalents of amide base was critical for the success of the annulation. As is described in Figure 4.8, the annulation occurs via different stages: 1) a condensation to form the ring, which generates a phenoxide; 2) elimination of the phenylsulfanol, which usually requires heating. The use of the phenyl ester, however, facilitated both of these steps, and both reactions took place even at −78 °C. Therefore two sources of acidic protons, phenol and phenylsulphanol, are generated before the end of the reaction, which might potentially quench the anionic annulation donor or related anionic intermediates (Figure 4.8). By using two extra equivalents of base, the acidic species are quenched before the full consumption of the annulation donor. By using a total of 3 equivalents of amide base, tetracyclic product **4.28** was obtained in high yield.

Figure 4.8 Optimization of sulfoxide annulation.

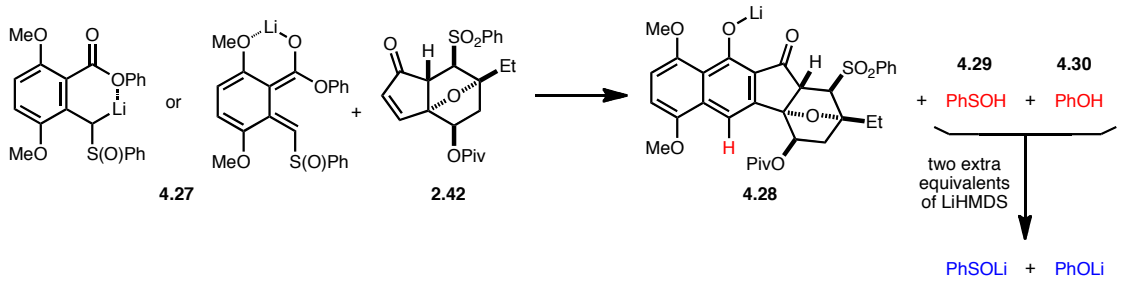

The tetracycle **4.28** was advanced to the targeted new dimerization precursor in four steps (Scheme 4.7). A sequence of reactions used to prepare dimerization precursor **2.62** was identically applied.[8] First the C5 ketone was masked as a dioxolane to give compound **4.29**. During the reaction 5-10% of orthoester byproduct **4.32** was detected. It is believed that the reaction takes place through a retro-Claisen reaction of initially formed product **4.29**, which is initiated by protonation with TfOH, followed by oxocarbenium ion trapping. It is believed that TfOH is generated by reaction of TMSOTf with water. Therefore rigorously anhydrous conditions were required to maximize the yield. The protected tetracycle was then alkylated to give allyl ether **4.33**. Unfortunately, the reaction was contaminated with formation of the C11 allylation product **4.34**. After

Scheme 4.7 Synthesis of dimerization precursor **4.13**.

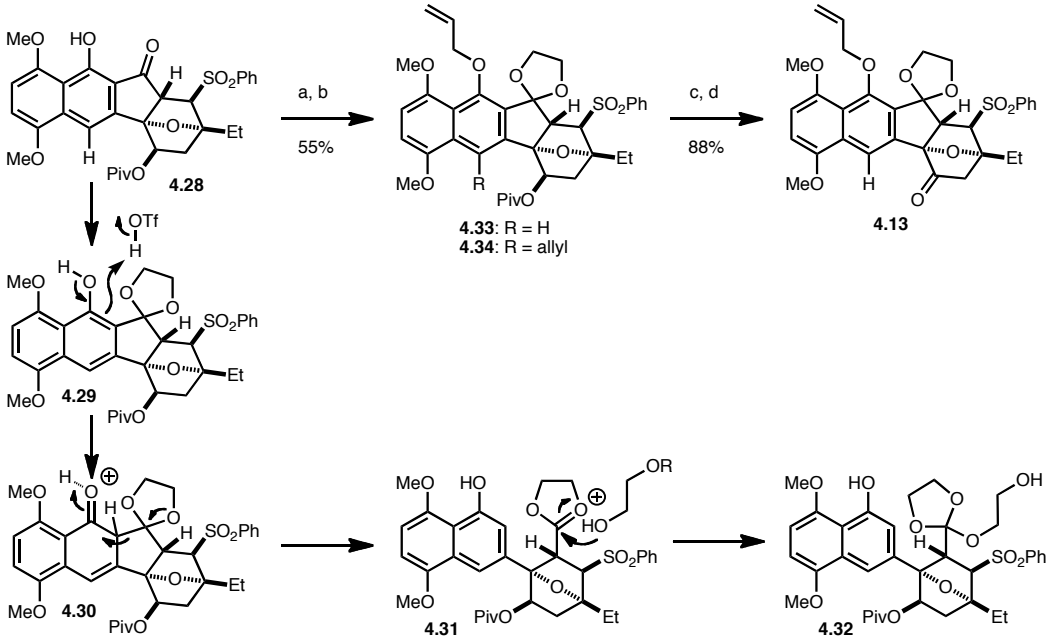

Reagents and conditions: (a) 1,2-Bis(trimethylsilyloxy)ethane, TMSOTf, CH_2Cl_2, 23 °C; (b) Allyl bromide, Cs_2CO_3, DMF, 23 °C; (c) $NaBHEt_3$, THF, 0 °C; (d) TPAP, NMO, 4 Å MS, CH_2Cl_2, 23 °C.

(8) See Scheme 2.18 and 2.19.

full protection, the pivalate ester was converted to the ketone uneventfully to provide the new dimerization precursor **4.13**.

As we anticipated, oxanorbornanone **4.13** underwent smooth dimerization (Scheme 4.8).[9] In the initial attempt, less than 20% of symmetric dimer **4.12** was isolated from a 0.02 M solution of **4.13** in 16 hours. Since the reaction is a bimolecular reaction, an increase in concentration should enhance the conversion. 0.06 or 0.07 M solution provided the product in a synthetically useful yield in three to four days. Due to problems with solubility, it was not possible to increase the concentration further. The dimerization reaction was reasonably scalable and reproducible. During the course of future studies more than 9 g of dimer **4.12** was prepared in several different batches.

Scheme 4.8 Oxidative enolate dimerization of oxanorbornanone **4.13**.

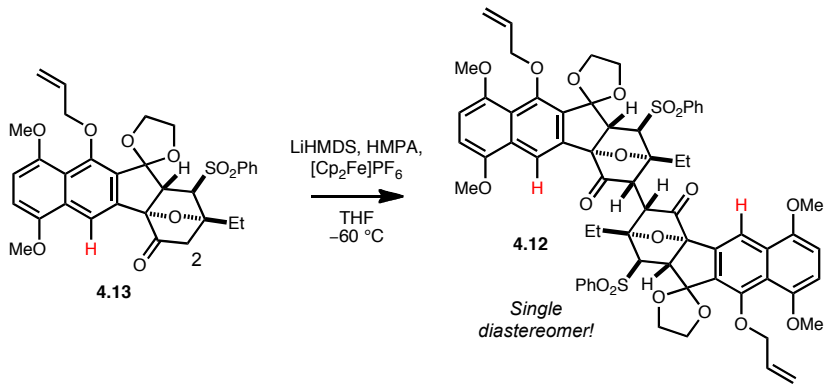

Time (h)	Concentration (mol/L)	Yield (%)
16	0.02	less than 20
72	0.06	60
84	0.06	71
96	0.07	80

(9) Lee, H. G.; Ahn, J. Y.; Lee, A. S.; Shair, M. D., *Chem.–Eur. J.* **2010**, *16*, 13058-13062.

The product was isolated as a single diastereomer and the orientation of the C2–C2' connectivity was unambiguously assigned by nOe study (Figure 4.9). The proton at the C2 position showed a strong nOe cross peak with the $C4_a$ proton, a phenomenon which is possible only when the connectivity is *exo* (Figure 4.9a). An *endo* connectivity could not provide such an nOe correlation (Figure 4.9b).

Figure 4.9 Stereochemistry of C2–C2' bond.

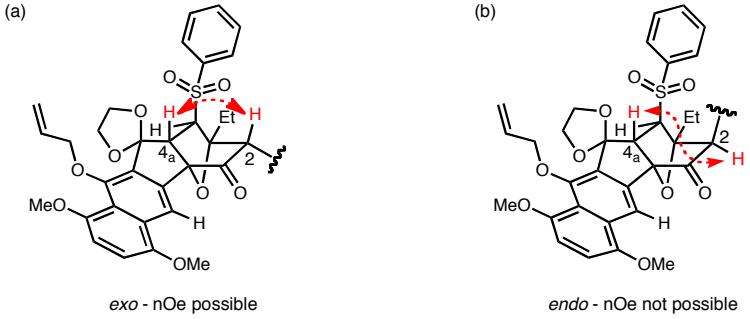

The oxanorbornane structure is not soley responsible for the great stereochemical outcome of the dimerization. Amy Lee, a coworker in this project, attempted a similar dimerization with a substrate having a substituent at C4 with the opposite relative stereochemistry (Figure 4.10).[10] The dimerization precursor provided only *exo-endo* product in 44% yield. No *exo-exo* dimer was detected. It is believed that the bulky phenyl

Figure 4.10 Effect of C4 stereochemistry in the diastereoselectivity of the dimerization.

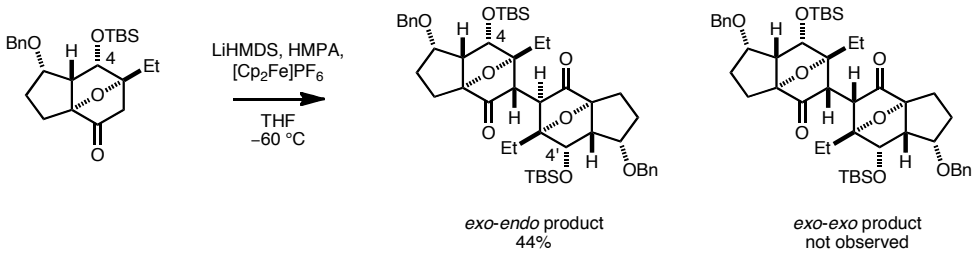

(10) Lee, A. S., Unpublished result, Harvard University, Cambridge, MA.

sulfonyl group in **4.13**, with an A-value of 2.5, reinforces the *exo*-*exo* selectivity of the reaction.

4.3. X-Ray Crystal Structure of the Dimer.

Although the full connectivity and stereochemistry of the symmetric dimer **4.12** could be elucidated by using solution state spectroscopic methods, no information regarding the relative orientation of each half is known. To investigate this area a single crystal X-ray structure of the dimer was obtained. Simply by removing the flexible allyl protecting group, the dimeric product **4.35** was obtained as a crystalline solid (Scheme 4.9).[11]

Scheme 4.9 Removal of allyl protecting group in dimer **4.12**.

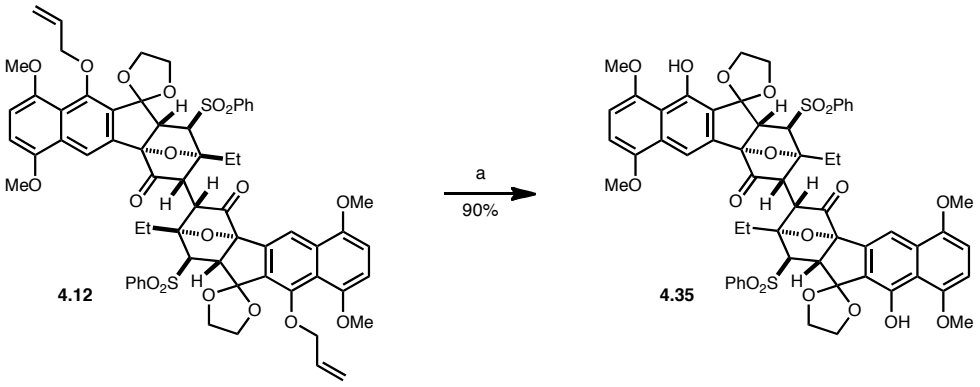

Reagents and conditions: (a) $PdCl_2(PPh_3)_2$, Bu_3SnH, AcOH, CH_2Cl_2, 0 °C.

The crystal structure of **4.35** is shown in Figure 4.11. All the relative

Figure 4.11 X-ray crystal structure of dimer **4.35**.

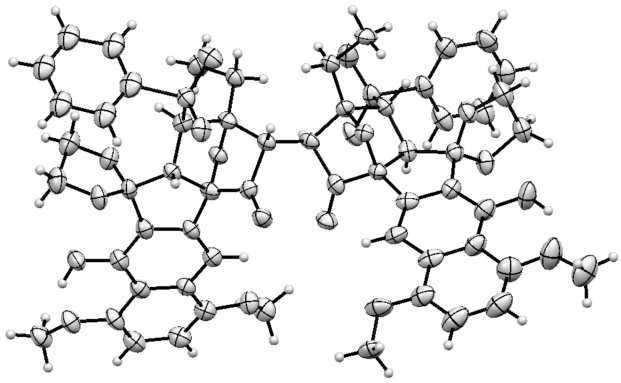

stereochemistry of the molecule confirmed the results gained from the NMR data, assuring the correct C2–C2' connectivity. Interestingly, the molecule possesses a conformation where the two naphthyl rings are oriented in the same direction.

The crystal structure revealed that the C11 hydrogen atom is in close proximity to the C1' ketone oxygen atom (and conversely the C11' hydrogen and C1 ketone oxygen). In fact the interatomic distance between H11 and O1' is 3.01 Å, only 0.29 Å greater than the sum of their van der Waals radii (Figure 4.12). The close contact between the C11 substituent and O1' may explain why the first dimerization with the C11 allyloxy group failed (Scheme 4.1). If the precursor with a C11 allyloxy group had dimerized, it would have suffered a non bonded interaction with O1'.

Figure 4.12 Interatomic distance between the C11 hydrogen atom and the C1' oxygen atom.

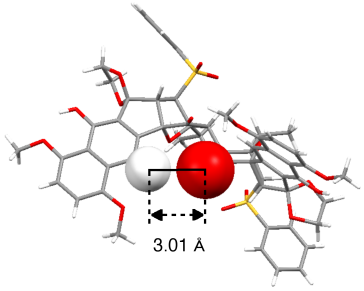

Closer inspection of the crystal structure showed that the dihedral angle for H2C2C2'H2' is 142 ° (Figure 4.13). It is a structure that closely resembles the postulated structure with the 180 ° dihedral angle discussed in Figure 4.3. It seems that the distorted H2C2C2'H2' dihedral angle is the result of alleviating non-bonded interactions in two different ways. A dihedral angle greater than 142 ° would result steric repulsion between the two ethyl groups, as in the structure with the 180 ° dihedral angle. And a smaller dihedral angle than 142 ° would put H11 and O1' (and H11' and O1) in close proximity,,

generating contact between these two atoms, an interaction discussed in Figure 4.12. Therefore the central dihedral angle is locked in 142 °, which balances these two interactions. Also the naphthyl rings of the dimer are highly distorted (see the side view of Figure 4.13), which suggests existence of additional repulsion between substituents of the two naphthyl rings.

Figure 4.13 H2C2C2'H2' dihedral angle of dimer **4.35**.

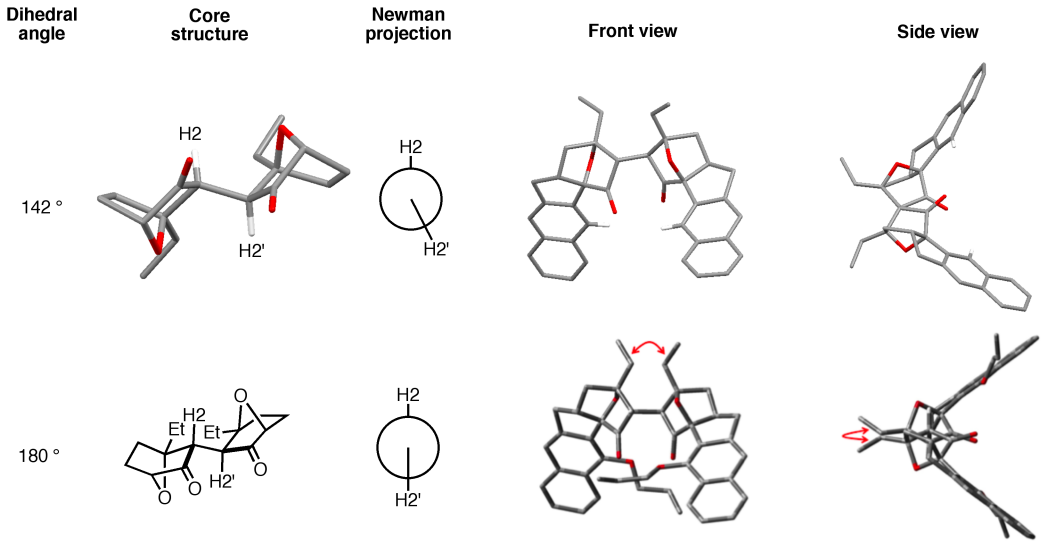

The presence of C2–C2' torsional strain in **4.35** and the potential for severe non-bonded interactions in the crystal structure suggested to us that there may be a measurable barrier to rotation about the C2–C2' bond, resulting in atropisomerism.[12] Unfortunately, heating to 140 °C or cooling to –80 °C did not result in a change in the ^{1}H NMR spectrum of **4.35**, preventing us from determining whether dimer **4.35** exhibits atropisomerism.

(12) Oki, M., "Topics in Stereochemistry"; John Wiley & Sons: New York, 1983; Vol. 14, pp. 1-81.

If there is a significant barrier to rotation, it can be speculated that the two reaction partners are approaching each other near 180 ° H2C2C2'H2' dihedral angle, or in between a 120 ° and 240 ° dihedral angle range. Then the product thus formed does not undergo further rotation through C2–C2' bond and stays with 142 ° dihedral angle, which accompanies distortion of other parts of the molecule. It is not clear why other modes of approach, such as dimerization in 0-120 ° or 240-360 ° range, are not observed.

In summary, successful formation of the targeted dimeric structure **4.12** was achieved (Figure 4.14). The desired annulation precursor **4.13** was prepared by using a modified Hauser annulation of sulfoxide **4.27** and enonoe **2.42**. Key to the success was control of a non-obvious remote steric effect of the C11 substituent, as well as careful control of temperature to avoid side reactions. The X-ray crystal structure of the dimer has revealed that the interaction between the C11 substituent and the C1' carbonyl

Figure 4.14 Summary of chapter 4.

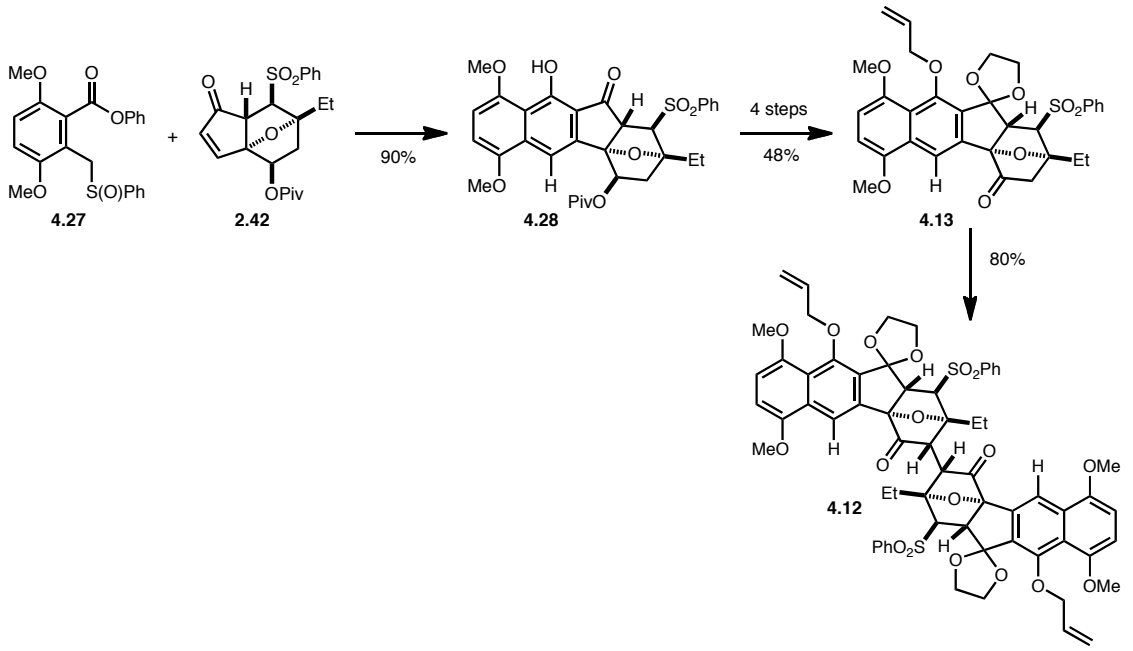

oxygen atom may be responsible for the unsuccessful dimerization when the C11 substituent was larger than a hydrogen atom.

Chapter 5

Attempted Completion of the Synthesis

5.1. Introduction of the C4 Hydroxyl Group

In chapter 4, the successful oxidative dimerization reaction to form the full carbon skeleton of the lomaiviticin aglycone was discussed.[1] With the dimer in hand, the focus of research shifted to finishing the synthesis of the lomaiviticin aglycone.

Figure 5.1 describes plans for the rest of the synthesis. First a ketal protecting group of dimer **4.12** at C5 would be removed to expose a handle for the key oxygen-bridge opening in the oxanorbornanone D-ring (**5.1**). With the handle in place, a cascade reaction discussed in section 1.4 would be investigated in the real system (**5.1** to **5.4**).[2] The reaction involves an elimination to cleave $C11_b$–O bond (**5.1** to **5.2**) and displacement of allylic sulfone at the C4 position with an oxygen nucleophile (**5.2** to **5.3**). It is expected that the initially formed product **5.3** would exist as a bishemiketal (**5.4**) as in the natural product lomaiviticin B. The next step would be removal of the allyl protecting group and subsequent introduction of hydrazone functionality at the C5 position (**5.5**). As was observed in previous studies, removal of B-ring protecting group is

---

(1) Lee, H. G.; Ahn, J. Y.; Lee, A. S.; Shair, M. D., *Chem.–Eur. J.* **2010**, *16*, 13058-13062.

(2) Krygowski, E. S.; Murphy-Benenato, K.; Shair, M. D., *Angew. Chem. Int. Ed.* **2008**, *47*, 1680-1684.

crucial for the successful introduction of a nucleophile at the C5 position.[3] Next, a global oxidation of B and B' rings, as well as the C5 and C5' hydrazones would provide protected the lomaiviticin aglycone (not shown). The selective oxidation of an unprotected phenol in the presence of a proximal alkylated hydroquinone is well documented in the literature.[4] It should be noted that the transformation works even in the presence of an electron-withdrawing group attached to the phenol ring; therefore the

Figure 5.1 Synthetic plans to complete synthesis of the lomaiviticin aglycone.

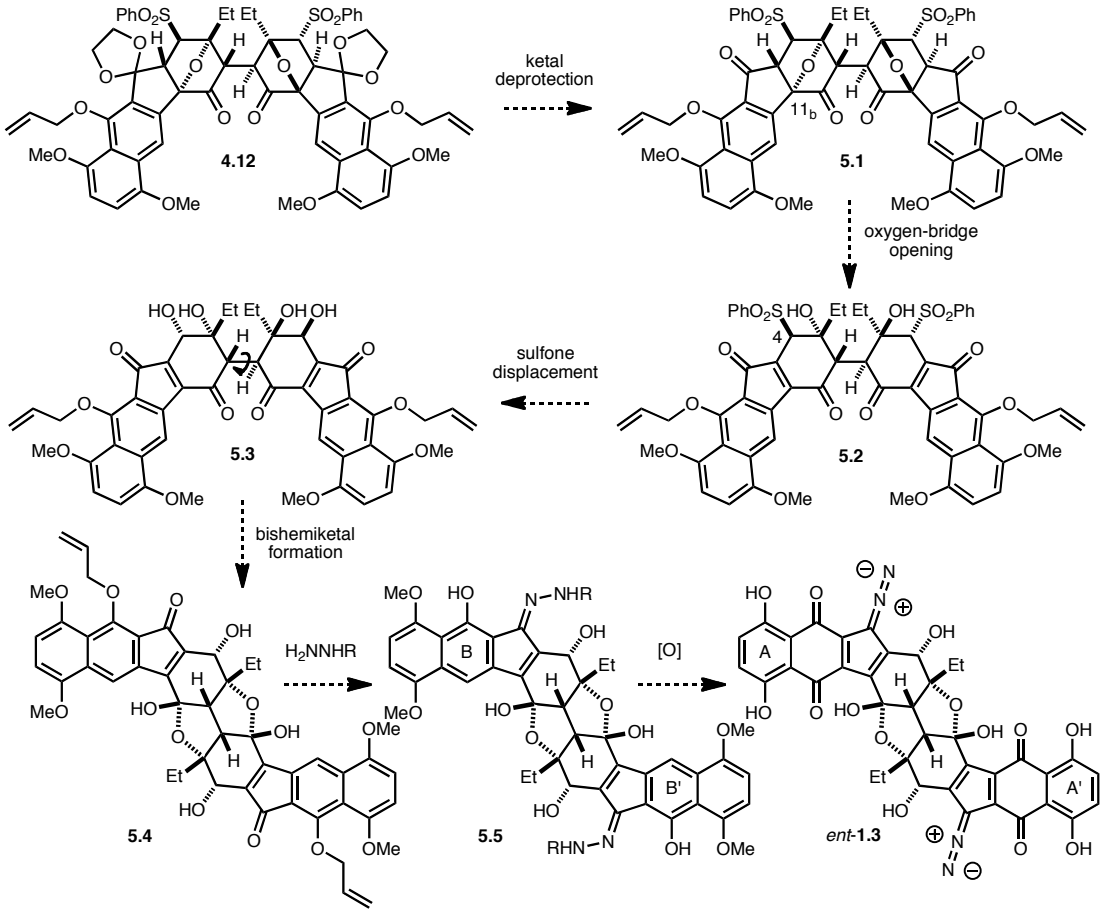

(3) See Scheme 2.18.

(4) (a) Magnus, P.; Eisenbeis, S. A.; Fairhurst, R. A.; Iliadis, T.; Magnus, N. A.; Parry, D., *J. Am. Chem. Soc.* **1997**, *119*, 5591-5605. (b) Couladouros, E. A.; Strongilos, A. T., *Eur. J. Org. Chem.* **2002**, *2002*, 3341-3350.

presence of C5 hydrazone, a partly electron donating group, should not be problematic. Finally, nucleophilic removal of the methyl protecting groups in the A-ring would provide the aglycone of the natural product.

Although this plan looked straightforward, we had contingency plans to deal with unpredicted reactivities of the intermediates. As was observed in the model study, the central 1,4-diketone system may form a cyclic hydrate as in **1.104** when a ketone functionality is exposed at C5 position. Although, the model core **1.104** underwent the desired cascade reaction to provide **1.106**, attempts to isomerize the product to the lomaiviticin B core **5.6** failed under acidic conditions (Figure 5.2).

Figure 5.2 Attempted isomerization of model core.

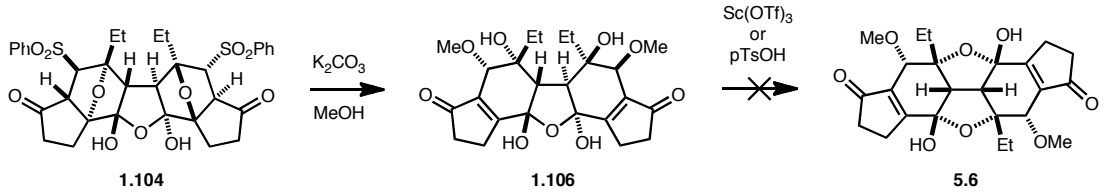

In the real synthesis, however, we expected that the naphthoquinone AB-rings could facilitate the isomerization (Figure 5.3). It was believed that the cyclic hydrate **5.7** would undergo identical cascade reactions to provide compound **5.8**, which may be reluctant to liberate water to form a bishemiketal such as **5.4**. However, if the B-ring phenol is oxidized to a quinone, the core pocket would not be spacious enough to accommodate two extra oxygen atoms, inferred from the crystal structure of the dimer (Figure 4.12). Therefore, it was believed that bisquinone **5.10** would be forced to lose a central water molecule and undergo bishemiketal formation. Further oxidation and removal of methyl protecting groups would provide lomaiviticin aglycone *ent*-**1.3**.

Figure 5.3 Alternative plans to complete synthesis of lomaiviticin aglycone.

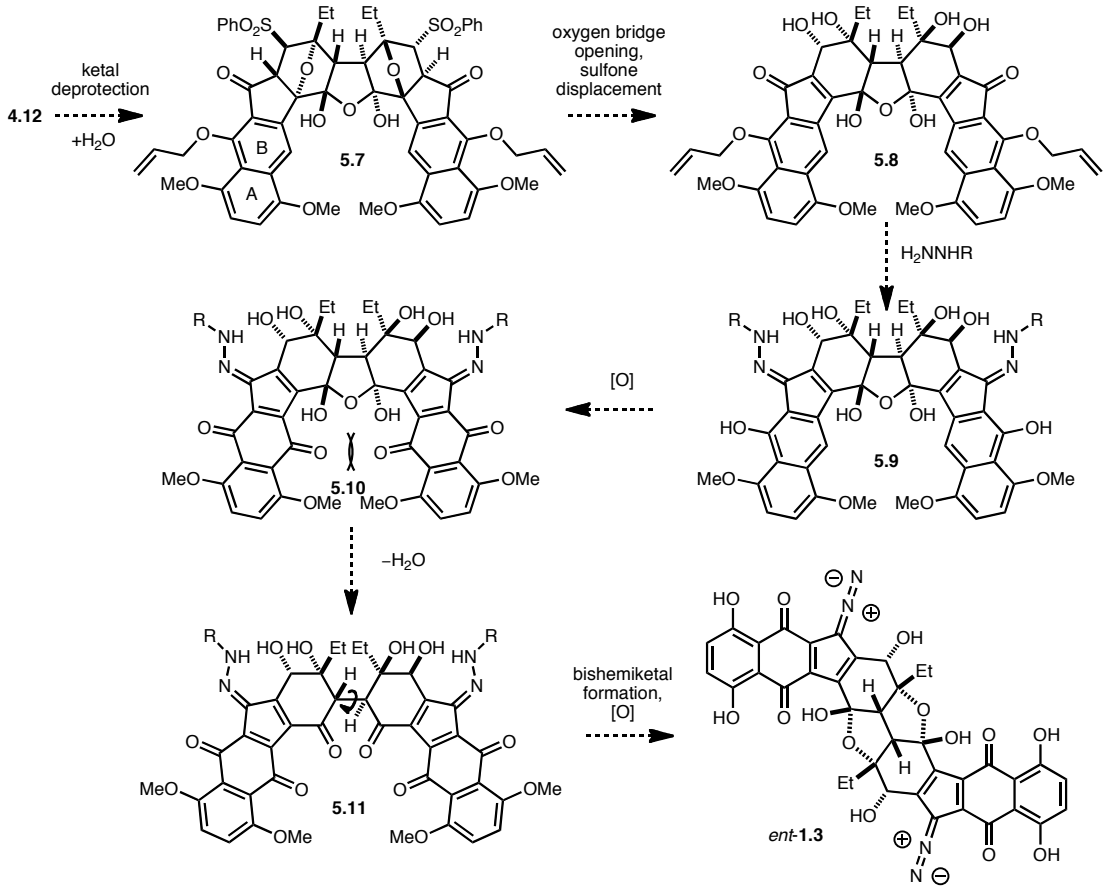

The original strategy for the oxygen bridge-opening relied on the donation of electron density from the $C4_a$ position (Figure 5.4). Either the C5–$C4_a$ enolate (**5.13**) or the C4–$C4_a$ enolate (**5.14**) may facilitate such a transformation, although the C5–$C4_a$

Figure 5.4 $C4_a$-assisted oxygen-bridge opening.

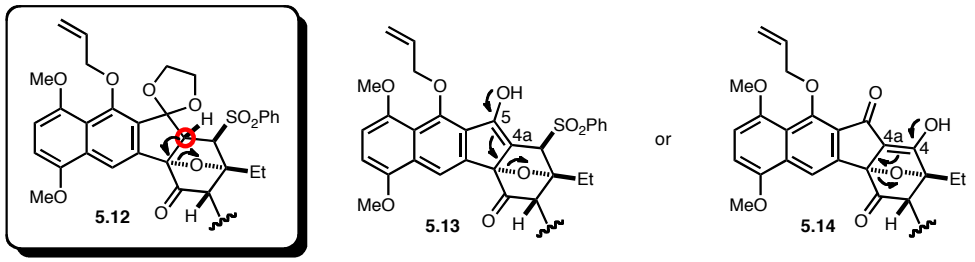

enolate is a better candidate due to greater orbital overlap.[5] Therefore, a strategy involving the C5–$C4_a$ enolate was tested initially.

As a prelude to enolate formation, C5 ketone was revealed by removal of the dioxolane protecting group (Scheme 5.1). Treatment of dimer **4.12** with TfOH in acetone/water released ethylene glycol, exposing two ketone functionalities at C5 and C5' in 78% yield. As was expected, the product exists as a stable cyclic hydrate **5.7**. Unfortunately, ketone **5.7** did not undergo the desired cascade reaction. Investigation of a large number of bases in protic solvent (e.g., MeOH, EtOH, *t*-BuOH, or water) only resulted in slow decomposition of the starting material. Stronger bases such as LDA, LiHMDS, KO*t*-Bu, or KO*t*-Pn, in THF decomposed **5.7** even more quickly.

Scheme 5.1 Attempted oxygen-bridge opening of **5.7**.

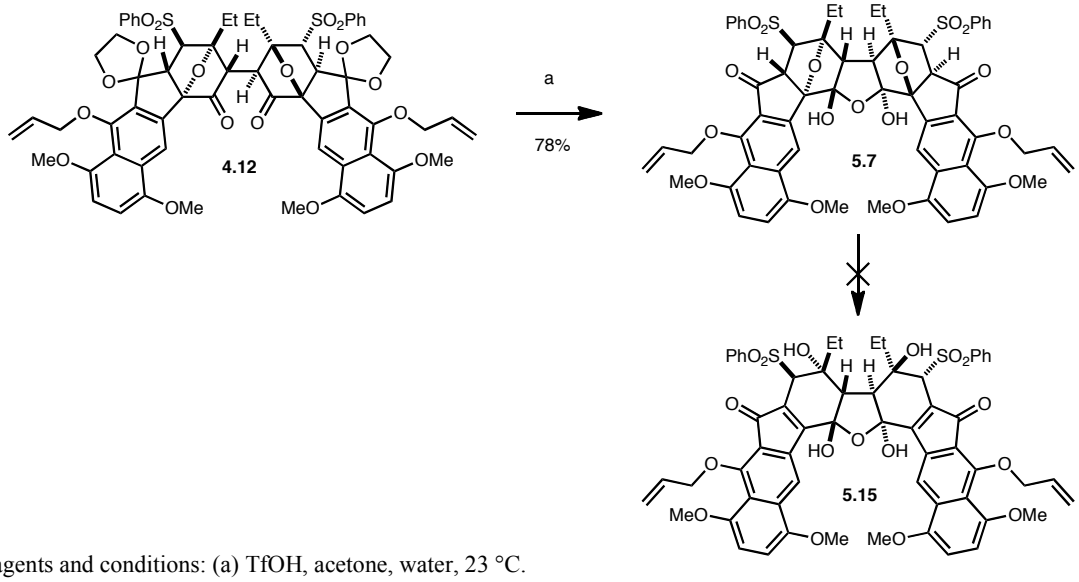

Reagents and conditions: (a) TfOH, acetone, water, 23 °C.

(5) (a) McMorris, T. C.; Staake, M. D.; Kelner, M. J., *J. Org. Chem.* **2004**, *69*, 619-623. (b) Jung, M. E.; Min, S.-J., *Tetrahedron* **2007**, *63*, 3682-3701.

The pathway of decomposition is not clear, since no characterizable compound was isolated in the reaction (Figure 5.5). The decomposition may arise from dehydration across the C1, C1' ketone **5.1** under basic conditions. Or we cannot exclude the possibility that the desired product **5.15** underwent decomposition. An antiaromatic indenone product **5.15** may be in equilibrium with the starting material through reclosure and may undergo unwanted nucleophilic attack under the reaction conditions.

Figure 5.5 Possible decomposition pathway of **5.7**.

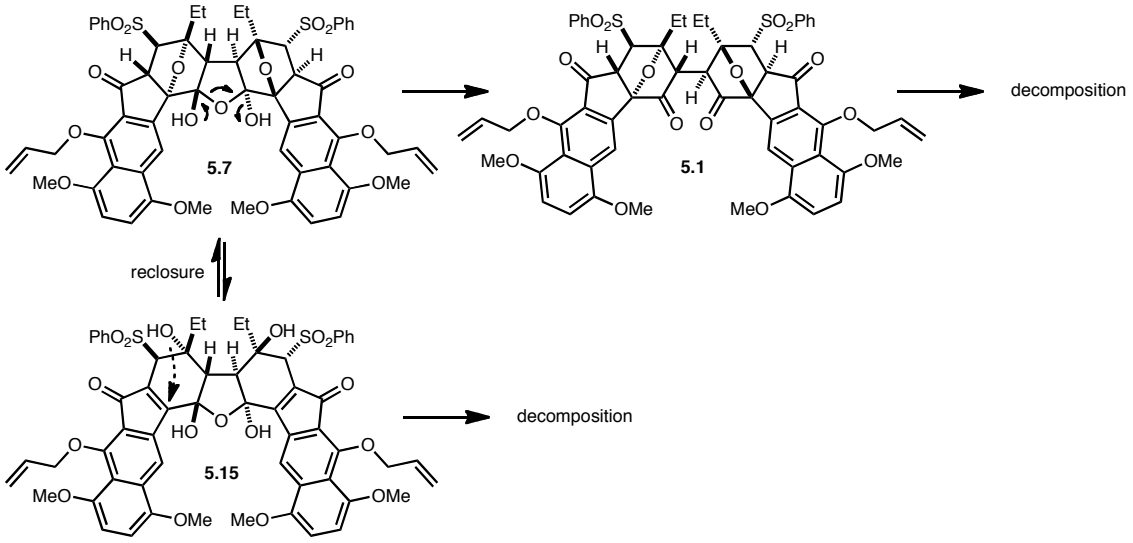

In order to test the first hypothesis, we decided to protect the central cyclic hydrate in a base-tolerant form. Of the numerous conditions used, MeOTf/NaHMDS combination worked best (Scheme 5.2). When the THF solution of NaHMDS is added to the cold premixed solution of **5.7** and MeOTf, the two hydroxyl groups of the cyclic hydrate were cleanly masked as methyl ethers. Methyl ether **5.16** was much more tolerant to basic conditions. However, the reactivity pattern was completely different from that of the model system. When **5.16** was treated with KOH in aqueous THF solution, β-hydroxy

ketone **5.17** was isolated as a major product together with two other diastereomers.[6] **5.17** contained (4*R*, 4'*R*) configuration and the structure was unequivocally assigned by X-ray crystallography.

Scheme 5.2 Sulfone displacement of dimer **5.16**.

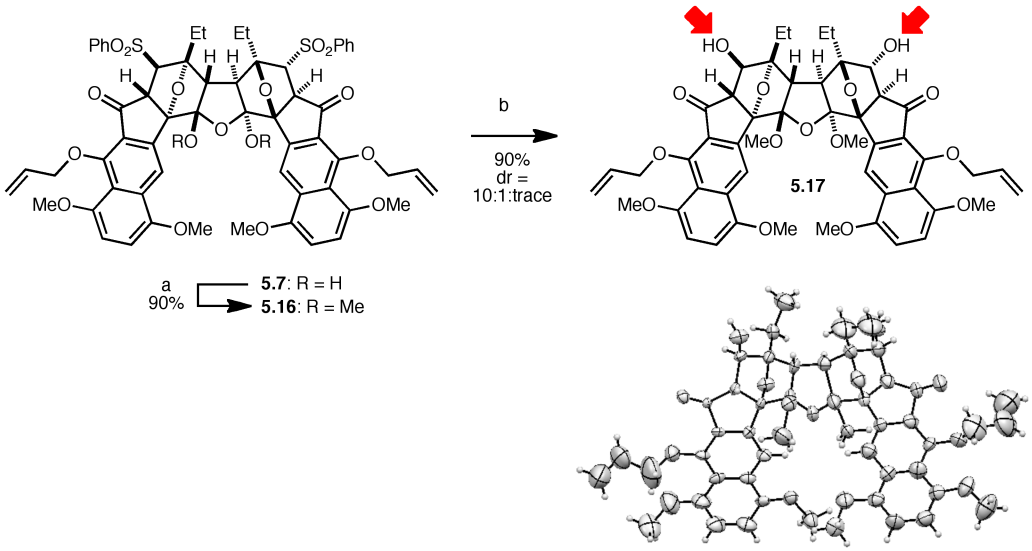

Reagents and conditions: (a) MeOTf, NaHMDS, THF, −78 °C; (b) KOH, H_2O, THF, 23 °C.

The suspected reaction pathway is described in Figure 5.6. First, ketone **5.16** underwent enolate formation to give **5.18** under the given reaction conditions. The potassium enolate **5.18** did not undergo desired oxygen bridge opening to form **5.19**. Instead, the C4 sulfone at another β position was eliminated to form enone intermediate **5.20**, followed by hydroxide addition across the *Re* (convex) face to the β-hydroxy ketone **5.17**. Obviously, the mode of hydroxide attack was governed by the overall concavity of the molecule, rather than the local predisposition of the oxanorbornane ring.

(6) The minor diastereomers were assigned to be unsymmetric (4*R*, 4'*S*)-diastereomer and symmetric (4*S*, 4'*S*)-diastereomer.

Figure 5.6 Proposed mechanism for formation of **5.17**.

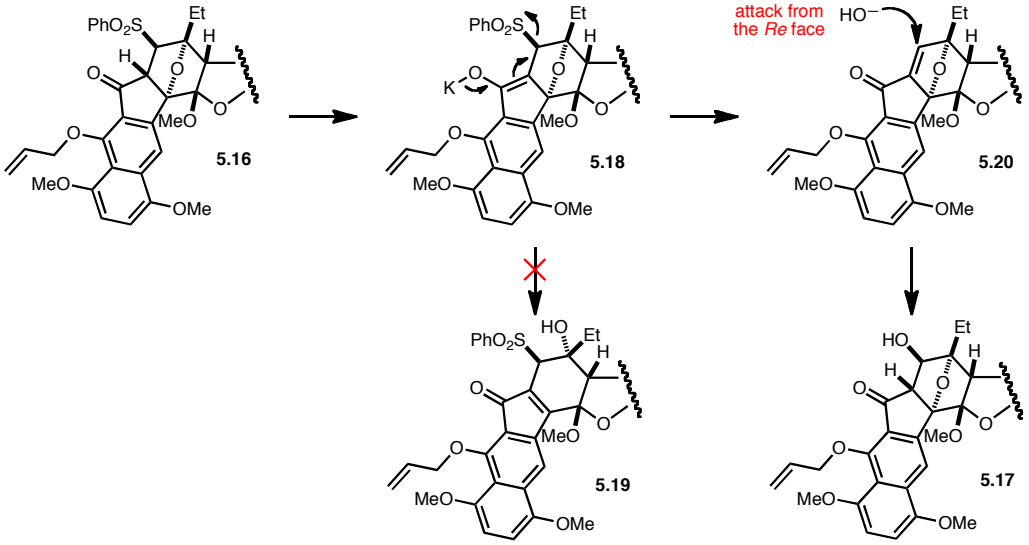

This scenario was partially supported by an independent synthesis of enone **5.20** (Scheme 5.3). Enone **5.20**, prepared from a mesylation/elimination sequence from β-hydroxy ketone **5.17**, regenerated **5.17** under the identical reaction conditions.

Scheme 5.3 Independent synthesis of enone **5.19**.

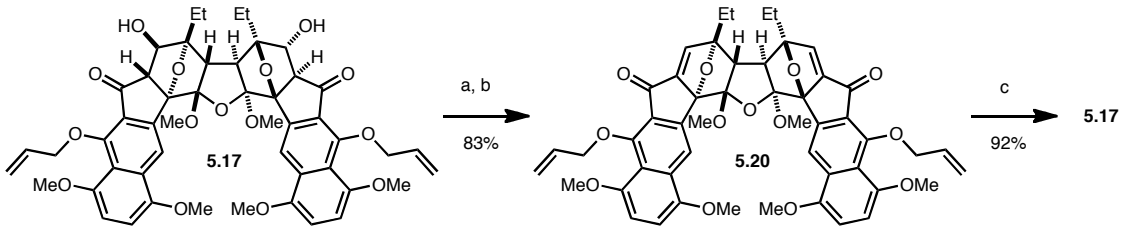

Reagents and conditions: (a) MsCl, Et_3N, CH_2Cl_2, 0 °C; (b) K_2CO_3, THF, H_2O, 0 °C; (c) KOH, THF, H_2O, 23 °C.

Although the desired $C11_b$–O bond scission was not realized at this stage, β-hydroxy ketone **5.17** was a useful intermediate in that the C4 hydroxyl group was introduced in a stereoselective manner. Therefore, compound **5.17** was used as the starting point of all remaining strategies for the rest of the investigation.

β-Hydroxyketone **5.17** did not undergo further oxygen-bridge opening (Scheme 5.4); **5.17** was highly stable under a variety of basic conditions and only decomposition was observed under forcing conditions. Even 1,3-diketone **5.22**, an oxidation product of **5.17**, did not undergo this transformation. The fact that the system did not eliminate oxygen substituent suggested inherent innertness of the system, possibly originating from the antiaromatic character of the potential product. Therefore, a strategy that does not involve formation of antiaromatic intermediate was sought in the future.

Scheme 5.4 Attempted oxygen bridge opening of **5.17**.

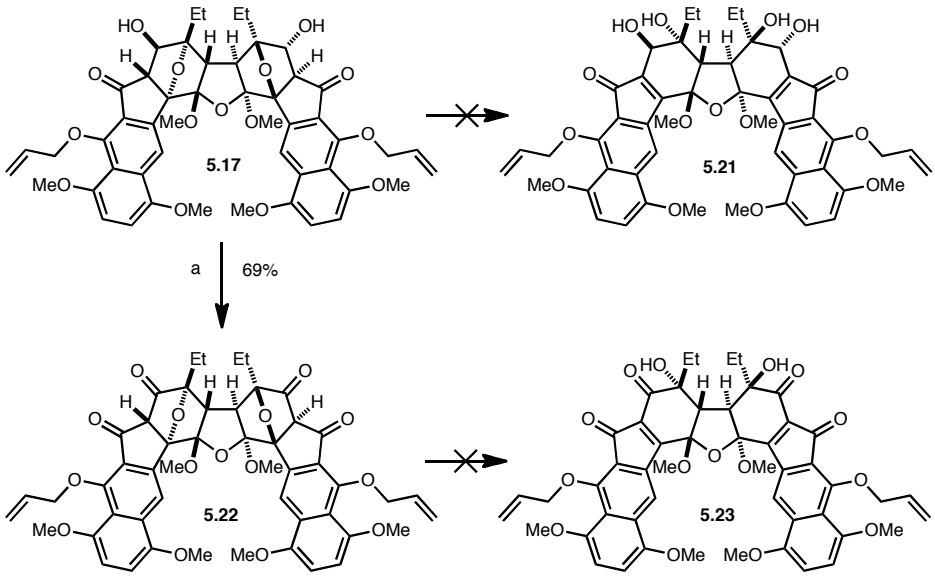

Reagents and conditions: (a) $(COCl)_2$, DMSO, CH_2Cl_2, −78 °C; then DIEA, 23 °C.

5.2. Reductive Approaches to C11$_b$–O Bond Cleavage

After encountering unexpected reactivity that disfavor the desired cascade reaction, alternative approaches were sought. The first approach involves donation of electron density from the C1 carbon (Figure 5.7). One-electron reduction of the C1 ketone would generate a ketyl radical species at the C1 position (**5.25**), which can undergo a ring-opening reaction to provide the lomaiviticin D-ring structure.[7]

Figure 5.7 Oxygen bridge opening assisted from C1.

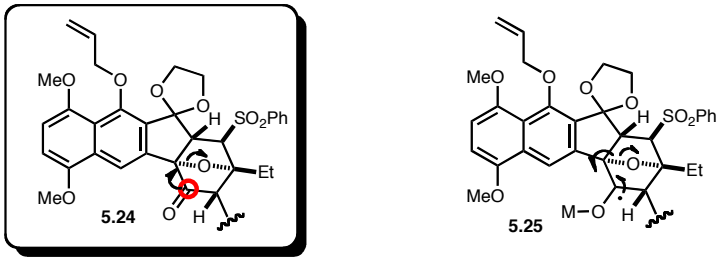

The revised overall synthetic plan is summarized in Figure 5.8. Reduction of both C1 and C1' ketone would provide lomaiviticin D and D' ring structure as compound

Figure 5.8 Revised synthetic plan.

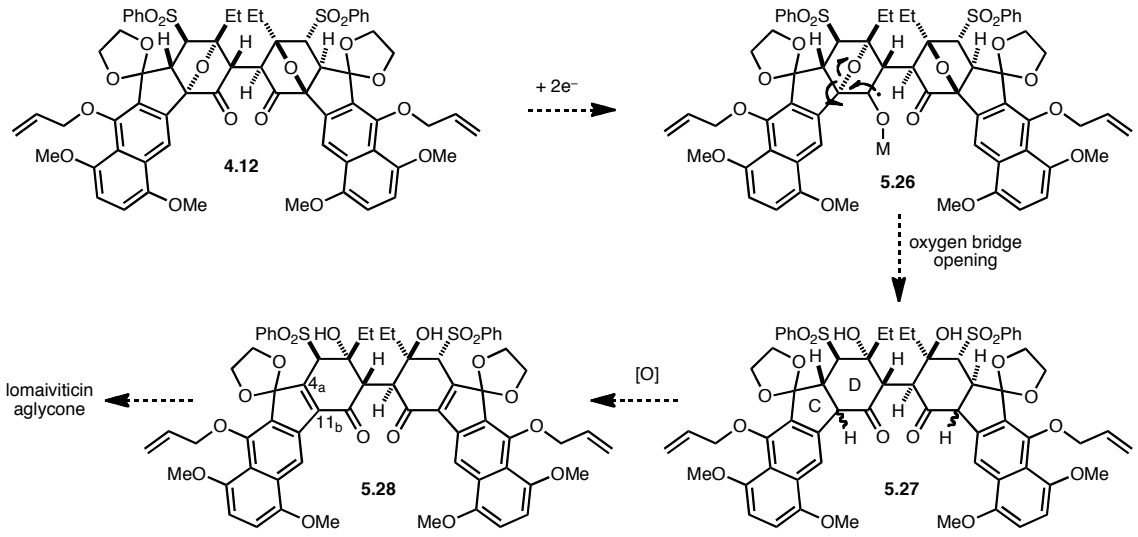

5.27. One drawback of this strategy is that an extra oxidation is required to install a C–C double bond at the CD-ring junction. A benzylic oxidation of **5.27** would provide intermediate **5.28**, which has desired oxidation state at $C4_a$ and $C11_b$. For the rest of the synthesis, strategies discussed in the previous section were applied.

To test the idea, dimer **4.12** was treated with freshly prepared SmI_2 in the presence of protic solvent (Scheme 5.5).[8] To our surprise, however, a diol **5.28** was isolated as the major product, along with a small amount of monomer **4.13**.[9] No desired product **5.27** was isolated.

Scheme 5.5 Attempted oxygen bridge opening of **4.12** under reductive conditions.

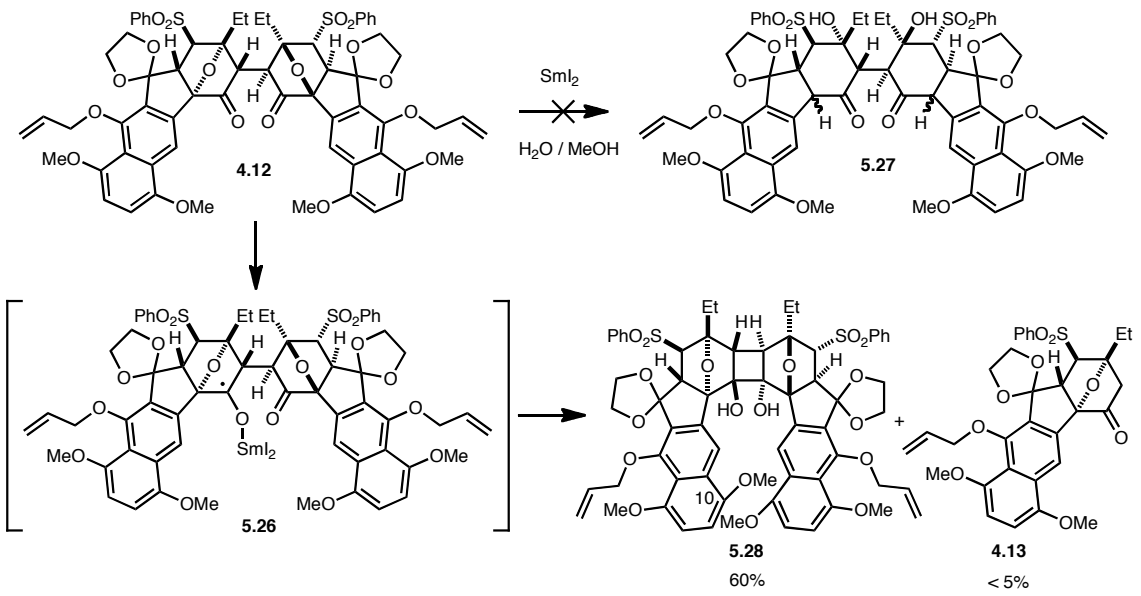

(7) Jae Young Ahn performed experiments associated with this approach.

(8) For review, see: (a) Molander, G. A.; Harris, C. R., *Chem. Rev.* **1996**, *96*, 307-338. (b) Edmonds, D. J.; Johnston, D.; Procter, D. J., *Chem. Rev.* **2004**, *104*, 3371-3404.

(9) A similar reaction pathway of the DD' core was observed in the model study. See: Krygowski, E. S., Ph. D. Thesis, Harvard University, Cambridge, MA, 2008.

Apparently, the initially formed ketyl radical species undergoes either an intramolecular pinacol coupling (path I), or C2–C2' bond cleavage (path II) (Figure 5.9). Pinacol coupling product **5.28** was characterized only by ^{1}H NMR and HRMS. No ^{13}C NMR was acquirable due to the marginal stability of the compound. It should be noted that the chemical shift of protons at the C11 methoxy group is much more upfield than was expected (**5.28**: δ = 2.62 ppm in $CDCl_3$, **4.12**: δ = 3.83 ppm in $CDCl_3$). It is believed that the magnetic anisotropy, arising from the naphthyl ring on the other end of the molecule, is responsible for the abnormal upfield chemical shift.

Figure 5.9 Formation of compound **5.28** and **4.13**.

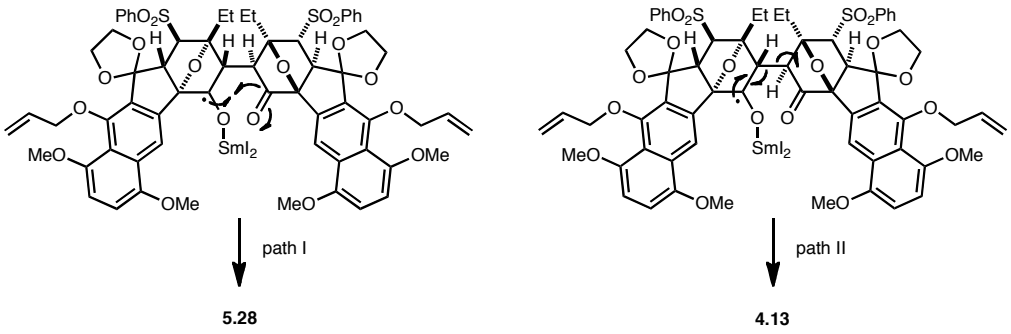

The undesired reactivity was rationalized based on the crystal structure of the dimer **4.35** (Figure 5.10). In the crystal structure, the C1 and C1' ketones are in close proximity, only 2.74 Å away from each other (Figure 5.10a). Therefore, as soon as one ketone is reduced, it may undergo pinacol coupling with the other ketone. The regeneration of monomer **4.13** is understood on the basis of orbital alignment (Figure 5.10b). The σ* orbital of the $C11_b$–O bond is sitting almost orthogonal to the π orbital of the C1 ketone, which may have the identical orientation as the half-filled orbital of the reduced species. On the other hand, the σ* orbital of C2-C2' bond is parallel to the C1 π

orbital. Thus, C2-C2' bond cleavage is more favorable than the desired C11$_b$–O bond cleavage.

Figure 5.10 Aspects of the crystal structure **4.35** help explain the formation of **5.28** and **4.13**.

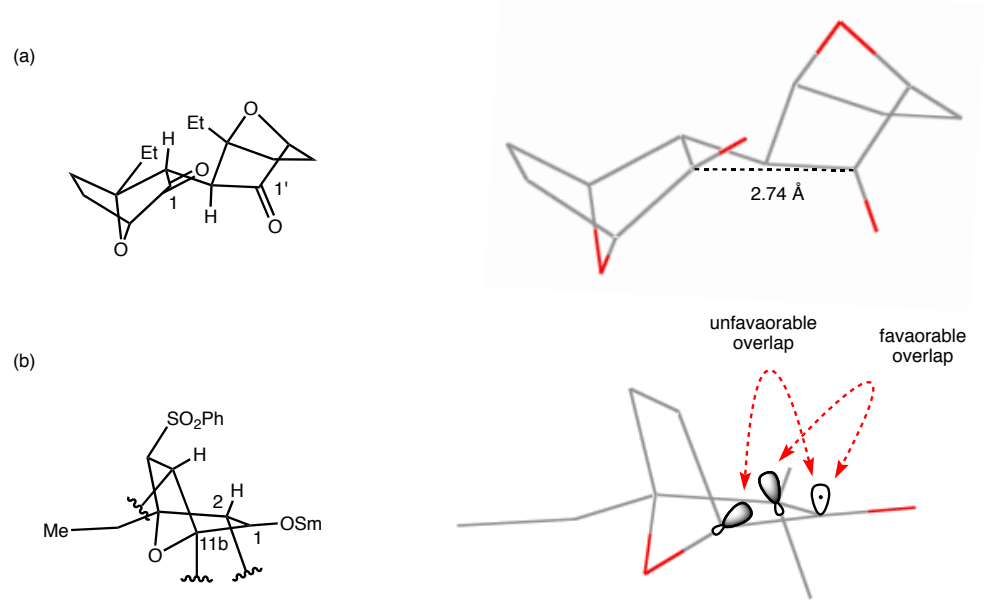

5.3. Attempted B-Ring Oxidation

The next strategy for $C11_b$–O bond cleavage relied on the assistance from the $C11_a$ position of the electron-rich naphthyl ring (Figure 5.11). In order to donate electron density to the σ* orbital of $C11_b$–O bond, oxdation of B-ring to a hydroquinone, such as **5.30**, was required.

Figure 5.11 Oxygen bridge opening assisted from $C11_a$.

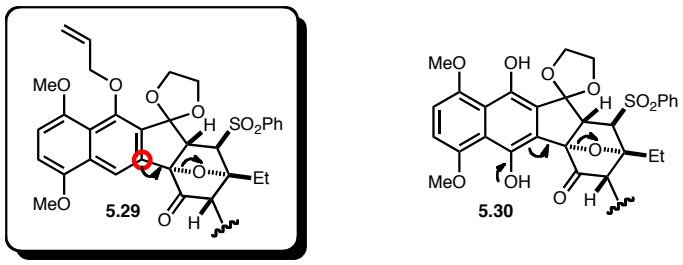

Synthetic plans involving this strategy are outlined in Figure 5.12. First, B-ring of the dimer **4.12** would be oxidized to the hydroquinone oxidation state to give intermediate **5.31**. The next step involved elimination of the benzylic oxygen substituent

Figure 5.12 Revised synthetic plan involving B-ring oxidation.

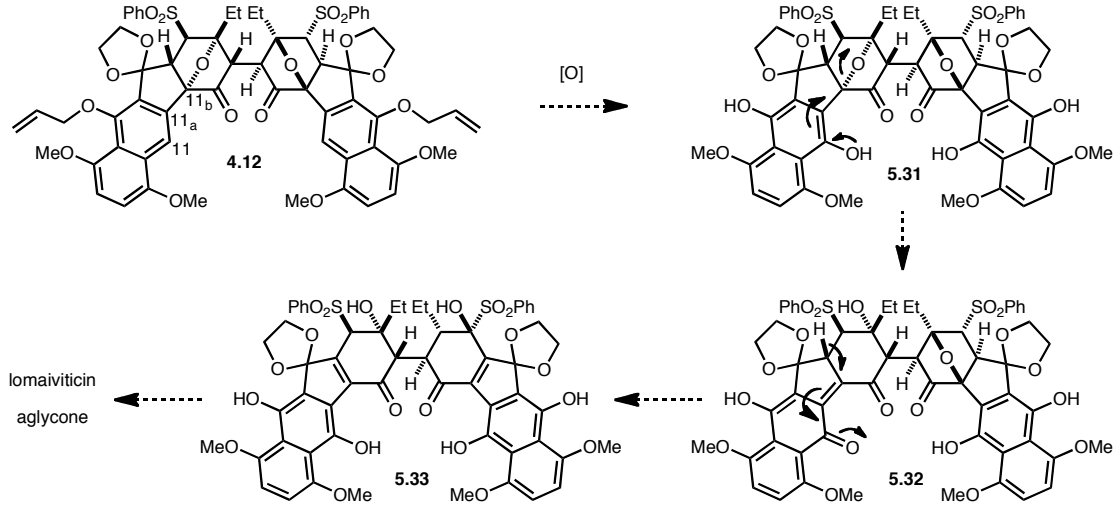

proximal to $C11_b$ with the assistance of the C11 phenol to form a quinone methide species such as **5.32**. Analogous eliminations of heteroatom leaving groups are well documented in the literature.[10] Next, the highly unstable quinone methide species **5.32** would undergo deprotonative rearomatization to provide a hydroquinone species such as **5.33**. Intermediate **5.33** was expected to be converted to the lomaiviticin aglycone with a similar strategy described in section 5.1.

The prerequisite for this strategy was oxidation of the B-ring phenol to a quinone or a hydroquinone (Scheme 5.6). Dimer **5.34** was chosen to be the most favorable oxidation substrate because the electron-withdrawing ketone, which retards the oxidation of naphthyl ring, was masked as a ketal. Ketal **5.34**, however, did not undergo the desired oxidation under standard conditions such as CAN, DDQ, PIFA, salcomine/O_2, or Fremy's salt. **5.35** or **5.36**, B-ring phenol intermediates having a ketone oxidation state at the C5 position, did not undergo any oxidation either. In all cases, starting material rapidly decomposed or did not react at all.

Scheme 5.6 Attempted oxidation of B-ring phenol.

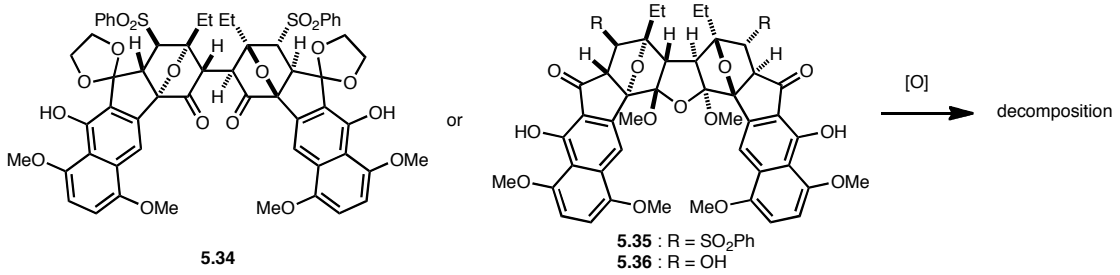

5.34

5.35 : R = SO_2Ph
5.36 : R = OH

In an effort to improve oxidation propensity, a partially electron-donating functional group, a hydrazone, was installed at C5 (Scheme 5.7). The hydrazone would

(10) Kende, A. S.; Johnson, S., *J. Org. Chem.* **1985**, *50*, 727-729.

be used as a handle for the oxidation of the B-ring as well as a precursor to the C5 diazo group. By using a standard protocol, ketones **5.35** and **5.36** were successfully converted to the corresponding tosyl hydrazones **5.37** and **5.38**, respectively. However, only decomposition was observed upon treatment of **5.37** or **5.38** with various oxidants.

Scheme 5.7 Attempted oxidation of B-ring phenol with hydrazone functionality at C5.

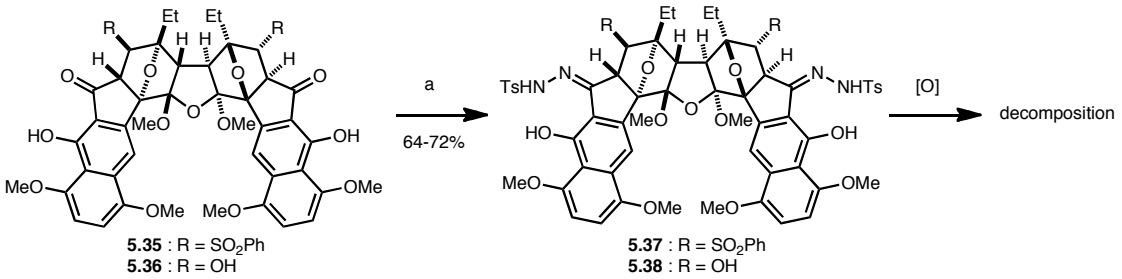

5.35 : R = SO_2Ph
5.36 : R = OH

5.37 : R = SO_2Ph
5.38 : R = OH

Reagents and conditions: (a) $TsNHNH_2$, HCl (aq), CH_2Cl_2/*i*-PrOH, 23 °C.

As was discussed previously about the **4.35** crystal structure, extremely little space is available between two naphthyl rings of the dimeric species (Figure 4.12). Therefore, we hypothesized that more space would be available by removing the cyclic hydrate of the dimer. However, all attempts to remove methyl-protected cyclic hydrate in aqueous acidic media were unsuccessful (Scheme 5.8). No 1,4-diketone, such as **5.39** or **5.40**, was detected prior to the decomposition of the starting material. This result is in accordance with the previous observation that the C1 ketal deprotection in the monomeric

Scheme 5.8 Attempted cyclic hydrate deprotection in the dimer.

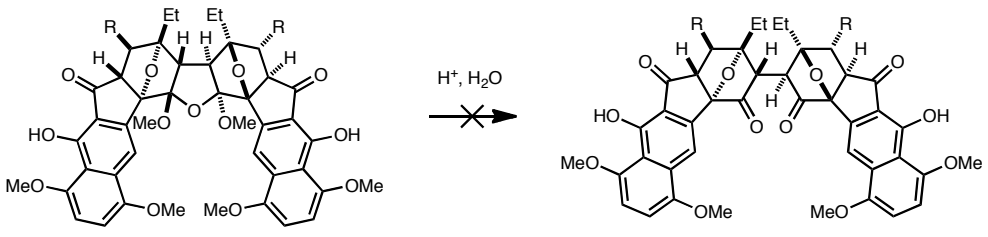

5.35 : R = SO_2Ph
5.36 : R = OH

5.39 : R = SO_2Ph
5.40 : R = OH

system was highly challenging (Scheme 2.8).

The only possible oxidation of the naphthyl ring was distal A-ring oxidation (Scheme 5.9). β-Hydroxy ketone **5.17** underwent smooth A-ring oxidation to the corresponding quinone **5.41** in the presence of AgO only when the B-ring allyl protecting group was present. Quinone **5.41** was easily reduced to the hydroquinone **5.42**. This mild oxidation/reduction sequence could potentially be used for the removal of the methyl protecting group of the A-ring at the end of the synthesis.

Scheme 5.9 Oxidation of A ring.

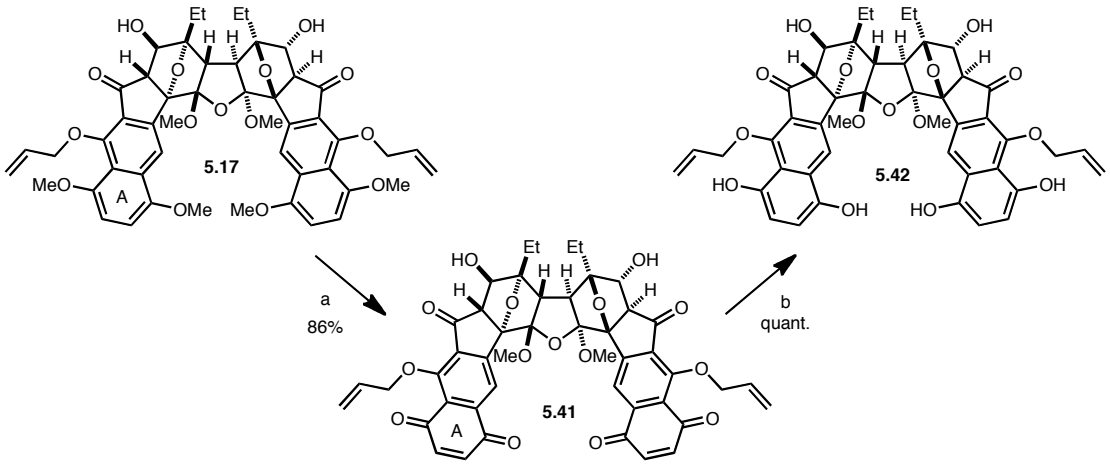

Reagents and conditions: (a) AgO, HNO_3, dioxane, H_2O, 0 °C; (b) $Na_2S_2O_4$, HCl(aq.), dioxane, H_2O, 23 °C.

5.4. Oxidation of the B-Ring

Confronted with the challenge of $C11_b$–O bond cleavage, a strategy that did not involve generation of an antiaromatic intermediate was conceived (Figure 5.13). By removing the carbonyl group at the C5 position, the elimination product would be an indene, such as **5.44**, instead of an antiaromatic indenone. By targeting an aromatic intermediate, it was anticipated that we would be able to isolate the desired elimination product. However, use of C5 methylene intermediates such as **5.43** would necessitate a major modification in the synthetic plan.

Figure 5.13 Strategy involving C5 methylene intermediates.

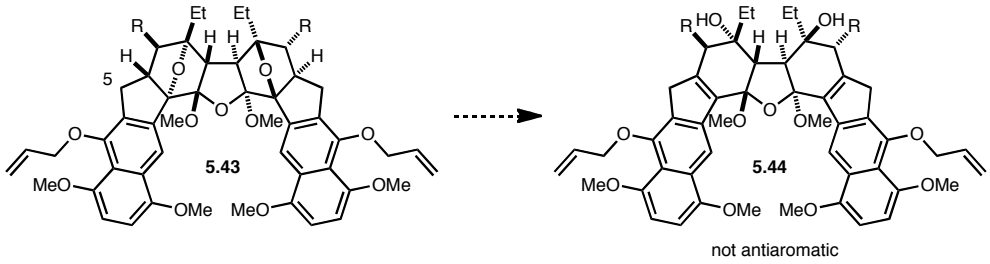

The overall post-elimination transformations would be almost identical to the previously discussed strategies, except for the introduction of C5 diazo group. Since the C5 carbonyl group would not be present, the hydrazone formation/oxidation sequence is not applicable. Instead, a Regitz diazo transfer utilized in the kinamycin F synthesis by Herzon would be utilized (Figure 5.14).[11] To apply this strategy, oxidation of the B-ring to a quinone oxidation state would have to be accompanied, as in the B-ring of compound **5.45**.

(11) Woo, C. M.; Lu, L.; Gholap, S. L.; Smith, D. R.; Herzon, S. B., *J. Am. Chem. Soc.* **2010**, *132*, 2540-2541.

Figure 5.14 Herzon's diazo transfer reaction in the synthesis of kinamycin F.

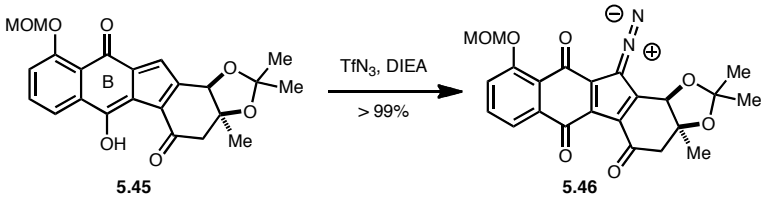

Accordingly, the synthetic challenge was reduced to removal of C5 carbonyl group. After extensive experimentations, a practical route to remove C5 carbonyl group was found (Scheme 5.10). β-Hydroxy ketone **5.17** was chosen as the starting point, since it already contained C4 oxygen functionality. **5.17** was treated with $LiBHEt_3$ and the resulting tetraol was peracetylated to provide tetraacetate **5.47**. **5.47** underwent ionic reduction in the presence of Et_3SiH and TfOH to liberate C5 acetate. It should be noted that use of a strong acid in a narrow temperature window was crucial for this transformation. The reaction was slow below −15 °C, and decomposition started took place above −10 °C. Other less acidic proton donors were not effective. The C4 acetate

Scheme 5.10 Removal of the C5 carbonyl group.

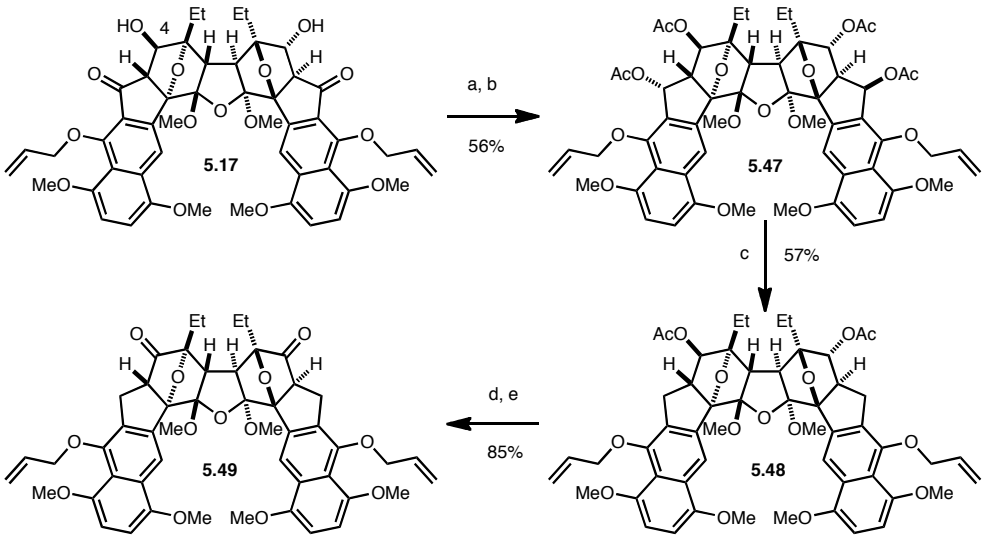

Reagents and conditions: (a) $LiBHEt_3$, THF, −78 °C; (b) Ac_2O, DMAP, CH_2Cl_2, 23 °C; (c) Et_3SiH, TfOH, CH_2Cl_2, −13 °C; (d) K_2CO_3, MeOH, 23 °C; (e) TPAP, NMO, 4 Å MS, CH_2Cl_2, 23 °C.

reduction product **5.48** was converted to C4 ketone **5.49** in two steps involving acetate removal and Ley oxidation.

Since the C5 carbonyl group was no longer present in **5.49** , a C5–$C4_a$ enolate was not available (Figure 5.4). Therefore, only two options of electron-density donation remained: C4–$C4_a$ enolate or $C11_a$ (Figure 5.15). A strategy involving the C4–$C4_a$ enolate as a handle for $C11_b$–O bond cleavage was investigated initially.

Figure 5.15 Possible source of electron density to cleave $C11_b$–O bond.

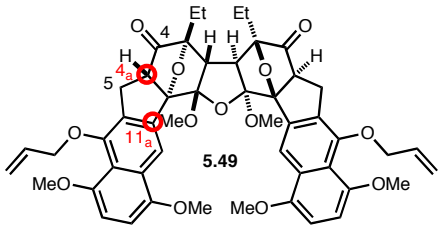

To our disappointment, ketone **5.49** did not undergo desired $C11_b$–O bond cleavage under a variety of conditions (Scheme 5.11). It was highly stable towards bulky strong bases and underwent decomposition when exposed to nucleophilic bases or strong acids.

Scheme 5.11 Attempted $C11_b$–O cleavage using a C4–$C4_a$ enolate.

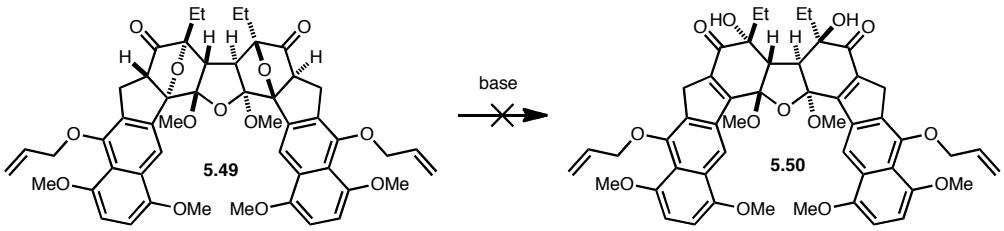

One benefit of this investigation was that we could introduce C4 hydroxyl group with the stereochemistry of the natural product (Scheme 5.12). By delivering a hydride from the convex face of the molecule, diketone **5.49** was reduced to the C4, C4' diol **5.51**

in 81% yield. The delivery of hydride was highly diastereoselective, and the orientation of hydride attack is in accordance with prior observations regarding hydroxide attack (Scheme 5.2).

Scheme 5.12 Diastreoselective reeduction of the C4 ketone.

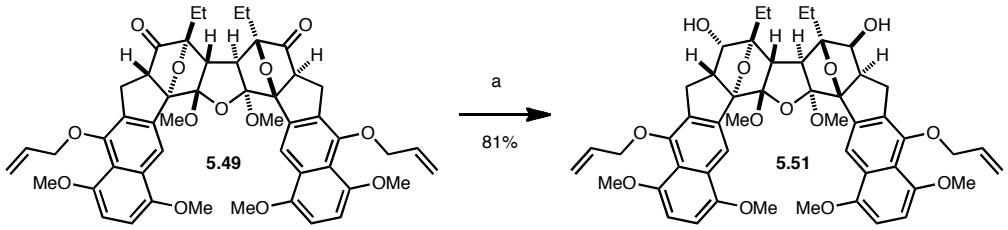

Reagents and conditions: (a) $LiBHEt_3$, THF, −78 °C.

At this point we focused on B-ring of the dimer in order to reveal another source of electron density, as was discussed in Figure 5.15. Unlike the previously unsuccessful oxidation of the B-ring, a practical oxidation protocol was found by using C5-methylene intermediates (Scheme 5.13). When diol **5.51** was deallylated and treated with a hypervalent iodine oxidant, an oxidized product **5.53** was isolated as the major product. Surprisingly, the B-ring of the molecule possessed a hydroquinone oxidation state in a very unusual 4-hydroxy cyclohexadienone form, an unaromatized tautomer of hydroquinone. To our delight, exposure of compound **5.53** to a second oxidant provided quinone **5.54** in 78% yield over two steps. It was believed that removal of electron-withdrawing heteroatom substituents at C5, which inductively hampered the B-ring oxidation, facilitated the oxidation reaction.

Scheme 5.13 Oxidation of the B-ring.

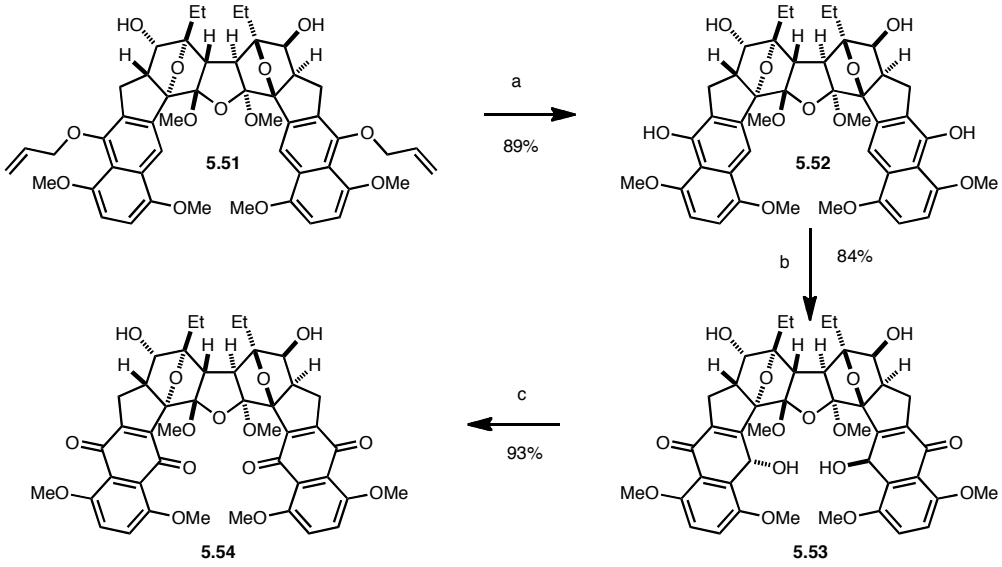

Reagents and conditions: (a) $PdCl_2(PPh_3)_2$, Bu_3SnH, AcOH, CH_2Cl_2, 0 °C; (b) $PhI(OCOCF_3)_2$, CH_3CN, H_2O, 0 °C; (c) DDQ, benzene, 50 °C.

A similar oxidation is known in a hindered setting (Figure 5.16). Schreiber and coworkers found that oxidation of phenol **5.55** takes place with the intermediacy of 4-hydroxy cyclohexadienone **5.56**, eventually providing quinone **5.57**.[12]

Figure 5.16 Schreiber's oxidation of phenol to 4-hydroxy cyclohexadienenone.

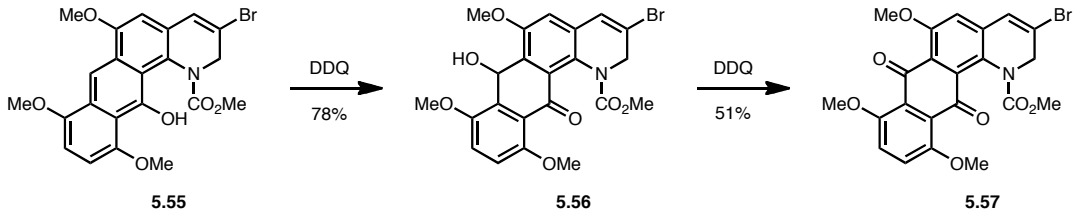

With the oxidized B-ring in hand, a synthetic plan to use it as a source of electron density was devised (Figure 5.17). The first strategy was to use a reduced form of the B-ring, such as hydroquinone **5.58** (path I). As was explained in Figure 5.12, hydroquinone

(12) Chikashita, H.; Porco, J. A.; Stout, T. J.; Clardy, J.; Schreiber, S. L., *J. Org. Chem.* **1991**, *56*, 1692-1694.

5.58 may undergo formation of quinone methide **5.59**, followed by rearomatizition to give **5.60**. Alternatively, a tautomeric form of quinone **5.54**, **5.61**, can also participate in a related sequence (path II). With a similar mechanistic rationale, intermediate **5.62** may be obtained, which may undergo [1,5]-hydride shift to regenerate quinone functionality in the B-ring.

Figure 5.17 B ring assisted $C11_b$–O bond cleavage.

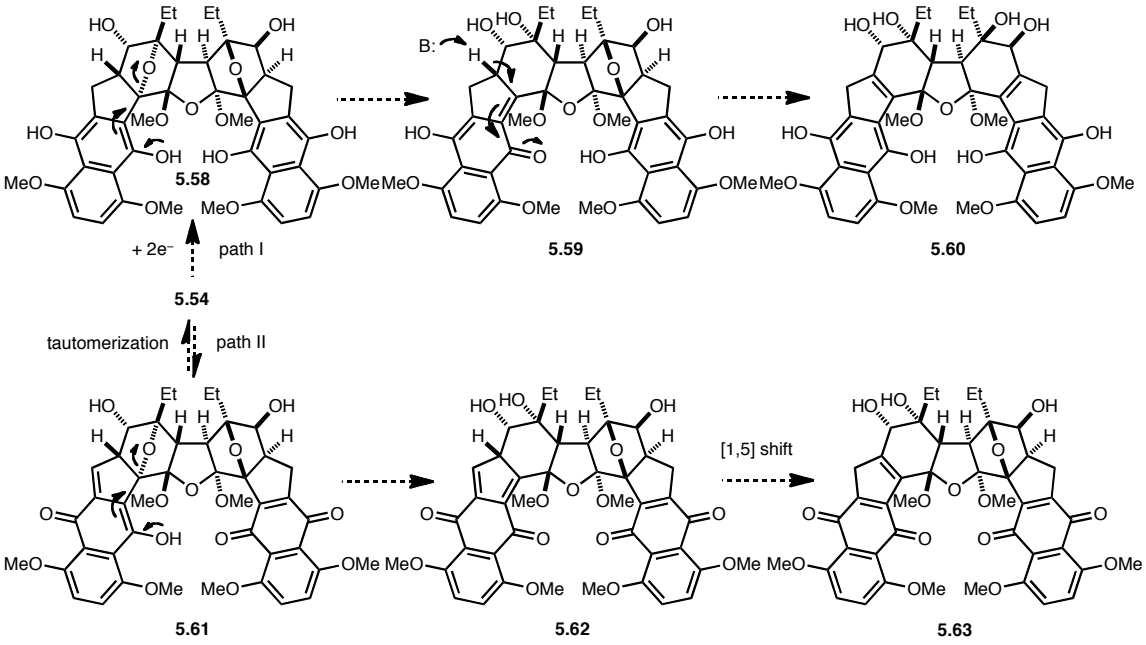

The strategy involving path II was investigated first. When **5.54** was exposed to bases, whose conjugate acid pK_a is greater than 12, decomposition took place (Scheme 5.14). Interestingly, when **5.54** was exposed to a tertiary amine, such as Et_3N, electron transfer between the quinone and the amine took place, providing hydroquinone **5.58** and Et_3NO. Residual water or oxygen may be the oxygen source leading to amine oxide. Upon isolation, hydroquinone **5.58** was quickly oxidized back to quinone **5.54**, with a half life of 30 minutes.

Scheme 5.14 Attempted $C11_b$–O bond cleavage of **5.54**.

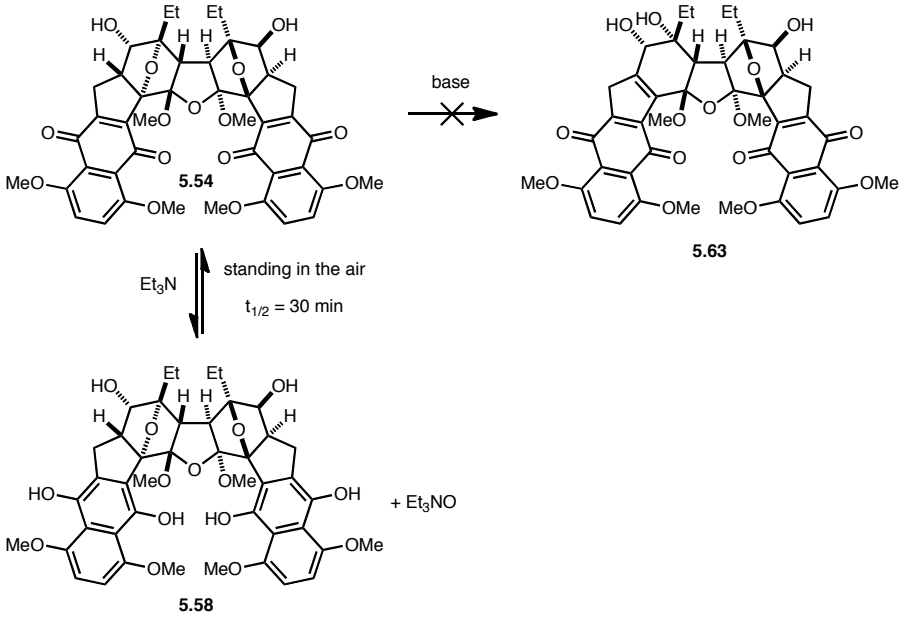

Next, path II was investigated. Due to the short life time of the hydroquinone, a model monomeric hydroquinone was used instead (Scheme 5.15). The corresponding quinone **5.68** was prepared in 9 steps from compound **4.28** with approximately 10% overall yield.

Scheme 5.15 Synthesis of model quinone **5.68**.

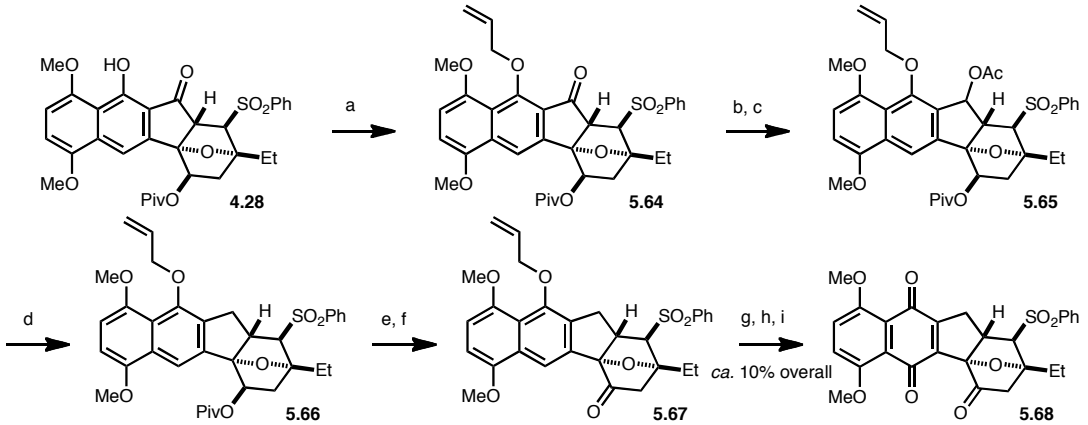

Reagents and conditions: (a) Allyl alcohol, DIAD, PPh_3, THF, 23 °C; (b) $NaBH_4$, MeOH, 0 °C; (c) Ac_2O, Et_3N, CH_2Cl_2, 23 °C; (d) Et_3SiH, TfOH, CH_2Cl_2, −13 °C; (e) $NaBHEt_3$, THF, 0 °C; (f) TPAP, NMO, CH_2Cl_2, 4 Å MS; (g) $PdCl_2(PPh_3)_2$, Bu_3SnH, AcOH, CH_2Cl_2, 0 °C; (h) $PhI(OCOCF_3)_2$, CH_3CN, H_2O, 0 °C; (i) DDQ, benzene, 50 °C.

The quinone was easily reduced to hydroquinone **5.69** upon exposure to Et_3N or $Na_2S_2O_4$ (Scheme 5.16a). Hydroquinoe **5.69** did not undergo the desired $C11_b$–O bond cleavage. Instead, oxidation of the B-ring to either a quinone or an epoxide was the dominant reaction pathway (Scheme 5.16b). Although use of rigorously degassed solvent partially retarded this unwawnted oxidation, complete obstruction was not achievable. The oxidation of hydroquinone to the corresponding epoxide under basic conditions has been documented.[13] It is proposed that both $^1O_2$ and $^3O_2$ may be responsible for the transformation.

Scheme 5.16 Attempted $C11_b$–O bond cleavage of monomeric quinone **5.68** or hydroquinone **5.69**.

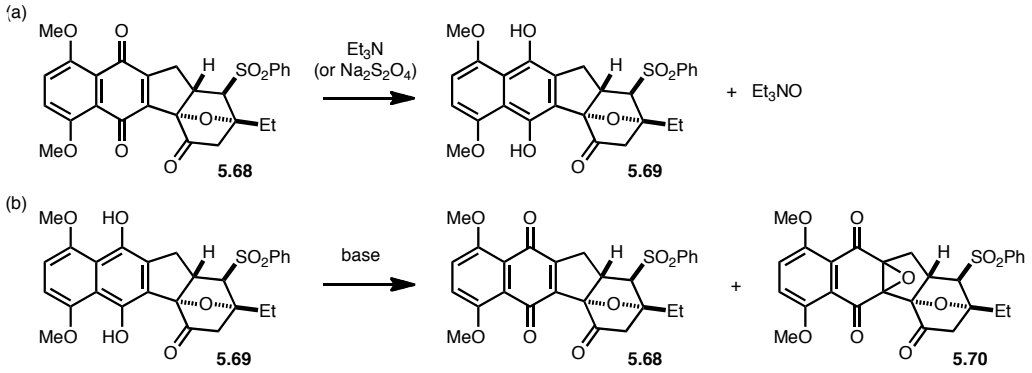

The introduction of diazo functionality was also investigated (Scheme 5.17). Quinone **5.54** was not an ideal substrate for Regitz diazo transfer (Scheme 5.17a). Unlike Herzon's intermediate **5.45**, **5.54** was not capable of forming a fulvene-type tautomer, which has a greater C5 nucleophilicity than the quinone tautomer. We then focused on conversion of an azide to the diazo group (Scheme 5.17b).[14] Azide **5.72** could be

(13) (a) Paquette, L. A.; Bellamy, F.; Boehm, M. C.; Gleiter, R., *J. Org. Chem.* **1980**, *45*, 4913-4921. (b) De, S. R.; Ghorai, S. K.; Mal, D., *J. Org. Chem.* **2009**, *74*, 1598-1604.

(14) Myers, E. L.; Raines, R. T., *Angew. Chem. Int. Ed.* **2009**, *48*, 2359-2363.

prepared from intermediate **5.64** in 10 steps. However, the desired oxidation did not take place. Instead, oxidation of phosphine **5.87** with concomitant reduction of quinone **5.72** took place.

Scheme 5.17 Attempted diazo group introduction.

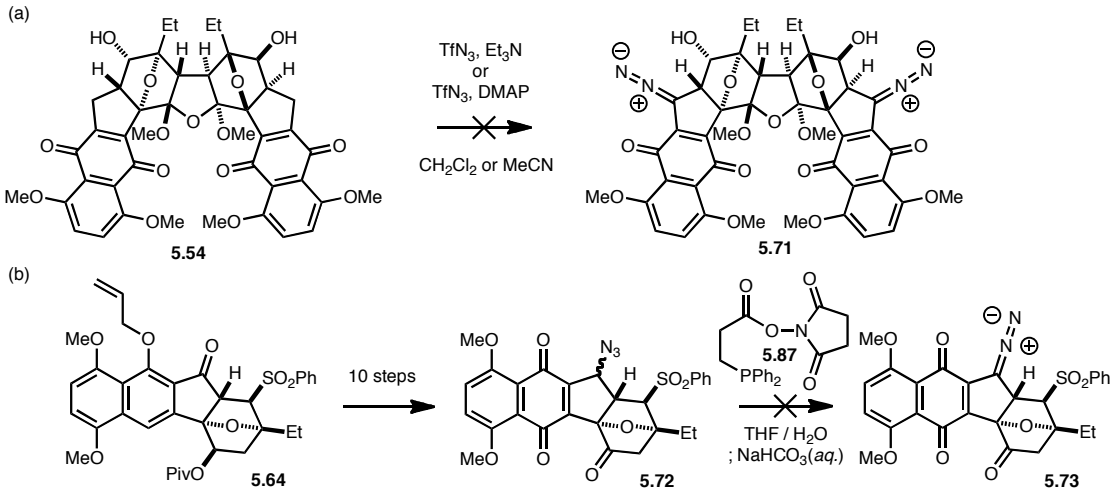

While we were addressing challenges associated with $C11_b$–O bond cleavage, an article demonstrating the futillity of our current approach was published from the Herzon group (Figure 5.18).[15] In this article, synthetic diazofluorene **5.74** was exposed to reductive conditions and subsequently underwent addition of a solvent molecule with corresponding loss of stereochemical integrity at the C4 position. The authors isolated intermediate **5.75** in the course of the reaction and postulated this arose from quinone methide intermediate **5.76**.

(15) Mulcahy, S. P.; Woo, C. M.; Ding, W.; Ellestad, G. A.; Herzon, S. B., *Chem. Sci.* **2012**, *3*, 1070.

Figure 5.18 Herzon's reductive solvolysis of daizofluorene **5.87**.

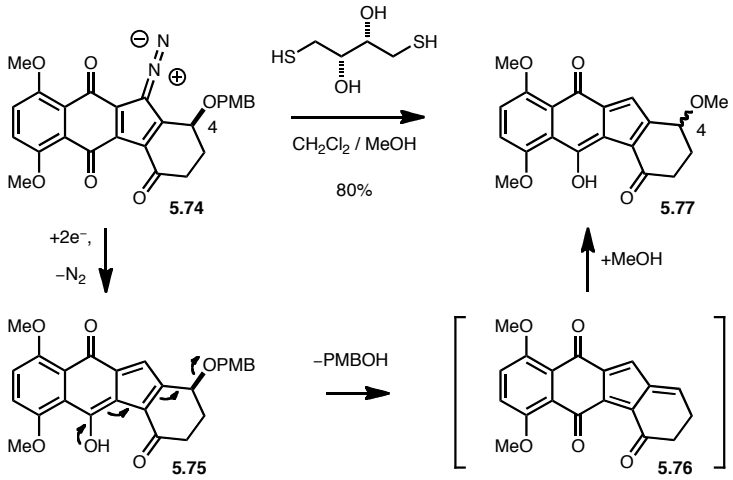

Although we may eventually effect the desired $C11_b$–O bond (i.e., **5.54** to **5.63**), the product may be in equilibrium with a fulvene tautomer **5.78** based on Herzon's result (Figure 5.19). Compound **5.78** may be highly prone to elimination of the C4 oxygen substituent to form a quinone methide species **5.79**, before undergoing diazo transfer.

Figure 5.19 Problems associated with the current strategy.

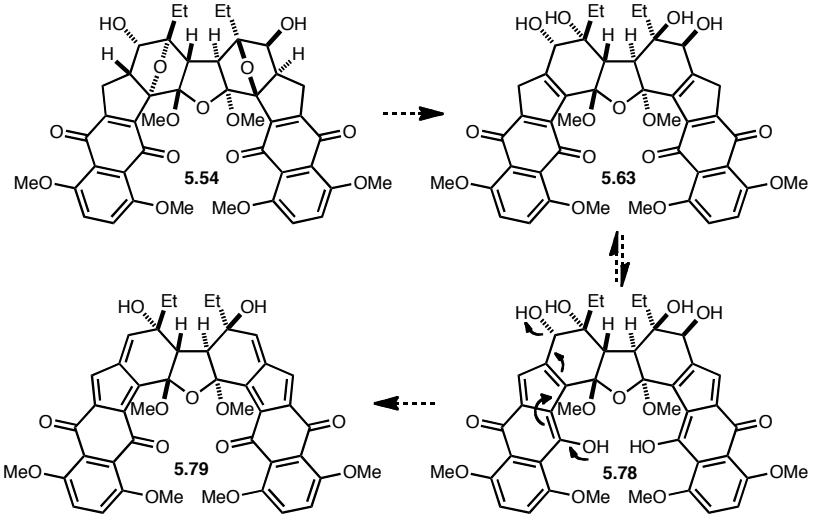

Chapter 6

Summary and Outlook

In summary, the full carbon skeleton of the lomaiviticin aglycone could be constructed by using a late-stage oxidative enolate dimerization strategy, although the dimeric product could not be elaborated to the synthetic target (Figure 6.1). The starting point of the synthesis was oxanorbornanone intermediate **1.101**, which is accesible in large quantities in an enantio-enriched form. By using a serendipitously discovered reductive transesterification protocol, oxanorbornanone **1.101** was transformed to allyl ester **2.36**, where the C1 and C5 oxygens are differentiated. Allyl ester **2.36** was converted to the key annulation precursor enone **2.42**, which was subjected to the modified Hauser annulation with sulfoxide **4.27** to provide tetracyclic intermediate **4.28**. Tetracycle **4.28** was advanced to the desired dimerization precursor **4.13**. In order to prepare **4.13** for a successful dimerization, a judicious choice of protecting group strategy was critical. **4.13** underwent successful oxidative enolate dimerization in a stereoselective manner to give dimer **4.12** in a synthetically practical yield. During the course of this study, a remarkable remote steric effect of the C11 substituent was disclosed. In addition, careful control of the reaction temperature was required to minimize side reactions. Upon removal of the C5 ketal of dimer **4.12**, we discovered thata single molecule of water had been incorporated into the central 1,4-ketone moiety to form stable cyclic hydrate **5.7**. Ketone **5.7** exhibited a completely different reaction profile from the model core toward basic fragmentation reaction conditions. Instead of going through the anticipated $C11_b$–O bond cleavage, the C4 sulfone was displaced with net retention of stereochemistry. In

order to avoid the difficulty associated with B-ring oxidation, due to inductive destabilization, the C5 carbonyl group was removed to give intermediate **5.51**. During the course of prepraring **5.51**, the C4 stereochemistry was adjusted to that of the natural

Figure 6.1 Summary of the synthesis.

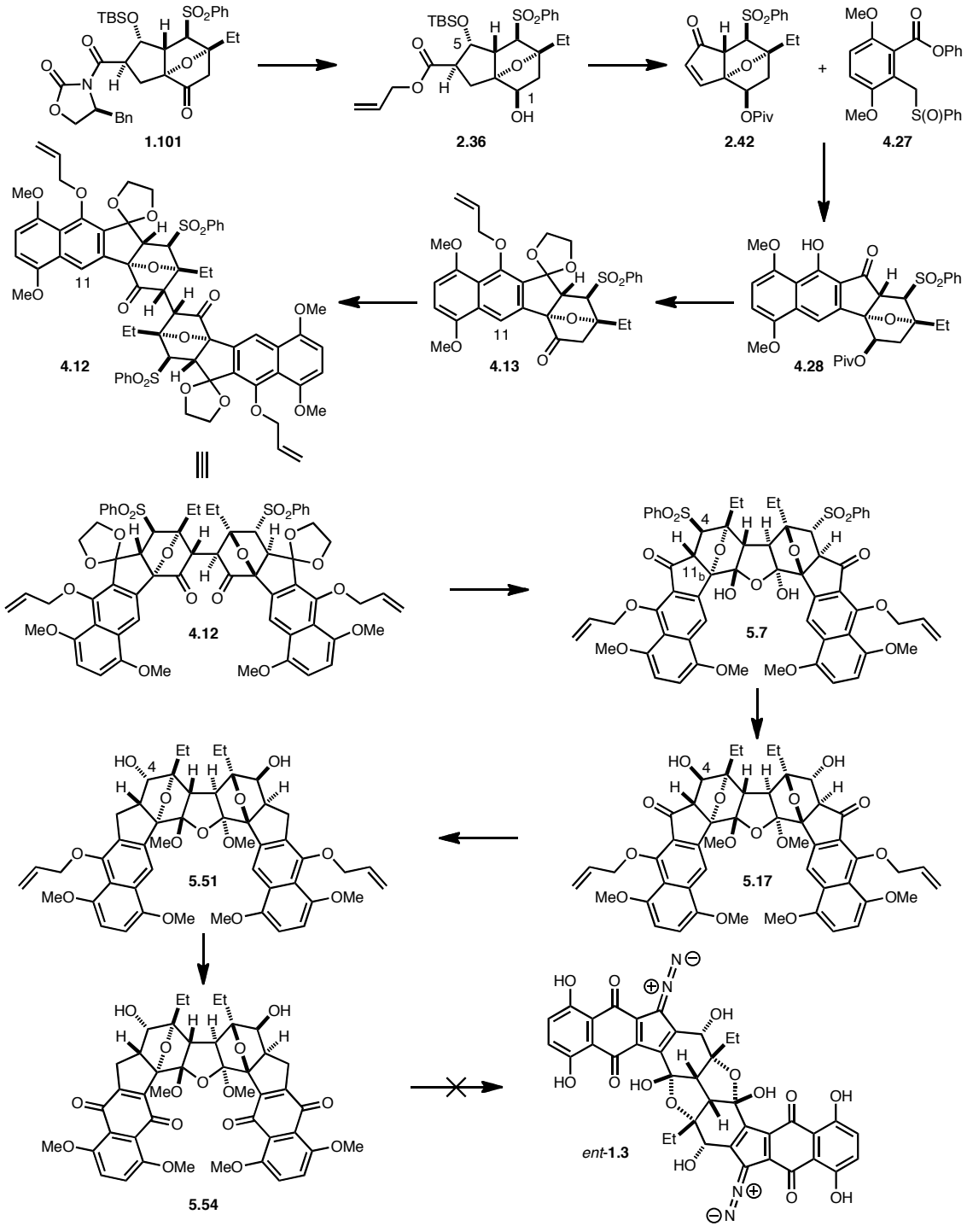

product. Intermediate **5.51** was advanced to the B-ring quinone **5.54**. Quinone **5.54** differs from the lomaiviticin aglycone (*ent*-**1.3**) in three aspects: 1) existence of the $C11_b$–O bond–the oxygen bridge; 2) lack of the C5 diazo functionality; 3) the central 1,4-diketone moiety locked in a methyl protected cyclic hydrate form.

Obviously, there was a major discrepancy in the ability of the oxanorbornane $C11_b$–O bond to undergo cleavage between the model system and the forefront intermediates. It seems that subtle electronic and conformational modifications arising from the AB-ring of the latter is the reason for the difference in the elimination behavior of the oxanorbornanes. Since we were not able to cleave the $C11_b$–O bond of the oxanorbornane, and hence could not expect stabilization of the C5 diazo group, we were unable to successfully introduce the diazo group. In addition, the existence of a central cyclic hydrate has made significant differences in manipulating the forefront intermediates due to the steric reasons.

One possible solution to address this problem would be to cleave the $C11_b$–O bond at an earlier stage. Since the oxanorbornane structure is essential for the diastereoselectivity of the dimerization, the cleavage should take place at a post dimerization stage. Therefore an intermediate resembling the model CDD'C' core might undergo the desired $C11_b$–O bond cleavage after dimerization, which could then be expanded to the full structure of the aglycone. However a way of introducing the A and B rings is not clear. Currently realization of this strategy is an active subject of research in the Shair group.

Appendix 1

Experimental Section

General Procedures. All reactions were performed in oven or flame-dried glassware under a positive pressure of argon unless noted otherwise. Flash column chromatography was performed either as described by Still et al. (Still, W. C.; Kahn, M.; Mitra, A. *J. Org. Chem*. **1978***, 43*, 2923-2925.), employing E. Merck silica gel 60 (230-400 mesh ASTM). Tetrahydrofuran, diethyl ether, dichloromethane, toluene, and dimethylformamide were degassed with argon and passed through a solvent purification system (designed by J.C. Meyer of Glass Contour) utilizing alumina columns. TLC analyses were performed on 250 μm Silica Gel 60F254 plates purchased from EM science.

Instrumentation. ^{1}H and ^{13}C NMR spectra were recorded on a Varian INOVA600, INOVA500, or INOVA500C spectrometer. Chemical shifts for proton and carbon resonances are reported in ppm (δ) relative to chloroform-d (δ 7.26 ppm, 77.0 ppm respectively). Mass spectra were obtained from the Harvard University Mass Spectrometry Laboratory.

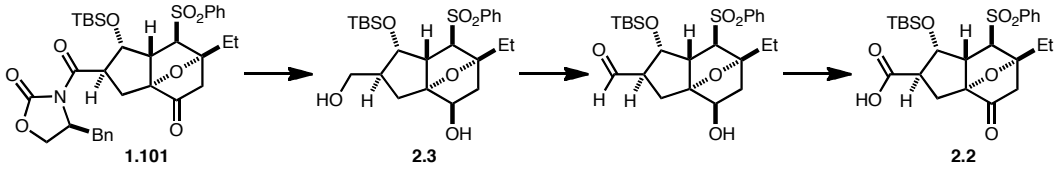

To a flask containing 0.5 mL of diethyl ether was added MeOH (0.0167 mL, 0.412 mmol, 1.10 equiv). Then the solution was cooled to 0 °C and 2.0 M THF solution of $LiBH_4$ (0.206 mL, 0.412 mmol, 1.10 equiv) was added in one portion. Then the mixture was cannulated to the 0 °C solution of ketone **1.101** (245 mg, 0.375 mmol, 1.00 equiv) in 2.0 mL of diethyl ether. The pale yellow solution was vigorously stirred at 0 °C for 30 min. Upon completion of the reaction, the mixture was quenched with saturated aqueous NH_4Cl solution (5mL), and the aqueous phase was extracted with diethyl ether (3 × 5 mL). The combined organic layer was dried over anhydrous $MgSO_4$ and filtered through celite. The crude product was purified by flash column chromatography (EtOAc/hexane = 1/2 to 2/1) to provide diol **2.3** (143 mg, 0.296 mmol, 79%).

To a solution of oxalyl chloride (0.152 mL, 1.74 mmol, 6.00 equiv) in dichloromethane (3 mL) was added DMSO (0.123 mL, 1.74 mmol, 6.00 equiv) over a 5 minute period at –78 °C. Gas evolution was observed. 30 minutes later, a solution of diol **2.3** (140 mg, 0.290 mmol, 1.00 equiv) in 2 mL of dichloromethane (plus 2 × 0.5 mL rinse) was cannulated to the reaction mixture over a 5 minute period. After stirring for 30 minutes, Et_3N (0.485 mL, 3.48 mmol, 12.0 equiv) was added in one portion to give a white suspension. The reaction system was warmed to 0 °C over 30 minutes and diluted with 50 mL of diethyl ether. The resulting slurry was filtered through a pad of celite/florisil and the filter cake was washed with diethyl ether. After concentration, the crude aldehyde was used for the next step without further purification.

The intermediate aldehyde was dissolved in 10 mL of *t*-BuOH together with 2-methyl-2-butene (0.307 mL, 2.90 mmol, 10.0 equiv). The mixture was cooled to 0 °C and a solution of $NaClO_2$ (164 mg, 1.45 mmol, 5.00 equiv) and $NaH_2PO_4 \cdot H_2O$ (200 mg, 1.45 mmol, 5.00 equiv) in 10 mL of water was added by a dropping funnel over 30 minutes. After addition, the reaction mixture was slowly warmed to 23 °C over 1 hour. Then the mixture was quenched with water (20 mL) and the aqueous phase was extracted with diethyl ether (3 × 10 mL). The combined organic layer was dried over anhydrous Na_2SO_4 and filtered through celite. The crude acid **2.2** (126 mg, 0.255 mmol, 88%) was used for the next step without further purification. ^{1}H NMR (500 MHz, $CDCl_3$) δ = 7.87 (d, *J* = 7.3 Hz, 2H), 7.67 (t, *J* = 1.0 Hz, 1H), 7.58 (t, *J* = 7.8 Hz, 2H), 4.23 (d, *J* = 5.0 Hz, 1H), 4.09 (q, *J* = 7.3 Hz, 1H), 4.01 (d, *J* = 5.0 Hz, 1H), 3.32 (d, *J* = 18.3 Hz, 1H), 3.15 - 3.09 (m, 1H), 3.03 (t, *J* = 5.7 Hz, 1H), 2.51 (dd, *J* = 5.5, 15.1 Hz, 1H), 2.35 (d, *J* = 17.9 Hz, 1H), 2.26 (dd, *J* = 9.2, 15.1 Hz, 1H), 1.94 (q, *J* = 7.5 Hz, 3H), 0.97 (t, *J* = 7.3 Hz, 3H), 0.78 (s, 9H), -0.05 (s, 3H), -0.34 ppm (s, 3H); HRMS (ESI) calcd for $C_{24}H_{38}O_7SSi$ [M+H$^+$] 495.1873, found: 495.1866.

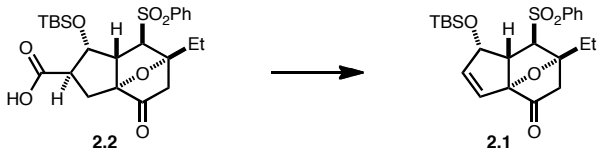

To the solution of acid **2.2** (81.0 mg, 0.164 mmol, 1.00 equiv) in 10 mL of benzene were added $Pb(OAc)_4$ (145 mg, 0.327 mmol, 2.00 equiv) and $Cu(OAc)_2 \cdot H_2O$ (8.2 mg, 0.041 mmol, 0.250 equiv). Then trifluoroacetic acid (0.0505 mL, 0.655 mmol, 4.00 equiv) was added to the solution. The mixture was heated to 80 °C and vigorously stirred. In 3 hours, the mixture was cooled to 23 °C and quenched with water (10mL). The aqueous phase

was extracted with diethyl ether (3 × 10 mL) and the combined organic layer was dried over anhydrous $MgSO_4$. After concentration, the crude product was purified by flash column chromatography (EtOAc/hexane = 1/10 to 1/5) to provide olefin **2.1** (31.0 mg, 0.0689 mmol, 42%) as a pale yellow film. ^{1}H NMR (500 MHz, $CDCl_3$) δ = 7.90 (d, *J* = 7.8 Hz, 2H), 7.71 - 7.66 (m, 1H), 7.62 - 7.55 (m, *J* = 7.8 Hz, 2H), 6.26 (dd, *J* = 2.3, 6.0 Hz, 1H), 6.04 (d, *J* = 6.0 Hz, 1H), 4.36 (dd, *J* = 2.3, 6.4 Hz, 1H), 4.10 (d, *J* = 6.0 Hz, 1H), 3.48 (d, *J* = 18.3 Hz, 1H), 3.01 (t, *J* = 6.4 Hz, 1H), 2.43 (d, *J* = 17.4 Hz, 1H), 2.09 - 1.93 (m, 2H), 1.00 (t, *J* = 7.3 Hz, 3H), 0.77 (s, 9H), -0.05 (s, 3H), -0.26 ppm (s, 3H); HRMS (ESI) calcd for $C_{23}H_{32}NaO_5SSi$ [M+Na^+] 471.1637, found: 471.1665.

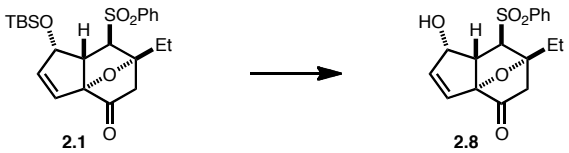

TBS ether **2.1** (51.0 mg, 0.114 mmol, 1 equiv) was dissolved in 3 mL of acetonitrile. To the solution was added 0.5 mL of aqueous solution of hydrofluoric acid in one portion at 23 °C. After stirring for 16 hours, the mixture was slowly quenched with saturated solution of $NaHCO_3$, and the aqueous phase was extracted with dichloromethane (3 × 10 mL). The combined organic layer was dried over anhydrous $MgSO_4$ and concentrated. The crude product was purified by flash column chromatography (EtOAc/hexane = 1/2 to 1/1) to provide alcohol **2.8** (36 mg, 0.107 mmol, 94%) as a white film. ^{1}H NMR (500 MHz, $CDCl_3$) δ = 7.93 (d, *J* = 7.3 Hz, 2H), 7.73 - 7.67 (m, 1H), 7.64 - 7.58 (m, 2H), 6.34 (dd, *J* = 2.4, 5.9 Hz, 1H), 6.09 (d, *J* = 5.9 Hz, 1H), 4.05 - 4.00 (m, 2H), 3.47 (d, *J* = 18.1 Hz, 1H), 2.86 (t, *J* = 6.6 Hz, 1H), 2.52 (dd, *J* = 1.2, 18.3 Hz, 1H), 2.11 (quind, *J* = 7.4,

14.4 Hz, 2H), 1.28 - 1.23 ppm (m, 3H); HRMS (ESI) calcd for $C_{16}H_{22}NO_5S$ [M+NH_4^+] 352.1219, found: 352.1201.

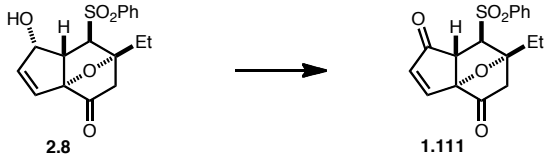

To the solution of alcohol **2.8** (8.3 mg, 0.025 mmol, 1.00 equiv) in 1 mL of dichloromethane was added Dess-Martin periodinane (15.8 mg, 0.0370 mmol, 1.50 equiv) in one portion. The mixture was vigorously stirred at 23 °C. 3 hour later, the reaction mixture was quenched with saturated aqueous $NaHCO_3$ solution (1 mL) and the aqueous phase was extracted with diethyl ether (3 × 2 mL). The combined organic layer was dried over anhydrous $MgSO_4$ and concentrated. The crude product was purified by flash column chromatography (EtOAc/hexane = 1/5) to provide enone **1.111** (7.5 mg, 0.0225 mmol, 90%) as a white film. ^{1}H NMR (500 MHz, $CDCl_3$) δ = 7.92 (d, *J* = 7.3 Hz, 2H), 7.73 - 7.65 (m, 1H), 7.59 - 7.62 (m, 2H), 7.48 (d, *J* = 5.8 Hz, 1H), 6.29 (d, *J* = 5.9 Hz, 1H), 3.64 (d, *J* = 6.5 Hz, 1H), 3.51 (d, *J* = 18.0 Hz, 1H), 3.24 (d, *J* = 6.6 Hz, 1H), 2.61 (d, *J* = 18.3 Hz, 1H), 2.18 (quind, *J* = 7.4, 14.2 Hz, 2H), 1.05 ppm (t, *J* = 7.5 Hz, 3H); HRMS (ESI) calcd for $C_{17}H_{20}NO_5S$ [M+NH_4^+] 350.1062, found: 350.1077.

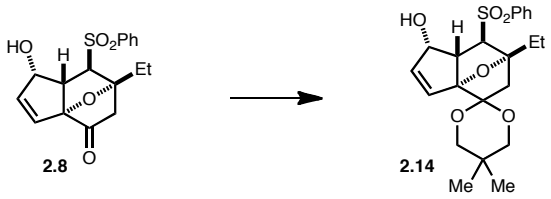

Ketone **2.8** (8.2 mg, 0.025 mmol, 1.00 equiv) was dissolved in 2 mL of benzene. To the solution were added 2,2-dimethylpropane-1,3-diol (5.1 mg, 0.049 mmol, 2.00 equiv) and

p-TsOH·H_2O (0.5 mg, 0.0025 mmol, 0.100 equiv). Then the reaction flask was equipped with a Dean-Stark condenser and the mixture was heated to reflux for 2 hours. After completion of the reaction, the mixture was cooled to 23 °C and diluted with 10 mL of diethyl ether. The organic phase was washed with saturated aqueous solution of $NaHCO_3$ (3 × 5 mL). After concentration, the crude product was purified by flash column chromatography (EtOAc/hexane = 1/1) to provide dioxane **2.14** (8.3 mg, 0.020 mmol, 79%) as a pale yellow solid. ^{1}H NMR (500 MHz, $CDCl_3$) δ = 7.95 (d, *J* = 7.3 Hz, 2H), 7.66 (t, *J* = 7.8 Hz, 1H), 7.60 - 7.55 (m, 2H), 6.26 - 6.21 (m, 2H), 3.93 (d, *J* = 7.3 Hz, 1H), 3.87 (br. s, 1H), 3.63 - 3.55 (m, 3H), 3.51 - 3.46 (m, 1H), 3.28 (t, *J* = 6.6 Hz, 1H), 3.10 (d, *J* = 13.3 Hz, 1H), 2.19 - 2.09 (m, 1H), 2.07 (d, *J* = 13.3 Hz, 1H), 2.03 - 1.94 (m, 1H), 1.15 (s, 3H), 1.05 (t, *J* = 7.6 Hz, 3H), 0.77 ppm (s, 3H); HRMS (ESI) calcd for $C_{22}H_{28}NaO_6S$ [M+Na^+] 443.1504, found: 443.1493.

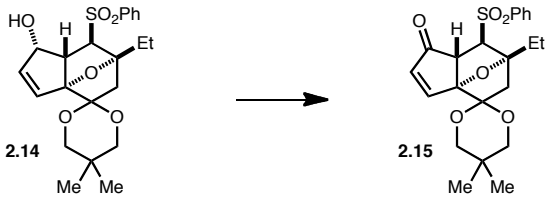

To the solution of alcohol **2.14** (8.3 mg, 0.020 mmol, 1.00 equiv) in 1 mL of dichloromethane was added Dess-Martin periodinane (12.7 mg, 0.030 mmol, 1.50 equiv) in one portion. The mixture was vigorously stirred at 23 °C. 1.5 hour later, the reaction mixture was quenched with saturated aqueous $NaHCO_3$ solution (1 mL) and the aqueous phase was extracted with diethyl ether (3 × 2 mL). The combined organic layer was dried over anhydrous $MgSO_4$ and concentrated. The crude product was purified by flash column chromatography (EtOAc/hexane = 1/5) to provide enone **2.15** (7.7 mg, 0.0184

mmol, 92%) as a white film. ^{1}H NMR (500 MHz, $CDCl_3$) δ = 7.92 (d, *J* = 7.3 Hz, 2H), 7.73 - 7.69 (m, 1H), 7.62 - 7.58 (m, 2H), 7.58 (d, *J* = 6.0 Hz, 1H), 6.20 (d, *J* = 6.0 Hz, 1H), 3.71 (d, *J* = 6.9 Hz, 1H), 3.68 - 3.52 (m, 4H), 3.11 (d, *J* = 13.3 Hz, 2H), 2.23 - 2.18 (m, 1H), 2.18 - 2.15 (m, *J* = 1.0 Hz, 1H), 2.01 (td, *J* = 7.7, 14.9 Hz, 1H), 1.19 (s, 3H), 1.01 (t, *J* = 7.3 Hz, 3H), 0.80 ppm (s, 3H); HRMS (ESI) calcd for $C_{22}H_{27}O_6S$ [M+H$^+$] 419.1528, found: 419.1542.

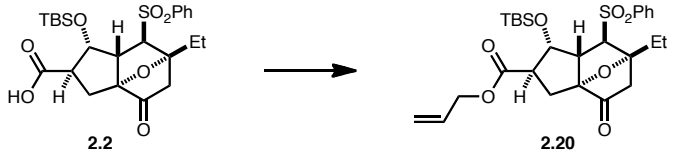

To the solution of acid **2.2** (8.2 mg, 0.0216 mmol, 1.00 equiv) in 2 mL of DMF were added allyl bromide (0.0020 mL, 0.0237 mmol, 1.10 equiv) and Cs_2CO_3 (7.0 mg, 0.0216 mmol, 1.00 equiv), successively. The heterogeneous mixture was vigorously stirred at 23 °C. 1 hour later, the reaction mixture was quenched with saturated aqueous solution of NH_4Cl, and the aqueous phase was extracted with diethyl ether (3 × 5 mL). The combined organic layer was washed with saturated aqueous solution of LiCl (2 × 5 mL), and dried over anhydrous $MgSO_4$. After concentration, the crude product was purified by flash column chromatography (EtOAc/hexane = 1/10 to 1/5) to provide allyl ester **2.20** (8.3 mg, 0.0197 mmol, 91%) as a white film. ^{1}H NMR (500 MHz, $CDCl_3$) δ = 7.88 (d, *J* = 7.3 Hz, 2H), 7.72 - 7.66 (m, *J* = 7.3 Hz, 1H), 7.61 - 7.56 (m, 2H), 5.97 - 5.87 (m, 1H), 5.34 (dd, *J* = 1.4, 17.4 Hz, 1H), 5.28 (dd, *J* = 0.9, 10.5 Hz, 1H), 4.61 (d, *J* = 6.0 Hz, 2H), 4.23 (dd, *J* = 2.1, 6.6 Hz, 1H), 4.05 (dd, *J* = 1.1, 5.3 Hz, 1H), 3.35 (d, *J* = 17.9 Hz, 1H), 3.16 - 3.11 (m, *J* = 2.5, 3.0 Hz, 1H), 3.06 - 3.02 (m, 1H), 2.47 (dd, *J* = 6.0, 15.1 Hz, 1H), 2.37 (dd, *J* = 1.4, 18.3 Hz, 1H), 2.27 (dd, *J* = 8.7, 15.1 Hz, 1H), 1.96 (q, *J* = 7.5 Hz, 2H),

1.00 (t, *J* = 7.6 Hz, 3H), 0.80 (s, 9H), -0.06 (s, 3H), -0.31 ppm (s, 3H); HRMS (ESI) calcd for $C_{27}H_{39}O_7SSi$ [M+H$^+$] 535.2186, found: 535.2199.

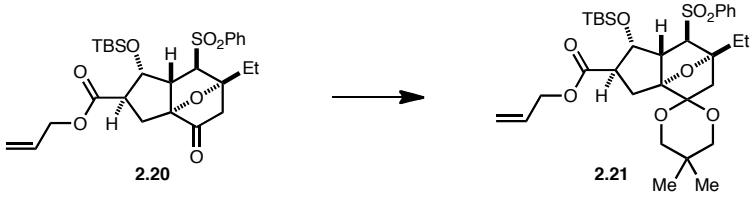

Ketone **2.20** (28.3 mg, 0.0529 mmol, 1.00 equiv) was dissolved in 2 mL of benzene. To the solution were added 2,2-dimethylpropane-1,3-diol (6.1 mg, 0.0582 mmol, 1.10 equiv) and *p*-TsOH·H_2O (1.0 mg, 0.0529 mmol, 0.100 equiv). Then the reaction flask was equipped with a Dean-Stark condenser and the mixture was heated to reflux for 6 hours. After completion of the reaction, the mixture was cooled to 23 °C and diluted with 10 mL of diethyl ether. The organic phase was washed with saturated aqueous solution of $NaHCO_3$ (3 × 5 mL). After concentration, the crude product was purified by flash column chromatography (EtOAc/hexane = 1/10) to provide dioxane **2.21** (32.0 mg, 0.0513 mmol, 97%) as white foam. ^{1}H NMR (500 MHz, $CDCl_3$) δ = 7.91 (d, *J* = 7.3 Hz, 2H), 7.64 (dd, *J* = 7.2, 7.3 Hz, 1H), 7.58 - 7.53 (m, 2H), 5.97 - 5.87 (m, 1H), 5.37 - 5.29 (m, 1H), 5.25 (d, *J* = 10.5 Hz, 1H), 4.58 (dd, *J* = 6.0, 12.4 Hz, 2H), 4.28 (dd, *J* = 2.7, 6.9 Hz, 1H), 3.98 (d, *J* = 5.5 Hz, 1H), 3.55 - 3.38 (m, 4H), 3.03 - 2.98 (m, 1H), 2.96 (d, *J* = 13.3 Hz, 1H), 2.36 - 2.32 (m, 2H), 1.94 - 1.86 (m, 1H), 1.82 (d, *J* = 13.3 Hz, 1H), 1.85 - 1.77 (m, 1H), 0.94 (t, *J* = 7.3 Hz, 3H), 0.78 (s, 9H), -0.10 (s, 3H), -0.31 ppm (s, 3H); ^{13}C NMR (125 MHz, $CDCl_3$) δ = 173.3, 140.8, 133.6, 132.0, 129.3, 128.4, 128.3, 118.5, 104.4, 98.4, 90.2, 73.9, 73.3, 70.5, 65.8, 65.5, 54.8, 49.2, 38.9, 30.2, 29.7, 27.9, 27.7, 25.8, 22.5, 21.8,

17.8, 8.1, -4.7, -5.4 ppm; HRMS (ESI) calcd for $C_{32}H_{49}O_8SSi$ [M+H$^+$] 621.2917, found: 621.2945.

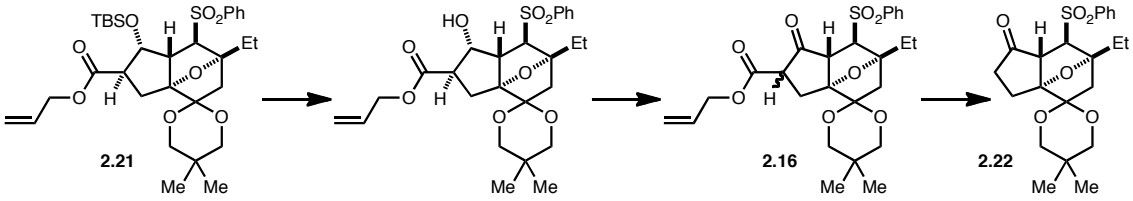

TBS ether **2.21** (64.0 mg, 0.103 mmol, 1.00 equiv) was dissolved in 5 mL of THF. The mixture was cooled to 0 °C and 1.0 M THF solution of TBAF (0.113 mL, 0.113 mmol, 1.10 equiv) was added in one portion. The reaction mixture was warmed to 23 °C and vigorously stirred for 2 hour. Then the mixture was quenched with saturated aqueous solution of NH_4Cl (5 mL), and the aqueous phase was extracted with EtOAc (3 × 5 mL). The combined organic layer was dried over anhydrous $MgSO_4$ and concentrated. The crude alcohol was used for the next step without further purification.

To the solution of the crude alcohol in 3 mL of dichloromethane was added Dess-Martin periodinane (65.5 mg, 0.155 mmol, 1.50 equiv) in one portion. The mixture was vigorously stirred at 23 °C. 1.5 hour later, the reaction mixture was quenched with saturated aqueous $NaHCO_3$ solution (5 mL) and the aqueous phase was extracted with diethyl ether (3 × 5 mL). The combined organic layer was dried over anhydrous $MgSO_4$ and concentrated. The crude product was purified by flash column chromatography (EtOAc/hexane = 1/5) to provide ketone **2.16** (44.5 mg, 0.0883 mmol, 85% over two steps) as white film.

To the solution of β-keto ester **2.16** (21.0 mg, 0.0416 mmo, 1.00 equiv) in 5 mL of toluene was added $PdCl_2(PPh_3)_2$ (0.6 mg, 0.00083 mmol, 0.0200 equiv), followed by

Bu_3SnH (0.0121 mL, 0.0458 mmol, 1.10 equiv). The mixture was stirred at 23 °C for 30 minutes, then heated to reflux for 30 minutes. The mixture was concentrated under reduced pressure and the crude product was purified by flash column chromatography (EtOAc/hexane = 1/5) to provide ketone **2.22** (15.6 mg, 0.0370 mmol, 89%) as white foam. ^{1}H NMR (500 MHz, $CDCl_3$) δ = 7.90 (d, *J* = 7.3 Hz, 2H), 7.70 - 7.65 (m, 1H), 7.60 - 7.54 (m, 2H), 3.67 - 3.57 (m, 4H), 3.51 - 3.41 (m, 4H), 3.04 (d, *J* = 12.8 Hz, 1H), 2.48 - 2.22 (m, 6H), 2.13 (qd, *J* = 7.5, 14.9 Hz, 1H), 1.98 (d, *J* = 12.8 Hz, 1H), 2.06 - 1.95 (m, 1H), 1.22 (s, 3H), 0.98 (t, *J* = 7.3 Hz, 3H), 0.77 ppm (s, 3H); HRMS (ESI) calcd for $C_{22}H_{29}O_6S$ [M+H$^+$] 421.1685, found: 421.1683.

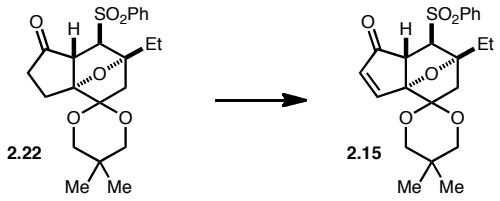

Ketone **2.22** (20.3 mg, 0.0483 mmol, 1.00 equiv) was dissolved in 5 mL of toluene. To the solution was added benzeneseleninic anhydride (20.9 mg, 0.0579 mmol, 1.20 equiv), followed by $NaHCO_3$ (6.1 mg, 0.0725 mmol, 1.50 mmol). The mixture was heated to reflux, while the progress of the reaction was monitored by NMR. In 5 hours, the reaction mixture was quenched with water and the aqueous phase was extracted with diethyl ether (3 × 5 mL). After concentration, the crude product was purified by flash column chromatography (EtOAc/hexane = 1/5) to provide enone **2.15** (16.1 mg, 0.0382 mmol, 79%) as white foam. The product was identical to the previously prepared compound in all aspects.

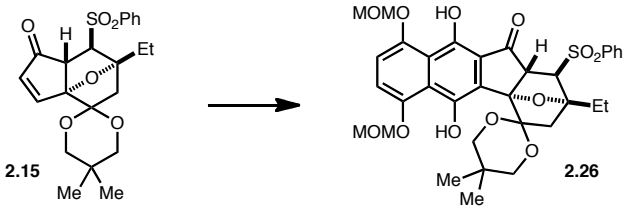

A two-neck flask was flame dried with a cold finger on it and charged with HMDS (0.0555 mL, 0.263 mmol, 5.00 equiv) in 0.5 mL of THF, and 1.60 M hexane solution of *n*-BuLi (0.164 mL, 0.263 mmol, 5.00 equiv), successively at –78 °C. 10 minutes later HMPA (45.8 μL, 0.263 mmol, 5.00 equiv) was added to the LiHMDS solution. In another 10 minutes, cyanophthalide **2.10** (44.0 mg, 0.158 mmol, 3.00 equiv) in 0.5 mL of THF (plus 2 × 0.3 mL rinse) was cannulated into the reaction mixture to give a bright yellow solution. The solution was stirred at –78 °C for 20 minutes, then enone **2.15** (22.0 mg, 0.0526 mmol, 1.00 equiv) in 0.5 mL of THF (plus 2 × 0.3 mL rinse) was cannulated to the reaction mixture. Stirring was continued at –78 °C for 10 minutes, then the reaction system was heated to 50 °C for 20 minutes. After completion of the reaction, the mixture was cooled to 23 °C, and quenched with saturated aqueous solution of NH_4Cl, and the aqueous phase was extracted with dichloromethane (3 × 10 mL). After concentration, the crude product was purified by flash column chromatography (EtOAc/hexane = 1/3 to 1/1.5) to provide tetracycle **2.26** (14.4 mg, 0.0216 mmol, 41%) as bright yellow foam. ^{1}H NMR (500 MHz, $CDCl_3$) δ = 10.39 (s, 1H), 10.36 (s, 1H), 7.98 (d, *J* = 7.8 Hz, 2H), 7.74 - 7.70 (m, 1H), 7.64 - 7.60 (m, 2H), 7.15 (d, *J* = 8.8 Hz, 1H), 7.06 (d, *J* = 8.8 Hz, 1H), 5.29 (s, 2H), 5.17 - 5.11 (m, 2H), 4.20 (d, *J* = 6.8 Hz, 1H), 3.91 - 3.86 (m, 1H), 3.85 - 3.79 (m, 1H), 3.76 - 3.68 (m, 2H), 3.64 (d, *J* = 6.3 Hz, 1H), 3.58 (s, 3H), 3.51 (s, 3H), 3.31 - 3.26 (m, 1H), 2.25 (d, *J* = 12.8 Hz, 1H), 2.30 - 2.20 (m, 1H), 2.16 - 2.06 (m, 1H), 1.24 (s, 3H), 1.02 (t, *J* = 7.3 Hz, 3H), 0.85 ppm (s, 3H); ^{13}C NMR (125 MHz, $CDCl_3$) δ = 199.0, 151.8,

150.3, 149.4, 145.1, 139.9, 134.2, 129.4, 128.5, 121.0, 120.1, 115.5, 112.5, 106.2, 98.5, 96.4, 93.5, 92.3, 74.3, 71.3, 68.3, 56.9, 56.8, 56.4, 39.1, 36.6, 30.5, 27.9, 22.3, 21.6, 8.1 ppm; HRMS (ESI) calcd for $C_{34}H_{39}O_{12}S$ [M+H$^+$] 671.2162, found: 671.2134.

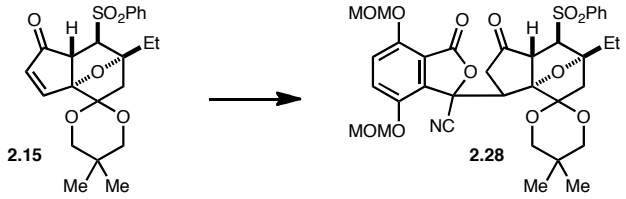

Without heating, in the reaction above, Michael adduct **2.28** was isolated in 45% yield. ^{1}H NMR (500 MHz, $CDCl_3$) δ = 7.86 (d, *J* = 7.3 Hz, 2H), 7.70 - 7.65 (m, 1H), 7.60 - 7.54 (m, 2H), 7.30 (d, *J* = 9.2 Hz, 1H), 7.18 (d, *J* = 9.2 Hz, 1H), 5.28 (s, 2H), 5.24 (d, *J* = 6.9 Hz, 1H), 5.12 (d, *J* = 6.9 Hz, 1H), 3.89 (t, *J* = 10.1 Hz, 1H), 3.77 (d, *J* = 5.0 Hz, 1H), 3.67 - 3.55 (m, 2H), 3.49 (s, 3H), 3.45 (s, 3H), 3.54 - 3.42 (m, 2H), 3.30 (d, *J* = 4.6 Hz, 1H), 2.88 (d, *J* = 12.8 Hz, 1H), 2.82 - 2.67 (m, 2H), 1.96 - 1.83 (m, 2H), 1.79 (d, *J* = 13.3 Hz, 1H), 1.35 (s, 3H), 0.78 (s, 3H), 0.75 ppm (t, *J* = 7.3 Hz, 3H); ^{13}C NMR (125 MHz, $CDCl_3$) δ = 208.8, 164.9, 150.1, 146.5, 139.8, 134.3, 134.1, 129.3, 128.3, 128.2, 121.0, 118.9, 115.5, 115.4, 104.2, 95.3, 94.8, 94.4, 91.3, 75.8, 74.3, 70.1, 69.8, 58.1, 56.5, 56.4, 40.3, 39.2, 36.9, 30.1, 29.7, 27.4, 22.5, 21.7, 7.7 ppm; HRMS (ESI) calcd for $C_{35}H_{40}NO_{12}S$ [M+H$^+$] 698.2271, found: 698.2264.

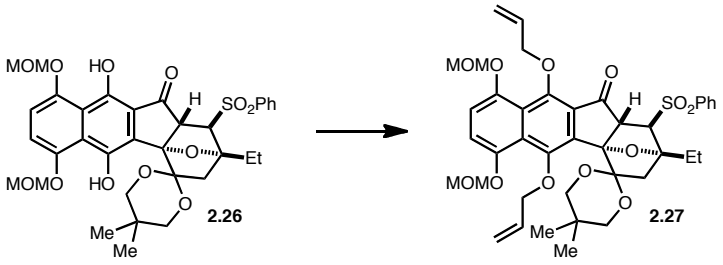

Hydroquinone **2.26** (156 mg, 0.233 mmol, 1.00 equiv) was dissolved in 5 mL of DMF. To the solution was added allyl bromide (0.099 mL, 1.17 mmol, 5.00 equiv) *n*-Bu_4NI (86 mg, 0.233 mmol, 1.00 equiv), and Cs_2CO_3 (227 mg, 0.699 mmol, 3.00 equiv), successively. The heterogeneous mixture was stirred at 23 °C for 2 hours. After completion of the reaction, the reaction system was quenched with saturated aqueous solution of NH_4Cl, and the aqueous phase was extracted with dichloromethane (3 × 10 mL). The combined organic layer was dried over anhydrous Na_2SO_4 and concentrated. The crude product was purified by flash column chromatography (EtOAc/hexane = 1/4 to 1/3) to provide bisallyl ether **2.27** (159 mg, 0.212 mmol, 91%) as bright yellow foam. ^1H NMR (500 MHz, $CDCl_3$) δ = 7.99 (d, *J* = 7.3 Hz, 2H), 7.73 - 7.68 (m, 1H), 7.63 - 7.58 (m, 2H), 7.19 - 7.16 (m, 1H), 7.12 - 7.09 (m, 1H), 6.19 - 6.04 (m, 2H), 5.38 - 5.30 (m, 1H), 5.25 - 5.16 (m, 1H), 5.15 (s, 2H), 5.14 - 5.08 (m, 2H), 4.62 (dd, *J* = 4.9, 11.2 Hz, 1H), 4.43 (d, *J* = 5.9 Hz, 2H), 4.34 - 4.32 (m, 1H), 3.63 - 3.55 (m, 4 H), 3.17 (d, *J* = 13.2 Hz, 1H), 2.21 (dd, *J* = 1.0, 13.2 Hz, 1H), 2.11 (dq, *J* = 2.2, 7.4 Hz, 2H), 1.08 (s, 3H), 0.98 (t, *J* = 7.3 Hz, 3H), 0.80 ppm (s, 3H); HRMS (ESI) calcd for $C_{40}H_{47}O_{12}S$ $[M+H^+]$ 751.2788, found: 751.2801.

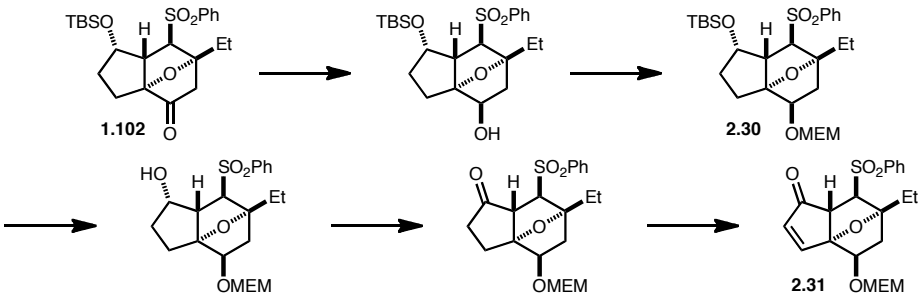

Ketone **1.102** (29.0 mg, 0.0640 mmol, 1.00 equiv) was dissolved in 3 mL of MeOH and cooled to 0 °C. To the solution was added $NaBH_4$ (24.0 mg, 0.640 mmol, 10.0 equiv) in

one portion. After stirring for 5 minutes, the mixture was quenched with saturated aqueous solution of NH_4Cl (5mL), then the aqueous phase was extracted with ethyl acetated (3 × 10 mL). The combined organic layer was dried over anhydrous $MgSO_4$ and concentrated. The crude product was used for the next step without further purification.

The crude alcohol was dissolved in 5 mL of dichloromethane. To the solution was added MEMCl (0.0219 mL, 0.192 mmol, 3.00 eqiv), followed by DIEA (0.0557 mL, 0.320 mmol, 5.00 equiv) and the mixture was heated to reflux for 12 hours. At the end of the reaction, the reaction mixture was quenched with water and the aqueous phase was extracted with dichloromethane (3 × 10 mL). The combined organic layer was dried over anhydrous Na_2SO_4 and concentrated. The crude product was purified by flash column chromatography (EtOAc/hexane = 1/3 to 1/2) to provide the corresponding MEM ether (30.8 mg, 0.0570 mmol, 89%) as colorless film.

The MEM ether (16.8 mg, 0.0310 mmol, 1.00 equiv) was dissolved in 5 mL of THF. To the solution was added 1.0 M THF solution of TBAF (0.0341 mL, 0.0341 mmol, 1.10 equiv) in one portion. The reaction mixture was vigorously stirred at 23 °C for 12 hours. At the end of the reaction, the mixture was quenched with saturated aqueous solution of NH_4Cl (5 mL), and the aqueous phase was extracted with EtOAc (3 × 10 mL). The combined organic layer was dried over anhydrous $MgSO_4$ and concentrated. The crude alcohol was used for the next step without further purification.

The intermediate alcohol was charged in a flask with 5 mL of dichloromethane. To the solution was added TPAP (0.5 mg, 0.00160 mmol, 0.0500 equiv), followed by NMO (5.4 mg, 0.0470 mmol, 1.50 equiv) and 20 mg of 4 Å MS. The heterogeneous mixture was

vigorously stirred for 1 hour at 23 °C. At the end of the reaction, the reaction system was diluted with 10 mL of diethyl ether and filtered through silica gel. After concentration, the crude ketone was used for the next step without further purification.

The ketone was dissolved in 5 mL of toluene. To the solution was added benzeneseleninic anhydride (16.7 mg, 0.0465 mmol, 1.50 equiv), followed by $NaHCO_3$ (7.8 mg, 0.0930 mmol, 3.00 mmol). The mixture was heated to reflux, while the progress of the reaction was monitored by NMR. In 5 hours, the reaction mixture was quenched with water and the aqueous phase was extracted with diethyl ether (3 × 5 mL). After concentration, the crude product was purified by flash column chromatography (EtOAc/hexane = 1/2 to 1/1) to provide enone **2.31** (9.4 mg, 0.0223 mmol, 72% over three steps) as white foam. ^{1}H NMR (500 MHz, $CDCl_3$) δ = 7.97 - 7.92 (m, 2H), 7.74 - 7.69 (m, 1H), 7.64 - 7.58 (m, 2H), 7.41 (d, *J* = 5.9 Hz, 1H), 6.15 (d, *J* = 6.3 Hz, 1H), 4.86 - 4.80 (m, 2H), 4.41 (dd, *J* = 3.9, 9.8 Hz, 1H), 3.82 - 3.77 (m, 2H), 3.71 - 3.65 (m, 1H), 3.60 - 3.51 (m, 3H), 3.39 (s, 3H), 2.80 (dd, *J* = 4.4, 13.7 Hz, 1H), 2.29 (ddd, *J* = 1.5, 10.3, 13.7 Hz, 1H), 2.10 (qd, *J* = 7.5, 15.0 Hz, 1H), 1.97 (qd, *J* = 7.5, 15.0 Hz, 1H), 0.98 ppm (t, *J* = 7.6 Hz, 3H); HRMS (ESI) calcd for $C_{21}H_{26}NaO_7S$ [M+Na$^+$] 445.1297, found: 445.1311.

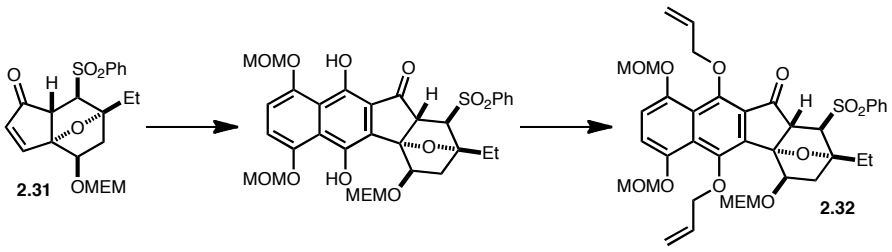

A two-neck flask was flame dried with a cold finger on it and charged with HMDS (0.0175 mL, 0.0830 mmol, 5.00 equiv) in 0.5 mL of THF, and 1.60 M hexane solution of *n*-BuLi (0.0520 mL, 0.0830 mmol, 5.00 equiv), successively at –78 °C. 10 minute later HMPA (0.0144 mL, 0.0830 mmol, 5.00 equiv) was added to the LiHMDS solution. In another 10 minutes, cyanophthalide **2.10** (13.9 mg, 0.0497 mmol, 3.00 equiv) in 0.5 mL of THF (plus 2 × 0.3 mL rinse) was cannulated into the reaction mixture to give a bright yellow solution. The solution was stirred at –78 °C for 20 min, then enone **2.31** (7.0 mg, 0.0166 mmol, 1.00 equiv) in 0.5 mL of THF (plus 2 × 0.3 mL rinse) was cannulated to the reaction mixture. Stirring was continued at –78 °C for 10 minutes, then the reaction system was heated to 50 °C for 20 minutes. After completion of the reaction, the mixture was cooled to 23 °C, and quenched with saturated aqueous solution of NH_4Cl, and the aqueous phase was extracted with dichloromethane (3 × 10 mL). After concentration, the crude product was used for the next step without further purification.

The crude hydroquinone was dissolved in 3 mL of DMF. To the solution was added allyl bromide (0.0070 mL, 0.0830 mmol, 5.00 equiv) *n*-Bu_4NI (6.1 mg, 0.0166 mmol, 1.00 equiv), and Cs_2CO_3 (16.2 mg, 0.0498 mmol, 3.00 equiv), successively. The heterogeneous mixture was stirred at 23 °C for 2 hours. After completion of the reaction, the reaction system was quenched with saturated aqueous solution of NH_4Cl (5 mL), and the aqueous phase was extracted with dichloromethane (3 × 5 mL). The combined organic layer was dried over anhydrous Na_2SO_4 and concentrated. The crude product was purified by flash column chromatography (EtOAc/hexane = 1/2) to provide bisallyl ether **2.32** (4.0 mg, 0.00531 mmol, 32% over two steps) as bright yellow foam. ^1H NMR (500 MHz, $CDCl_3$) δ = 8.00 (d, *J* = 7.8 Hz, 2H), 7.74 - 7.68 (m, 1H), 7.65 - 7.58 (m, 2H), 7.21

(d, *J* = 8.8 Hz, 1H), 7.11 (d, *J* = 8.8 Hz, 1H), 6.14 (ddd, *J* = 5.4, 11.0, 16.8 Hz, 1H), 5.51 - 5.43 (m, 1H), 5.40 - 5.21 (m, 3H), 5.20 - 5.11 (m, 2H), 4.89 - 4.77 (m, 2H), 4.61 - 4.38 (m, 4 H), 4.24 (d, *J* = 6.3 Hz, 1H), 3.87 - 3.81 (m, 1H), 3.70 (d, *J* = 6.3 Hz, 1H), 3.66 - 3.60 (m, 2H), 3.55 (s, 3H), 3.51 (s, 3H), 3.49 - 3.45 (m, 2H), 3.33 (s, 3H), 2.82 (dd, *J* = 3.9, 13.7 Hz, 1H), 2.38 - 2.29 (m, 1H), 2.05 (q, *J* = 7.3 Hz, 2H), 0.97 ppm (t, *J* = 7.3 Hz, 3H); HRMS (ESI) calcd for $C_{39}H_{47}O_{13}S$ [M+H$^+$] 755.2737, found: 755.2761.

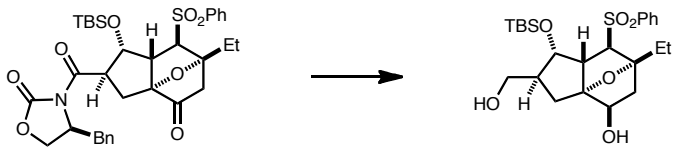

1.101 **2.3**

To the solution of ketone **1.101** (48.0 mg, 0.0734 mmol, 1.00 equiv) in 0.5 mL of MeOH was added $NaBH_4$ (28.0 mg, 0.734 mmol, 10.0 equiv). In 5 minutes, the starting material was fully consumed. Then the mixture was quenched with water (2 mL), and the aqueous phase was extracted with diethyl ether (3 × 5 mL). The combined organic layer was dried over anhydrous $MgSO_4$ and filtered through celite. The crude product was purified by flash column chromatography (EtOAc/hexane = 1/2 to 2/1) to provide diol **2.3** (24.1 mg, 0.0499 mmol, 68%). The product was identical to the previously prepared compound in all aspects.

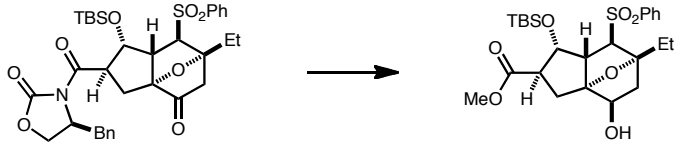

1.101 **2.35**

To the solution of ketone **1.101** (15.8 mg, 0.0241 mmol, 1.00 equiv) in 0.5 mL of MeOH was added $NaBH_4$ (4.6 mg, 0.121 mmol, 5.00 equiv). In 5 minutes, the starting material

was fully consumed. Then the mixture was quenched with anhydrous acetone (2 mL), and the mixture was warmed to 23 °C. The volatiles were removed under reduced pressure, and the resulting suspension was quenched with 2 mL of water. The aqueous phase was extracted with diethyl ether (3 × 5 mL). The combined organic layer was dried over anhydrous $MgSO_4$ and filtered through celite. The crude product was purified by flash column chromatography (EtOAc/hexane = 1/2) to provide methyl ester **2.35** (8.5 mg, 0.0169 mmol, 70%). ^{1}H NMR (500 MHz, $CDCl_3$) δ = 7.90 (d, *J* = 7.8 Hz, 2H), 7.70 - 7.65 (m, 1H), 7.61 - 7.56 (m, 2H), 4.40 (dd, *J* = 3.7, 8.1 Hz, 1H), 4.19 (d, *J* = 8.8 Hz, 1H), 4.10 - 4.04 (m, 1H), 3.70 (s, 3H), 3.43 (dd, *J* = 4.4, 7.8 Hz, 1H), 3.36 - 3.28 (m, 1H), 3.04 (d, *J* = 3.9 Hz, 1H), 2.49 (dd, *J* = 2.9, 14.2 Hz, 1H), 2.27 (dd, *J* = 8.3, 14.2 Hz, 1H), 2.18 - 2.06 (m, 2H), 1.74 (q, *J* = 7.3 Hz, 2H), 0.91 (t, *J* = 7.6 Hz, 3H), 0.76 (s, 9 H), -0.10 (s, 3H), -0.35 ppm (s, 3H); HRMS (ESI) calcd for $C_{25}H_{39}O_7SSi$ [M+H$^+$] 511.2186, found: 511.2205.

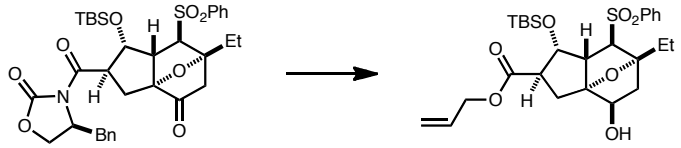

A round bottomed flask was charged with $NaBH_4$ (654 mg, 17.3 mmol, 2.00 equiv). Then allyl alcohol (15 mL) was added to give a turbid suspension. After cooling to –78 °C, a solution of oxazolidinone **1.101** (5.65 g, 8.64 mmol, 1.00 equiv) in 10 mL of diethyl ether (plus 2 × 2 mL rinse) was cannulated to the reaction mixture. 5 minutes later, the pale yellow suspension was quenched with 20 mL of anhydrous acetone at –78 °C, then warmed to room temperature over 15 minutes. Volatiles were removed under reduced pressure and the residue was quenched with 50 mL of water. Then the aqueous phase was

extracted with diethyl ether (3 × 50 mL) and the combined organic layers were dried over $MgSO_4$. After concentration, the crude product was purified by flash column chromatography (EtOAc/hexane = 1/4) to give allyl ester **2.36** (4.13 g, 7.69 mmol, 89%) as a colorless oil. ^{1}H NMR (500 MHz, $CDCl_3$) **δ** = 7.88 (d, *J* = 7.8 Hz, 2H), 7.66 (t, *J* = 7.6 Hz, 1H), 7.56 (t, *J* = 7.8 Hz, 2H), 5.88 (dddd, *J* = 16.9, 11.0, 5.6, 5.6 Hz, 1H), 5.17 - 5.38 (m, 2H), 4.58 (d, *J* = 5.4 Hz, 2H), 4.37 (dd, *J* = 7.6, 3.7 Hz, 1H), 4.13 - 4.22 (m, 1H), 4.04 (d, *J* = 4.4 Hz, 1H), 3.41 (dd, *J* = 7.6, 4.6 Hz, 1H), 3.29 (d, *J* = 8.3 Hz, 1H), 3.05 (ddd, *J* = 8.3, 8.3, 3.9 Hz, 1H), 2.47 (dd, *J* = 14.2, 2.9 Hz, 1H), 2.27 (dd, *J* = 14.4, 8.1 Hz, 1H), 2.05 - 2.16 (m, 2H), 1.73 (q, *J* = 7.7 Hz, 2H), 0.90 (t, *J* = 7.3 Hz, 3H), 0.74 (s, 9H), -0.12 (s, 3H), -0.37 ppm (s, 3H); ^{13}C NMR (125 MHz, $CDCl_3$) δ = 174.0, 140.2, 134.0, 131.7, 129.5, 128.2, 118.6, 97.6, 90.3, 73.5, 72.1, 67.0, 65.5, 55.4, 48.1, 39.8, 30.4, 27.6, 25.7, 17.7, 8.1, -4.7, -5.8 ppm; HRMS (ESI) calcd for $C_{27}H_{44}NO_7Si$ [M+NH_4^+] 554.2602, found: 554.2616.

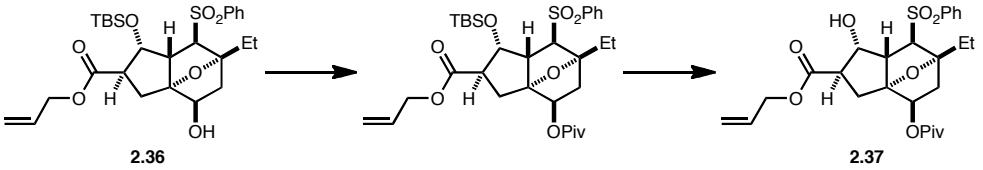

To the solution of allyl ester **2.36** (3.48 g, 6.48 mmol, 1.00 equiv) in 10 mL of dichloromethane was added pyridine (1.20 mL, 9.72 mmol, 1.50 equiv), followed by trimethylacetyl chloride (1.05 mL, 13.0 mmol, 2.00 equiv). The mixture was heated under reflux for 24 hours. After completion of the reaction, the mixture was quenched with saturated aqueous NH_4Cl solution (10 mL), and the aqueous phase was extracted with diethyl ether (3 × 20 mL). The combined organic layers were dried over $MgSO_4$ and concentrated. The crude product was purified by flash column chromatography

(EtOAc/hexane = 1/10 to 1/8).

To the solution of the trimethylacetyl ester in 25 mL of THF was added 1.0 M TBAF solution in THF (7.78 mL, 7.78 mmol, 1.20 equiv) at room temperature. 16 hours later, the mixture was quenched with saturated aqueous NH_4Cl solution (20 mL), and the aqueous phase was extracted with diethyl ether (3 × 50 mL). Then the combined organic layers were dried over $MgSO_4$. The crude product was purified by flash column chromatography (EtOAc/hexane = 1/4 to 1/3) to give compound **2.37** (2.99 g, 5.90 mmol, 91% over two steps) as a colorless oil. ^{1}H NMR (500 MHz, $CDCl_3$) δ = 7.85 - 7.93 (m, 2H), 7.66 (d, *J* = 7.3 Hz, 1H), 7.57 (t, *J* = 8.0, 8.0 Hz, 2H), 5.82 - 5.92 (m, 1H), 5.20 - 5.32 (m, 2H), 4.87 (dd, *J* = 10.1, 3.9 Hz, 1H), 4.52 - 4.63 (m, 2H), 4.17 (dd, *J* = 8.7, 6.4 Hz, 1H), 3.99 (dd, *J* = 6.2, 1.6 Hz, 1H), 3.45 (dd, *J* = 8.7, 6.2 Hz, 1H), 3.07 (ddd, *J* = 10.0, 7.0, 7.0 Hz, 1H), 2.54 (dd, *J* = 14.0, 3.9 Hz, 1H), 2.17 - 2.26 (m, 2H), 1.98 (dd, *J* = 14.4, 10.3 Hz, 1H), 1.87 (br. s, 1H), 1.74 (q, *J* = 7.6 Hz, 2H), 1.27 (s, 9H), 0.87 ppm (t, *J* = 7.4 Hz, 3H); ^{13}C NMR (125 MHz, $CDCl_3$) δ = 178.2, 172.9, 140.0, 133.9, 131.7, 129.3, 128.1, 118.5, 94.1, 89.8, 72.5, 72.3, 66.8, 65.5, 52.5, 47.1, 38.7, 36.5, 29.4, 27.2, 27.1, 7.7 ppm; HRMS (ESI) calcd for $C_{26}H_{35}O_8S$ [M+H$^+$] 507.2047, found: 507.2046.

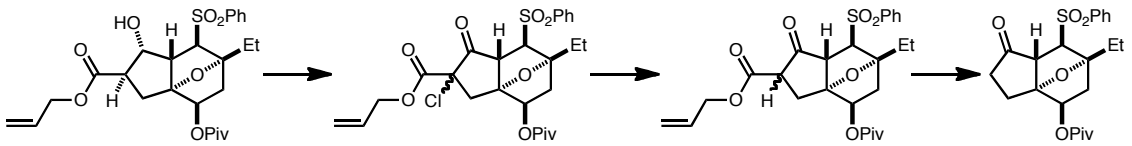

To a solution of oxalyl chloride (1.54 mL, 17.7 mmol, 3.00 equiv) in dichloromethane (30 mL) was added DMSO (1.26 mL, 17.7 mmol, 3.00 equiv) over a 5-minute period at –78 °C. Gas evolution was observed. 30 minutes later, a solution of alcohol **2.37** (2.99 g,

5.90 mmol, 1.00 equiv) in 15 mL of dichloromethane (plus 2 × 5 mL rinse) was cannulated to the reaction mixture over a 5-minute period. After stirring for 30 minutes, Et_3N (4.11 mL, 29.5 mmol, 5.00 equiv) was added in one portion to give a white suspension. The reaction system was warmed to room temperature over 30 minutes and diluted with 50 mL of diethyl ether. The resulting slurry was filtered through a pad of celite/florisil and the filter cake was washed with diethyl ether. After concentration, the crude α-chloro β-keto ester **2.39** was used for the next step without further purification.

The α-chloro β-keto ester **2.39** was dissolved in acetic acid (20 mL) and to the solution was added zinc dust at room temperature. The heterogeneous mixture was vigorously stirred for 2 hours, then diluted with dichloromethane (20 mL) before being filtered through a celite pad. After concentration under reduced pressure, the mixture was azeotroped with toluene to further remove residual acetic acid. The crude product was purified by flash column chromatography (EtOAc/hexane = 1/5 to 1/3) to give β-keto ester **2.40** (2.85 g, 5.66 mmol, 96% over two steps) as a colorless oil.

To a solution of β-keto ester **2.40** (10.1 g, 20.0 mmol, 1.00 equiv) in 60 mL of toluene was added acetic acid (5.72 mL, 100 mmol, 5.00 equiv), $PdCl_2(PPh_3)_2$ (702 mg, 1.00 mmol, 0.050 equiv), and *n*-Bu_3SnH (5.92 mL, 22.0 mmol, 1.10 equiv), successively at 0 °C. After full conversion to the corresponding β-keto acid, the mixture was heated to reflux for 30 minutes. After completion of the decarboxylation, volatiles were removed under reduced pressure and the crude product was purified by flash column chromatography (EtOAc/hexane = 1/7 to 1/5) to give ketone **2.41** (7.15 g, 17.0 mmol, 85%) as a white foam. ^{1}H NMR (500 MHz, $CDCl_3$) δ = 7.89 (dd, *J* = 8.0, 1.1 Hz, 2H), 7.68 (tt, *J* = 7.3, 1.0 Hz, 1H), 7.59 (t, *J* = 7.8, 7.8 Hz, 2H), 4.97 (dd, *J* = 10.3, 3.4 Hz,

1H), 3.48 (dd, *J* = 5.0, 1.8 Hz, 1H), 3.42 (d, *J* = 5.0 Hz, 1H), 2.60 (dd, *J* = 14.2, 3.2 Hz, 1H), 2.44 (dd, *J* = 10.3, 6.2 Hz, 2H), 2.31 (ddd, *J* = 14.3, 10.2, 2.1 Hz, 1H), 2.12 - 2.26 (m, 2H), 1.96 (qd, *J* = 7.5, 1.8 Hz, 2H), 1.30 (s, 9H), 0.95 ppm (t, *J* = 7.6 Hz, 3H); ^{13}C NMR (125 MHz, $CDCl_3$) δ = 213.9, 178.1, 140.0, 134.0, 129.3, 128.1, 92.5, 91.4, 72.8, 71.1, 54.2, 38.8, 36.8, 36.5, 27.2, 27.1, 23.2, 8.0 ppm; HRMS (ESI) calcd for $C_{22}H_{32}NO_6S$ [M+NH_4^+] 438.1945, found: 438.1902.

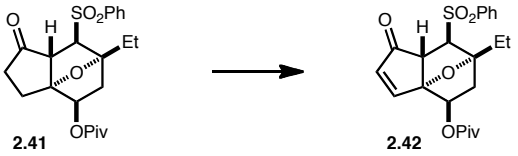

LiHMDS solution was generated by adding *n*-BuLi (2.36 M in hexanes, 3.85 mL, 9.08mmol, 1.10 equiv) to a solution of HMDS (1.92 mL, 9.08 mmol, 1.10 equiv) in 70 mL of THF and stirring for 40 minutes at –78 °C. Then a solution of ketone **2.41** (3.47g, 8.25 mmol, 1.00 equiv) in 25 mL of THF (plus 2 × 5 mL rinse) was cannulated to the reaction mixture to give a pale yellow solution. After stirring for 30 minutes, a solution of phenylselenyl bromide (2.14 g, 9.08 mmol, 1.10 equiv) in 10 mL of THF was cannulated to the reaction mixture to give a deep yellow solution. In 5 minutes, the reaction was quenched with saturated aqueous NH_4Cl, and the aqueous phase was extracted with diethyl ether (3 × 50 mL). The crude selenide was concentrated under reduced pressure and was dissolved in 1:1 dichloromethane/THF. After cooling to 0 °C, a 30 wt% aqueous solution of H_2O_2 (1.85 mL, 18.2 mmol, 2.20 equiv) was added. The mixture was stirred at 0 °C for 4 hours then quenched with a 0.1 M aqueous solution of $Na_2S_2O_3$ (30 mL). The aqueous phase was extracted with diethyl ether (3 × 50 mL) and the combined organic layers were dried with $MgSO_4$. The crude enone was purified by flash column

chromatography (EtOAc/hexane = 1/7 to 1/5) to give enone **2.42** (2.52 g, 6.02 mmol, 73%) as a colorless oil. ^{1}H NMR (500 MHz, $CDCl_3$) δ = 7.92 (dd, *J* = 8.5, 1.1 Hz, 2H), 7.72 (tt, *J* = 7.8, 1.0 Hz, 1H), 7.62 (dd, *J* = 8.2, 8.2 Hz, 2H), 7.45 (d, *J* = 5.5 Hz, 1H), 6.14 (d, *J* = 5.5 Hz, 1H), 5.23 (dd, *J* = 10.3, 3.9 Hz, 1H), 3.64 (d, *J* = 6.9 Hz, 1H), 3.60 (dd, *J* = 6.4, 1.4 Hz, 1H), 2.82 (dd, *J* = 14.0, 3.9 Hz, 1H), 2.43 (ddd, *J* = 14.2, 10.1, 1.8 Hz, 1H), 2.09 (dq, *J* = 15.0, 7.4 Hz, 1H), 1.98 (dq, *J* = 14.9, 7.4 Hz, 1H), 1.27 (s, 9H), 0.99 ppm (t, *J* = 7.3 Hz, 3H); ^{13}C NMR (125 MHz, $CDCl_3$) δ = 202.8, 178.3, 152.5, 140.0, 138.6, 134.1, 129.4, 128.2, 95.0, 91.8, 72.6, 68.3, 52.2, 38.8, 37.3, 27.8, 27.1, 7.9 ppm; HRMS (ESI) calcd for $C_{22}H_{27}O_6S$ [M+H$^+$] 419.1523, found: 419.1514.

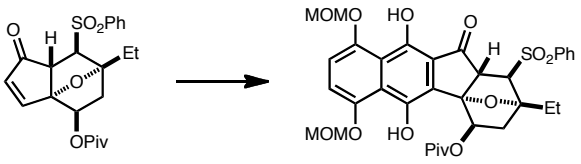

2.42 **2.43**

LiHMDS-HMPA solution was prepared in a two neck flask equipped with a cold finger by mixing 1.60 M hexane solution of *n*-BuLi (0.0520 mL, 0.0832 mmol, 1.20 equiv), HMDS (0.0176 mL, 0.0832 mmol, 1.20 equiv), and HMPA (0.0145 mL, 0.0832 mmol, 1.20 equiv) in 1.0 mL of THF at –78 °C. 20 minutes later, cyanophthalide **2.10** (23.0 mg, 0.0832 mmol, 1.20 equiv) in 0.5 mL of THF (plus 0.5 mL rinse) was cannulated to the LiHMDS-HMPA solution to give a bright yellow solution. 30 minutes later, enone **2.42** (29.0 mg, 0.0693 mmol, 1.00 equiv) in 1 mL of THF (plus 0.5 mL rinse) was cannulated to the reaction mixture at –78 °C. The mixture was stirred at –78 °C for 30 minutes, and warmed to 23 °C over 30 minutes. Then the flask was heated to 50 °C for 20 minutes. The mixture was cooled to 23 °C and quenched with saturated aqueous solution of

NH_4Cl, and the aqueous phase was extracted with dichloromethane (3 × 5 mL). The combined organic layer was dried over anhydrous Na_2SO_4 and concentrated. The crude product was purified by flash column chromatography (EtOAc/hexane = 1/2 to 1.5/1) to provide hydroquinone **2.43** (39.5 mg, 0.0589 mmol, 85%). ^{1}H NMR (500 MHz, $CDCl_3$) δ = 10.17 (s, 1H), 9.52 (s, 1H), 7.98 (d, *J* = 7.8 Hz, 2H), 7.71 (d, *J* = 7.8 Hz, 1H), 7.67 - 7.59 (m, 2H), 7.19 (d, *J* = 8.8 Hz, 1H), 7.02 (d, *J* = 8.8 Hz, 1H), 6.20 (dd, *J* = 3.7, 10.0 Hz, 1H), 5.39 - 5.34 (m, 2H), 5.32 (s, 2H), 4.15 (d, *J* = 6.3 Hz, 1H), 3.79 (d, *J* = 5.9 Hz, 1H), 3.56 (s, 3H), 3.52 (s, 3H), 2.75 (dd, *J* = 3.4, 14.2 Hz, 1H), 2.58 (d, *J* = 11.7 Hz, 1H), 2.20 (dd, *J* = 7.6, 14.9 Hz, 1H), 2.11 - 2.00 (m, 1H), 1.23 (s, 9 H), 1.01 ppm (t, *J* = 7.3 Hz, 3H); HRMS (ESI) calcd for $C_{34}H_{42}NO_{12}S$ [M+NH_4^+] 688.2428, found: 688.2422.

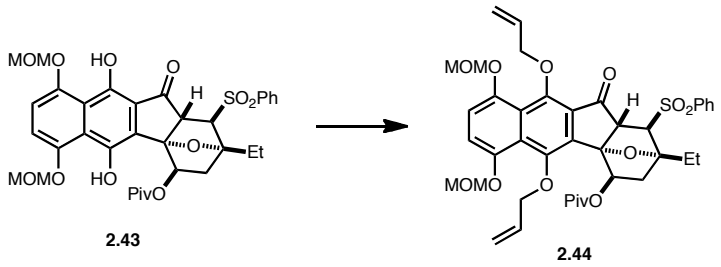

To the solution of hydroquinone **2.43** (10.0 mg, 0.0150 mmol, 1.00 equiv) and PPh_3 (11.8 mg, 0.0450 mmol, 3.00 equiv) in 0.8 mL of THF were added allyl alcohol (0.0031 mL, 0.0450 mmol, 3.00 equiv) and DIAD (0.0089 mL, 0.0450 mmol, 3.00 equiv) at 23 °C. The reaction flask was attached to a cold finger, then the mixture was heated to 50 °C for 1 hour. After completion of the reaction, the mixture was concentrated under reduced pressure. The crude product was purified by flash column chromatography (EtOAc/hexane = 1/5 to 1/10) to provide bisallyl ether **2.44** (10.0 mg, 0.0133 mmol, 89%). ^{1}H NMR (500 MHz, $CDCl_3$) δ = 7.97 (d, *J* = 7.8 Hz, 2H), 7.71 (d, *J* = 7.3 Hz, 1H),

7.66 - 7.60 (m, 2H), 7.24 (d, *J* = 8.8 Hz, 1H), 7.14 (d, *J* = 8.3 Hz, 1H), 6.15 (dd, *J* = 5.9, 11.2 Hz, 2H), 6.08 (dd, *J* = 3.7, 10.0 Hz, 1H), 5.45 (d, *J* = 17.1 Hz, 1H), 5.39 - 5.30 (m, 2H), 5.24 (d, *J* = 10.3 Hz, 1H), 5.20 - 5.14 (m, 4 H), 4.98 (s, 1H), 4.55 (d, *J* = 5.4 Hz, 1H), 4.49 (dd, *J* = 6.3, 10.7 Hz, 1H), 4.45 (d, *J* = 3.9 Hz, 2H), 4.17 (d, *J* = 6.3 Hz, 1H), 3.75 (d, *J* = 5.9 Hz, 1H), 3.55 (s, 3H), 3.52 (s, 3H), 2.73 (dd, *J* = 3.4, 14.2 Hz, 1H), 2.57 (d, *J* = 10.7 Hz, 1H), 2.07 - 1.98 (m, 2H), 1.19 (s, 9 H), 0.97 ppm (t, *J* = 7.3 Hz, 3H); HRMS (ESI) calcd for $C_{40}H_{47}O_{12}S$ [$M+H^+$] 751.2788, found: 751.2801.

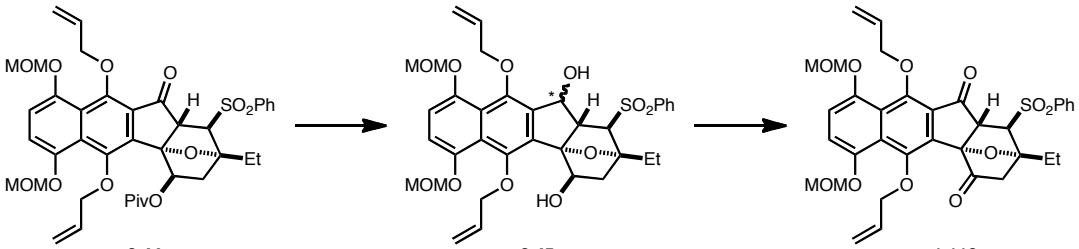

To the solution of ester **2.44** (26.7 mg, 0.0356 mmol, 1.00 equiv) in 1 mL of dichloromethane was added 1.0 M toluene solution of DIBAL-H (0.0710 mL, 0.0710 mmol, 2.00 equiv) at –78 °C. After stirring for 2 hours, the mixture was quenched with saturated aqueous solution of potassium sodium tartrate (2 mL) and warmed to 23 °C. After stirring for 1 hour, the aqueous phase was extracted with dichloromethane (3 × 5 mL), and the combined organic layer was dried over anhydrous Na_2SO_4. After concentration, the crude diol **2.45** was used for the next step without further purification.

To the solution of oxalyl chloride (0.0310 mL, 0.356 mmol, 10.0 equiv) in 1.5 mL of dichloromethane was added DMSO (0.0250 mL, 0.356 mmol, 10.0 equiv) at –78 °C. 30 minutes later, diol **2.45** in 1 mL of dichloromethane (plus 2 × 0.5 mL rinse) was cannulated to the reaction mixture. 1 hour later, Et_3N (0.0740 mL, 0.534 mmol, 15 equiv)

was added in one portion, and the reaction system was warmed to 23 °C over 1 hour. The mixture was diluted with 5 mL of diethyl ether and filtered over a fluorisil pad. After concentration, the crude product was purified by flash column chromatography (EtOAc/hexane = 1/4 to 1/3) to provide ketone **2.46** (14.0 mg, 0.0210 mmol, 59% over two steps). ^{1}H NMR (500 MHz, $CDCl_3$) δ = 7.95 (d, *J* = 7.6 Hz, 2H), 7.77 - 7.71 (m, 1H), 7.67 - 7.61 (m, 2H), 7.29 - 7.25 (m, 1H), 7.16 (d, *J* = 8.7 Hz, 1H), 6.16 - 6.01 (m, 2H), 5.42 - 5.30 (m, 2H), 5.26 - 5.12 (m, 6 H), 4.63 (dd, *J* = 5.2, 11.6 Hz, 1H), 4.53 - 4.45 (m, 2H), 4.38 (dd, *J* = 5.3, 11.4 Hz, 1H), 3.84 (d, *J* = 5.5 Hz, 1H), 3.58 (d, *J* = 5.5 Hz, 1H), 3.55 (s, 3H), 3.52 (s, 3H), 2.74 (d, J = 17.9 Hz, 1H), 2.22 - 2.22 (m, 1H), 2.26 - 2.19 (m, 1H), 1.06 ppm (t, J = 7.3 Hz, 3H); ^{13}C NMR (125 MHz, $CDCl_3$) δ = 202.7, 194.8, 152.0, 151.4, 150.1, 149.2, 139.4, 134.4, 133.9, 133.8, 129.6, 128.3, 128.1, 126.9, 126.2, 126.1, 118.1, 117.8, 116.7, 115.8, 97.5, 97.0, 92.6, 90.7, 76.9, 76.9, 68.4, 59.6, 56.5, 56.5, 45.1, 36.6, 29.7, 27.8, 24.7, 7.9 ppm; HRMS (ESI) calcd for $C_{35}H_{37}O_{11}S$ [M+H$^+$] 665.2057, found: 665.2059.

2.42 **2.59**

LiHMDS-HMPA solution was prepared in a two neck flask equipped with a cold finger by mixing 0.80 M hexane solution of *n*-BuLi (0.266 mL, 0.213 mmol, 1.05 equiv), HMDS (0.047.1 mL, 0.223 mmol, 1.10 equiv), and HMPA (37.1 μL, 0.213 mmol, 1.05 equiv) in 2.5 mL of THF at –78 °C. 20 minutes later, cyanophthalide **2.58** (46.7 mg, 0.213 mmol, 1.05 equiv) in 1.5 mL of THF (plus 0.5 mL rinse) was cannulated to the

LiHMDS-HMPA solution to give a bright yellow solution. 30 minutes later, enone **2.42** (85.0 mg, 0.203 mmol, 1.00 equiv) in 1 mL of THF (plus 0.5 mL rinse) was cannulated to the reaction mixture at –78 °C. The mixture was stirred at –78 °C for 30 minutes, and warmed to 23 °C over 30 minutes. Then the flask was heated to 50 °C for 20 minutes. The mixture was cooled to 23 °C and quenched with saturated aqueous solution of NH_4Cl, and the aqueous phase was extracted with dichloromethane (3 × 5 mL). The combined organic layer was dried over anhydrous Na_2SO_4 and concentrated. The crude product was purified by flash column chromatography (EtOAc/hexane = 1/1 to 2/1) to provide hydroquinone **2.59** (111 mg, 0.172 mmol, 85%). ^{1}H NMR (500 MHz, $CDCl_3$) δ = 10.18 (s, 1H), 9.54 (s, 1H), 7.97 (d, *J* = 7.6 Hz, 2H), 7.73 - 7.65 (m, 1H), 7.64 - 7.57 (m, 2H), 6.77 (d, *J* = 8.7 Hz, 1H), 6.67 (d, *J* = 8.7 Hz, 1H), 6.20 (dd, *J* = 3.3, 10.0 Hz, 1H), 4.12 (d, *J* = 6.2 Hz, 1H), 3.96 (s, 3H), 3.95 (s, 3H), 3.78 (d, *J* = 6.0 Hz, 1H), 2.74 (dd, *J* = 3.4, 14.0 Hz, 1H), 2.61 - 2.50 (m, 1H), 2.17 (td, *J* = 7.4, 14.8 Hz, 1H), 2.10 - 1.99 (m, 1H), 1.22 (s, 9H), 1.01 ppm (t, *J* = 7.3 Hz, 3H); ^{13}C NMR (125 MHz, $CDCl_3$) δ = 198.5, 178.0, 153.0, 151.2, 147.7, 145.4, 140.1, 133.9, 129.2, 128.2, 128.2, 120.9, 119.3, 118.7, 118.2, 107.9, 106.0, 92.9, 89.1, 71.4, 68.8, 56.8, 56.6, 55.9, 38.7, 38.5, 27.6, 27.1, 8.0 ppm; HMRS (ESI) calcd for $C_{32}H_{35}O_{10}S$ [M+H$^+$] 611.1951, found: 611.1988.

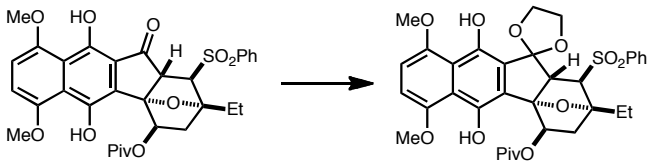

2.59 **2.60**

To a solution of ketone **2.59** (26.3 mg, 0.0430 mmol, 1.00 equiv) in 1 mL of dichloromethane was added 1,2-bis(trimethylsilyloxy)ethane (0.0211 mL, 0.0860 mmol,

2.00 equiv), followed by TMSOTf (0.0078 mL, 0.0430 mmol, 1.00 equiv) at 23 °C. The reaction was vigorously stirred for 36 hours. Upon completion of the reaction, the mixture was quenched with saturated aqueous $NaHCO_3$ at 0 °C and the aqueous phase was extracted with dichloromethane (3 × 5 mL). The combined organic layers were dried over Na_2SO_4 and the crude product was purified by flash column chromatography (EtOAc/hexane = 1/1.5 to 1/1) to give dioxolane **2.60** (21.4 mg, 0.0327 mmol, 76%) as a pale yellow solid. ^{1}H NMR (500 MHz, $CDCl_3$) δ = 9.56 (s, 1H), 9.48 (s, 1H), 8.02 (d, *J* = 7.6 Hz, 2H), 7.72 - 7.65 (m, 1H), 7.63 - 7.56 (m, 2H), 6.62 - 6.56 (m, 2H), 6.21 (dd, *J* = 3.3, 10.2 Hz, 1H), 4.20 - 4.03 (m, 4 H), 3.94 (s, 3H), 3.93 (s, 3H), 3.30 - 3.22 (m, 1H), 3.03 - 2.96 (m, 1H), 2.72 (dd, *J* = 3.3, 13.8 Hz, 1H), 2.52 - 2.42 (m, 1H), 2.16 - 2.06 (m, 1H), 2.03 - 1.95 (m, 1H), 1.21 (s, 9 H), 1.05 ppm (t, *J* = 7.3 Hz, 3H); ^{13}C NMR (125 MHz, $CDCl_3$) δ = 178.3, 151.5, 151.5, 145.2, 142.7, 141.0, 133.5, 129.1, 128.8, 127.5, 118.6, 117.7, 116.7, 113.2, 104.7, 104.1, 92.6, 91.8, 71.3, 67.3, 65.6, 56.6, 56.3, 55.0, 38.7, 38.2, 36.6, 29.7, 27.6, 27.1, 24.6, 8.0 ppm; HRMS (ESI) calcd for $C_{34}H_{38}NaO_{11}S$ [M+Na^+] 677.2027, found: 677.2044.

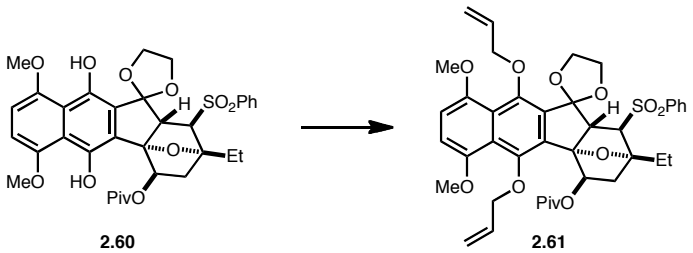

To a solution of hydroquinone **2.60** (20.3 mg, 0.0310 mmol, 1.00 equiv) in 0.6 mL of DMF was added allyl bromide (0.0027 mL, 0.310 mmol, 10.0 equiv), followed by Cs_2CO_3 (30.3 mg, 0.0930 mmol, 3.00 equiv). The resulting red solution was vigorously stirred for 2 hours, then the reaction was quenched with saturated aqueous NH_4Cl, and

the aqueous phase was extracted with dichloromethane (3 × 5 mL). After drying over Na_2SO_4 and concentrating under reduced pressure, the crude product was purified by flash column chromatography (EtOAc/hexane = 1/3) to give bisallyl ether **2.61** (19.8 mg, 0.0270 mmol, 87%) as a pale yellow foam. ^{1}H NMR (500 MHz, $CDCl_3$) δ = 8.00 (d, *J* = 7.6 Hz, 2H), 7.70 - 7.64 (m, 1H), 7.63 - 7.55 (m, 2H), 6.78 (s, 2H), 6.23 - 6.07 (m, 2H), 6.02 (dd, *J* = 2.5, 9.8 Hz, 1H), 5.40 (dd, *J* = 8.7, 17.2 Hz, 2H), 5.28 (d, *J* = 10.5 Hz, 1H), 5.20 (d, *J* = 10.5 Hz, 1H), 4.46 - 4.37 (m, 3H), 4.36 - 4.30 (m, 1H), 4.14 - 4.05 (m, 3H), 4.01 (d, *J* = 5.3 Hz, 1H), 3.86 (s, 3H), 3.81 (s, 3H), 3.23 (br. s, 1H), 2.98 (br. s, 1H), 2.65 (dd, *J* = 2.7, 14.0 Hz, 1H), 2.56 - 2.46 (m, 1H), 1.98 (q, *J* = 7.1 Hz, 2H), 1.19 (s, 9 H), 1.02 ppm (t, *J* = 7.2 Hz, 3H); ^{13}C NMR (125 MHz, CDCl3) δ = 177.8, 150.8, 150.7, 150.3, 148.1, 140.8, 135.7, 135.1, 134.0, 133.6, 129.1, 128.6, 128.2, 125.1, 124.8, 117.4, 115.8, 113.3, 108.0, 107.5, 92.7, 91.8, 77.6, 76.6, 71.7, 69.1, 66.7, 65.4, 57.0, 56.8, 54.9, 38.6, 36.8, 29.6, 27.6, 27.1, 8.1 ppm; HRMS (ESI) calcd for $C_{40}H_{46}NaO_{11}S$ [M+Na^+] 757.2653, found: 757.2748.

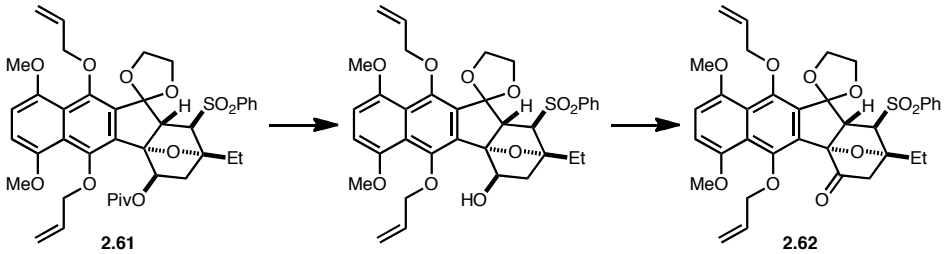

The trimethylacetyl ester **2.61** (9.2 mg, 0.0125 mmol, 1.00 equiv) was dissolved in 1 mL of THF and cooled to 0 °C. To the solution was added 1.0 M $NaBHEt_3$ solution in THF (0.0625 mL, 0.0625 mmol, 5.00 equiv) via syringe. The mixture was vigorously stirred at 0 °C for 2 hours. After completion of the reaction, the mixture was quenched with saturated aqueous NH_4Cl and the aqueous phase was extracted with dichloromethane (3 ×

1 mL). After drying over Na_2SO_4 and concentrating under reduced pressure, the crude product was purified by flash column chromatography (EtOAc/hexane = 1/2 to 1/1.5) to give the corresponding alcohol as a white foam.

A flask was charged with the alcohol, TPAP (0.2 mg, 0.000630 mmol, 0.0500 equiv), NMO (2.2 mg, 0.0188 mmol, 1.50 equiv), and 4 Å MS (5 mg), then 0.5 mL of dichloromethane was added. The reaction was vigorously stirred at room temperature for 2 hours. After completion of the reaction, the mixture was diluted with 3 mL of diethyl ether and the resulting suspension was filtered through a pad of celite. After concentration, the crude product was purified by flash column chromatography (EtOAc/hexane = 1/3 to 1/2) to give ketone **2.62** (7.3 mg, 0.0113 mmol, 90% over two steps) as a white solid. ^{1}H NMR (500 MHz, $CDCl_3$) δ = 8.00 (d, *J* = 7.6 Hz, 2H), 7.74 - 7.67 (m, 1H), 7.65 - 7.59 (m, 2H), 6.84 - 6.77 (m, 2H), 6.17 - 6.01 (m, 2H), 5.42 - 5.30 (m, 2H), 5.24 - 5.16 (m, 2H), 4.53 (dd, *J* = 5.3, 11.4 Hz, 1H), 4.42 - 4.36 (m, 1H), 4.33 (d, *J* = 5.5 Hz, 1H), 4.31 (d, *J* = 5.7 Hz, 1H), 4.12 - 4.06 (m, 1H), 4.05 - 3.98 (m, 2H), 3.86 (s, 3H), 3.83 (s, 3H), 3.54 (d, *J* = 5.3 Hz, 1H), 3.42 (d, *J* = 17.9 Hz, 1H), 3.26 (d, *J* = 6.4 Hz, 1H), 2.77 (q, *J* = 6.0 Hz, 1H), 2.70 (dd, *J* = 1.0, 17.7 Hz, 1H), 2.36 - 2.25 (m, 1H), 2.25 - 2.17 (m, 1H), 1.12 ppm (t, *J* = 7.4 Hz, 3H); ^{13}C NMR (125 MHz, $CDCl_3$) δ = 204.3, 151.0, 150.8, 150.1, 148.1, 140.1, 135.6, 135.1, 134.5, 134.0, 129.3, 128.9, 125.6, 125.1, 123.1, 116.4, 116.0, 113.8, 108.5, 107.9, 93.9, 92.5, 77.2, 76.8, 68.2, 66.8, 65.3, 58.7, 57.1, 57.0, 44.7, 29.7, 27.9, 8.1 ppm; HRMS (ESI) calcd for $C_{35}H_{37}O_{10}S$ [$M+H^+$] 649.2102, found: 649.2090.

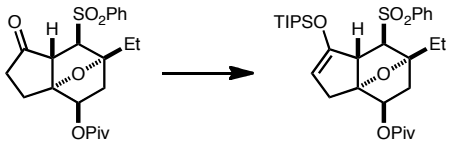

2.41 **3.2**

To the cooled (–78 °C) solution of ketone **2.41** (115 mg, 0.273 mmol, 1.00 equiv) in 3 mL of THF was added 1.0 M THF solution of NaHMDS (0.328 mL, 0.328 mmol, 1.20 equiv). The mixture was stirred at –78 °C for 1 hour. Then TIPSOTf was added to the reaction mixture to give a pale yellow solution. The mixture was stirred at –78 °C for 1.5 hour before being warmed to 23 °C over 30 minutes. After completion of the reaction, it was quenched with saturated aqueous solution of NH_4Cl (5 mL), and the aqueous phase was extracted with diethyl ether (3 × 5 mL). After concentration, the crude product was purified by flash column chromatography (EtOAc/hexane = 1/20 to 1/10) to provide enolsilane **3.2** (156 mg, 0.270 mmol, 99%). ^{1}H NMR (500 MHz, $CDCl_3$) δ = 7.89 (d, *J* = 8.0 Hz, 2H), 7.62 (d, *J* = 7.6 Hz, 1H), 7.57 - 7.51 (m, 2H), 4.92 (dd, *J* = 3.4, 10.1 Hz, 1H), 4.49 (br. s, 1H), 4.05 (d, *J* = 4.8 Hz, 1H), 3.61 (d, *J* = 4.6 Hz, 1H), 2.61 (dd, *J* = 3.5, 14.1 Hz, 1H), 2.52 - 2.45 (m, 1H), 2.36 (dd, *J* = 2.5, 16.3 Hz, 1H), 2.27 - 2.19 (m, 1H), 1.78 - 1.69 (m, 2H), 1.02 - 0.94 (m, 21H), 0.86 ppm (t, J = 7.3 Hz, 3H); HRMS (ESI) calcd for $C_{31}H_{48}NaO_6SSi$ [M+Na^+] 599.2839, found: 599.2860.

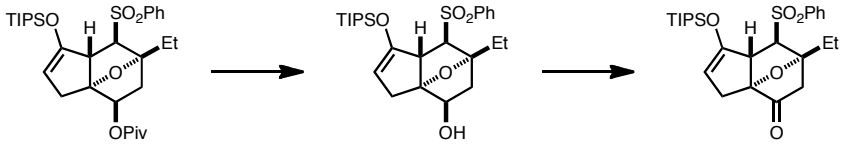

3.2 **3.3**

The trimethylacetyl ester **3.2** (25.0 mg, 0.0430 mmol, 1.00 equiv) was dissolved in 1 mL of THF and cooled to 0 °C. To the solution was added 1.0 M $NaBHEt_3$ solution in THF

(0.215 mL, 0.215 mmol, 5.00 equiv) via syringe. The mixture was vigorously stirred at 0 °C for 2 hours. After completion of the reaction, the mixture was quenched with saturated aqueous NH_4Cl and the aqueous phase was extracted with dichloromethane (3 × 1 mL). After drying over Na_2SO_4 and concentrating under reduced pressure, the crude product was purified by flash column chromatography (EtOAc/hexane = 1/5 to 1/4) to give the corresponding alcohol as a white foam.

A flask was charged with the alcohol, TPAP (0.8 mg, 0.00215 mmol, 0.0500 equiv), NMO (7.6 mg, 0.0645 mmol, 1.50 equiv), and 4 Å MS (10 mg), then 1 mL of dichloromethane was added. The reaction was vigorously stirred at 23 °C for 2 hours. After completion of the reaction, the mixture was diluted with 3 mL of diethyl ether and the resulting suspension was filtered through a pad of celite. After concentration, the crude product was purified by flash column chromatography (EtOAc/hexane = 1/20 to 1/10) to give ketone **3.3** (19.8 mg, 0.0404 mmol, 94% over two steps) as a white solid. ^{1}H NMR (500 MHz, $CDCl_3$) δ = 7.89 (d, *J* = 7.8 Hz, 2H), 7.67 - 7.62 (m, 1H), 7.58 - 7.53 (m, 2H), 4.53 (d, *J* = 1.6 Hz, 1H), 3.68 (d, *J* = 4.6 Hz, 1H), 3.64 (br. s, 1H), 3.37 (d, *J* = 18.1 Hz, 1H), 2.85 (d, *J* = 16.7 Hz, 1H), 2.45 (d, *J* = 18.1 Hz, 1H), 2.30 (dd, *J* = 2.7, 16.7 Hz, 1H), 2.10 - 2.00 (m, 2H), 1.00 (t, *J* = 7.4 Hz, 3H), 0.96 - 0.89 ppm (m, 21H); ^{13}C NMR (125 MHz, $CDCl_3$) δ = 206.7, 150.8, 140.4, 133.9, 129.4, 128.4, 99.0, 94.9, 88.9, 67.7, 54.9, 44.9, 27.6, 27.1, 17.8, 17.8, 12.6, 7.7 ppm; HRMS (ESI) calcd for $C_{26}H_{39}O_5SSi$ [M+H$^+$] 491.2287, found: 491.2266.

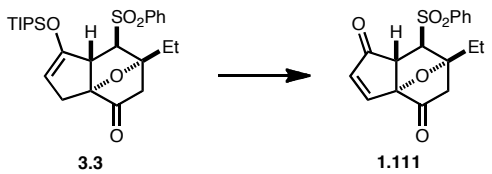

To the solution of enolsilane **3.3** (10.9 mg, 0.0222 mmol, 1.00 equiv) and $Pd(OAc)_2$ (0.5 mg, 0.00222 mmol, 0.100 equiv) in 0.5 mL of DMSO was heated to 80 °C under oxygen atmosphere. In 9 hours, the mixture was quenched with saturated aqueous soluution of $NaHCO_3$ (2 mL) and the aqueous phase was extracted with EtOAc (3 × 5 mL). The combined organic layer was washed with water and brine, then the crude product was purified by flash column chromatography (EtOAc/hexane = 1/5) to provide enone **1.111** (5.2 mg, 0.0158 mmol, 71%). The product was identical to the previously prepared compound in all aspects.

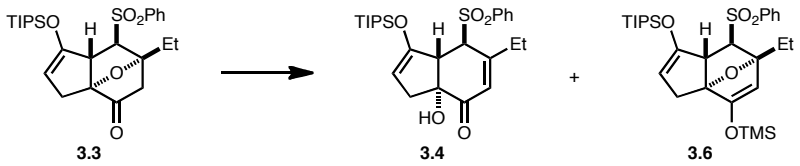

β-elimination product **3.4**

^{1}H NMR (500 MHz, $CDCl_3$) δ = 7.84 (d, *J* = 7.3 Hz, 2H), 7.65 - 7.60 (m, 1H), 7.57 - 7.51 (m, 2H), 5.49 (s, 1H), 4.56 (d, *J* = 2.3 Hz, 1H), 3.53 - 3.43 (m, 2H), 3.19 (d, *J* = 8.7 Hz, 1H), 2.72 (d, *J* = 16.3 Hz, 1H), 2.57 (td, *J* = 7.5, 14.6 Hz, 2H), 2.36 (d, *J* = 16.0 Hz, 1H), 1.29 (t, *J* = 7.6 Hz, 3H), 1.02 - 0.90 ppm (m, 21H); HRMS (ESI) calcd for $C_{26}H_{39}O_5SSi$ [$M+H^+$] 491.2287, found: 491.2295.

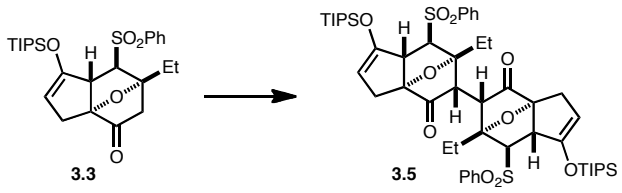

To the solution of HMDS (0.0876 mL, 0.415 mmol, 1.67 equiv) in 1 mL of THF was added 0.84 M hexane solution of *n*-BuLi (0.494 mL, 0.415 mmol, 1.67 equiv) and HMPA

(0.0722 mL, 0.415 mmol, 1.67 equiv) at –78 °C. 40 minutes later, ketone **3.3** (122 mg, 0.249 mmol, 1.00 equiv) in 1 mL of THF (plus 0.3 mL rinse) was cannulated. 1 hour later, $[Cp_2Fe]PF_6$ (247 mg, 0.747 mmol, 3.00 equiv) was added from the solid addition adaptor and the reaction system was warmed to –60 °C. 16 hours later, the mixture was quenched with saturated aqueous solution of NH_4Cl and warmed to 23 °C. The aqueous phase was extracted with diethyl ether (3 × 5 mL), and the combined organic layer was dried over anhydrous $MgSO_4$. After concentration, the crude product was purified by flash column chromatography (EtOAc/hexane = 1/20 to 1/10) to provide dimer **3.5** (69.0 mg, 0.142 mmol, 57%). ^{1}H NMR (500 MHz, $CDCl_3$) δ = 7.93 (d, *J* = 7.3 Hz, 2H), 7.68 - 7.62 (m, 1H), 7.61 - 7.56 (m, 2H), 4.55 (br. s, 1H), 4.08 (s, 1H), 3.92 (d, *J* = 5.0 Hz, 1H), 3.68 (d, *J* = 3.7 Hz, 1H), 2.80 (d, *J* = 16.7 Hz, 1H), 2.37 - 2.31 (m, 1H), 2.34 - 2.25 (m, 1H), 1.85 (dd, *J* = 7.4, 14.8 Hz, 1H), 1.02 - 0.94 (m, 21H), 0.95 - 0.92 ppm (m, 3H); ^{13}C NMR (125 MHz, $CDCl_3$) δ = 205.8, 150.8, 140.0, 134.0, 129.5, 128.4, 128.3, 99.3, 93.3, 90.5, 66.2, 53.8, 48.5, 27.1, 24.2, 17.8, 12.6, 7.7 ppm; HRMS (ESI) calcd for $C_{52}H_{78}NO_{10}S_2Si_2$ [M+NH_4^+] 996.4600, found: 996.4600.

To the solution of dimer **3.5** (30.5 mg, 0.0311 mmol, 1.00 equiv) and $Pd(OAc)_2$ (14.0 mg, 0.0622 mmol, 2.00 equiv) in 3 mL of DMSO was heated to 80 °C under oxygen atmosphere. In 16 hours, the mixture was quenched with saturated aqueous soliution of $NaHCO_3$ (5 mL) and the aqueous phase was extracted with EtOAc (3 × 10 mL). The

combined organic layer was washed with water and brine, then the crude product was purified by flash column chromatography (EtOAc/hexane = 1/5) to provide enone **3.8** (12.5 mg, 0.0183 mmol, 59%). ^{1}H NMR (500 MHz, $CDCl_3$) δ = 7.96 (d, *J* = 7.8 Hz, 2H), 7.79 - 7.72 (m, 1H), 7.69 - 7.61 (m, 2H), 7.54 (d, *J* = 5.7 Hz, 1H), 6.27 (d, *J* = 5.7 Hz, 1H), 3.92 (s, 1H), 3.80 (d, *J* = 6.6 Hz, 1H), 3.69 (d, *J* = 6.4 Hz, 1H), 3.33 (br. s, 1H), 2.98 (s, 1H), 2.23 - 1.94 (m, 2H), 1.10 ppm (t, *J* = 6.9 Hz, 3H); ^{13}C NMR (125 MHz, $CDCl_3$) δ = 202.2, 149.6, 140.1, 139.4, 134.4, 129.5, 128.3, 114.2, 95.6, 93.3, 65.6, 54.0, 52.6, 25.0, 8.4 ppm; HRMS (ESI) calcd for $C_{34}H_{32}KO_{11}S_2$ [M+K^+] 719.1018, found: 719.1002.

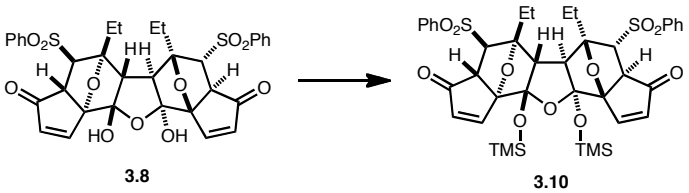

To the solution of dimer **3.8** (16.9 mg, 0.0248 mmol, 1.00 equiv) was dissolved in 0.2 mL of TMSCN. The mixture was heated to 80 °C for 8 hours. Upon completion of the reaction, volatiles were removed by azeotroping with toluene. After concentration, the crude product was purified by flash column chromatography (EtOAc/hexane = 1/6 to 1/4) to provide enone **3.10** (11.9 mg, 0.0144 mmol, 58%). ^{1}H NMR (500 MHz, $CDCl_3$) δ = 7.96 (d, *J* = 7.8 Hz, 2H), 7.76 - 7.70 (m, 1H), 7.68 - 7.60 (m, 2H), 7.50 (d, *J* = 5.4 Hz, 1H), 6.27 (d, *J* = 5.9 Hz, 1H), 3.75 (s, 1H), 3.72 (d, *J* = 6.8 Hz, 1H), 3.62 (d, *J* = 6.8 Hz, 1H), 2.01 (dd, *J* = 7.3, 14.6 Hz, 1H), 1.95 - 1.83 (m, 1H), 1.05 - 0.95 (m, 3H), 0.13 ppm (s, 18 H); HRMS (ESI) calcd for $C_{40}H_{48}NaO_{11}S$ [M+Na^+] 847.2069, found: 847.2068.

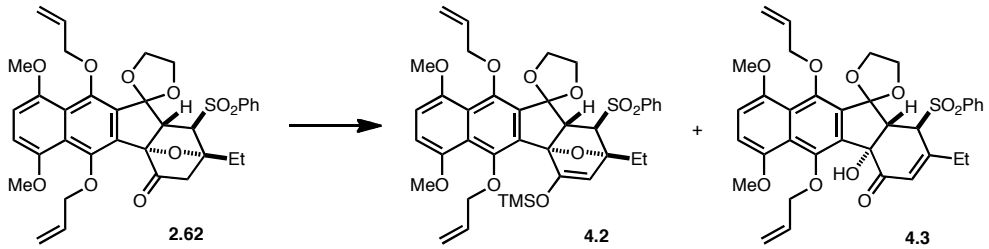

Enolsilane **4.2**

^{1}H NMR (600 MHz, $CDCl_3$) δ = 7.99 (d, *J* = 7.9 Hz, 2H), 7.66 (s, 1H), 7.61 - 7.55 (m, 2H), 6.86 - 6.82 (m, 1H), 6.81 - 6.77 (m, 1H), 6.20 - 6.07 (m, 2H), 5.37 (dd, *J* = 10.4, 17.1 Hz, 2H), 5.14 (s, 1H), 5.22 - 5.13 (m, 2H), 4.48 - 4.37 (m, 2H), 4.36 - 4.30 (m, 1H), 4.11 - 4.04 (m, 2H), 3.90 (d, *J* = 4.4 Hz, 1H), 3.85 (s, 3H), 3.84 (s, 3H), 3.48 (d, *J* = 7.0 Hz, 1H), 3.30 (d, *J* = 4.4 Hz, 1H), 3.25 - 3.18 (m, 1H), 3.05 (br. s, 1H), 2.54 - 2.44 (m, 1H), 2.03 - 1.96 (m, 1H), 1.05 (t, *J* = 7.2 Hz, 3H), 0.29 ppm (s, 9 H); HRMS (ESI) calcd for $C_{38}H_{44}NaO_{10}SSi$ [M+Na^+] 743.2322, found: 743.2329.

β-Elimination product **4.3**

^{1}H NMR (600 MHz, $CDCl_3$) δ = 7.91 (d, *J* = 7.9 Hz, 2H), 7.68 - 7.64 (m, 1H), 7.59 - 7.53 (m, 2H), 6.78 (q, *J* = 8.5 Hz, 2H), 6.17 (td, *J* = 5.5, 11.3 Hz, 1H), 5.93 (dd, *J* = 5.6, 11.1 Hz, 1H), 5.56 (s, 1H), 5.45 (d, *J* = 17.3 Hz, 1H), 5.31 - 5.23 (m, 2H), 5.15 (d, *J* = 10.5 Hz, 1H), 4.49 (dd, *J* = 5.6, 11.7 Hz, 1H), 4.43 - 4.38 (m, 1H), 4.38 - 4.33 (m, 2H), 4.27 - 4.20 (m, 2H), 4.07 (q, *J* = 6.9 Hz, 2H), 3.85 (s, 3H), 3.77 (s, 3H), 3.63 (dd, *J* = 6.0, 15.7 Hz, 1H), 3.21 (t, *J* = 4.8 Hz, 1H), 2.97 (dd, *J* = 4.2, 15.7 Hz, 1H), 2.55 (q, *J* = 7.4 Hz, 2H), 1.29 - 1.23 ppm (m, 3H); HRMS (ESI) calcd for $C_{35}H_{37}O_{10}S$ [M+H^+] 649.2107, found: 649.2111.

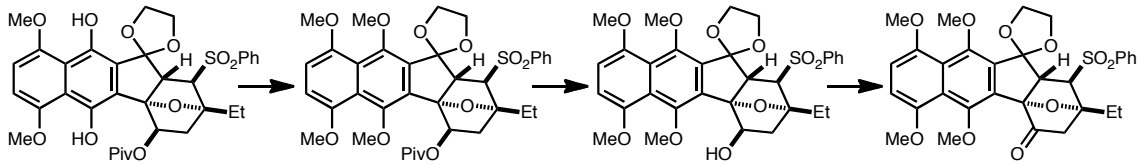

2.60 **4.10**

To the solution of hydroquinone **2.60** (13.9 mg, 0.0212 mmol, 1.00 equiv) in 0.5 mL of THF was added 0.92 M THF solution of NaHMDS (0.0692 mL, 0.0637 mmol, 3.00 equiv) at –78 °C. In 5 minutes MeOTf (0.0233 mL, 0.212 mmol, 10.0 equiv) was added via syringe. 5 minutes later, the mixture was warmed to 23 °C over 10 minutes. The reaction mixture was quenched with saturated aqueous solution of NH_4Cl, and the aqueous phase was extracted with diethyl ether (3 × 2 mL). After concentration, the crude product was purified by flash column chromatography (EtOAc/hexane = 1/1).

The dimethyl hydroquinoe was dissolved in 0.5 mL of THF and mixture was cooled to 0 °C. To the solution was added 1.0 M THF solution of $NaBHEt_3$ (0.106 mL, 0.106 mmol, 5.00 equiv) via syringe. In 5 minutes, the mixture was quenched with saturated aqueous solution of NH_4Cl, and the aqueous phase was extracted with diethyl ether (3 × 2 mL). After concentration, the crude product was used for the next step without further purification.

A flask was charged with the alcohol, TPAP (0.4 mg, 0.00106 mmol, 0.05 equiv), NMO (5.0 mg, 0.0424 mmol, 2.00 equiv), and 10 mg of 4 Å MS. Then the mixture was dissolved in 1 mL of dichloromethane, and the mixture was vigorously stirred at 23 °C. In 2 hours the mixture was diluted with 5 mL of diethyl ether and filtered through a pad of silica gel. After concentration, the crude product was purified by flash column chromatography (EtOAc/hexane = 1/1) to provide ketone **4.10** (5.9 mg, 0.00996 mmol,

47% over three steps). ^{1}H NMR (500 MHz, $CDCl_3$) δ = 7.99 (d, *J* = 8.0 Hz, 2H), 7.73 - 7.66 (m, 1H), 7.63 - 7.56 (m, 2H), 6.86 - 6.75 (m, 2H), 4.10 - 4.02 (m, 2H), 3.99 (q, *J* = 6.6 Hz, 1H), 3.88 (s, 3H), 3.87 (s, 3H), 3.77 (s, 3H), 3.72 (s, 3H), 3.55 (d, *J* = 5.3 Hz, 1H), 3.46 (d, *J* = 17.6 Hz, 1H), 3.41 (br. s, 1H), 3.20 (q, *J* = 6.7 Hz, 1H), 2.90 (q, *J* = 6.0 Hz, 1H), 2.76 (d, *J* = 17.9 Hz, 1H), 2.25 (tt, *J* = 7.4, 14.3 Hz, 2H), 1.12 ppm (t, *J* = 7.3 Hz, 3H); ^{13}C NMR (125 MHz, $CDCl_3$) δ = 204.6, 151.2, 150.8, 150.6, 149.3, 140.0, 135.0, 134.0, 129.2, 128.7, 128.2, 125.5, 124.6, 122.6, 113.6, 108.2, 107.5, 93.7, 92.4, 70.5, 67.7, 66.7, 65.1, 63.7, 63.3, 58.7, 56.9, 56.7, 44.9, 27.7, 26.4, 8.0 ppm; HRMS (ESI) calcd for $C_{31}H_{32}NaO_{10}S$ [M+Na^+] 619.1608, found: 619.1604.

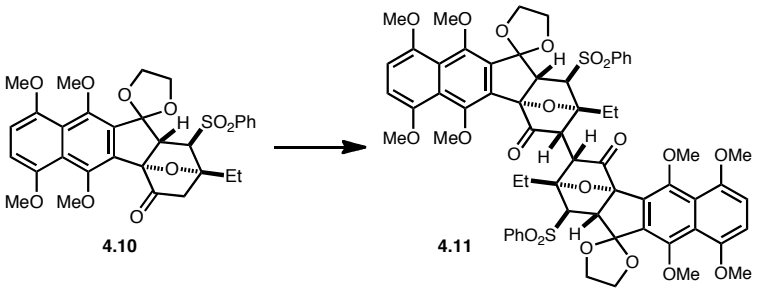

To the solution of HMDS (0.0193 mL, 0.0915 mmol, 1.70 equiv) in 0.6 mL of THF was added 0.71 M hexane solution of *n*-BuLi (0.129 mL, 0.0915 mmol, 1.70 equiv), followed by HMPA (0.0188 mL, 0.108 mmol, 2.00 equiv) at –78 °C. 40 minutes later ketone **4.10** (32.1 mg, 0.0538 mmol, 1.00 equiv) in 1 mL of THF (plus 2 × 0.5 mL rinse) was cannulated to the mixture. The resulting pale yellow solution was vigorously stirred at –78 °C for 2 hours. Then $[Cp_2Fe]PF_6$ (53.4 mg, 0.161 mmol, 3.00 equiv) was added from the solid addition adaptor. In 10 minutes the reaction system was warmed to –60 °C and stirred for 12 hours. The reaction mixture was quenched with saturated aqueous solution of NH_4Cl (5 mL), and the aqueous phase was extracted with dichloromethane (3 × 5 mL).

After concentration, the crude product was purified by flash column chromatography (EtOAc/hexane = 2/1 to 4/1) to provide marginally stable dimer **4.11**. HRMS (ESI) cald for $C_{62}H_{62}NaO_{20}S_2$ [M+Na^+] 1213.3169, found: 1213.3160.

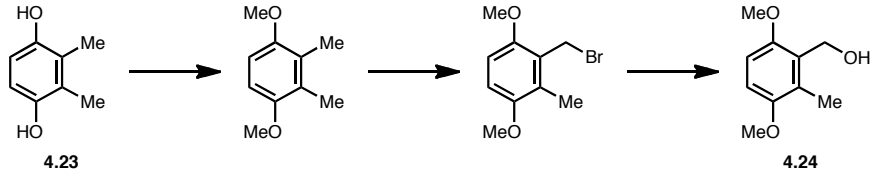

4.23 **4.24**

To the solution of 2,3-dimethylhydroquinone (5.00 g, 36.2 mmol, 1.00 equiv) in 100 mL of anhydrous acetone was added Me_2SO_4 (7.55 mL, 79.6 mmol, 2.20 equiv), followed by K_2CO_3 (11.0 g, 79.6 mmol, 2.20 equiv). The suspension was heated to reflux for 12 hours. Upon completion of the reaction, the mixture was cooled to 23 °C, and volatiles were removed under reduced pressure. The resulting suspension was quenched with 100 mL of water, and the aqueous phase was extracted with diethyl ether (3 × 50 mL). After concentration, the crude product was used for the next step without further purification.

The dimethoxybenzene was dissolved in 50 mL of CCl_4 together with NBS (6.44 g, 36.2 mmol, 1.00 equiv), and AIBN (297 mg, 1.81 mmol, 0.0500 equiv). The mixture was heated to reflux for 50 minutes, then cooled to 23 °C. Volatiles were removed under reduced pressure, and the resulting suspension was diluted with 100 mL of 1:2 mixture of EtOAc and hexane. The suspension was filtered through a pad of silica gel and concentrated. The crude product was used for the next step without further purification.

The arylbromide was dissolved in 80 mL of dioxane and 20 mL of water. To the solution was added $CaCO_3$ (7.25 g, 72.4 mmol, 2.00 equiv). The mixture was heated to 50 °C with vigorous stirring for 6 hours. After completion of the reaction, the reaction system was

quenched with 10% aqueous HCl, and the aqueous phase was extracted with diethyl ether (3 × 50 mL). After concentration, the crude product was purified by flash column chromatography (EtOAc/hexane = 1/5 to 1/3) to provide alcohol **4.24** (4.02 g, 22.1 mmol, 61% over three steps). ^{1}H NMR (500 MHz, $CDCl_3$) δ = 6.80 - 6.65 (m, 2H), 4.76 (d, *J* = 6.8 Hz, 2H), 3.82 (s, 3H), 3.78 (s, 3H), 2.27 ppm (s, 3H); HRMS (ESI) calcd for $C_{10}H_{15}O_3$ [M+H$^+$] 183.1021, found: 183.1022.

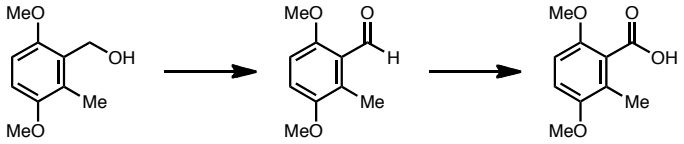

4.24 **4.25**

Alcohol **4.24** (6.33 g, 34.7 mmol, 1.00 equiv), TPAP, (610 mg, 1.74 mmol, 0.0500 equiv), NMO (6.10 g, 52.1 mmol, 1.50 equiv), and 17.4 g of 4 Å MS were charged in a flask. The mixture was dissolved in 100 mL of dichloromethane, and the reaction mixture was vigorously stirred for 2 hours. After completion of the reaction, the reaction system was diluted with 100 mL of diethyl ether, and filter over a pad of silica gel. After concentration, the crude product was used for the next step without further purification.

The aldehyde was dissolved in 100 mL of *t*-BuOH together with 2-methyl-2-butene (36.7 mL, 347 mmol, 10.0 equiv). The mixture was cooled to 0 °C, and a solution of $NaClO_2$ (19.6 g, 174 mmol, 5.00 equiv) and $NaH_2PO_4{\cdot}H_2O$ (24.0 g, 174 mmol, 5.00 equiv) in 100 mL of water was added by a dropping funnel over 30 minutes. After addition, the reaction mixture was slowly warmed to 23 °C over 1 hour. Then the mixture was quenched with water (100 mL) and the aqueous phase was extracted with dichloromethane (3 × 10 mL). The combined organic layer was dried over anhydrous

Na_2SO_4 and filtered through celite. The crude acid **4.25** (5.72 g, 29.1 mmol, 84% over two steps) was used for the next step without further purification. ^{1}H NMR (600 MHz, $CDCl_3$) δ = 6.87 (d, *J* = 8.8 Hz, 1H), 6.77 (d, *J* = 8.8 Hz, 1H), 3.86 (s, 3H), 3.80 (s, 3H), 2.31 ppm (s, 3H); HRMS (ESI) calcd for $C_{10}H_{12}NaO_4$ [M+Na$^+$] 219.0633, found: 219.0647.

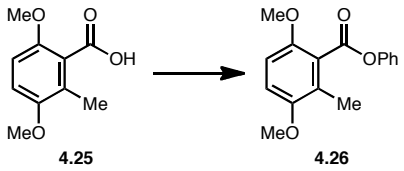

Acid **4.25** (4.88 g, 24.9 mmol, 1.00 equiv) was dissolved in 100 mL of benzene together with DMF (6.52 mL, 74.7 mmol, 3.00 equiv). After cooling to 0 °C, oxalyl chloride (5.78 mL, 74.7 mmol, 3.00 equiv) was added to the reaction mixture over a 10 minute period. The mixture was warmed to 23 °C and vigorously stirred for 2 hours. Then the reaction mixture was filtered over a pad of celite and concentrated under reduced pressure. The resulting oil was dissolved in 100 mL of dichloromethane and phenol (2.34 g, 24.9 mmol, 1.00 equiv) was added. The mixture was cooled to 0 °C, then pyridine (10.0 mL, 124 mmol, 5.00 equiv) was added dropwise over 5 minutes. After stirring for 6 hours, the mixture was quenched with 100 mL of water and the aqueous phase was extracted with diethyl ether (3 × 50 mL). After concentration, the crude product was purified by flash column chromatography (EtOAc/hexane = 1/15 to 1/10) to give phenyl ester **4.26** (5.28 g, 19.4 mmol, 78%). ^{1}H NMR (600 MHz, $CDCl_3$) δ = 7.43 (t, *J* = 7.9 Hz, 2H), 7.31 - 7.23 (m, 3H), 6.87 (d, *J* = 9.1 Hz, 1H), 6.78 (d, *J* = 8.8 Hz, 1H), 3.85 (s, 3H), 3.82 (s, 3H), 2.31 ppm (s, 3H); HRMS (ESI) calcd for $C_{16}H_{17}O_4$ [M+H$^+$] 273.1127, found: 273.1131.

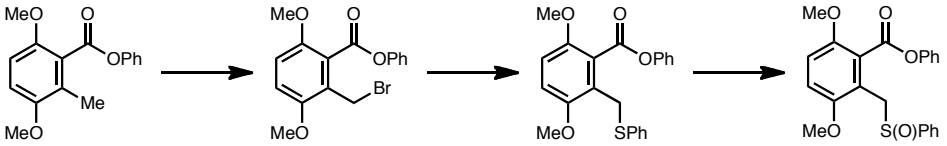

Compound **4.26** (510 mg, 1.87 mmol, 1.00 equiv) was was dissolved in 10 mL of CCl_4 together with NBS (400 mg, 2.25 mmol, 1.20 equiv), and AIBN (30.7 mg, 0.187 mmol, 0.100 equiv). The mixture was heated to reflux for 3 hours, then cooled to 23 °C. Volatiles were removed under reduced pressure, and the resulting suspension was diluted with 50 mL of 1:2 mixture of EtOAc and hexane. The suspension was filtered through a pad of silica gel and concentrated. The crude product was used for the next step without further purification.

The crude aryl bromide was dissolved in 10 mL of DMF and cooled to 0 °C. To the solution was added NaSPh (272 mg, 2.06 mmol, 1.10 equiv), and the reaction mixture was warmed to 23 °C. After stirring for 1 hour, the mixture was quenched with 10 mL of water, and the aqueous phase was extracted with diethyl ether (3 × 20 mL). After concentration, the crude product was used for the next step without further purification.

The crude sulfide was dissolved in 10 mL of methanol. To the solution was added 2 mL of water, followed by $NaIO_4$ (600 mg, 2.81 mmol, 1.50 equiv) to give a white suspension. The mixture was vigorously stirred at 23 °C for 24 hours. After completion of the reaction, volatiles were removed under reduced pressure and the resulting oil was quenched with 10 mL of water. The aqueous phase was extracted with diethyl ether (3 × 20 mL). The combined organic layer was dried over anhydrous $MgSO_4$ and filtered. After concentration, the crude product was purified by flash column chromatography

(EtOAc/hexane = 1/2 to 1/1) to give sulfoxide **4.27** (511 mg, 1.29 mmol, 69% over three steps) as colorless oil. ^{1}H NMR (600 MHz, $CDCl_3$) δ = 7.56 (dd, *J* = 1.9, 7.2 Hz, 2H), 7.51 - 7.46 (m, 2H), 7.46 - 7.42 (m, 3H), 7.40 (d, *J* = 7.6 Hz, 2H), 7.35 - 7.29 (m, 1H), 6.94 (d, *J* = 9.1 Hz, 1H), 6.84 (d, *J* = 9.1 Hz, 1H), 4.52 (d, *J* = 12.6 Hz, 1H), 4.41 (d, *J* = 12.3 Hz, 1H), 3.89 (s, 3H), 3.55 ppm (s, 3H); ^{13}C NMR (125 MHz, $CDCl_3$) δ = 165.6, 151.5, 150.9, 150.7, 143.5, 130.7, 129.2, 128.4, 125.8, 124.7, 124.0, 121.7, 118.1, 112.8, 112.6, 56.6, 55.7, 55.7, 54.9 ppm; HRMS (ESI) calcd for $C_{22}H_{20}NaO_5S$ [M+Na^+] 419.0924, found: 419.0847.

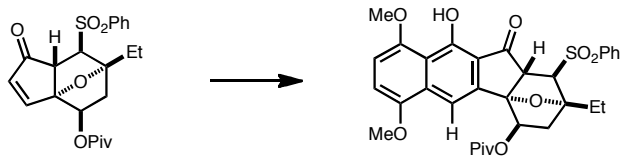

2.42 **4.28**

A solution of sulfoxide **4.27** (575 mg, 1.45 mmol, 1.05 equiv) in 2 mL of THF (plus 1 mL rinse) was cannulated to a solution of LiHMDS (4.14 mmol, 3.00 equiv) in 12 mL of THF to give a bright yellow solution at –78 °C. The resulting solution was stirred at –60 °C for 6 hours to give an orange solution. The mixture was cooled to –78 °C again and a solution of enone **2.42** (577 mg, 1.38 mmol, 1.00 equiv) in 2 mL of THF (plus 1 mL rinse) was added to the reaction. In 10 minutes, the mixture was quenched with saturated aqueous NH_4Cl, and the aqueous phase was extracted with dichloromethane (3 × 20 mL). The crude product was purified by flash column chromatography (EtOAc/hexane = 1/1.5 to 1.5/1) to give phenol **4.28** (650 mg, 1.09 mmol, 79%) as bright yellow foam. ^{1}H NMR (500 MHz, $CDCl_3$) δ = 10.63 (s, 1H), 7.98 (dd, *J* = 8.5, 1.1 Hz, 2H), 7.92 (s, 1H), 7.71 (tt, *J* = 7.8, 1.0 Hz, 1H), 7.62 (dd, *J* = 8.2, 8.2 Hz, 2H), 6.82 (d, *J* = 8.2 Hz, 1H), 6.77 (d, *J* =

8.2 Hz, 1H), 5.71 (dd, *J* = 9.8, 3.4 Hz, 1H), 4.13 (d, *J* = 6.0 Hz, 1H), 4.00 (s, 3H), 3.94 (s, 3H), 3.82 (dd, *J* = 6.0, 1.8 Hz, 1H), 2.79 (dd, *J* = 13.7, 3.7 Hz, 1H), 2.59 (ddd, *J* = 14.3, 10.0, 1.8 Hz, 1H), 2.16 (dq, *J* = 15.0, 7.4 Hz, 1H), 2.05 (dq, *J* = 15.0, 7.4 Hz, 1H), 1.21 (s, 9H), 0.99 ppm (t, *J* = 7.3 Hz, 3H); ^{13}C NMR (125 MHz, $CDCl_3$) δ = 198.0, 178.1, 155.8, 152.1, 150.4, 140.1, 138.4, 134.0, 131.6, 129.3, 128.2, 118.0, 116.6, 109.6, 107.3, 105.8, 93.9, 89.5, 70.9, 69.6, 56.8, 55.9, 55.9, 38.7, 38.3, 27.7, 27.0, 8.0 ppm; HRMS (ESI) calcd for $C_{32}H_{35}O_9S$ [M+H$^+$] 595.1996, found: 595.1996.

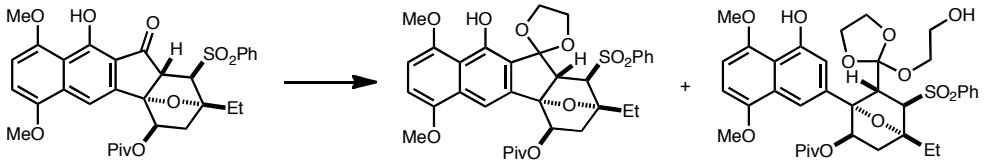

To a solution of **4.28** (650 mg, 1.09 mmol, 1.00 equiv) in 3 mL of dichloromethane was added 1,2-(bistrimethylsilyloxy)ethane (0.534 mL, 2.18 mmol, 2.00 equiv), followed by TMSOTf (0.197 mL, 1.09 mmol, 1.00 equiv) at room temperature. The reaction was vigorously stirred for 2 days. Upon completion of the reaction, the mixture was quenched with saturated aqueous $NaHCO_3$ at 0 °C and the aqueous phase was extracted with dichloromethane (3 × 10 mL). The combined organic layers were dried over Na_2SO_4 and the crude product was purified by flash column chromatography (EtOAc/hexane = 1/2.5 to 1/2) to give dioxolane **4.29** (501 mg, 0.785 mmol, 72%) as a pale yellow solid. ^{1}H NMR (500 MHz, $CDCl_3$) δ = 10.02 (d, *J* = 1.0 Hz, 1H), 8.02 (d, *J* = 7.3 Hz, 2H), 7.79 (s, 1H), 7.69 (t, *J* = 7.3 Hz, 1H), 7.61 (dd, *J* = 7.8, 7.8 Hz, 2H), 6.66 (d, *J* = 8.8 Hz, 1H), 6.62 (d, *J* = 8.8 Hz, 1H), 5.59 (dd, *J* = 10.0, 3.7 Hz, 1H), 4.10 - 4.20 (m, 3H), 4.08 (d, *J* = 5.9 Hz, 1H), 3.96 (s, 3H), 3.90 (s, 3H), 3.23 (ddd, *J* = 6.3, 6.3, 6.3 Hz, 1H), 2.98 (ddd, *J* =

6.3, 6.3, 6.3 Hz, 1H), 2.74 (dd, *J* = 14.2, 3.4 Hz, 1H), 2.49 - 2.57 (m, 1H), 2.06 - 2.15 (m, 1H), 1.98 - 2.06 (m, 1H) 1.18 (s, 9H), 1.04 ppm (t, *J* = 7.3 Hz, 3H); ^{13}C NMR (125 MHz, $CDCl_3$) δ = 178.4, 151.0, 150.7, 150.6, 140.9, 134.0, 133.6, 129.7, 129.1, 128.8, 125.8, 117.2, 113.3, 108.9, 104.6, 103.8, 93.7, 92.0, 71.6, 68.5, 67.3, 65.6, 56.6, 55.7, 55.4, 38.7, 37.8, 27.8, 27.1, 8.0 ppm; HRMS (ESI) calcd for $C_{34}H_{39}O_{10}S$ [M+H$^+$] 639.2258, found: 639.2260.

Byproduct **4.32**

^{1}H NMR (500 MHz, $CDCl_3$) δ = 9.38 (s, 1H), 7.89 (d, *J* = 7.3 Hz, 2H), 7.71 (d, *J* = 1.4 Hz, 1H), 7.61 (d, *J* = 7.8 Hz, 1H), 7.57 - 7.49 (m, 2H), 6.91 (d, *J* = 1.4 Hz, 1H), 6.68 - 6.58 (m, 2H), 4.94 (dd, *J* = 3.7, 10.5 Hz, 1H), 4.29 (d, *J* = 6.9 Hz, 1H), 4.20 (dd, *J* = 1.4, 6.9 Hz, 1H), 3.97 (s, 3H), 3.88 (s, 3H), 3.55 (br. s. 2H), 3.42 (dd, *J* = 4.1, 6.9 Hz, 1H), 3.40 - 3.34 (m, 1H), 3.28 - 3.17 (m, 2H), 3.05 - 2.97 (m, 1H), 2.88 - 2.80 (m, 1H), 2.68 (dd, *J* = 3.7, 14.2 Hz, 1H), 2.49 (dd, *J* = 1.8, 10.5 Hz, 1H), 2.16 - 2.00 (m, 2H), 1.46 (s, 9 H), 1.14 ppm (t, *J* = 7.3 Hz, 3H); ^{13}C NMR (125 MHz, $CDCl_3$) δ = 177.6, 169.8, 154.0, 150.3, 149.7, 139.9, 135.1, 133.9, 129.3, 128.0, 127.7, 115.0, 110.0, 108.8, 103.6, 103.1, 89.3, 88.5, 78.0, 72.0, 69.6, 68.0, 63.8, 61.6, 56.2, 55.4, 50.3, 38.8, 37.1, 27.2, 27.2, 8.0 ppm; HRMS (ESI) calcd for $C_{36}H_{48}NO_{12}S$ [M+NH_4^+] 718.2892, found: 718.2892.

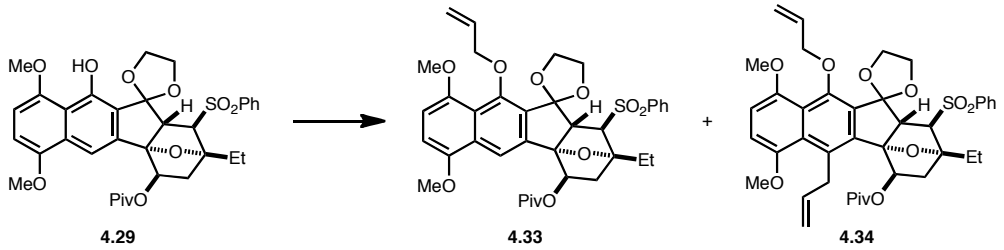

To a solution of phenol **4.29** (1.62 g, 2.54 mmol, 1.00 equiv) in 8 mL of DMF was added

allyl bromide (0.241 mL, 2.79 mmol, 1.10 equiv), followed by Cs_2CO_3 (909 mg, 2.79 mmol, 1.10 equiv). The resulting red solution was vigorously stirred for 2 hours, then the reaction was quenched with saturated aqueous NH_4Cl, and the aqueous phase was extracted with dichloromethane (3 × 20 mL). After drying over Na_2SO_4 and concentrating under reduced pressure, the crude product was purified by flash column chromatography (EtOAc/hexane = 1/4 to 1/3) to give allyl ether **4.33** (1.32 g, 1.94 mmol, 76%) as a pale yellow foam. ^{1}H NMR (500 MHz, $CDCl_3$) δ = 8.13 (s, 1H), 8.02 (d, *J* = 7.3 Hz, 2H), 7.69 (t, *J* = 7.3 Hz, 1H), 7.61 (dd, *J* = 7.8, 7.8 Hz, 2H), 6.76 (d, *J* = 8.7 Hz, 1H), 6.71 (d, *J* = 8.7 Hz, 1H), 6.15 (dddd, *J*=17.2, 10.5, 5.2, 5.2 Hz, 1H), 5.63 (dd, *J* = 10.1, 3.7 Hz, 1H), 5.41 (dd, *J* = 17.4, 1.8 Hz, 1H), 5.21 (dd, *J* = 10.8, 1.6 Hz, 1H), 4.36 - 4.50 (m, 2H), 4.04 - 4.16 (m, 4H), 3.93 (s, 3H), 3.85 (s, 3H), 3.19 - 3.27 (m, 1H), 2.95 - 3.03 (m, 1H), 2.71 (dd, *J* = 14.0, 3.4 Hz, 1H), 2.53 (ddd, *J* = 14.2, 10.1, 1.8 Hz, 1H), 1.93 - 2.10 (m, 2H), 1.19 (s, 9H), 0.98 - 1.05 ppm (t, *J* = 7.3 Hz, 3H); ^{13}C NMR (125 MHz, $CDCl_3$) δ = 178.4, 152.1, 150.3, 150.2, 140.9, 135.2, 135.1, 133.7, 132.8, 130.4, 129.2, 128.7, 122.8, 116.0, 114.4, 113.6, 107.2, 104.5, 93.7, 91.7, 76.7, 71.6, 68.9, 66.8, 65.4, 57.0, 55.8, 55.4, 38.7, 37.4, 27.7, 27.1, 8.1 ppm; HRMS (ESI) calcd for $C_{37}H_{43}O_{10}S$ [$M+H^+$] 679.2571, found: 679.2545.

Byproduct **4.34**

^{1}H NMR (600 MHz, $CDCl_3$) δ = 8.01 (d, *J* = 7.3 Hz, 2H), 7.68 (d, *J* = 7.3 Hz, 1H), 7.63 - 7.58 (m, 2H), 6.81 - 6.72 (m, 2H), 6.15 (dd, *J* = 5.7, 11.3 Hz, 1H), 5.63 - 5.55 (m, 1H), 5.40 (dd, *J* = 1.2, 17.3 Hz, 1H), 5.21 (d, *J* = 10.5 Hz, 1H), 4.91 (d, *J* = 10.3 Hz, 1H), 4.44 (d, *J* = 4.1 Hz, 2H), 4.19 (d, *J* = 6.2 Hz, 1H), 4.14 (d, J = 6.4 Hz, 1H), 4.03 (t, *J* = 6.0 Hz, 2H), 3.83 (s, 3H), 3.77 (s, 3H), 2.66 (dd, *J* = 3.2, 14.1 Hz, 1H), 2.47 (br. s, 1H), 2.00 -

1.88 (m, 2H), 1.16 (s, 9 H), 1.01 ppm (d, J = 14.9 Hz, 3H); HRMS (ESI) calcd for $C_{40}H_{47}O_{10}S$ [M+H$^+$] 719.2890, found: 719.2889.

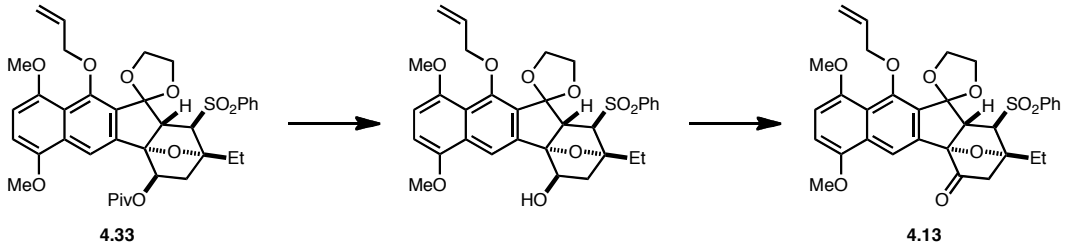

The trimethylacetyl ester **4.33** (1.32 g, 1.94 mmol, 1.00 equiv) was dissolved in 12 mL of THF and cooled to 0 °C. To the solution was added 1.0 M $NaBHEt_3$ solution in THF (9.72 mL, 9.72 mmol, 5.00 equiv) via syringe. The mixture was vigorously stirred at 0 °C for 2 hours. After completion of the reaction, the mixture was quenched with saturated aqueous NH_4Cl and the aqueous phase was extracted with dichloromethane (3 × 20 mL). After drying over Na_2SO_4 and concentrating under reduced pressure, the crude product was purified by flash column chromatography (EtOAc/hexane = 1/2 to 1/1.5) to give the corresponding alcohol (1.15 g, 1.93 mmol, 99%) as a white foam.

A flask was charged with the alcohol (270 mg, 0.454 mmol, 1.00 equiv), TPAP (8.0 mg, 0.0227 mmol, 0.0500 equiv), NMO (80.0 mg, 0.681 mmol, 1.50 equiv), and 4Å MS (230 mg), then 5 mL of dichloromethane was added. The reaction was vigorously stirred at room temperature for 2 hours. After completion of the reaction, the mixture was diluted with 10 mL of diethyl ether and the resulting suspension was filtered through a pad of celite. After concentration, the crude product was purified by flash column chromatography (EtOAc/hexane = 1/3 to 1/2) to give ketone **4.13** (240 mg, 0.405 mmol, 89%) as a white solid. ^{1}H NMR (500 MHz, $CDCl_3$) δ = 8.14 (s, 1H), 8.01 (dd, J = 8.5,

1.1 Hz, 2H), 7.72 (tt, *J* = 7.5, 1.2 Hz, 1H), 7.63 (dd, *J* = 8.2, 8.2 Hz, 2H), 6.78 (d, *J* = 8.7 Hz, 1H), 6.72 (d, *J* = 8.7 Hz, 1H), 6.14 (dddd, *J* = 17.2, 10.5, 5.4, 5.4 Hz, 1H), 5.36 - 5.42 (m, 1H), 5.19 - 5.24 (m, 1H), 4.32 - 4.46 (m, 2H), 4.09 - 4.20 (m, 2H), 4.03 (ddd, *J* = 6.9, 6.9, 6.9 Hz, 1H), 3.91 (s, 3H), 3.85 (s, 3H), 3.60 (d, *J* = 5.5 Hz, 1H), 3.53 (d, *J* = 18.3 Hz, 1H), 3.27 (ddd, *J* = 6.4, 6.4, 6.4 Hz, 1H), 2.81 (ddd, *J* = 6.4, 6.4, 6.4 Hz, 1H), 2.71 (dd, *J* = 18.1, 1.6 Hz, 1H), 2.24 (qd, *J* = 7.4, 2.5 Hz, 2H), 1.11 ppm (t, *J* = 7.3 Hz, 3H); ^{13}C NMR (125 MHz, $CDCl_3$) δ = 204.9, 152.1, 150.3, 150.1, 140.1, 135.1, 134.0, 130.6, 129.5, 129.3, 128.8, 128.3, 122.9, 117.2, 116.2, 113.6, 107.5, 104.7, 93.8, 91.9, 76.9, 67.8, 66.9, 65.3, 58.7, 56.8, 55.7, 44.5, 27.8, 7.9 ppm; HRMS (ESI) calcd for $C_{32}H_{33}O_9S$ [M+H$^+$] 593.1840, found: 593.1837.

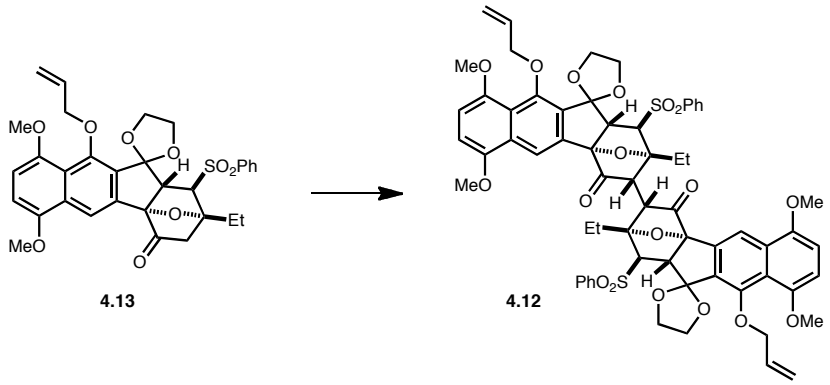

A two-neck flask was equipped with a solid addition adaptor containing $[Cp_2Fe]PF_6$ (2.32 g, 7.00 mmol, 5.00 equiv). To the flask was added 8 mL of THF, HMDS (0.502 mL, 2.38 mmol, 1.70 equiv), *n*-BuLi solution (2.29 M in hexanes, 1.04 mL, 2.38 mmol, 1.70 equiv), and HMPA (0.487 mL, 2.80 mmol, 2.00 equiv) at –78°C, successively. 40 minutes later a solution of ketone **4.13** (830 mg, 1.40 mmol, 1.00 equiv) in 10 mL of THF (plus 2 × 1 mL rinse) was cannulated to the LiHMDS-HMPA solution to give a pale yellow solution. 2 hours later, $[Cp_2Fe]PF_6$ was added to the reaction system from the

solid addition adaptor. The initially deep blue suspension turned yellowish-green in 30 minutes. The reaction mixture was stirred at –60 °C for 3 days. The reaction mixture was quenched with saturated aqueous NH_4Cl and warmed to room temperature. The aqueous phase was extracted with dichloromethane (3 × 20 mL) and the combined organic layers were dried over Na_2SO_4. The crude product was purified by flash column chromatography (EtOAc/hexane = 1/1 to 1.5/1) to give dimer **4.12** (665 mg, 1.12 mmol, 80%) as a pale yellow solid. ^{1}H NMR (500 MHz, $CDCl_3$) δ = 8.32 (s, 2H), 8.04 (d, *J* = 7.6 Hz, 4H), 7.71 (t, *J* = 7.1 Hz, 2H), 7.64 (dd, *J* = 7.3, 7.3 Hz, 4H), 6.75 (d, *J* = 8.5 Hz, 2H), 6.69 (d, *J* = 8.2 Hz, 2H), 6.14 (dddd, *J* = 15.8, 10.1, 4.8, 4.8 Hz, 2H), 5.40 (d, *J* = 17.2 Hz, 2H), 5.21 (d, *J* = 10.3 Hz, 2H), 4.48 (d, *J* = 95.0 Hz, 2H), 4.35 - 4.45 (m, 4H), 4.28 (s, 2H), 4.16 (ddd, *J* = 6.6, 6.6, 6.6 Hz, 2H), 4.07 (ddd, *J* = 6.2, 6.2, 6.2 Hz, 2H), 3.84 (s, 6H), 3.83 (s, 6H), 3.65 (d, *J* = 5.0 Hz, 2H), 3.27 - 3.34 (m, 2H), 2.94 - 3.02 (m, 2H), 2.44 – 2.57 (m, 2H), 2.20 - 2.31 (m, 2H), 1.20 ppm (t, *J* = 7.0 Hz, 6H); ^{13}C NMR (125 MHz, $CDCl_3$) δ = 205.3, 151.9, 150.5, 150.0, 140.0, 135.2, 135.1, 134.1, 130.8, 129.6, 129.5, 128.6, 122.8, 117.7, 116.0, 113.8, 107.3, 104.8, 93.9, 93.2, 76.8, 66.8, 65.4, 65.3, 58.2, 56.7, 55.9, 51.0, 24.6, 7.8 ppm; HRMS (ESI) calcd for $C_{64}H_{63}O_{18}S_2$ [M+H$^+$] 1183.3450, found: 1183.3501.

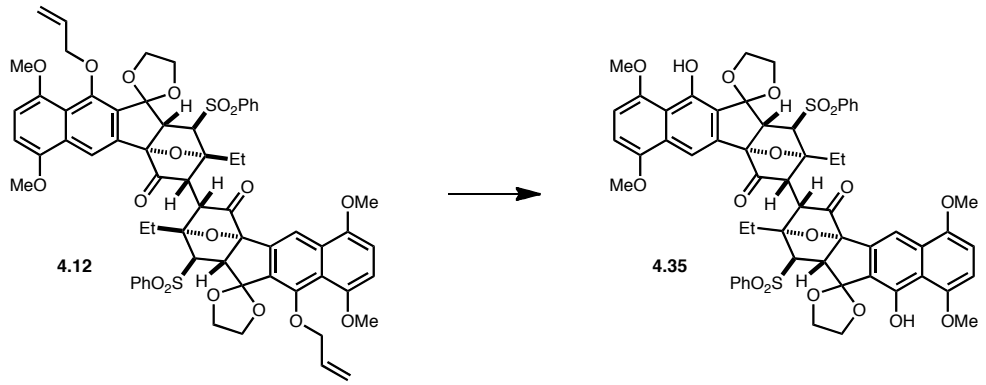

To the solution of dimer **4.12** (19.7 mg, 0.0166 mmol, 1.00 equiv), in 0.5 mL of dichloromethane was added acetic acid (0.0095 mL, 0.166 mmol, 10.0 equiv), *n*-Bu_3SnH (0.0098 mL, 0.0365 mmol, 2.2 equiv), and $PdCl_2(PPh_3)_2$ (1.2 mg, 0.00166 mmol, 0.100 equiv), successively at 0 °C. In 30 minutes, volatiles were removed under reduced pressure, and the crude product was purified by flash column chromatography (EtOAc/hexane = 2/1 to 4/1) to give dimer **4.35** (16.4 mg, 0.0149 mmol, 90%) as white solid. The product was recrystallized over dichloromethane/pentane for X-ray analysis.

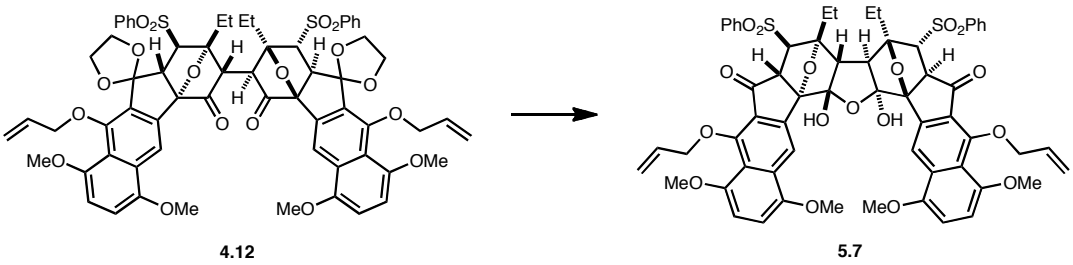

To the solution of dioxolane **4.12** (128 mg, 0.108 mmol, 1.00 equiv) in 3 mL of acetone was added 0.5 mL of water. The solution was cooled to 0 °C and 0.5 mL of TfOH was added dropwise over 5 minutes. The mixture was warmed to 23 °C and vigorously stirred for 24 hours. At the end of the reaction, the reaction system was cooled to 0 °C and 10 mL of saturated aqueous $NaHCO_3$ solution was added. The aqueous phase was quenched with dichloromethane (3 × 10 mL), and the combined organic layer was dried over Na_2SO_4 and filtered. After concentration the crude product was purified by flash column chromatography (EtOAc/hexane = 1/1 to 1.5/1) to give ketone **5.7** (94.0 mg, 0.0844 mmol, 78%) as bright yellow solid. ^{1}H NMR (500 MHz, $CDCl_3$) δ = 9.00 (s, 1H), 8.06 (d, *J* = 7.3 Hz, 2H), 7.80 - 7.73 (m, 1H), 7.72 - 7.63 (m, 2H), 6.92 - 6.82 (m, 2H), 6.26 - 6.13 (m, 1H), 5.39 (d, *J* = 17.2 Hz, 1H), 5.26 (d, *J* = 10.1 Hz, 1H), 4.65 - 4.53 (m, 2H), 4.20 (d, *J* = 6.0 Hz, 1H), 4.09 (d, *J* = 6.2 Hz, 1H), 4.08 (br. s, 1H), 3.90 (s, 3H), 3.80 (s,

3H), 3.63 (br. s, 1H), 2.28 - 2.07 (m, 2H), 1.06 ppm (t, J = 7.1 Hz, 3H); ^{13}C NMR (125 MHz, $CDCl_3$) δ = 197.2, 155.9, 152.3, 150.2, 139.8, 136.4, 134.3, 134.1, 132.6, 129.5, 128.4, 128.3, 126.5, 123.0, 117.8, 117.7, 115.8, 108.6, 107.3, 93.7, 90.2, 76.8, 67.5, 57.2, 56.8, 55.7, 54.0, 24.7, 8.4 ppm; HRMS (ESI) calcd for $C_{60}H_{56}NaO_{17}S_2$ [M+Na^+] 1135.2851, found: 1135.2847.

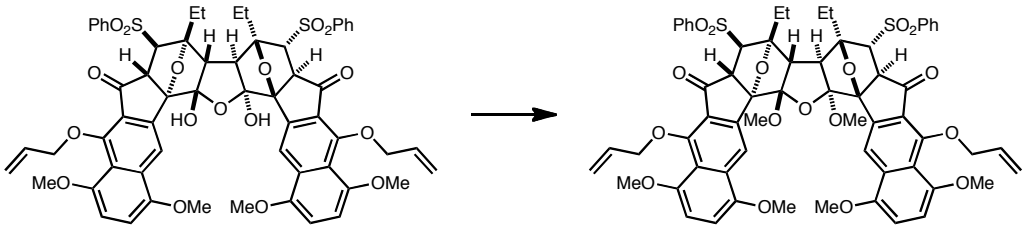

To the solution of cyclic hydrate **5.7** (11.4 mg, 0.0101 mmol, 1.00 equiv) in 0.5 mL of THF was added MeOTf (0.00340 mL, 0.0302, 3.00 equiv). The solution was cooled to –78 °C, then 0.92 M THF solution of NaHMDS (0.0231 mL, 0.0212 mmol, 2.10 equiv) was added to the reaction system via syringe. In 5 minutes, the mixture was quenched with saturated aqueous solution of NH_4Cl, and the aqueous phase was extracted with dichloromethane (3 × 5 mL). The combined organic layer was dried over Na_2SO_4 and filtered. After concentration the crude product was purified by flash column chromatography (EtOAc/hexane = 1/1.5 to 1/1) to provide methyl ether **5.16** (10.4 mg, 0.00911 mmol, 90%). ^{1}H NMR (500 MHz, $CDCl_3$) δ = 9.00 (s, 1H), 8.06 (d, J = 7.3 Hz, 2H), 7.78 - 7.71 (m, 1H), 7.70 - 7.63 (m, 2H), 6.91 - 6.82 (m, 2H), 6.25 - 6.14 (m, 1H), 5.40 (dd, J = 1.1, 17.2 Hz, 1H), 5.26 (d, J = 10.1 Hz, 1H), 4.69 - 4.62 (m, 1H), 4.60 - 4.54 (m, 1H), 4.14 (d, J = 5.5 Hz, 1H), 4.12 (s, 1H), 4.09 (d, J = 6.0 Hz, 1H), 3.90 (s, 3H), 3.82 (s, 3H), 3.58 (s, 3H), 2.32 - 2.22 (m, 1H), 2.17 (qd, J = 7.5, 14.9 Hz, 1H), 1.04 ppm

(t, J = 7.1 Hz, 3H); ^{13}C NMR (125 MHz, $CDCl_3$) δ = 197.7, 155.9, 152.5, 150.1, 140.2, 138.4, 134.1, 134.0, 132.6, 129.4, 128.3, 126.1, 122.8, 119.5, 117.7, 117.4, 108.2, 107.8, 93.8, 90.8, 76.9, 67.6, 58.1, 57.1, 56.1, 54.2, 53.1, 24.5, 8.6 ppm; HRMS (ESI) calcd for $C_{62}H_{60}NaO_{17}S_2$ [M+Na^+] 1163.3164, found: 1163.3166.

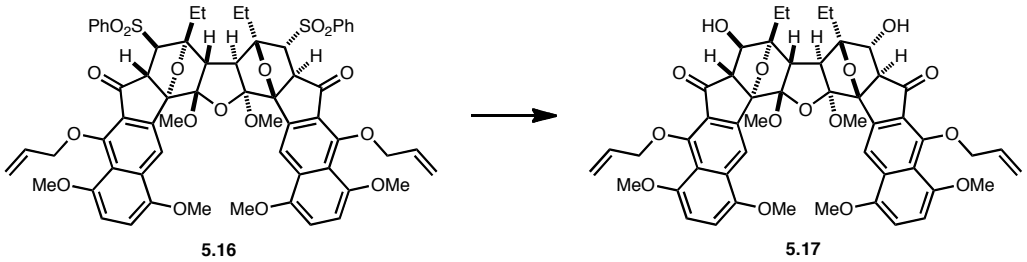

To the solution of sulfone **5.16** (31.0 mg, 0.0272 mmol, 1.00 equiv) in 0.5 mL of THF and 0.5 mL of water was added KOH (15.0 mg, 0.272 mmol, 10.0 equiv) at 0 °C. The mixture was warmed to 23 °C and vigorously stirred for 12 hours. Upon completion of the reaction, the reaction system was quenched with saturated aqueous solution of NH_4Cl, and the aqueous phase was extracted with dichloromethane (3 × 5 mL). The combined organic layer was dried over Na_2SO_4 and filtered. After concentration, the crude product was purified by flash column chromatography (EtOAc/hexane = 1/1.5 to 1/1) to provide diol **5.17** (21.9 mg, 0.0245 mmol, 90%) as a 10:1 diastereomeric mixture. ^{1}H NMR (500 MHz, $CDCl_3$) δ = 8.97 (s, 1H), 6.92 - 6.81 (m, 2H), 6.39 - 6.25 (m, 1H), 5.53 - 5.46 (m, 1H), 5.31 (d, J = 10.1 Hz, 1H), 4.76 (dd, J = 5.7, 10.8 Hz, 1H), 4.70 - 4.62 (m, 2H), 3.94 (s, 3H), 3.84 (s, 3H), 3.49 (s, 3H), 3.39 (s, 1H), 3.37 (d, J = 3.2 Hz, 1H), 2.01 - 1.92 (m, 2H), 1.03 ppm (t, J = 7.6 Hz, 3H); ^{13}C NMR (125 MHz, $CDCl_3$) δ = 201.2, 156.1, 152.6, 150.1, 140.4, 134.3, 132.8, 126.7, 122.7, 120.4, 117.8, 117.1, 107.9, 107.6, 91.4, 89.7, 77.3, 64.0, 57.1, 56.1, 53.8, 49.8, 29.7, 24.0, 7.8 ppm; HRMS (ESI) calcd for $C_{50}H_{53}O_{15}$

[M+H$^+$] 893.3384, found: 893.3389. The product was recrystallized over dichloromethane/pentane for X-ray analysis.

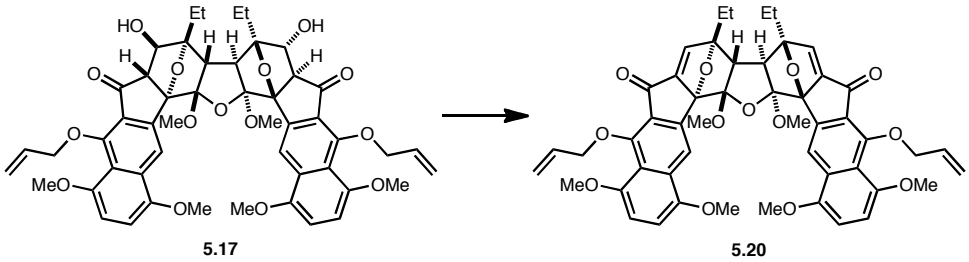

To the solution of diol **5.17** (3.5 mg, 0.00392 mmol, 1.00 equiv) in 0.5 mL of dichloromethane was added Et_3N (0.0054 mL, 0.0392 mmol, 10.0 equiv), followed by MsCl (0.0015 mL, 0.0196 mmol, 5.00 equiv) at 0 °C. In 30 minutes the reaction mixture was quenched with 1 mL of water, and the aqueous phase was extracted with dichloromethane (3 × 2 mL). The combined organic layer was dried over Na_2SO_4 and filtered. After concentration the crude mesylate was dissolved in 0.5 mL of THF and 0.5 mL of water, and the solution was cooled to 0 °C. To the solution was added K_2CO_3 (5.3 mg, 0.0392 mmol, 10.0 equiv). The mixture was vigorously stirred at 0 °C for 3 hr before completion of the reaction. At the end of the reaction, the mixture was quenched with 1 mL of saturated aqueous solution of NH_4Cl, and the aqueous phase was extracted with dichloromethane (3 × 2 mL). The combined organic layer was dried over Na_2SO_4 and filtered. After concentration the crude product was purified by flash column chromatography (EtOAc/hexane = 1/1.5 to 1/1) to provide enone **5.20** (2.8 mg, 0.00327 mmol, 83%). ^{1}H NMR (600 MHz, $CDCl_3$) δ = 8.28 (s, 1H), 6.95 (s, 1H), 6.80 (s, 2H), 6.39 - 6.30 (m, 1H), 5.50 - 5.46 (m, 1H), 5.33 - 5.29 (m, 1H), 4.80 - 4.75 (m, 1H), 4.71 - 4.67 (m, 1H), 3.92 (s, 3H), 3.75 (s, 3H), 3.40 (s, 3H), 2.81 (s, 1H), 2.16 - 2.08 (m, 1H),

2.04 - 1.95 (m, 1H), 1.12 ppm (t, J = 7.5 Hz, 3H); HRMS (ESI) calcd for $C_{50}H_{49}O_{13}$ [M+H$^+$] 857.3168, found: 857.3175.

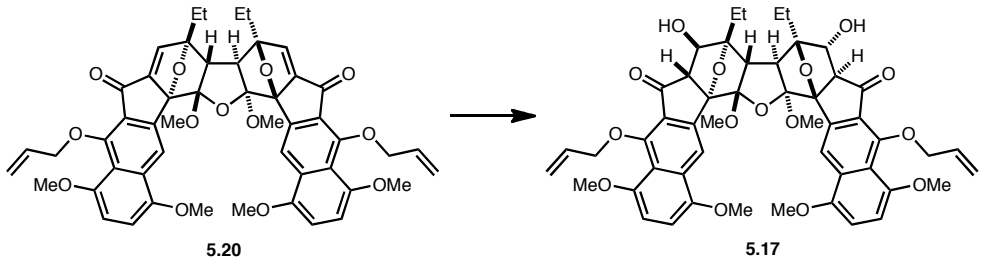

To the solution of enone **5.20** (2.8 mg, 0.00327 mmol, 1.00 equiv) in 0.5 mL of THF and 0.5 mL of water was added KOH (4.5 mg, 0.0327, 10.0 equiv) at 0 °C. The solution was warmed to 23 °C and vigorously stirred for 6 hours. Upon completion of the reaction, the mixture was quenched with 1 mL of saturated aqueous solution of NH_4Cl, and the aqueous phase was extracted with dichloromethane (3 × 2 mL). The combined organic layer was dried over Na_2SO_4 and filtered. After concentration the crude product was purified by flash column chromatography (EtOAc/hexane = 1/1.5 to 1/1) to provide diol **5.17** (2.7 mg, 0.00302 mmol, 92%). The product was identical to the previously prepared compound in all aspects.

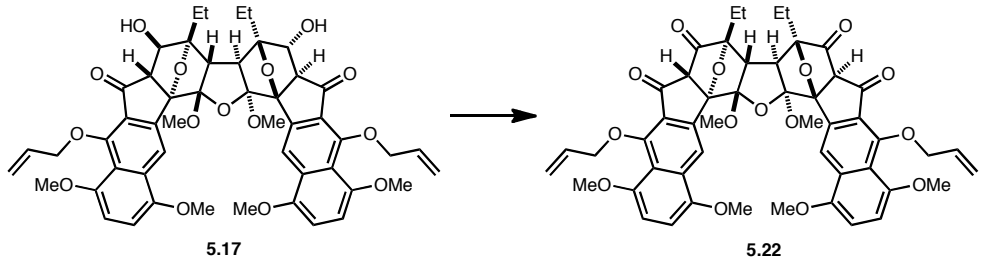

To the solution of oxalyl chloride (0.0022 mL, 0.0251 mmol, 4.00 equiv) in 0.5 mL of dichloromethane was added DMSO (0.0018 mL, 0.0251 mmol, 4.00 equiv) at –78 °C. In 20 minutes, diol **5.17** (5.6 mg, 0.00627 mmol, 1.00 equiv) in 0.3 mL of dichloromethane

(plus 0,2 mL rinse) was cannulated to the reaction mixture. The reaction mixture was stirred for 20 minutes, then DIEA (0.0070 mL, 0.0502 mmol, 8.00 equiv) was added in one portion. The reaction system was vigorously stirred for 30 minutes, then quenched with water. The mixture was warmed to 23 °C, and the aqueous phase was extracted with dichloromethane (3 × 2 mL). The combined organic layer was dried over Na_2SO_4 and filtered. After concentration the crude product was purified by flash column chromatography (EtOAc/hexane = 1/2 to 1/1.2) to provide ketone **5.22** (3.8 mg, 0.00433 mmol, 69%). ^{1}H NMR (600 MHz, $CDCl_3$) δ = 9.00 (s, 1H), 6.97 - 6.88 (m, 2H), 6.36 - 6.27 (m, 1H), 5.48 (d, *J* = 17.3 Hz, 1H), 5.31 (d, *J* = 10.3 Hz, 1H), 4.78 (dd, *J* = 5.9, 10.8 Hz, 1H), 4.66 (dd, *J* = 6.2, 10.3 Hz, 1H), 3.95 (s, 3H), 3.90 (s, 1H), 3.88 (s, 3H), 3.56 (s, 3H), 2.82 (s, 1H), 1.94 - 1.80 (m, 2H), 0.97 ppm (t, *J* = 7.3 Hz, 3H); ^{13}C NMR (125 MHz, $CDCl_3$) δ = 200.5, 188.5, 157.4, 152.7, 150.0, 138.7, 134.0, 132.4, 125.8, 122.9, 120.8, 118.2, 118.1, 116.6, 108.3, 108.2, 93.3, 89.0, 77.4, 64.7, 57.1, 56.1, 54.4, 54.2, 20.6, 7.5 ppm; HRMS (ESI) calcd for $C_{50}H_{53}O_{15}$ [M+H$^+$] 893.3379, found: 893.3266.

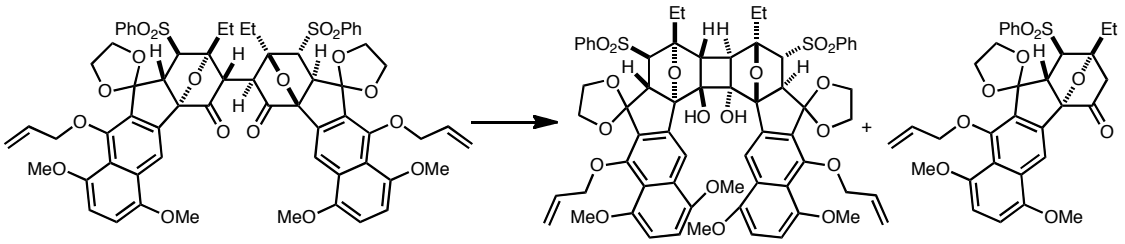

Ketone **4.12** (29.0 mg, 0.0245 mmol, 1.00 equiv) was dissolved in 1 mL of MeOH containing 0.3 mL of water. The solution was cooled to 0 °C and freshly prepared 1.0 M THF solution of SmI_2 (0.0980 mL, 0.0980 mmol, 4.00 equiv) was added via syringe. The mixture was stirred for 2 hours, then quenched with water. The aqueous phase was

extracted with dichloromethane (3 × 2 mL). The combined organic layer was dried over Na_2SO_4 and filtered. After concentration the crude product was purified by flash column chromatography (EtOAc/hexane = 1/1 to 1/1.2) to provide diol **5.28** (17.4 mg, 0.0147 mmol, 60%) and approximately 1 mg of monomer **4.13**. ^{1}H NMR (500 MHz, $CDCl_3$) δ = 8.74 (s, 1H), 8.09 (d, *J* = 7.8 Hz, 2H), 7.70 (d, *J* = 7.3 Hz, 1H), 7.66 - 7.61 (m, 2H), 6.68 (d, *J* = 8.3 Hz, 1H), 6.31 (d, *J* = 8.3 Hz, 1H), 6.24 - 6.13 (m, 1H), 5.43 (d, *J* = 16.1 Hz, 1H), 5.25 (d, *J* = 10.7 Hz, 1H), 4.47 (d, *J* = 4.9 Hz, 1H), 4.52 - 4.44 (m, 1H), 4.41 - 4.38 (m, 1H), 4.38 - 4.35 (m, 1H), 4.22 (s, 1H), 4.17 (d, *J* = 6.8 Hz, 1H), 4.10 - 4.04 (m, 1H), 3.83 (s, 3H), 3.49 - 3.43 (m, 1H), 3.36 (s, 1H), 2.62 (s, 3H), 2.38 - 2.18 (m, 1H), 1.23 ppm (br. s. 3H); HRMS (ESI) calcd for $C_{64}H_{64}NaO_{18}S_2$ [M+Na^+] 1207.3426, found: 1207.3400.

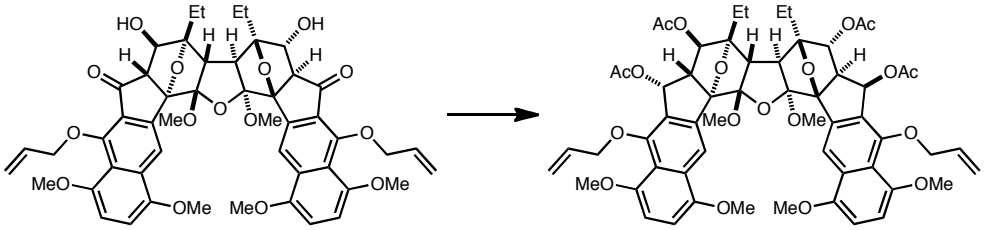

5.17 **5.47**

To the solution of ketone **5.17** (80.0 mg, 0.0896 mmol, 1.00 equiv) in 2 mL of THF was added 1.0 M THF solution of $LiBHEt_3$ (0.448 mL, 0.448 mmol, 5.00 equiv) at –78 °C. In 5 minutes the mixture was quenched with saturated aqueous solution of NH_4Cl (5 mL), then the aqueous phase was extracted with dichloromethane (3 × 2 mL). The combined organic layer was dried over Na_2SO_4 and filtered. After concentration the crude product was purified by flash column chromatography (EtOAc/hexane = 2/1 to 3/1) to give intermediate tetraol.

The alcohol was dissolved in 3 mL of dichloromethane and to the solution was added Ac_2O (0.0423 mL, 0.448 mmol, 5.00 equiv) and DMAP (109 mg, 0.896 mmol, 10.0 equiv) at 0 °C. The mixture was warmed to 23 °C and stirred for 2 hours. Upon completion of the reaction, the reaction system was quenched with 5 mL of water, and the aqueous phase was extracted with dichloromethane (3 × 5 mL). The combined organic layer was dried over Na_2SO_4 and filtered. After concentration the crude product was purified by flash column chromatography (EtOAc/hexane = 1/1.5 to 1/1) to give tetraacetate **5.47** (53.4 mg, 0.0502 mmol, 56%) as a pale yellow film. ^{1}H NMR (500 MHz, $CDCl_3$) δ = 8.86 (s, 1H), 6.89 (d, *J* = 7.8 Hz, 1H), 6.79 (d, *J* = 8.3 Hz, 1H), 6.75 - 6.70 (m, 1H), 6.30 - 6.18 (m, 1H), 5.40 (d, *J* = 17.6 Hz, 1H), 5.37 (br. s, 1H), 5.29 (d, *J* = 10.3 Hz, 1H), 4.59 (dd, *J* = 5.9, 10.3 Hz, 1H), 4.53 - 4.45 (m, 1H), 3.92 (s, 3H), 3.75 (s, 3H), 3.34 (s, 3H), 3.27 - 3.22 (m, 1H), 3.17 (s, 1H), 2.18 (s, 3H), 2.13 (s, 3H), 2.06 - 1.96 (m, 1H), 1.85 (qd, *J* = 7.0, 14.5 Hz, 1H), 1.03 ppm (t, *J* = 7.1 Hz, 3H); ^{13}C NMR (125 MHz, $CDCl_3$) δ = 170.0, 169.6, 153.1, 150.4, 150.0, 136.0, 134.4, 134.3, 130.8, 128.3, 122.4, 120.3, 117.4, 117.2, 106.4, 104.5, 95.2, 89.3, 76.6, 75.5, 69.6, 56.6, 55.9, 53.4, 52.9, 50.6, 23.6, 21.0, 20.9, 7.3 ppm; HRMS (ESI) calcd for $C_{58}H_{68}NO_{19}S_2$ [M+NH_4^+] 1082.4380, found: 1082.4413.

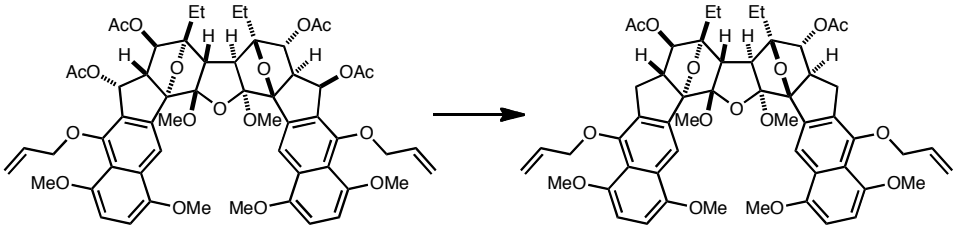

Tetraacetate **5.47** (13.8 mg, 0.0130 mmol, 1.00 mmol) was dissolved in 0.8 mL of dichloromethane, and the solution was cooled to –15 °C. To the solution was added Et_3SiH (0.0208 mL, 0.130 mmol, 10.0 quiv), followed by TfOH (0.00011 mL, 0.00130 mmol, 0.100 equiv). The resulting dark green solution was vigorously stirred at –13 °C for 6 hours. At the end of the reaction, the mixture was quenched with saturated aqueous solution of $NaHCO_3$ (2 mL), then the aqueous phase was extracted with dichloromethane (3 × 5 mL). The combined organic layer was dried over Na_2SO_4 and filtered. After concentration the crude product was purified by flash column chromatography (EtOAc/hexane = 1/3 to 1/2.5) to give tetraacetate **5.48** (7.0 mg, 0.00741 mmol, 57%) as a pale yellow film. ^{1}H NMR (500 MHz, $CDCl_3$) δ = 8.85 (s, 1H), 6.77 (d, *J* = 8.3 Hz, 1H), 6.65 (d, *J* = 8.3 Hz, 1H), 6.29 - 6.16 (m, 1H), 5.44 (d, *J* = 17.1 Hz, 1H), 5.29 (d, *J* = 10.3 Hz, 1H), 5.01 (d, *J* = 2.9 Hz, 1H), 4.49 (d, *J* = 5.4 Hz, 2H), 3.92 (s, 3H), 3.75 (s, 3H), 3.37 (s, 3H), 3.14 (s, 1H), 3.18 - 3.09 (m, 1H), 3.07 - 2.98 (m, 1H), 2.17 (s, 3H), 2.03 - 1.86 (m, 2H), 1.02 ppm (t, *J* = 7.3 Hz, 3H); ^{13}C NMR (125 MHz, $CDCl_3$) δ = 170.7, 150.7, 149.7, 136.6, 136.4, 134.7, 129.4, 128.3, 122.3, 120.3, 117.1, 117.0, 106.7, 103.1, 96.5, 88.6, 83.4, 75.0, 56.9, 55.8, 53.5, 51.3, 50.3, 33.4, 24.0, 21.2, 7.6 ppm; HRMS (ESI) calcd for $C_{54}H_{61}O_{15}$ [M+H$^+$] 949.4010, found: 949.4026.

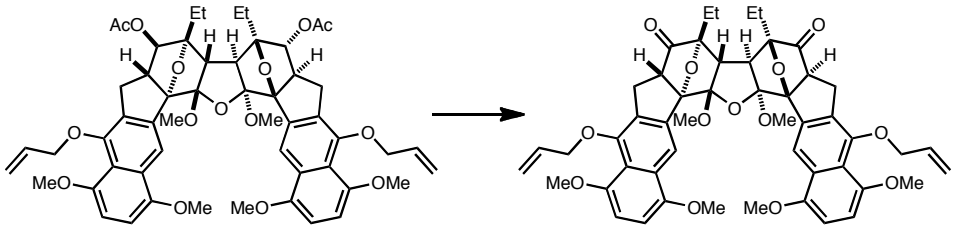

5.48 **5.49**

Acetate **5.48** (7.0 mg, 0.00741 mmol, 1.00 equiv) was dissolved in 0.5 mL of MeOH and the solution was cooled to 0 °C. To the solution was added K_2CO_3 (10.2 mg, 0.0741 mmol, 10.0 equiv). The mixture was warmed to 23 °C and stirred for 1 hour. After completion of the reaction, the reaction system was quenched with saturated aqueous solution of NH_4Cl (1 mL), and the aqueous phase was extracted with dichloromethane (3 × 2 mL). The combined organic layer was dried over Na_2SO_4 and filtered. After concentration the crude product was used for the next step without further purification.

The diol was dissolved in 1 mL of dichloromethane. To the solution was added NMO (2.6 mg, 0.0222, 3.00 equiv), 10 mg of 4 Å MS, and TPAP (0.1 mg, 0.000371 mmol, 0.05 equiv). After stirring for 30 minutes the mixture was diluted with 5 mL of diethyl ether, and filtered over a pad of silica gel. After concentration the crude product was purified by flash column chromatography (EtOAc/hexane = 1/3 to 1/2) to give ketone **5.49** (5.4 mg, 0.00627 mmol, 85%) as a pale yellow film. ^{1}H NMR (500 MHz, $CDCl_3$) δ = 8.90 (s, 1H), 6.82 (d, *J* = 8.2 Hz, 1H), 6.71 (d, *J* = 8.7 Hz, 1H), 6.26 - 6.12 (m, 1H), 5.43 (dd, *J* = 1.4, 16.9 Hz, 1H), 5.28 (d, *J* = 10.5 Hz, 1H), 4.55 - 4.44 (m, 2H), 3.93 (s, 3H), 3.82 (s, 3H), 3.62 - 3.53 (m, 1H), 3.49 (s, 3H), 3.47 - 3.40 (m, 1H), 3.12 (dd, *J* = 8.7, 16.0 Hz, 1H), 2.73 (s, 1H), 1.88 (tt, *J* = 7.2, 13.9 Hz, 2H), 1.00 ppm (t, *J* = 7.3 Hz, 3H); ^{13}C NMR (125 MHz, $CDCl_3$) δ = 211.9, 151.3, 150.7, 149.8, 136.0, 135.6, 134.5, 129.4, 122.5, 120.9, 117.4, 116.7, 110.7, 107.4, 103.8, 95.8, 91.8, 75.4, 57.0, 55.9, 54.1, 54.0, 53.7, 27.9, 22.7, 7.7 ppm; HRMS (ESI) calcd for $C_{50}H_{53}O_{13}$ [M+H$^+$] 861.3486, found: 861.3488.

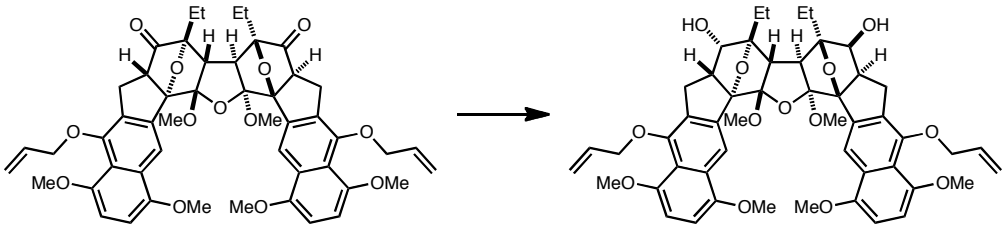

To the solution of ketone **5.49** (20.0 mg, 0.0232 mmol, 1.00 equiv) in 2 mL of THF was added 1.0 M THF solution of $LiBHEt_3$ (0.0511 mL, 0.0511 mmol, 2.20 equiv) at –78 °C. In 5 minutes the mixture was quenched with saturated aqueous solution of NH_4Cl (2 mL), and the aqueous phase was extracted with dichloromethane (3 × 5 mL). The combined organic layer was dried over Na_2SO_4 and filtered. After concentration the crude product was purified by flash column chromatography (EtOAc/hexane = 1/2 to 1/1) to give diol **5.51** (16.3 mg, 0.0188 mmol, 81%) as a pale yellow film. ^{1}H NMR (600 MHz, $CDCl_3$) δ = 8.78 (s, 1H), 6.77 (d, *J* = 8.5 Hz, 1H), 6.66 (d, *J* = 8.5 Hz, 1H), 6.22 (dt, *J* = 5.4, 11.2 Hz, 1H), 5.44 (d, *J* = 17.3 Hz, 1H), 5.28 (d, *J* = 10.3 Hz, 1H), 4.56 - 4.45 (m, 1H), 4.28 (dd, *J* = 6.9, 11.0 Hz, 1H), 3.93 (s, 3H), 3.78 (s, 3H), 3.51 - 3.45 (m, 1H), 3.32 (s, 3H), 3.28 (d, J = 9.1 Hz, 1H), 2.36 (s, 1H), 2.07 - 1.96 (m, 1H), 1.83 (d, J = 11.1 Hz, 1H), 1.91 - 1.78 (m, 1H), 1.02 ppm (t, J = 7.5 Hz, 3H); HRMS (ESI) calcd for $C_{50}H_{56}NaO_{13}$ [M+Na^+] 887.3619, found: 887.3655.

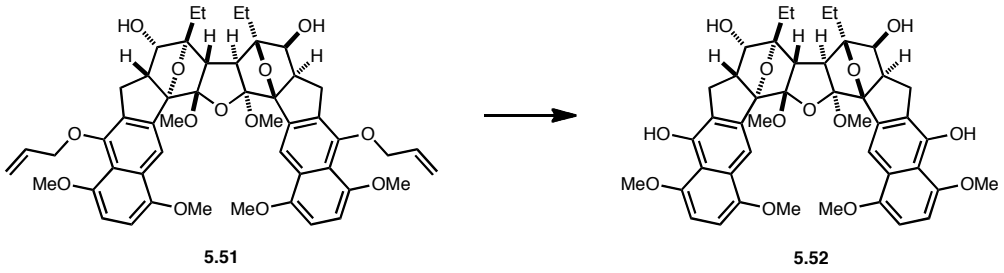

To the solution of allyl ether **5.51** (8.0 mg, 0.00925 mmol, 1.00 equiv) in 1 mL of dichloromethane was added 0.010 mL of AcOH, Bu_3SnH (0.0055 mL, 0.0203 mmol, 2.20 equiv), and $PdCl_2(PPh_3)_2$ (0.3 mg, 0.000460 mmol, 0.0500 equiv) at 0 °C. In 30 minutes, volatiles were removed under reduced pressure and the crude product was purified by flash column chromatography (EtOAc/hexane = 1/1 to 2/1) to give phenol **5.52** (6.5 mg, 0.00828 mmol, 90%) as colorless film. ^{1}H NMR (500 MHz, $CDCl_3$) δ = 9.59 (s, 1H), 8.48 (s, 1H), 6.67 (d, *J* = 8.3 Hz, 1H), 6.58 (d, *J* = 8.3 Hz, 1H), 4.26 (dd, *J* = 6.8, 10.7 Hz, 1H), 4.03 (s, 3H), 3.77 (s, 3H), 3.54 - 3.46 (m, 1H), 3.33 (s, 3H), 3.18 (d, *J* = 9.3 Hz, 2H), 2.35 (s, 1H), 2.08 - 1.96 (m, 1H), 1.92 - 1.76 (m, 1H), 1.01 ppm (t, *J* = 7.6 Hz, 3H); HRMS (ESI) calcd for $C_{44}H_{49}O_{13}S$ [M+H$^+$] 785.3173, found: 785.3177.

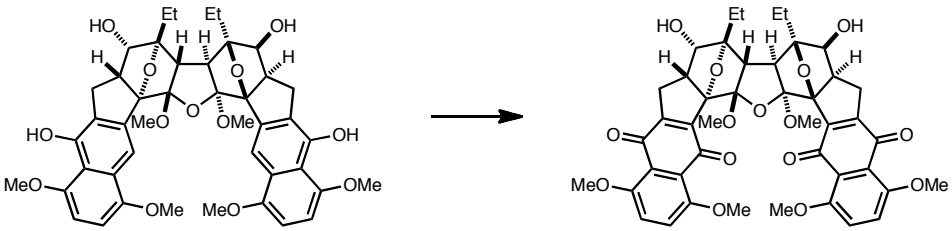

Phenol **5.52** (32.5 mg, 0.0414 mmol, 1.00 equiv) was dissolved in 1 mL of acetonitrile and 1 mL of water, and the mixture was cooled to 0 °C. To the solution was added PIFA (89.0 mg, 0.207 mmol, 5.00 equiv) in one portion, and the mixture was vigorously stirred for 30 minutes. After full consumption of the starting material the mixture was quenched with saturated aqueous solution of NaS_2O_3 (1 mL), and the aqueous phase was extracted with dichloromethane (3 × 5 mL). The combined organic layer was dried over Na_2SO_4 and filtered. After concentration the crude product was used for the next step.

The intermediate cyclohexadienone was dissolved in 2 mL of benzene and DDQ (28.1 mg, 0.124 mmol, 3.00 equiv) was added to the solution. The mixture was heated to 50 °C for 3 hours, then cooled to 23 °C. After concentration, the crude product was purified by prep TLC (EtOAc/acetone=1/1) to give the quinone **5.54** (26.2 mg, 0.0323 mmol, 78% over two steps) as red solid. ^{1}H NMR (500 MHz, $CDCl_3$) δ = 7.33 - 7.29 (m, 1H), 7.25 - 7.21 (m, 1H), 4.05 (br. s, 1H), 3.97 (s, 3H), 3.86 (s, 3H), 3.61 (s, 3H), 3.44 - 3.32 (m, 2H), 3.11 - 3.02 (m, 1H), 2.96 - 2.85 (m, 1H), 2.06 - 1.95 (m, 1H), 1.83 (qd, *J* = 7.3, 14.6 Hz, 1H), 0.94 (t, *J* = 7.6 Hz, 3H); HRMS (ESI) calcd for $C_{44}H_{48}NaO_{15}$ [M+Na^+] 839.2885, found: 839.2780.

Appendix 2

X-Ray Crystalographic Data

X-Ray Crystallography: A crystal mounted on a diffractometer was collected data at 100 K. The intensities of the reflections were collected by means of a Bruker APEX II CCD diffractometer ($Mo_{K\alpha}$ radiation, λ=0.71073 Å), and equipped with an Oxford Cryosystems nitrogen flow apparatus. The collection method involved 0.5° scans in ω at 28° in 2θ. Data integration down to 0.82 Å resolution was carried out using SAINT V7.46 A (Bruker diffractometer, 2009) with reflection spot size optimisation. Absorption corrections were made with the program SADABS (Bruker diffractometer, 2009). The structure was solved by the direct methods procedure and refined by least-squares methods again F^2 using SHELXS-97 and SHELXL-97 (Sheldrick, 2008). Non-hydrogen atoms were refined anisotropically, and hydrogen atoms were allowed to ride on the respective atoms. Crystal data as well as details of data collection and refinement are summarized in Table 1, geometric parameters are shown in Table 2 and hydrogen-bond parameters are list in Table 3. The Ortep plots produced with SHELXL-97 program, and the other drawings were produced with Accelrys DS Visualizer 2.0 (Accelrys, 2007).

Compound 4.35

Table 1.1 Experimental details

	Dimer
Crystal data	
Chemical formula	$C_{64}H_{68}Cl_2O_{18}S_2$
M_r	1260.20
Crystal system, space group	Monoclinic, $P2_1$

Table 1.1 (Continued)

Temperature (K)	100
a, *b*, *c* (Å)	13.7688 (10), 13.2782 (10), 17.2333 (12)
b (°)	110.610 (4)
V (Å^3)	2949.0 (4)
Z	2
Radiation type	Mo *K*a
m (mm^{-1})	0.26
Crystal size (mm)	0.32 × 0.24 × 0.16
Data collection	
Diffractometer	CCD area detector diffractometer
Absorption correction	Multi-scan *SADABS* (Sheldrick, 2009)
T_{min}, T_{max}	0.922, 0.960
No. of measured, independent and observed [$I > 2s(I)$] reflections	36391, 11575, 7985
R_{int}	0.066
Refinement	
$R[F^2 > 2s(F^2)]$, $wR(F^2)$, S	0.070, 0.189, 1.09
No. of reflections	11575
No. of parameters	769
No. of restraints	38
H-atom treatment	H-atom parameters constrained
$D\rho_{max}$, $D\rho_{min}$ (e Å^{-3})	0.76, -0.64
Absolute structure	Flack H D (1983), Acta Cryst. A39, 876-881
Flack parameter	0.05 (9)

Computer programs: *APEX2* v2009.3.0 (Bruker-AXS, 2009), *SAINT* 7.46A (Bruker-AXS, 2009), *SHELXS97* (Sheldrick, 2008), *SHELXL97* (Sheldrick, 2008), Bruker *SHELXTL*.

Table 1.2 Geometric parameters (Å, º)

S1—O2	1.411 (4)	C28—H28B	0.9800
S1—O3	1.423 (4)	C28—H28C	0.9800
S1—C20	1.744 (6)	C29—H29A	0.9800
S1—C3	1.778 (5)	C29—H29B	0.9800
S2—O12	1.403 (4)	C29—H29C	0.9800
S2—O13	1.424 (4)	C31—C32	1.532 (7)

Table 1.2 (Continued)

S2—C50	1.747 (5)	C31—C47	1.538 (7)
S2—C33	1.776 (5)	C31—H31A	1.0000
O1—C2	1.440 (6)	C32—C48	1.509 (7)
O1—C16	1.444 (6)	C32—C33	1.558 (7)
O4—C5	1.398 (6)	C33—C34	1.505 (7)
O4—C26	1.416 (7)	C33—H33A	1.0000
O5—C5	1.404 (6)	C34—C46	1.534 (7)
O5—C27	1.439 (6)	C34—C35	1.547 (7)
O6—C7	1.320 (6)	C34—H34A	1.0000
O6—H6O	0.8800	C35—C36	1.499 (7)
O7—C9	1.374 (6)	C36—C37	1.355 (7)
O7—C28	1.451 (6)	C36—C45	1.391 (7)
O8—C12	1.367 (6)	C37—C38	1.397 (8)
O8—C29	1.417 (6)	C38—C43	1.409 (8)
O9—C17	1.198 (6)	C38—C39	1.441 (8)
O11—C32	1.425 (6)	C39—C40	1.343 (9)
O11—C46	1.440 (6)	C40—C41	1.403 (10)
O14—C56	1.381 (10)	C40—H40A	0.9500
O14—C35	1.389 (6)	C41—C42	1.356 (9)
O14—C56B	1.51 (3)	C41—H41A	0.9500
O15—C57B	1.23 (4)	C42—C43	1.399 (8)
O15—C35	1.420 (6)	C43—C44	1.415 (8)
O15—C57	1.491 (11)	C44—C45	1.349 (7)
O16—C37	1.371 (7)	C44—H44A	0.9500
O16—H16O	0.8799	C45—C46	1.484 (7)
O17—C39	1.358 (8)	C46—C47	1.497 (7)
O17—C58	1.415 (8)	C48—C49	1.504 (7)
O18—C42	1.360 (8)	C48—H48A	0.9900
O18—C59B	1.40 (5)	C48—H48B	0.9900
O18—C59	1.444 (12)	C49—H49A	0.9800
O19—C47	1.201 (6)	C49—H49B	0.9800
C1—C17	1.533 (7)	C49—H49C	0.9800
C1—C31	1.536 (6)	C50—C55	1.354 (8)
C1—C2	1.549 (7)	C50—C51	1.368 (8)
C1—H1A	1.0000	C51—C52	1.365 (8)
C2—C18	1.495 (7)	C51—H51A	0.9500

Table 1.2 (Continued)

C2—C3	1.595 (7)	C52—C53	1.380 (9)
C3—C4	1.519 (7)	C52—H52A	0.9500
C3—H3A	1.0000	C53—C54	1.374 (9)
C4—C5	1.539 (7)	C53—H53A	0.9500
C4—C16	1.550 (6)	C54—C55	1.363 (8)
C4—H4A	1.0000	C54—H54A	0.9500
C5—C6	1.518 (7)	C55—H55A	0.9500
C6—C7	1.366 (7)	C56—C57	1.466 (16)
C6—C15	1.418 (7)	C56—H56A	0.9900
C7—C8	1.424 (7)	C56—H56B	0.9900
C8—C13	1.416 (7)	C57—H57A	0.9900
C8—C9	1.433 (7)	C57—H57B	0.9900
C9—C10	1.331 (7)	C56B—C57B	1.59 (5)
C10—C11	1.393 (8)	C56B—H56C	0.9900
C10—H10A	0.9500	C56B—H56D	0.9900
C11—C12	1.365 (8)	C57B—H57C	0.9900
C11—H11A	0.9500	C57B—H57D	0.9900
C12—C13	1.396 (7)	C58—H58A	0.9800
C13—C14	1.431 (7)	C58—H58B	0.9800
C14—C15	1.342 (7)	C58—H58C	0.9800
C14—H14A	0.9500	C59—H59A	0.9800
C15—C16	1.479 (7)	C59—H59B	0.9800
C16—C17	1.472 (7)	C59—H59C	0.9800
C18—C19	1.509 (8)	C59B—H59D	0.9800
C18—H18A	0.9900	C59B—H59E	0.9800
C18—H18B	0.9900	C59B—H59F	0.9800
C19—H19A	0.9800	C1S—Cl2S	1.732 (10)
C19—H19B	0.9800	C1S—Cl1S	1.743 (12)
C19—H19C	0.9800	C1S—H1SA	0.9900
C20—C25	1.367 (9)	C1S—H1SB	0.9900
C20—C21	1.388 (9)	C11S—C12S	1.483 (15)
C21—C22	1.379 (8)	C11S—H11B	0.9800
C21—H21A	0.9500	C11S—H11C	0.9800
C22—C23	1.314 (9)	C11S—H11D	0.9800
C22—H22A	0.9500	C12S—C13S	1.409 (11)
C23—C24	1.345 (9)	C12S—H12A	0.9900
C23—H23A	0.9500	C12S—H12B	0.9900

Table 1.2 (Continued)

C24—C25	1.391 (8)	C13S—C14S	1.385 (11)
C24—H24A	0.9500	C13S—H13A	0.9900
C25—H25A	0.9500	C13S—H13B	0.9900
C26—C27	1.479 (9)	C14S—C15S	1.500 (12)
C26—H26A	0.9900	C14S—H14B	0.9900
C26—H26B	0.9900	C14S—H14C	0.9900
C27—H27A	0.9900	C15S—H15A	0.9800
C27—H27B	0.9900	C15S—H15B	0.9800
C28—H28A	0.9800	C15S—H15C	0.9800
O2—S1—O3	119.2 (2)	C31—C32—C33	110.9 (4)
O2—S1—C20	109.5 (3)	C34—C33—C32	103.3 (4)
O3—S1—C20	108.5 (3)	C34—C33—S2	113.7 (3)
O2—S1—C3	108.8 (2)	C32—C33—S2	115.5 (3)
O3—S1—C3	107.2 (2)	C34—C33—H33A	108.0
C20—S1—C3	102.4 (3)	C32—C33—H33A	108.0
O12—S2—O13	118.5 (2)	S2—C33—H33A	108.0
O12—S2—C50	109.4 (2)	C33—C34—C46	101.0 (4)
O13—S2—C50	108.3 (3)	C33—C34—C35	119.3 (4)
O12—S2—C33	106.9 (2)	C46—C34—C35	104.9 (4)
O13—S2—C33	109.8 (2)	C33—C34—H34A	110.3
C50—S2—C33	102.8 (2)	C46—C34—H34A	110.3
C2—O1—C16	99.0 (3)	C35—C34—H34A	110.3
C5—O4—C26	108.4 (4)	O14—C35—O15	106.9 (4)
C5—O5—C27	106.4 (4)	O14—C35—C36	113.1 (4)
C7—O6—H6O	113.5	O15—C35—C36	113.1 (4)
C9—O7—C28	117.1 (4)	O14—C35—C34	112.7 (4)
C12—O8—C29	116.0 (4)	O15—C35—C34	108.6 (4)
C32—O11—C46	97.7 (3)	C36—C35—C34	102.4 (4)
C56—O14—C35	111.6 (6)	C37—C36—C45	120.1 (5)
C35—O14—C56B	104.1 (14)	C37—C36—C35	127.5 (5)
C57B—O15—C35	117 (2)	C45—C36—C35	112.4 (4)
C35—O15—C57	107.3 (6)	C36—C37—O16	118.1 (5)
C37—O16—H16O	115.5	C36—C37—C38	119.8 (5)
C39—O17—C58	117.8 (6)	O16—C37—C38	122.0 (5)
C42—O18—C59B	129 (2)	C37—C38—C43	119.2 (5)
C42—O18—C59	114.0 (6)	C37—C38—C39	122.9 (5)

Table 1.2 (Continued)

C17—C1—C31	110.3 (4)	C43—C38—C39	117.9 (5)
C17—C1—C2	99.5 (4)	C40—C39—O17	124.0 (6)
C31—C1—C2	111.7 (4)	C40—C39—C38	121.0 (6)
C17—C1—H1A	111.6	O17—C39—C38	115.1 (5)
C31—C1—H1A	111.6	C39—C40—C41	120.6 (6)
C2—C1—H1A	111.6	C39—C40—H40A	119.7
O1—C2—C18	110.2 (4)	C41—C40—H40A	119.7
O1—C2—C1	99.8 (4)	C42—C41—C40	119.6 (6)
C18—C2—C1	119.6 (4)	C42—C41—H41A	120.2
O1—C2—C3	98.5 (4)	C40—C41—H41A	120.2
C18—C2—C3	114.4 (4)	C41—C42—O18	123.4 (6)
C1—C2—C3	111.1 (4)	C41—C42—C43	122.2 (6)
C4—C3—C2	103.1 (4)	O18—C42—C43	114.3 (5)
C4—C3—S1	114.3 (3)	C42—C43—C38	118.6 (5)
C2—C3—S1	114.4 (3)	C42—C43—C44	121.0 (6)
C4—C3—H3A	108.2	C38—C43—C44	120.4 (5)
C2—C3—H3A	108.2	C45—C44—C43	117.3 (5)
S1—C3—H3A	108.2	C45—C44—H44A	121.4
C3—C4—C5	119.7 (4)	C43—C44—H44A	121.4
C3—C4—C16	101.5 (4)	C44—C45—C36	123.1 (5)
C5—C4—C16	105.5 (4)	C44—C45—C46	128.2 (5)
C3—C4—H4A	109.8	C36—C45—C46	108.8 (4)
C5—C4—H4A	109.8	O11—C46—C45	112.4 (4)
C16—C4—H4A	109.8	O11—C46—C47	102.7 (4)
O4—C5—O5	107.8 (4)	C45—C46—C47	126.2 (4)
O4—C5—C6	116.3 (4)	O11—C46—C34	102.5 (4)
O5—C5—C6	108.4 (4)	C45—C46—C34	104.8 (4)
O4—C5—C4	108.0 (4)	C47—C46—C34	105.9 (4)
O5—C5—C4	113.8 (4)	O19—C47—C46	127.5 (5)
C6—C5—C4	102.6 (4)	O19—C47—C31	128.2 (5)
C7—C6—C15	119.3 (5)	C46—C47—C31	104.0 (4)
C7—C6—C5	128.2 (5)	C49—C48—C32	115.3 (4)
C15—C6—C5	112.3 (4)	C49—C48—H48A	108.5
O6—C7—C6	117.4 (5)	C32—C48—H48A	108.5
O6—C7—C8	123.5 (5)	C49—C48—H48B	108.5
C6—C7—C8	118.9 (5)	C32—C48—H48B	108.5
C13—C8—C7	120.3 (4)	H48A—C48—H48B	107.5

Table 1.2 (Continued)

C13—C8—C9	116.8 (5)	C48—C49—H49A	109.5
C7—C8—C9	122.8 (5)	C48—C49—H49B	109.5
C10—C9—O7	124.1 (5)	H49A—C49—H49B	109.5
C10—C9—C8	121.2 (5)	C48—C49—H49C	109.5
O7—C9—C8	114.7 (5)	H49A—C49—H49C	109.5
C9—C10—C11	121.4 (5)	H49B—C49—H49C	109.5
C9—C10—H10A	119.3	C55—C50—C51	120.7 (5)
C11—C10—H10A	119.3	C55—C50—S2	120.3 (4)
C12—C11—C10	119.9 (5)	C51—C50—S2	119.1 (5)
C12—C11—H11A	120.1	C52—C51—C50	119.5 (6)
C10—C11—H11A	120.1	C52—C51—H51A	120.2
C11—C12—O8	123.3 (5)	C50—C51—H51A	120.2
C11—C12—C13	120.4 (5)	C51—C52—C53	120.3 (6)
O8—C12—C13	116.1 (4)	C51—C52—H52A	119.9
C12—C13—C8	120.1 (5)	C53—C52—H52A	119.9
C12—C13—C14	120.4 (5)	C54—C53—C52	119.0 (5)
C8—C13—C14	119.2 (4)	C54—C53—H53A	120.5
C15—C14—C13	117.9 (5)	C52—C53—H53A	120.5
C15—C14—H14A	121.0	C55—C54—C53	120.3 (6)
C13—C14—H14A	121.0	C55—C54—H54A	119.9
C14—C15—C6	123.6 (5)	C53—C54—H54A	119.9
C14—C15—C16	127.4 (5)	C50—C55—C54	120.1 (6)
C6—C15—C16	108.3 (4)	C50—C55—H55A	119.9
O1—C16—C17	103.4 (4)	C54—C55—H55A	119.9
O1—C16—C15	110.1 (4)	O14—C56—C57	106.6 (8)
C17—C16—C15	128.2 (4)	O14—C56—H56A	110.4
O1—C16—C4	102.5 (4)	C57—C56—H56A	110.4
C17—C16—C4	103.3 (4)	O14—C56—H56B	110.4
C15—C16—C4	106.4 (4)	C57—C56—H56B	110.4
O9—C17—C16	128.4 (5)	H56A—C56—H56B	108.6
O9—C17—C1	126.1 (5)	C56—C57—O15	103.0 (10)
C16—C17—C1	105.2 (4)	C56—C57—H57A	111.2
C2—C18—C19	113.9 (4)	O15—C57—H57A	111.2
C2—C18—H18A	108.8	C56—C57—H57B	111.2
C19—C18—H18A	108.8	O15—C57—H57B	111.2
C2—C18—H18B	108.8	H57A—C57—H57B	109.1
C19—C18—H18B	108.8	O14—C56B—C57B	102 (3)

Table 1.2 (Continued)

H18A—C18—H18B	107.7	O14—C56B—H56C	111.4
C18—C19—H19A	109.5	C57B—C56B—H56C	111.4
C18—C19—H19B	109.5	O14—C56B—H56D	111.4
H19A—C19—H19B	109.5	C57B—C56B—H56D	111.4
C18—C19—H19C	109.5	H56C—C56B—H56D	109.3
H19A—C19—H19C	109.5	O15—C57B—C56B	103 (3)
H19B—C19—H19C	109.5	O15—C57B—H57C	111.1
C25—C20—C21	121.3 (6)	O15—C57B—H57D	111.1
C25—C20—S1	119.4 (5)	C56B—C57B—H57D	111.1
C21—C20—S1	119.2 (5)	O17—C58—H58A	109.5
C22—C21—C20	117.0 (6)	O17—C58—H58B	109.5
C22—C21—H21A	121.5	H58A—C58—H58B	109.5
C20—C21—H21A	121.5	O17—C58—H58C	109.5
C23—C22—C21	121.5 (7)	H58A—C58—H58C	109.5
C23—C22—H22A	119.2	H58B—C58—H58C	109.5
C21—C22—H22A	119.2	O18—C59—H59A	109.5
C22—C23—C24	122.5 (6)	O18—C59—H59B	109.5
C22—C23—H23A	118.8	O18—C59—H59C	109.5
C24—C23—H23A	118.8	O18—C59B—H59D	109.5
C23—C24—C25	119.0 (6)	O18—C59B—H59E	109.5
C23—C24—H24A	120.5	H59D—C59B—H59E	109.5
C25—C24—H24A	120.5	O18—C59B—H59F	109.5
C20—C25—C24	118.7 (6)	H59D—C59B—H59F	109.5
C20—C25—H25A	120.7	H59E—C59B—H59F	109.5
C24—C25—H25A	120.7	Cl2S—C1S—Cl1S	112.6 (6)
O4—C26—C27	102.1 (4)	Cl2S—C1S—H1SA	109.1
O4—C26—H26A	111.4	Cl1S—C1S—H1SA	109.1
C27—C26—H26A	111.4	Cl2S—C1S—H1SB	109.1
O4—C26—H26B	111.4	Cl1S—C1S—H1SB	109.1
C27—C26—H26B	111.4	H1SA—C1S—H1SB	107.8
H26A—C26—H26B	109.2	C12S—C11S—H11B	109.5
O5—C27—C26	103.7 (5)	C12S—C11S—H11C	109.5
O5—C27—H27A	111.0	H11B—C11S—H11C	109.5
C26—C27—H27A	111.0	C12S—C11S—H11D	109.5
O5—C27—H27B	111.0	H11B—C11S—H11D	109.5
C26—C27—H27B	111.0	H11C—C11S—H11D	109.5
H27A—C27—H27B	109.0	C13S—C12S—C11S	106.4 (8)

Table 1.2 (Continued)

O7—C28—H28A	109.5	C13S—C12S—H12A	110.4
O7—C28—H28B	109.5	C11S—C12S—H12A	110.4
H28A—C28—H28B	109.5	C13S—C12S—H12B	110.4
O7—C28—H28C	109.5	C11S—C12S—H12B	110.4
H28A—C28—H28C	109.5	H12A—C12S—H12B	108.6
H28B—C28—H28C	109.5	C14S—C13S—C12S	110.1 (7)
O8—C29—H29A	109.5	C14S—C13S—H13A	109.6
O8—C29—H29B	109.5	C12S—C13S—H13A	109.6
H29A—C29—H29B	109.5	C14S—C13S—H13B	109.6
O8—C29—H29C	109.5	C12S—C13S—H13B	109.6
H29A—C29—H29C	109.5	H13A—C13S—H13B	108.2
H29B—C29—H29C	109.5	C13S—C14S—C15S	108.7 (8)
C32—C31—C1	115.5 (4)	C13S—C14S—H14B	110.0
C32—C31—C47	99.4 (4)	C15S—C14S—H14B	110.0
C1—C31—C47	112.0 (4)	C13S—C14S—H14C	110.0
C32—C31—H31A	109.8	C15S—C14S—H14C	110.0
C1—C31—H31A	109.8	H14B—C14S—H14C	108.3
C47—C31—H31A	109.8	C14S—C15S—H15A	109.5
O11—C32—C48	109.6 (4)	C14S—C15S—H15B	109.5
O11—C32—C31	101.4 (4)	H15A—C15S—H15B	109.5
C48—C32—C31	118.4 (4)	C14S—C15S—H15C	109.5
O11—C32—C33	100.0 (4)	H15A—C15S—H15C	109.5
C48—C32—C33	114.0 (4)	H15B—C15S—H15C	109.5
C16—O1—C2—C18	-176.5 (4)	C47—C31—C32—C48	-159.6 (4)
C16—O1—C2—C1	56.8 (4)	C1—C31—C32—C33	-174.3 (4)
C16—O1—C2—C3	-56.4 (4)	C47—C31—C32—C33	65.7 (4)
C17—C1—C2—O1	-40.8 (4)	O11—C32—C33—C34	35.1 (4)
C31—C1—C2—O1	75.6 (4)	C48—C32—C33—C34	151.9 (4)
C17—C1—C2—C18	-160.9 (4)	C31—C32—C33—C34	-71.3 (5)
C31—C1—C2—C18	-44.5 (6)	O11—C32—C33—S2	159.9 (3)
C17—C1—C2—C3	62.3 (5)	C48—C32—C33—S2	-83.3 (5)
C31—C1—C2—C3	178.7 (4)	C31—C32—C33—S2	53.5 (5)
O1—C2—C3—C4	36.2 (4)	O12—S2—C33—C34	174.4 (3)
C18—C2—C3—C4	153.1 (4)	O13—S2—C33—C34	44.7 (4)
C1—C2—C3—C4	-67.8 (5)	C50—S2—C33—C34	-70.5 (4)
O1—C2—C3—S1	161.0 (3)	O12—S2—C33—C32	55.2 (4)

Table 1.2 (Continued)

C18—C2—C3—S1	-82.1 (5)	O13—S2—C33—C32	-74.6 (4)
C1—C2—C3—S1	57.0 (5)	C50—S2—C33—C32	170.3 (4)
O2—S1—C3—C4	30.5 (4)	C32—C33—C34—C46	-1.1 (5)
O3—S1—C3—C4	160.5 (4)	S2—C33—C34—C46	-127.1 (3)
C20—S1—C3—C4	-85.4 (4)	C32—C33—C34—C35	-115.3 (4)
O2—S1—C3—C2	-88.1 (4)	S2—C33—C34—C35	118.7 (4)
O3—S1—C3—C2	41.9 (4)	C56—O14—C35—O15	4.0 (6)
C20—S1—C3—C2	156.0 (4)	C56B—O14—C35—O15	-18.2 (13)
C2—C3—C4—C5	-118.5 (4)	C56—O14—C35—C36	129.1 (6)
S1—C3—C4—C5	116.7 (4)	C56B—O14—C35—C36	106.9 (13)
C2—C3—C4—C16	-3.1 (5)	C56—O14—C35—C34	-115.3 (6)
S1—C3—C4—C16	-127.9 (4)	C56B—O14—C35—C34	-137.5 (12)
C26—O4—C5—O5	12.9 (6)	C57B—O15—C35—O14	3 (3)
C26—O4—C5—C6	-109.0 (5)	C57—O15—C35—O14	9.8 (8)
C26—O4—C5—C4	136.3 (4)	C57B—O15—C35—C36	-122 (3)
C27—O5—C5—O4	9.4 (5)	C57—O15—C35—C36	-115.3 (8)
C27—O5—C5—C6	136.1 (4)	C57B—O15—C35—C34	125 (3)
C27—O5—C5—C4	-110.4 (5)	C57—O15—C35—C34	131.7 (8)
C3—C4—C5—O4	-102.1 (5)	C33—C34—C35—O14	13.3 (6)
C16—C4—C5—O4	144.6 (4)	C46—C34—C35—O14	-98.8 (5)
C3—C4—C5—O5	17.6 (6)	C33—C34—C35—O15	-105.1 (5)
C16—C4—C5—O5	-95.7 (5)	C46—C34—C35—O15	142.8 (4)
C3—C4—C5—C6	134.5 (4)	C33—C34—C35—C36	135.1 (4)
C16—C4—C5—C6	21.2 (5)	C46—C34—C35—C36	23.0 (5)
O4—C5—C6—C7	52.5 (7)	O14—C35—C36—C37	-71.8 (7)
O5—C5—C6—C7	-69.1 (6)	O15—C35—C36—C37	49.9 (7)
C4—C5—C6—C7	170.2 (5)	C34—C35—C36—C37	166.6 (5)
O4—C5—C6—C15	-132.3 (4)	O14—C35—C36—C45	109.3 (5)
O5—C5—C6—C15	106.0 (5)	O15—C35—C36—C45	-129.0 (4)
C4—C5—C6—C15	-14.7 (5)	C34—C35—C36—C45	-12.3 (5)
C15—C6—C7—O6	175.6 (4)	C45—C36—C37—O16	-177.4 (5)
C5—C6—C7—O6	-9.5 (8)	C35—C36—C37—O16	3.8 (9)
C15—C6—C7—C8	-9.0 (7)	C45—C36—C37—C38	2.7 (8)
C5—C6—C7—C8	165.8 (5)	C35—C36—C37—C38	-176.1 (5)
O6—C7—C8—C13	179.0 (5)	C36—C37—C38—C43	0.8 (8)
C6—C7—C8—C13	3.9 (7)	O16—C37—C38—C43	-179.2 (5)
O6—C7—C8—C9	3.0 (8)	C36—C37—C38—C39	178.7 (6)

Table 1.2 (Continued)

C6—C7—C8—C9	-172.0 (5)	O16—C37—C38—C39	-1.3 (9)
C28—O7—C9—C10	-22.4 (8)	C58—O17—C39—C40	-11.3 (10)
C28—O7—C9—C8	156.1 (5)	C58—O17—C39—C38	168.5 (6)
C13—C8—C9—C10	-4.3 (8)	C37—C38—C39—C40	-175.6 (6)
C7—C8—C9—C10	171.7 (5)	C43—C38—C39—C40	2.3 (9)
C13—C8—C9—O7	177.1 (4)	C37—C38—C39—O17	4.7 (9)
C7—C8—C9—O7	-6.9 (7)	C43—C38—C39—O17	-177.4 (5)
O7—C9—C10—C11	179.1 (5)	O17—C39—C40—C41	-179.7 (6)
C8—C9—C10—C11	0.7 (8)	C38—C39—C40—C41	0.5 (10)
C9—C10—C11—C12	2.5 (8)	C39—C40—C41—C42	-2.8 (10)
C10—C11—C12—O8	-177.5 (5)	C40—C41—C42—O18	179.3 (6)
C10—C11—C12—C13	-1.8 (8)	C40—C41—C42—C43	2.1 (10)
C29—O8—C12—C11	23.4 (7)	C59B—O18—C42—C41	-23 (2)
C29—O8—C12—C13	-152.5 (5)	C59—O18—C42—C41	-5.3 (9)
C11—C12—C13—C8	-2.1 (8)	C59B—O18—C42—C43	155 (2)
O8—C12—C13—C8	173.9 (4)	C59—O18—C42—C43	172.2 (7)
C11—C12—C13—C14	-177.1 (5)	C41—C42—C43—C38	0.9 (9)
O8—C12—C13—C14	-1.1 (7)	O18—C42—C43—C38	-176.6 (5)
C7—C8—C13—C12	-171.2 (5)	C41—C42—C43—C44	179.6 (6)
C9—C8—C13—C12	5.0 (7)	O18—C42—C43—C44	2.1 (8)
C7—C8—C13—C14	3.9 (7)	C37—C38—C43—C42	175.0 (5)
C9—C8—C13—C14	-179.9 (5)	C39—C38—C43—C42	-3.0 (8)
C12—C13—C14—C15	168.6 (5)	C37—C38—C43—C44	-3.8 (8)
C8—C13—C14—C15	-6.5 (7)	C39—C38—C43—C44	178.2 (5)
C13—C14—C15—C6	1.4 (7)	C42—C43—C44—C45	-175.5 (5)
C13—C14—C15—C16	-167.3 (5)	C38—C43—C44—C45	3.2 (8)
C7—C6—C15—C14	6.6 (8)	C43—C44—C45—C36	0.3 (8)
C5—C6—C15—C14	-169.1 (5)	C43—C44—C45—C46	180.0 (5)
C7—C6—C15—C16	177.2 (5)	C37—C36—C45—C44	-3.3 (8)
C5—C6—C15—C16	1.5 (6)	C35—C36—C45—C44	175.7 (5)
C2—O1—C16—C17	-50.7 (4)	C37—C36—C45—C46	176.9 (5)
C2—O1—C16—C15	169.4 (4)	C35—C36—C45—C46	-4.1 (6)
C2—O1—C16—C4	56.5 (4)	C32—O11—C46—C45	168.7 (4)
C14—C15—C16—O1	72.2 (6)	C32—O11—C46—C47	-53.0 (4)
C6—C15—C16—O1	-97.9 (4)	C32—O11—C46—C34	56.8 (4)
C14—C15—C16—C17	-54.8 (8)	C44—C45—C46—O11	88.7 (6)
C6—C15—C16—C17	135.0 (5)	C36—C45—C46—O11	-91.6 (5)

Table 1.2 (Continued)

C14—C15—C16—C4	-177.4 (5)	C44—C45—C46—C47	-37.8 (8)
C6—C15—C16—C4	12.4 (5)	C36—C45—C46—C47	141.9 (5)
C3—C4—C16—O1	-31.1 (5)	C44—C45—C46—C34	-160.8 (5)
C5—C4—C16—O1	94.3 (4)	C36—C45—C46—C34	18.9 (5)
C3—C4—C16—C17	76.1 (4)	C33—C34—C46—O11	-33.1 (4)
C5—C4—C16—C17	-158.4 (4)	C35—C34—C46—O11	91.6 (4)
C3—C4—C16—C15	-146.8 (4)	C33—C34—C46—C45	-150.6 (4)
C5—C4—C16—C15	-21.3 (5)	C35—C34—C46—C45	-26.0 (5)
O1—C16—C17—O9	-162.2 (5)	C33—C34—C46—C47	74.2 (4)
C15—C16—C17—O9	-32.6 (8)	C35—C34—C46—C47	-161.2 (4)
C4—C16—C17—O9	91.3 (6)	O11—C46—C47—O19	-158.9 (5)
O1—C16—C17—C1	23.6 (4)	C45—C46—C47—O19	-28.6 (8)
C15—C16—C17—C1	153.2 (4)	C34—C46—C47—O19	93.9 (6)
C4—C16—C17—C1	-82.9 (4)	O11—C46—C47—C31	27.3 (4)
C31—C1—C17—O9	78.5 (6)	C45—C46—C47—C31	157.7 (5)
C2—C1—C17—O9	-164.0 (5)	C34—C46—C47—C31	-79.8 (4)
C31—C1—C17—C16	-107.1 (4)	C32—C31—C47—O19	-166.7 (5)
C2—C1—C17—C16	10.4 (5)	C1—C31—C47—O19	70.8 (6)
O1—C2—C18—C19	51.6 (6)	C32—C31—C47—C46	7.1 (4)
C1—C2—C18—C19	166.3 (5)	C1—C31—C47—C46	-115.5 (4)
C3—C2—C18—C19	-58.3 (6)	O11—C32—C48—C49	56.0 (6)
O2—S1—C20—C25	159.4 (5)	C31—C32—C48—C49	171.5 (4)
O3—S1—C20—C25	27.8 (6)	C33—C32—C48—C49	-55.2 (6)
C3—S1—C20—C25	-85.3 (5)	O12—S2—C50—C55	-141.4 (4)
O2—S1—C20—C21	-22.6 (6)	O13—S2—C50—C55	-10.9 (5)
O3—S1—C20—C21	-154.2 (5)	C33—S2—C50—C55	105.3 (5)
C3—S1—C20—C21	92.7 (5)	O12—S2—C50—C51	38.9 (5)
C25—C20—C21—C22	1.5 (9)	O13—S2—C50—C51	169.4 (4)
S1—C20—C21—C22	-176.5 (5)	C33—S2—C50—C51	-74.3 (5)
C20—C21—C22—C23	0.7 (9)	C55—C50—C51—C52	-0.6 (8)
C21—C22—C23—C24	-1.8 (10)	S2—C50—C51—C52	179.1 (4)
C22—C23—C24—C25	0.7 (10)	C50—C51—C52—C53	2.6 (9)
C21—C20—C25—C24	-2.5 (9)	C51—C52—C53—C54	-2.9 (9)
S1—C20—C25—C24	175.5 (5)	C52—C53—C54—C55	1.3 (9)
C23—C24—C25—C20	1.4 (9)	C51—C50—C55—C54	-1.0 (8)
C5—O4—C26—C27	-28.9 (6)	S2—C50—C55—C54	179.3 (5)
C5—O5—C27—C26	-26.8 (6)	C53—C54—C55—C50	0.7 (9)

Table 1.2 (Continued)

O4—C26—C27—O5	33.6 (6)	C35—O14—C56—C57	-16.3 (11)
C17—C1—C31—C32	-142.1 (4)	O14—C56—C57—O15	20.9 (13)
C2—C1—C31—C32	108.2 (5)	C35—O15—C57—C56	-18.8 (12)
C17—C1—C31—C47	-29.3 (6)	C56—O14—C56B—C57B	-89 (6)
C2—C1—C31—C47	-138.9 (4)	C35—O14—C56B—C57B	24 (3)
C46—O11—C32—C48	-176.0 (4)	C35—O15—C57B—C56B	13 (5)
C46—O11—C32—C31	58.1 (4)	C57—O15—C57B—C56B	-21 (14)
C46—O11—C32—C33	-55.9 (4)	O14—C56B—C57B—O15	-23 (4)
C1—C31—C32—O11	80.2 (5)	C11S—C12S—C13S—C14S	-177.5 (9)
C47—C31—C32—O11	-39.8 (4)	C12S—C13S—C14S—C15S	176.3 (9)
C1—C31—C32—C48	-39.7 (6)		

Table 1.3 Hydrogen-bond parameters

D—H···*A*	*D*—H (Å)	H···*A* (Å)	*D*···*A* (Å)	*D*—H···*A* (°)
O6—H6O···O7	0.88	1.82	2.535 (5)	136.3
O6—H6O···O9^{i}	0.88	2.55	3.032 (5)	115.0
O16—H16O···O17	0.88	1.78	2.496 (6)	137.1

Symmetry code(s): (i) -*x*+1, *y*+1/2, -*z*-1.

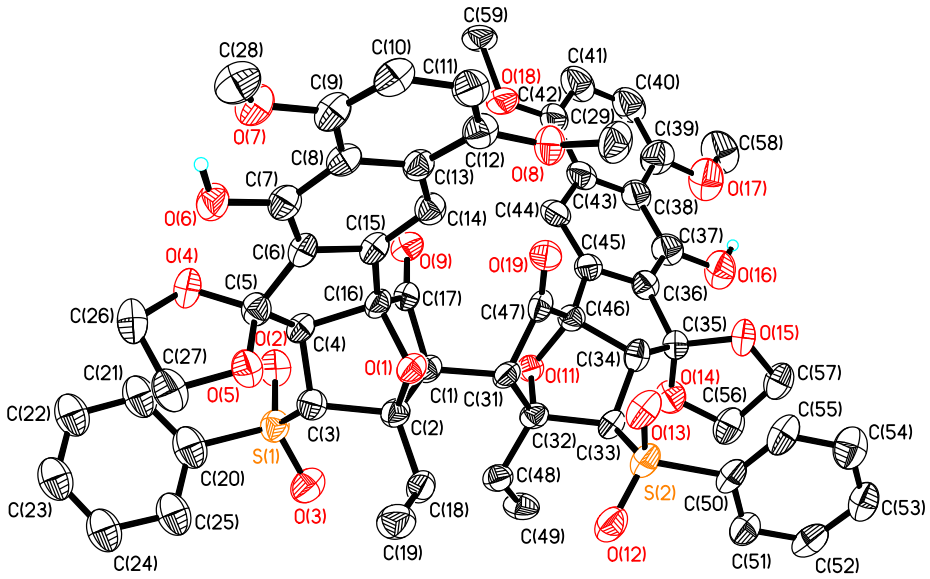

Figure 1.1 Perspective views showing 50% probability for two independent molecules (disorder part and the H atoms that ride on the C atoms have been omitted).

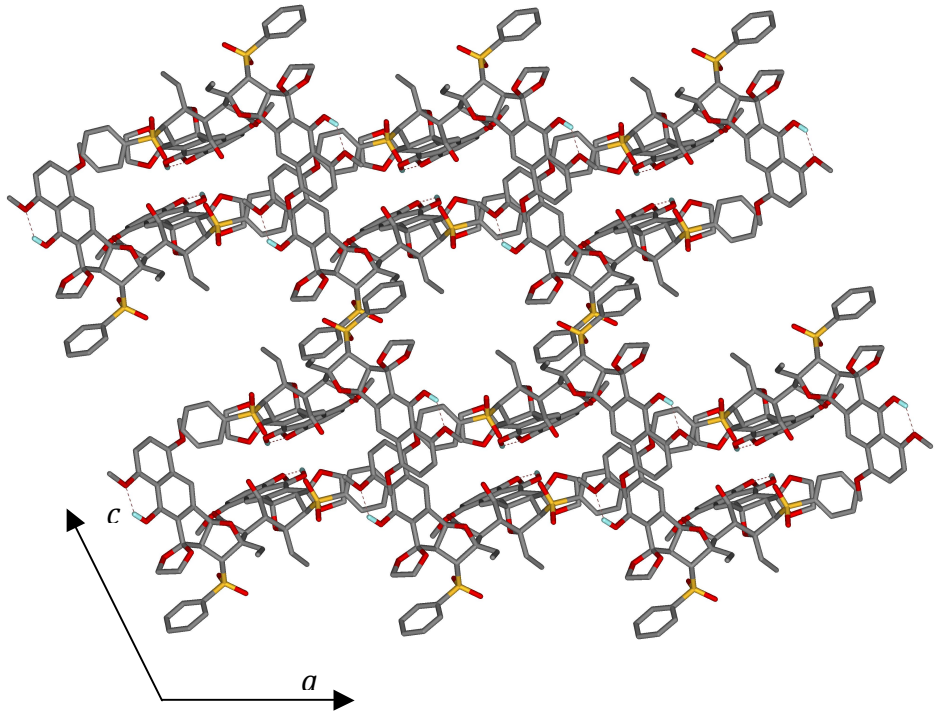

Figure 1.2. Three-dimensional supramolecular architecture viewed along the *b*-axis direction (disorder part, the H atoms ride on C atoms and solvents have been omitted).

Compound 5.17

NOTE: The intensity of this data is too weak (#Sigma %<2s up to 92.3 at 0.94 Ang.), since the crystal is micro -size. This result is NOT for publication.

Table 2.1 Experimental details

	V-108
Crystal data	
Chemical formula	$C_{50}H_{52}O_{15}$
M_r	892.92
Crystal system, space group	Monoclinic, $P2_1$
Temperature (K)	100
a, *b*, *c* (Å)	14.4713 (7), 22.2295 (9), 19.9174 (8)
b (°)	92.343 (2)
V (Å^3)	6401.9 (5)

Table 2.1 (Continued)

Z	4
Radiation type	Mo *K*a
m (mm^{-1})	0.07
Crystal size (mm)	0.24 × 0.06 × 0.04
Data collection	
Diffractometer	CCD area detector diffractometer
Absorption correction	Multi-scan *SADABS* (Sheldrick, 2009)
T_{min}, T_{max}	0.984, 0.997
No. of measured, independent and observed [$I > 2s(I)$] reflections	22193, 22193, 10735
R_{int}	0.095
Refinement	
$R[F^2 > 2s(F^2)]$, $wR(F^2)$, *S*	0.141, 0.307, 1.08
No. of reflections	22193
No. of parameters	1050
No. of restraints	1324
H-atom treatment	H-atom parameters constrained
$D\rho_{max}$, $D\rho_{min}$ (e $Å^{-3}$)	1.01, -0.82
Absolute structure	Flack H D (1983), Acta Cryst. A39, 876-881
Flack parameter	-2 (2)

Computer programs: *APEX2* v2009.3.0 (Bruker-AXS, 2009), *SAINT* 7.46A (Bruker-AXS, 2009), *SHELXS97* (Sheldrick, 2008), *SHELXL97* (Sheldrick, 2008), Bruker *SHELXTL*.

Table 2.2 Geometric parameters (Å, º)

O1—C2	1.581 (12)	O22—C53	1.461 (11)
O1—C16	1.633 (11)	O23—C55	1.117 (10)
O2—C3	1.458 (12)	O24—C65	1.343 (13)
O3—C5	1.116 (11)	O24—C87	1.457 (9)
O4—C8	1.355 (8)	O25—C90	0.890 (15)
O4—C37	1.442 (9)	O25—C59	1.298 (13)
O5—C12	1.358 (9)	O26—C91B	1.38 (2)
O5—C40	1.458 (15)	O26—C91	1.393 (15)

Table 2.2 (Continued)

O6—C9	1.420 (9)	O26—C62	1.457 (13)
O6—C41	1.434 (13)	O27—C67	1.368 (13)
O7—C42	1.442 (12)	O27—C92	1.501 (13)
O7—C17	1.553 (14)	O28—C69	1.463 (12)
O8—C33	1.434 (10)	O28—C83	1.465 (13)
O8—C19	1.486 (11)	O29—C70	1.438 (11)
O9—C20	1.471 (11)	O30—C72	1.151 (12)
O10—C22	1.145 (9)	O31—C82	1.415 (10)
O11—C32	1.379 (8)	O31—C95	1.437 (9)
O11—C45	1.422 (9)	O32—C76	1.411 (9)
O12—C48	1.428 (17)	O32—C98	1.476 (9)
O12—C26	1.432 (11)	O33—C79	1.315 (8)
O13—C29	1.270 (8)	O33—C99	1.417 (12)
O13—C49	1.619 (13)	O34—C84	1.427 (13)
O14—C34	1.435 (12)	O34—C100	1.464 (14)
O14—C50	1.536 (15)	O35—C84	1.441 (12)
O15—C17	1.184 (12)	O35—C67	1.489 (12)
O15—C34	1.347 (12)	C51—C68	1.448 (13)
C1—C18	1.421 (12)	C51—C52	1.547 (15)
C1—C2	1.494 (14)	C51—C67	1.631 (14)
C1—C17	1.774 (15)	C52—C53	1.409 (14)
C2—C35	1.462 (18)	C52—C85	1.567 (15)
C2—C3	1.488 (15)	C53—C54	1.623 (13)
C3—C4	1.517 (15)	C54—C66	1.250 (14)
C4—C5	1.425 (14)	C54—C55	1.341 (14)
C4—C16	1.462 (13)	C55—C56	1.632 (10)
C5—C7	1.630 (11)	C59—C60	1.3900
C9—C10	1.3900	C59—C64	1.3900
C9—C14	1.3900	C60—C61	1.3900
C10—C11	1.3900	C61—C62	1.3900
C11—C12	1.3900	C62—C63	1.3900
C12—C13	1.3900	C63—C64	1.3900
C13—C14	1.3900	C63—C58	1.3900
C13—C8	1.3900	C64—C65	1.3900
C14—C15	1.3900	C65—C56	1.3900
C15—C6	1.3900	C56—C57	1.3900

Table 2.2 (Continued)

C6—C7	1.3900	C57—C58	1.3900
C6—C16	1.494 (10)	C57—C66	1.516 (13)
C7—C8	1.3900	C66—C67	1.555 (15)
C16—C17	1.448 (14)	C68—C69	1.530 (14)
C18—C34	1.466 (14)	C68—C84	1.675 (14)
C18—C19	1.471 (12)	C69—C93	1.541 (16)
C19—C20	1.452 (13)	C69—C70	1.587 (14)
C19—C43	1.516 (13)	C70—C71	1.408 (15)
C20—C21	1.571 (12)	C71—C72	1.622 (16)
C21—C22	1.509 (11)	C71—C83	1.741 (16)
C21—C33	1.542 (11)	C72—C73	1.544 (10)
C22—C23	1.547 (8)	C76—C77	1.3900
C26—C27	1.3900	C76—C81	1.3900
C26—C31	1.3900	C77—C78	1.3900
C27—C28	1.3900	C78—C79	1.3900
C28—C29	1.3900	C79—C80	1.3900
C29—C30	1.3900	C80—C81	1.3900
C30—C31	1.3900	C80—C75	1.3900
C30—C25	1.3900	C81—C82	1.3900
C31—C32	1.3900	C82—C73	1.3900
C32—C23	1.3900	C73—C74	1.3900
C23—C24	1.3900	C74—C75	1.3900
C24—C25	1.3900	C74—C83	1.543 (11)
C24—C33	1.445 (9)	C83—C84	1.321 (15)
C33—C34	1.575 (13)	C85—C86	1.518 (16)
C35—C36	1.519 (9)	C87—C88	1.548 (9)
C37—C38	1.514 (9)	C88—C89	1.344 (9)
C38—C39	1.357 (9)	C88—C97^{i}	1.90 (2)
C43—C44	1.551 (16)	C93—C94	1.513 (17)
C45—C46	1.546 (9)	C95—C96	1.520 (9)
C46—C47	1.333 (9)	C96—C97	1.319 (10)
O21—C52	1.464 (13)	C97—C88^{ii}	1.90 (2)
O21—C66	1.602 (13)		

C2—O1—C16	90.9 (6)	C91B—O26—C91	45.4 (18)
C8—O4—C37	112.7 (9)	C91B—O26—C62	125.3 (17)
C12—O5—C40	121.2 (10)	C91—O26—C62	164.8 (19)

Table 2.2 (Continued)

C9—O6—C41	108.4 (7)	C67—O27—C92	116.9 (8)
C42—O7—C17	104.5 (7)	C69—O28—C83	98.3 (8)
C33—O8—C19	96.8 (6)	C82—O31—C95	166.0 (12)
C32—O11—C45	132.5 (9)	C76—O32—C98	153.1 (11)
C48—O12—C26	133.2 (12)	C79—O33—C99	114.7 (6)
C29—O13—C49	119.1 (7)	C84—O34—C100	113.6 (9)
C34—O14—C50	112.8 (9)	C84—O35—C67	121.2 (8)
C17—O15—C34	119.6 (9)	C68—C51—C52	132.6 (9)
C18—C1—C2	128.9 (9)	C68—C51—C67	107.6 (8)
C18—C1—C17	101.5 (8)	C52—C51—C67	102.8 (8)
C2—C1—C17	102.5 (8)	C53—C52—O21	103.9 (9)
C35—C2—C3	117.9 (11)	C53—C52—C51	114.5 (10)
C35—C2—C1	115.4 (10)	O21—C52—C51	95.0 (8)
C3—C2—C1	116.7 (9)	C53—C52—C85	123.3 (9)
C35—C2—O1	103.8 (10)	O21—C52—C85	104.7 (9)
C3—C2—O1	99.3 (8)	C51—C52—C85	110.5 (9)
C1—C2—O1	98.8 (7)	C52—C53—O22	114.2 (9)
O2—C3—C2	110.9 (8)	C52—C53—C54	100.4 (8)
O2—C3—C4	117.7 (9)	O22—C53—C54	119.1 (7)
C2—C3—C4	104.2 (9)	C66—C54—C55	124.0 (11)
C5—C4—C16	115.2 (9)	C66—C54—C53	106.8 (9)
C5—C4—C3	119.5 (9)	C55—C54—C53	115.2 (8)
C16—C4—C3	106.2 (9)	O23—C55—C54	145.8 (10)
O3—C5—C4	141.7 (11)	O23—C55—C56	118.0 (9)
O3—C5—C7	117.3 (9)	C54—C55—C56	96.1 (7)
C4—C5—C7	101.1 (7)	O25—C59—C60	116.9 (7)
C10—C9—C14	120.0	O25—C59—C64	122.1 (7)
C10—C9—O6	126.8 (4)	C60—C59—C64	120.0
C14—C9—O6	113.1 (4)	C61—C60—C59	120.0
C11—C10—C9	120.0	C60—C61—C62	120.0
C10—C11—C12	120.0	C63—C62—C61	120.0
O5—C12—C13	118.3 (4)	C63—C62—O26	115.2 (5)
O5—C12—C11	120.9 (4)	C61—C62—O26	124.7 (5)
C13—C12—C11	120.0	C62—C63—C64	120.0
C12—C13—C14	120.0	C62—C63—C58	120.0
C12—C13—C8	120.0	C64—C63—C58	120.0
C14—C13—C8	120.0	C65—C64—C63	120.0

Table 2.2 (Continued)

C15—C14—C13	120.0	C65—C64—C59	120.0
C15—C14—C9	120.0	C63—C64—C59	120.0
C13—C14—C9	120.0	O24—C65—C56	119.2 (7)
C6—C15—C14	120.0	O24—C65—C64	120.2 (7)
C15—C6—C7	120.0	C56—C65—C64	120.0
C15—C6—C16	128.3 (5)	C65—C56—C57	120.0
C7—C6—C16	111.6 (5)	C65—C56—C55	131.1 (5)
C8—C7—C6	120.0	C57—C56—C55	108.4 (5)
C8—C7—C5	132.2 (5)	C58—C57—C56	120.0
C6—C7—C5	107.6 (5)	C58—C57—C66	135.2 (6)
O4—C8—C7	116.1 (4)	C56—C57—C66	104.5 (6)
O4—C8—C13	123.6 (4)	C57—C58—C63	120.0
C7—C8—C13	120.0	C54—C66—C57	106.1 (10)
C17—C16—C4	125.7 (9)	C54—C66—C67	123.2 (11)
C17—C16—C6	122.5 (8)	C57—C66—C67	123.9 (9)
C4—C16—C6	104.0 (7)	C54—C66—O21	99.0 (8)
C17—C16—O1	98.8 (7)	C57—C66—O21	103.1 (8)
C4—C16—O1	97.7 (7)	C67—C66—O21	94.4 (8)
C6—C16—O1	101.5 (6)	O27—C67—O35	115.1 (8)
O15—C17—C16	132.7 (11)	O27—C67—C66	113.5 (9)
O15—C17—O7	112.0 (9)	O35—C67—C66	111.6 (9)
C16—C17—O7	107.1 (8)	O27—C67—C51	116.9 (9)
O15—C17—C1	101.9 (9)	O35—C67—C51	97.1 (7)
C16—C17—C1	97.3 (8)	C66—C67—C51	100.7 (8)
O7—C17—C1	98.6 (8)	C51—C68—C69	124.5 (9)
C1—C18—C34	104.8 (8)	C51—C68—C84	107.4 (8)
C1—C18—C19	123.5 (9)	C69—C68—C84	98.0 (7)
C34—C18—C19	105.4 (8)	O28—C69—C68	100.5 (8)
C20—C19—C18	117.4 (8)	O28—C69—C93	112.5 (10)
C20—C19—O8	100.8 (7)	C68—C69—C93	115.2 (9)
C18—C19—O8	98.1 (7)	O28—C69—C70	101.4 (7)
C20—C19—C43	110.9 (8)	C68—C69—C70	110.4 (8)
C18—C19—C43	119.1 (8)	C93—C69—C70	115.0 (9)
O8—C19—C43	107.3 (7)	C71—C70—O29	105.9 (9)
C19—C20—O9	115.4 (8)	C71—C70—C69	103.2 (8)
C19—C20—C21	102.6 (7)	O29—C70—C69	112.4 (8)
O9—C20—C21	109.0 (7)	C70—C71—C72	116.0 (11)

Table 2.2 (Continued)

C22—C21—C33	105.3 (7)	C70—C71—C83	104.2 (9)
C22—C21—C20	116.5 (7)	C72—C71—C83	93.7 (8)
C33—C21—C20	100.4 (7)	O30—C72—C73	120.0 (9)
O10—C22—C21	131.3 (8)	O30—C72—C71	124.4 (10)
O10—C22—C23	125.0 (7)	C73—C72—C71	115.0 (8)
C21—C22—C23	103.4 (6)	C77—C76—C81	120.0
C27—C26—C31	120.0	C77—C76—O32	117.2 (5)
C27—C26—O12	113.6 (5)	C81—C76—O32	122.7 (5)
C31—C26—O12	126.1 (5)	C76—C77—C78	120.0
C26—C27—C28	120.0	C79—C78—C77	120.0
C29—C28—C27	120.0	O33—C79—C78	125.2 (3)
O13—C29—C30	113.4 (4)	O33—C79—C80	114.8 (3)
O13—C29—C28	126.6 (4)	C78—C79—C80	120.0
C30—C29—C28	120.0	C79—C80—C81	120.0
C29—C30—C31	120.0	C79—C80—C75	120.0
C29—C30—C25	120.0	C81—C80—C75	120.0
C31—C30—C25	120.0	C82—C81—C80	120.0
C32—C31—C30	120.0	C82—C81—C76	120.0
C32—C31—C26	120.0	C80—C81—C76	120.0
C30—C31—C26	120.0	C73—C82—C81	120.0
O11—C32—C23	116.2 (4)	C73—C82—O31	112.1 (5)
O11—C32—C31	123.8 (4)	C81—C82—O31	127.7 (5)
C23—C32—C31	120.0	C82—C73—C74	120.0
C24—C23—C32	120.0	C82—C73—C72	132.9 (5)
C24—C23—C22	110.3 (4)	C74—C73—C72	107.1 (5)
C32—C23—C22	129.5 (4)	C75—C74—C73	120.0
C23—C24—C25	120.0	C75—C74—C83	126.7 (5)
C23—C24—C33	110.0 (4)	C73—C74—C83	113.3 (5)
C25—C24—C33	129.1 (4)	C74—C75—C80	120.0
C24—C25—C30	120.0	C84—C83—O28	103.6 (9)
O8—C33—C24	111.0 (7)	C84—C83—C74	129.8 (9)
O8—C33—C21	103.4 (6)	O28—C83—C74	105.3 (8)
C24—C33—C21	106.5 (6)	C84—C83—C71	108.0 (10)
O8—C33—C34	96.9 (7)	O28—C83—C71	97.5 (8)
C24—C33—C34	128.4 (7)	C74—C83—C71	107.8 (7)
C21—C33—C34	108.0 (7)	C83—C84—O34	123.2 (10)
O15—C34—O14	105.8 (8)	C83—C84—O35	117.2 (10)

Table 2.2 (Continued)

O15—C34—C18	110.9 (8)	O34—C84—O35	105.1 (9)
O14—C34—C18	112.2 (9)	C83—C84—C68	103.7 (9)
O15—C34—C33	111.6 (8)	O34—C84—C68	105.7 (8)
O14—C34—C33	114.6 (8)	O35—C84—C68	98.3 (7)
C18—C34—C33	101.9 (8)	C86—C85—C52	109.3 (9)
C2—C35—C36	108.3 (12)	O24—C87—C88	152 (2)
O4—C37—C38	104.7 (11)	C89—C88—C87	113.4 (13)
C39—C38—C37	112.1 (13)	C89—C88—C97^{i}	127.7 (14)
C19—C43—C44	117.9 (10)	C87—C88—C97^{i}	118.8 (14)
O11—C45—C46	107.1 (12)	C94—C93—C69	106.9 (10)
C47—C46—C45	113.3 (13)	O31—C95—C96	160 (2)
C52—O21—C66	95.0 (8)	C97—C96—C95	116.2 (15)
C65—O24—C87	110.2 (12)	C96—C97—C88^{ii}	143.3 (19)
C90—O25—C59	165 (2)		

C18—C1—C2—C35	28.5 (16)	C66—O21—C52—C85	-179.8 (8)
C17—C1—C2—C35	144.7 (12)	C68—C51—C52—C53	165.6 (10)
C18—C1—C2—C3	173.5 (9)	C67—C51—C52—C53	-65.4 (11)
C17—C1—C2—C3	-70.3 (10)	C68—C51—C52—O21	-86.6 (13)
C18—C1—C2—O1	-81.4 (11)	C67—C51—C52—O21	42.4 (9)
C17—C1—C2—O1	34.8 (9)	C68—C51—C52—C85	21.1 (16)
C16—O1—C2—C35	179.7 (9)	C67—C51—C52—C85	150.1 (9)
C16—O1—C2—C3	57.8 (8)	O21—C52—C53—O22	-156.1 (8)
C16—O1—C2—C1	-61.3 (8)	C51—C52—C53—O22	-53.9 (12)
C35—C2—C3—O2	83.5 (13)	C85—C52—C53—O22	85.6 (13)
C1—C2—C3—O2	-60.6 (12)	O21—C52—C53—C54	-27.4 (10)
O1—C2—C3—O2	-165.4 (8)	C51—C52—C53—C54	74.8 (10)
C35—C2—C3—C4	-148.9 (11)	C85—C52—C53—C54	-145.7 (11)
C1—C2—C3—C4	67.0 (11)	C52—C53—C54—C66	-12.1 (12)
O1—C2—C3—C4	-37.8 (10)	O22—C53—C54—C66	113.3 (10)
O2—C3—C4—C5	-105.6 (12)	C52—C53—C54—C55	129.8 (10)
C2—C3—C4—C5	131.1 (10)	O22—C53—C54—C55	-104.8 (10)
O2—C3—C4—C16	122.0 (10)	C66—C54—C55—O23	175.3 (16)
C2—C3—C4—C16	-1.4 (11)	C53—C54—C55—O23	41 (2)
C16—C4—C5—O3	173.3 (14)	C66—C54—C55—C56	-8.5 (12)
C3—C4—C5—O3	45 (2)	C53—C54—C55—C56	-143.1 (8)
C16—C4—C5—C7	-6.9 (11)	C90—O25—C59—C60	82 (9)

Table 2.2 (Continued)

C3—C4—C5—C7	-135.3 (9)	C90—O25—C59—C64	-110 (8)
C41—O6—C9—C10	-6.8 (9)	O25—C59—C60—C61	168.6 (8)
C41—O6—C9—C14	176.0 (6)	C64—C59—C60—C61	0.0
C14—C9—C10—C11	0.0	C59—C60—C61—C62	0.0
O6—C9—C10—C11	-177.0 (7)	C60—C61—C62—C63	0.0
C9—C10—C11—C12	0.0	C60—C61—C62—O26	-176.5 (9)
C40—O5—C12—C13	-167.5 (9)	C91B—O26—C62—C63	160 (2)
C40—O5—C12—C11	2.0 (12)	C91—O26—C62—C63	112 (7)
C10—C11—C12—O5	-169.3 (6)	C91B—O26—C62—C61	-24 (3)
C10—C11—C12—C13	0.0	C91—O26—C62—C61	-71 (7)
O5—C12—C13—C14	169.6 (6)	C61—C62—C63—C64	0.0
C11—C12—C13—C14	0.0	O26—C62—C63—C64	176.8 (8)
O5—C12—C13—C8	-10.4 (6)	C61—C62—C63—C58	180.0
C11—C12—C13—C8	180.0	O26—C62—C63—C58	-3.2 (8)
C12—C13—C14—C15	180.0	C62—C63—C64—C65	180.0
C8—C13—C14—C15	0.0	C58—C63—C64—C65	0.0
C12—C13—C14—C9	0.0	C62—C63—C64—C59	0.0
C8—C13—C14—C9	180.0	C58—C63—C64—C59	180.0
C10—C9—C14—C15	180.0	O25—C59—C64—C65	12.0 (9)
O6—C9—C14—C15	-2.6 (6)	C60—C59—C64—C65	180.0
C10—C9—C14—C13	0.0	O25—C59—C64—C63	-168.0 (9)
O6—C9—C14—C13	177.4 (6)	C60—C59—C64—C63	0.0
C13—C14—C15—C6	0.0	C87—O24—C65—C56	99.9 (13)
C9—C14—C15—C6	180.0	C87—O24—C65—C64	-71.0 (15)
C14—C15—C6—C7	0.0	C63—C64—C65—O24	170.8 (9)
C14—C15—C6—C16	-175.5 (6)	C59—C64—C65—O24	-9.2 (9)
C15—C6—C7—C8	0.0	C63—C64—C65—C56	0.0
C16—C6—C7—C8	176.2 (5)	C59—C64—C65—C56	180.0
C15—C6—C7—C5	-175.5 (5)	O24—C65—C56—C57	-170.9 (9)
C16—C6—C7—C5	0.7 (6)	C64—C65—C56—C57	0.0
O3—C5—C7—C8	8.7 (12)	O24—C65—C56—C55	0.0 (9)
C4—C5—C7—C8	-171.1 (5)	C64—C65—C56—C55	170.9 (7)
O3—C5—C7—C6	-176.6 (8)	O23—C55—C56—C65	8.6 (12)
C4—C5—C7—C6	3.6 (8)	C54—C55—C56—C65	-169.0 (6)
C37—O4—C8—C7	-95.6 (10)	O23—C55—C56—C57	-179.7 (8)
C37—O4—C8—C13	90.7 (10)	C54—C55—C56—C57	2.7 (7)
C6—C7—C8—O4	-173.9 (6)	C65—C56—C57—C58	0.0

Table 2.2 (Continued)

C5—C7—C8—O4	0.2 (7)	C55—C56—C57—C58	-172.7 (5)
C6—C7—C8—C13	0.0	C65—C56—C57—C66	174.8 (6)
C5—C7—C8—C13	174.2 (6)	C55—C56—C57—C66	2.1 (7)
C12—C13—C8—O4	-6.6 (6)	C56—C57—C58—C63	0.0
C14—C13—C8—O4	173.4 (6)	C66—C57—C58—C63	-172.9 (8)
C12—C13—C8—C7	180.0	C62—C63—C58—C57	180.0
C14—C13—C8—C7	0.0	C64—C63—C58—C57	0.0
C5—C4—C16—C17	156.9 (10)	C55—C54—C66—C57	10.5 (14)
C3—C4—C16—C17	-68.4 (13)	C53—C54—C66—C57	148.1 (8)
C5—C4—C16—C6	7.5 (11)	C55—C54—C66—C67	162.5 (10)
C3—C4—C16—C6	142.3 (8)	C53—C54—C66—C67	-59.8 (13)
C5—C4—C16—O1	-96.4 (9)	C55—C54—C66—O21	-96.1 (11)
C3—C4—C16—O1	38.3 (9)	C53—C54—C66—O21	41.6 (10)
C15—C6—C16—C17	20.5 (11)	C58—C57—C66—C54	167.0 (6)
C7—C6—C16—C17	-155.3 (8)	C56—C57—C66—C54	-6.6 (9)
C15—C6—C16—C4	171.1 (5)	C58—C57—C66—C67	15.2 (14)
C7—C6—C16—C4	-4.7 (8)	C56—C57—C66—C67	-158.4 (9)
C15—C6—C16—O1	-87.8 (6)	C58—C57—C66—O21	-89.4 (8)
C7—C6—C16—O1	96.4 (5)	C56—C57—C66—O21	97.0 (6)
C2—O1—C16—C17	69.9 (8)	C52—O21—C66—C54	-57.9 (10)
C2—O1—C16—C4	-58.2 (8)	C52—O21—C66—C57	-166.8 (8)
C2—O1—C16—C6	-164.2 (6)	C52—O21—C66—C67	66.8 (8)
C34—O15—C17—C16	-110.4 (14)	C92—O27—C67—O35	53.8 (12)
C34—O15—C17—O7	105.9 (10)	C92—O27—C67—C66	-76.6 (12)
C34—O15—C17—C1	1.4 (12)	C92—O27—C67—C51	166.8 (9)
C4—C16—C17—O15	174.0 (11)	C84—O35—C67—O27	103.1 (11)
C6—C16—C17—O15	-42.0 (18)	C84—O35—C67—C66	-125.5 (10)
O1—C16—C17—O15	67.8 (15)	C84—O35—C67—C51	-21.0 (11)
C4—C16—C17—O7	-41.1 (13)	C54—C66—C67—O27	-58.4 (14)
C6—C16—C17—O7	102.9 (9)	C57—C66—C67—O27	88.7 (12)
O1—C16—C17—O7	-147.3 (7)	O21—C66—C67—O27	-162.2 (8)
C4—C16—C17—C1	60.3 (12)	C54—C66—C67—O35	169.5 (10)
C6—C16—C17—C1	-155.7 (7)	C57—C66—C67—O35	-43.4 (13)
O1—C16—C17—C1	-45.9 (8)	O21—C66—C67—O35	65.7 (9)
C42—O7—C17—O15	81.6 (10)	C54—C66—C67—C51	67.4 (13)
C42—O7—C17—C16	-71.3 (9)	C57—C66—C67—C51	-145.5 (9)
C42—O7—C17—C1	-171.7 (7)	O21—C66—C67—C51	-36.5 (9)

Table 2.2 (Continued)

C18—C1—C17—O15	6.0 (11)	C68—C51—C67—O27	-94.5 (10)
C2—C1—C17—O15	-128.5 (9)	C52—C51—C67—O27	122.4 (10)
C18—C1—C17—C16	142.6 (8)	C68—C51—C67—O35	28.4 (10)
C2—C1—C17—C16	8.0 (10)	C52—C51—C67—O35	-114.7 (9)
C18—C1—C17—O7	-108.8 (8)	C68—C51—C67—C66	142.1 (9)
C2—C1—C17—O7	116.7 (8)	C52—C51—C67—C66	-1.0 (10)
C2—C1—C18—C34	106.7 (11)	C52—C51—C68—C69	-146.9 (11)
C17—C1—C18—C34	-9.9 (10)	C67—C51—C68—C69	85.8 (11)
C2—C1—C18—C19	-133.0 (11)	C52—C51—C68—C84	100.1 (12)
C17—C1—C18—C19	110.4 (10)	C67—C51—C68—C84	-27.3 (11)
C1—C18—C19—C20	169.5 (9)	C83—O28—C69—C68	-53.7 (8)
C34—C18—C19—C20	-70.5 (11)	C83—O28—C69—C93	-176.7 (9)
C1—C18—C19—O8	-83.9 (11)	C83—O28—C69—C70	59.9 (9)
C34—C18—C19—O8	36.1 (9)	C51—C68—C69—O28	-87.5 (11)
C1—C18—C19—C43	31.1 (14)	C84—C68—C69—O28	30.0 (9)
C34—C18—C19—C43	151.1 (9)	C51—C68—C69—C93	33.7 (14)
C33—O8—C19—C20	59.5 (8)	C84—C68—C69—C93	151.2 (9)
C33—O8—C19—C18	-60.5 (7)	C51—C68—C69—C70	166.1 (9)
C33—O8—C19—C43	175.5 (7)	C84—C68—C69—C70	-76.4 (9)
C18—C19—C20—O9	-55.5 (11)	O28—C69—C70—C71	-42.2 (10)
O8—C19—C20—O9	-160.6 (7)	C68—C69—C70—C71	63.7 (10)
C43—C19—C20—O9	86.0 (10)	C93—C69—C70—C71	-163.8 (10)
C18—C19—C20—C21	62.9 (10)	O28—C69—C70—O29	-155.8 (8)
O8—C19—C20—C21	-42.2 (8)	C68—C69—C70—O29	-50.0 (11)
C43—C19—C20—C21	-155.6 (8)	C93—C69—C70—O29	82.5 (12)
C19—C20—C21—C22	123.5 (8)	O29—C70—C71—C72	-131.2 (9)
O9—C20—C21—C22	-113.7 (8)	C69—C70—C71—C72	110.6 (10)
C19—C20—C21—C33	10.4 (9)	O29—C70—C71—C83	127.4 (8)
O9—C20—C21—C33	133.2 (7)	C69—C70—C71—C83	9.2 (11)
C33—C21—C22—O10	168.6 (8)	C70—C71—C72—O30	64.7 (16)
C20—C21—C22—O10	58.3 (12)	C83—C71—C72—O30	172.4 (11)
C33—C21—C22—C23	-18.3 (7)	C70—C71—C72—C73	-124.1 (10)
C20—C21—C22—C23	-128.6 (7)	C83—C71—C72—C73	-16.4 (11)
C48—O12—C26—C27	-28.5 (17)	C98—O32—C76—C77	-36 (2)
C48—O12—C26—C31	158.2 (12)	C98—O32—C76—C81	141.3 (19)
C31—C26—C27—C28	0.0	C81—C76—C77—C78	0.0
O12—C26—C27—C28	-173.8 (7)	O32—C76—C77—C78	177.2 (7)

Table 2.2 (Continued)

C26—C27—C28—C29	0.0	C76—C77—C78—C79	0.0
C49—O13—C29—C30	169.1 (6)	C99—O33—C79—C78	1.3 (8)
C49—O13—C29—C28	-8.6 (9)	C99—O33—C79—C80	-178.9 (5)
C27—C28—C29—O13	177.6 (6)	C77—C78—C79—O33	179.8 (6)
C27—C28—C29—C30	0.0	C77—C78—C79—C80	0.0
O13—C29—C30—C31	-177.9 (5)	O33—C79—C80—C81	-179.8 (5)
C28—C29—C30—C31	0.0	C78—C79—C80—C81	0.0
O13—C29—C30—C25	2.1 (5)	O33—C79—C80—C75	0.2 (5)
C28—C29—C30—C25	180.0	C78—C79—C80—C75	180.0
C29—C30—C31—C32	180.0	C79—C80—C81—C82	180.0
C25—C30—C31—C32	0.0	C75—C80—C81—C82	0.0
C29—C30—C31—C26	0.0	C79—C80—C81—C76	0.0
C25—C30—C31—C26	180.0	C75—C80—C81—C76	180.0
C27—C26—C31—C32	180.0	C77—C76—C81—C82	180.0
O12—C26—C31—C32	-7.1 (8)	O32—C76—C81—C82	2.9 (7)
C27—C26—C31—C30	0.0	C77—C76—C81—C80	0.0
O12—C26—C31—C30	172.9 (8)	O32—C76—C81—C80	-177.1 (7)
C45—O11—C32—C23	120.5 (16)	C80—C81—C82—C73	0.0
C45—O11—C32—C31	-59.3 (17)	C76—C81—C82—C73	180.0
C30—C31—C32—O11	179.8 (6)	C80—C81—C82—O31	-175.2 (8)
C26—C31—C32—O11	-0.2 (6)	C76—C81—C82—O31	4.8 (8)
C30—C31—C32—C23	0.0	C95—O31—C82—C73	-160 (6)
C26—C31—C32—C23	180.0	C95—O31—C82—C81	15 (6)
O11—C32—C23—C24	-179.8 (6)	C81—C82—C73—C74	0.0
C31—C32—C23—C24	0.0	O31—C82—C73—C74	175.9 (7)
O11—C32—C23—C22	6.2 (6)	C81—C82—C73—C72	177.3 (7)
C31—C32—C23—C22	-173.9 (5)	O31—C82—C73—C72	-6.8 (8)
O10—C22—C23—C24	-177.0 (7)	O30—C72—C73—C82	5.3 (14)
C21—C22—C23—C24	9.3 (6)	C71—C72—C73—C82	-166.3 (6)
O10—C22—C23—C32	-2.6 (10)	O30—C72—C73—C74	-177.1 (9)
C21—C22—C23—C32	-176.3 (4)	C71—C72—C73—C74	11.2 (9)
C32—C23—C24—C25	0.0	C82—C73—C74—C75	0.0
C22—C23—C24—C25	175.0 (4)	C72—C73—C74—C75	-177.9 (5)
C32—C23—C24—C33	-170.4 (5)	C82—C73—C74—C83	179.4 (6)
C22—C23—C24—C33	4.6 (5)	C72—C73—C74—C83	1.5 (7)
C23—C24—C25—C30	0.0	C73—C74—C75—C80	0.0
C33—C24—C25—C30	168.4 (6)	C83—C74—C75—C80	-179.3 (7)

Table 2.2 (Continued)

C29—C30—C25—C24	180.0	C79—C80—C75—C74	180.0
C31—C30—C25—C24	0.0	C81—C80—C75—C74	0.0
C19—O8—C33—C24	-165.7 (6)	C69—O28—C83—C84	60.3 (10)
C19—O8—C33—C21	-51.9 (7)	C69—O28—C83—C74	-161.2 (7)
C19—O8—C33—C34	58.5 (7)	C69—O28—C83—C71	-50.4 (8)
C23—C24—C33—O8	95.4 (6)	C75—C74—C83—C84	33.4 (15)
C25—C24—C33—O8	-73.9 (7)	C73—C74—C83—C84	-145.9 (11)
C23—C24—C33—C21	-16.4 (7)	C75—C74—C83—O28	-89.6 (7)
C25—C24—C33—C21	174.3 (4)	C73—C74—C83—O28	91.0 (7)
C23—C24—C33—C34	-146.6 (8)	C75—C74—C83—C71	167.1 (6)
C25—C24—C33—C34	44.1 (10)	C73—C74—C83—C71	-12.3 (9)
C22—C21—C33—O8	-95.2 (7)	C70—C71—C83—C84	-81.8 (12)
C20—C21—C33—O8	26.2 (8)	C72—C71—C83—C84	160.3 (9)
C22—C21—C33—C24	21.8 (8)	C70—C71—C83—O28	25.3 (11)
C20—C21—C33—C24	143.2 (6)	C72—C71—C83—O28	-92.7 (8)
C22—C21—C33—C34	162.8 (7)	C70—C71—C83—C74	134.0 (9)
C20—C21—C33—C34	-75.8 (8)	C72—C71—C83—C74	16.0 (10)
C17—O15—C34—O14	113.3 (10)	O28—C83—C84—O34	-157.8 (9)
C17—O15—C34—C18	-8.5 (14)	C74—C83—C84—O34	78.5 (16)
C17—O15—C34—C33	-121.4 (10)	C71—C83—C84—O34	-55.1 (13)
C50—O14—C34—O15	62.3 (11)	O28—C83—C84—O35	68.7 (11)
C50—O14—C34—C18	-176.6 (9)	C74—C83—C84—O35	-55.0 (16)
C50—O14—C34—C33	-61.1 (11)	C71—C83—C84—O35	171.5 (8)
C1—C18—C34—O15	11.9 (11)	O28—C83—C84—C68	-38.3 (10)
C19—C18—C34—O15	-119.7 (9)	C74—C83—C84—C68	-162.0 (10)
C1—C18—C34—O14	-106.2 (9)	C71—C83—C84—C68	64.5 (10)
C19—C18—C34—O14	122.2 (8)	C100—O34—C84—C83	-61.4 (14)
C1—C18—C34—C33	130.8 (8)	C100—O34—C84—O35	76.6 (11)
C19—C18—C34—C33	-0.9 (10)	C100—O34—C84—C68	179.9 (9)
O8—C33—C34—O15	82.3 (9)	C67—O35—C84—C83	-104.0 (12)
C24—C33—C34—O15	-41.5 (13)	C67—O35—C84—O34	115.0 (9)
C21—C33—C34—O15	-171.1 (8)	C67—O35—C84—C68	6.2 (11)
O8—C33—C34—O14	-157.4 (8)	C51—C68—C84—C83	134.9 (9)
C24—C33—C34—O14	78.8 (11)	C69—C68—C84—C83	4.9 (10)
C21—C33—C34—O14	-50.8 (10)	C51—C68—C84—O34	-94.2 (9)
O8—C33—C34—C18	-36.1 (9)	C69—C68—C84—O34	135.7 (8)
C24—C33—C34—C18	-159.9 (8)	C51—C68—C84—O35	14.2 (10)

Table 2.2 (Continued)

C21—C33—C34—C18	70.5 (9)	C69—C68—C84—O35	-115.9 (8)
C3—C2—C35—C36	52.3 (18)	C53—C52—C85—C86	-69.5 (14)
C1—C2—C35—C36	-163.2 (12)	O21—C52—C85—C86	172.5 (9)
O1—C2—C35—C36	-56.3 (15)	C51—C52—C85—C86	71.3 (11)
C8—O4—C37—C38	177.0 (11)	C65—O24—C87—C88	-124 (3)
O4—C37—C38—C39	-64 (2)	O24—C87—C88—C89	103 (3)
C20—C19—C43—C44	-86.9 (12)	O24—C87—C88—C97^{i}	-78 (4)
C18—C19—C43—C44	54.0 (13)	O28—C69—C93—C94	-62.2 (13)
O8—C19—C43—C44	164.0 (9)	C68—C69—C93—C94	-176.6 (10)
C32—O11—C45—C46	-179.2 (10)	C70—C69—C93—C94	53.2 (13)
O11—C45—C46—C47	-135 (2)	C82—O31—C95—C96	22 (10)
C66—O21—C52—C53	49.7 (9)	O31—C95—C96—C97	-146 (5)
C66—O21—C52—C51	-67.0 (8)	C95—C96—C97—C88^{ii}	-161 (2)

Symmetry code(s): (i) *x*, *y*, *z*-1; (ii) *x*, *y*, *z*+1.

Table 2.3 Hydrogen-bond parameters

D—H···*A*	*D*—H (Å)	H···*A* (Å)	*D*···*A* (Å)	*D*—H···*A* (°)
O2—H2O···O30^{i}	0.86	2.02	2.883 (11)	179.9
O9—H9O···O23^{ii}	0.86	1.90	2.757 (10)	180.0
O22—H22O···O10^{iii}	0.86	2.00	2.860 (9)	179.5
O29—H29O···O3^{iv}	0.86	2.13	2.992 (11)	179.9

Symmetry code(s): (i) *x*-1, *y*, *z*-1; (ii) *x*-1, *y*, *z*; (iii) *x*+1, *y*, *z*; (iv) *x*+1, *y*, *z*+1.

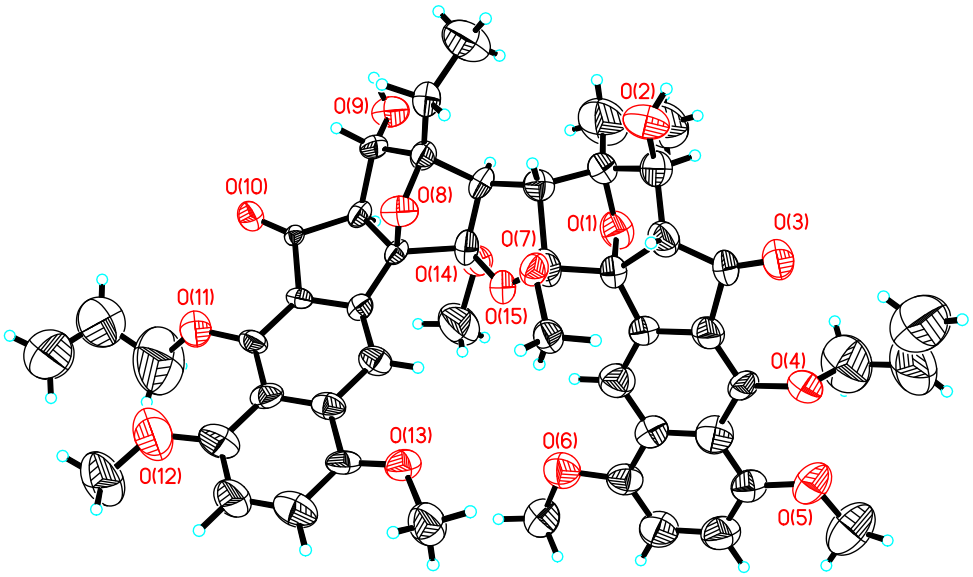

Figure 2.1a

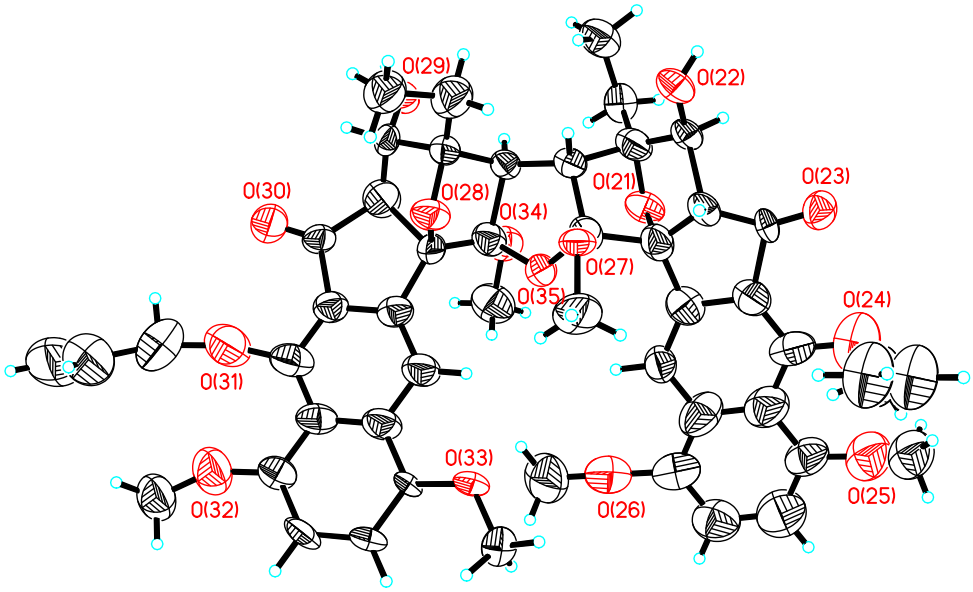

Figure 2.1b

Figure 2.1. Perspective views showing 50% (The disorder part has been omitted).

Appendix 3

Selected ^{1}H and ^{13}C Spectra

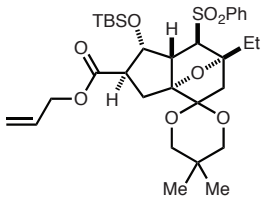
TBSO
H
SO2Ph
Et
O
O
H
O
O
O
Me
Me

2.21

10.5
10.0
9.5
9.0
8.5
8.0
7.5
7.0
6.5
6.0
5.5
5.0
4.5
4.0
3.5
3.0
2.5
2.0
1.5
1.0
0.5
0
-0.5

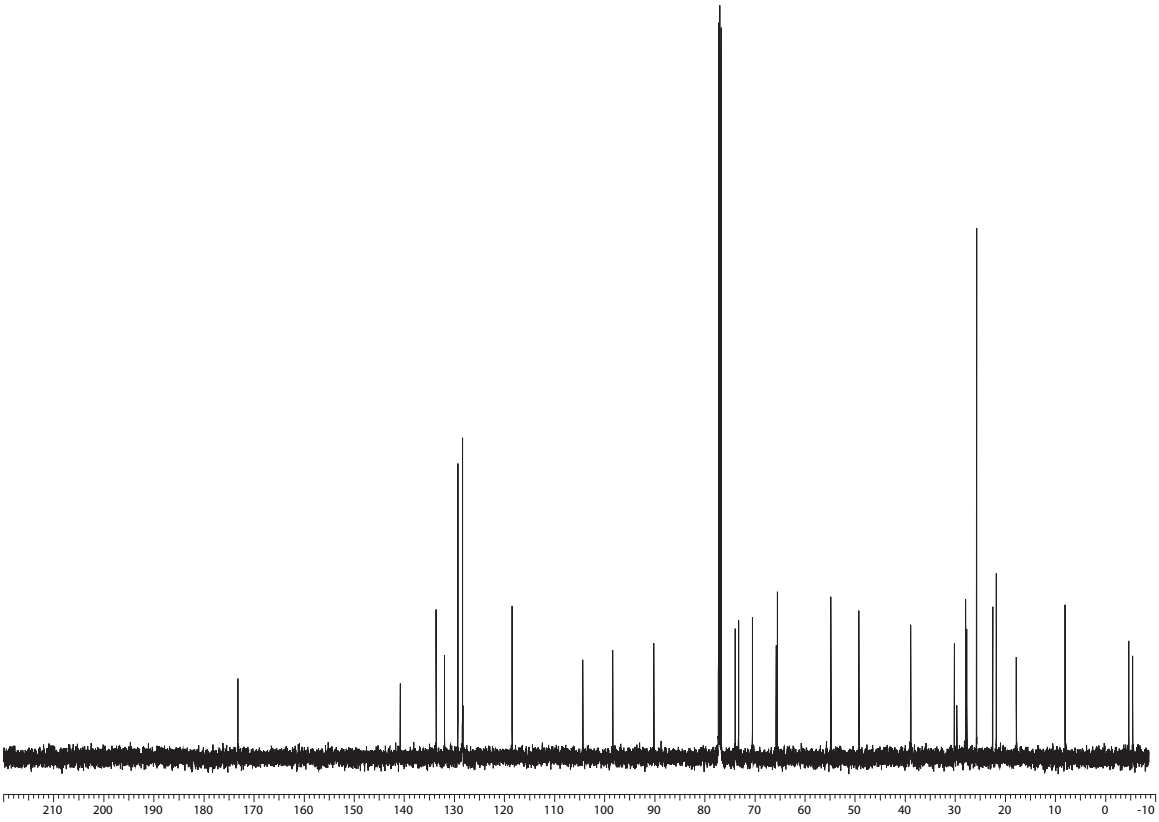
210
200
190
180
170
160
150
140
130
120
110
100
90
80
70
60
50
40
30
20
10
0
-10

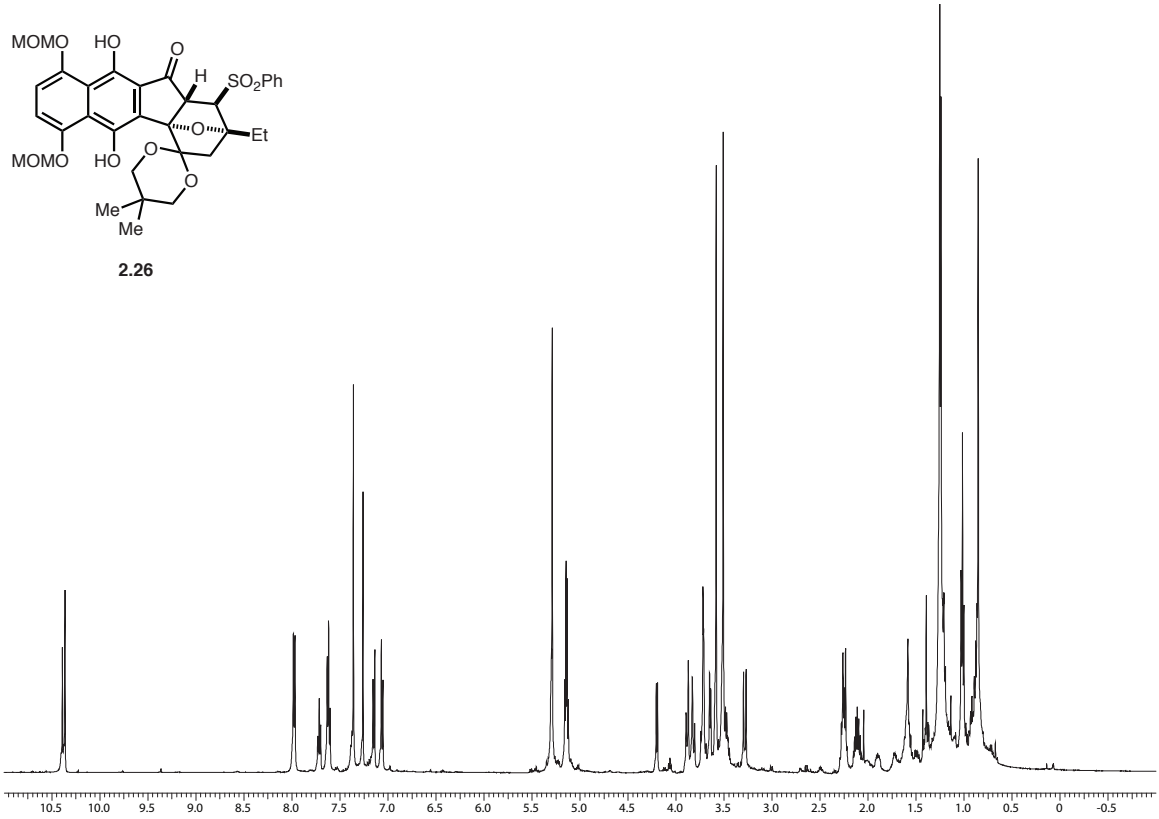
MOMO
HO
O
H
SO2Ph
Et
MOMO
HO
O
O
Me
Me
10.5 10.0 9.5 9.0 8.5 8.0 7.5 7.0 6.5 6.0 5.5 5.0 4.5 4.0 3.5 3.0 2.5 2.0 1.5 1.0 0.5 0 -0.5

2.26

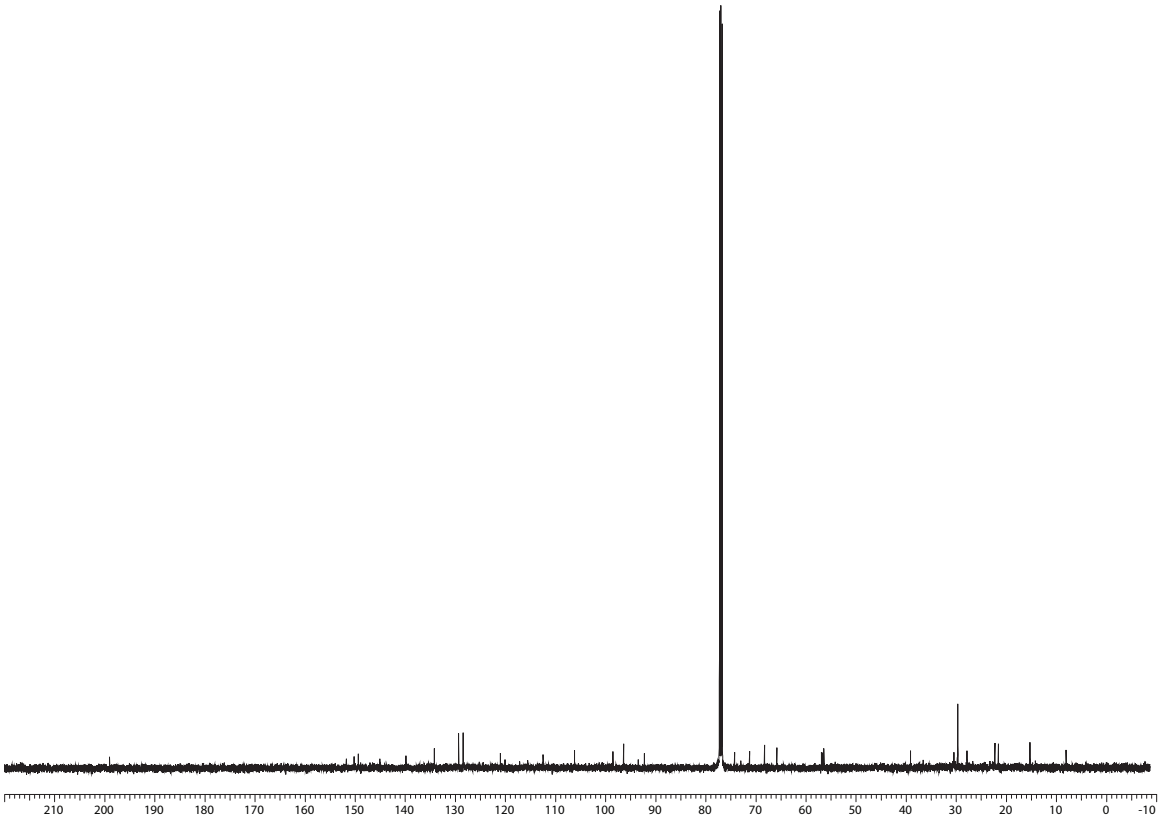
210 200 190 180 170 160 150 140 130 120 110 100 90 80 70 60 50 40 30 20 10 0 -10

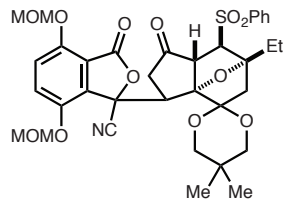
MOMO
O
O
H
SO2Ph
Et
O
O
NC
MOMO
O
O
Me
Me

2.28

10.5
10.0
9.5
9.0
8.5
8.0
7.5
7.0
6.5
6.0
5.5
5.0
4.5
4.0
3.5
3.0
2.5
2.0
1.5
1.0
0.5
0
-0.5

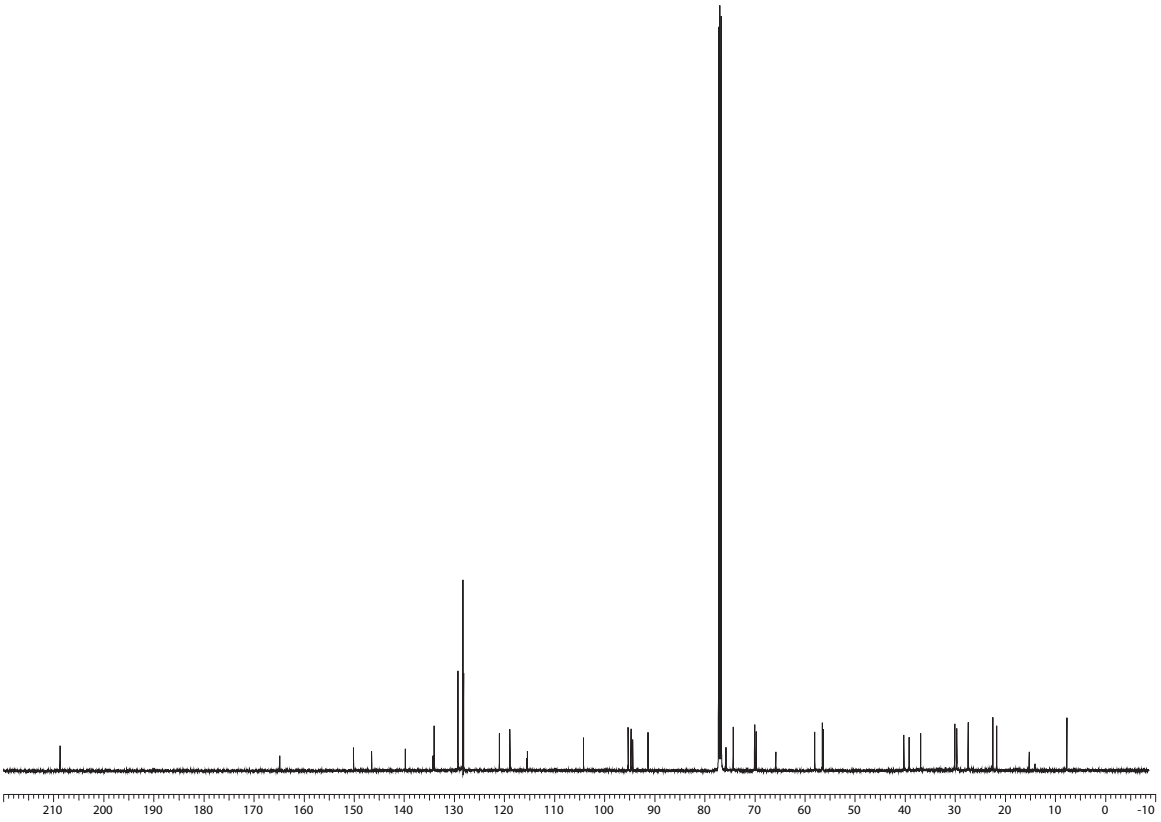
210
200
190
180
170
160
150
140
130
120
110
100
90
80
70
60
50
40
30
20
10
0
-10

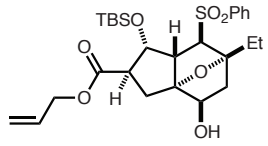
TBSO
H
SO2Ph
Et
O
O
H
O
OH

2.36

10.5 10.0 9.5 9.0 8.5 8.0 7.5 7.0 6.5 6.0 5.5 5.0 4.5 4.0 3.5 3.0 2.5 2.0 1.5 1.0 0.5 0 -0.5

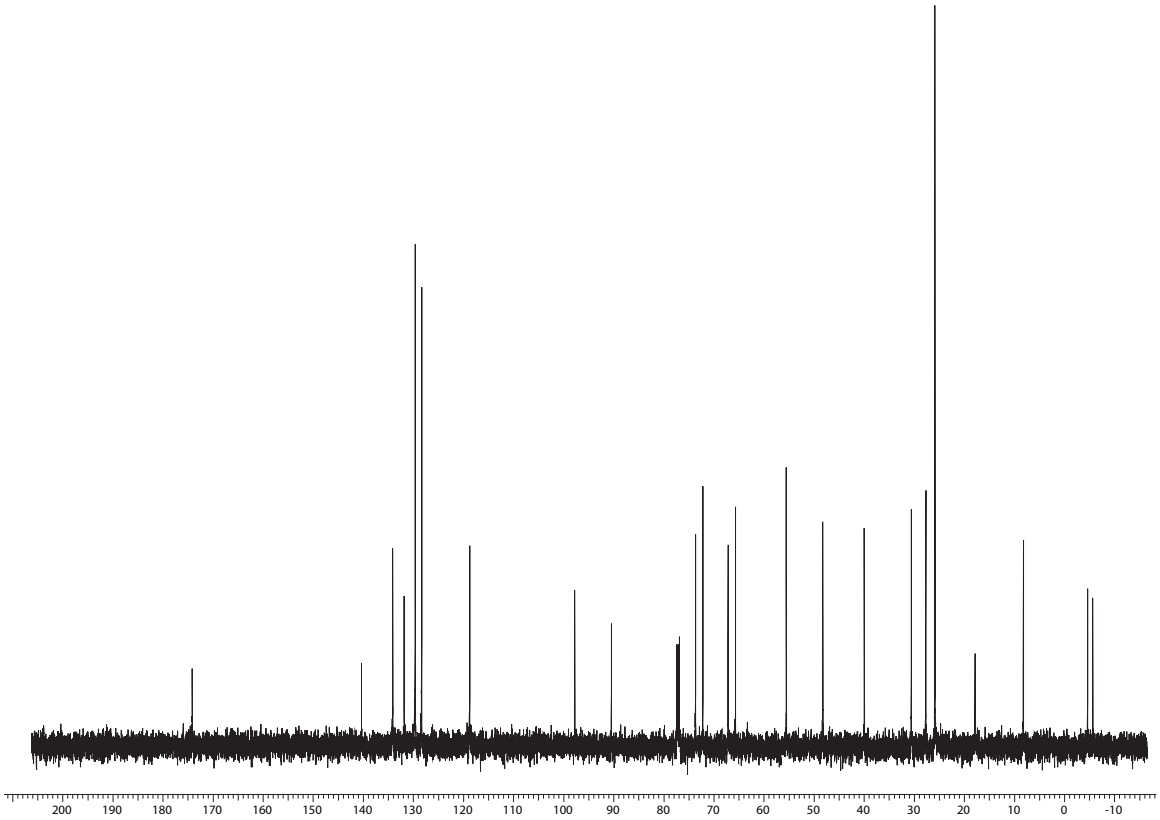
200 190 180 170 160 150 140 130 120 110 100 90 80 70 60 50 40 30 20 10 0 -10

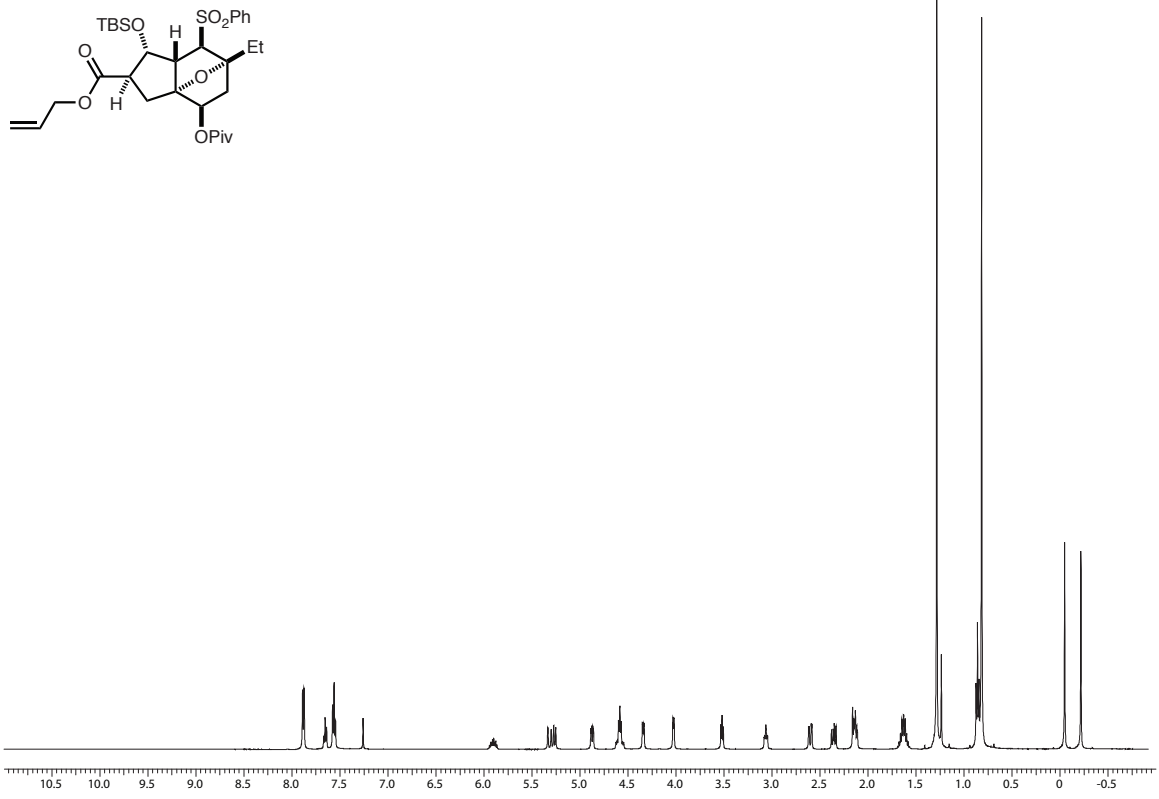
TBSO
H
SO2Ph
Et
O
O
H
O
OPiv
10.5 10.0 9.5 9.0 8.5 8.0 7.5 7.0 6.5 6.0 5.5 5.0 4.5 4.0 3.5 3.0 2.5 2.0 1.5 1.0 0.5 0 -0.5

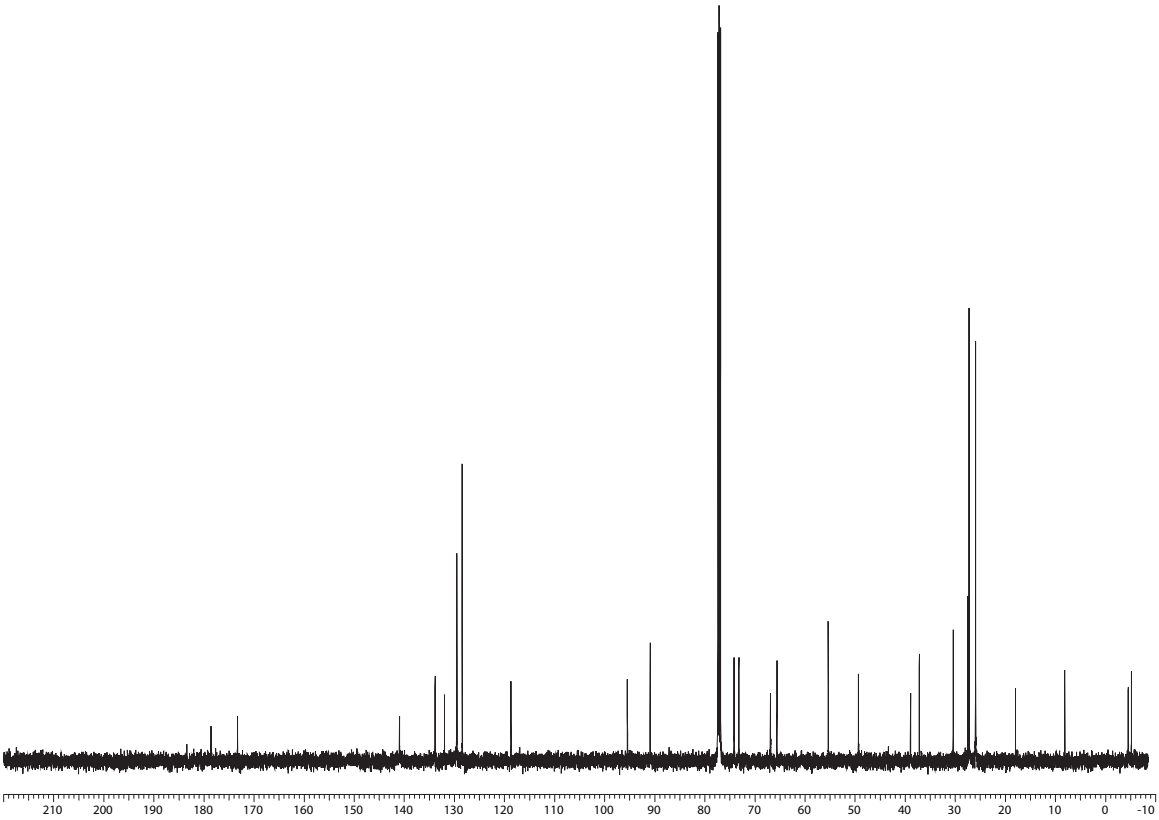
210 200 190 180 170 160 150 140 130 120 110 100 90 80 70 60 50 40 30 20 10 0 -10

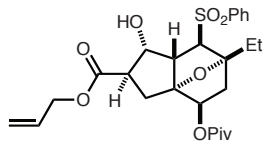
HO
H
SO2Ph
Et
O
O
O
H
OPiv

2.37

10.5 10.0 9.5 9.0 8.5 8.0 7.5 7.0 6.5 6.0 5.5 5.0 4.5 4.0 3.5 3.0 2.5 2.0 1.5 1.0 0.5 0 -0.5

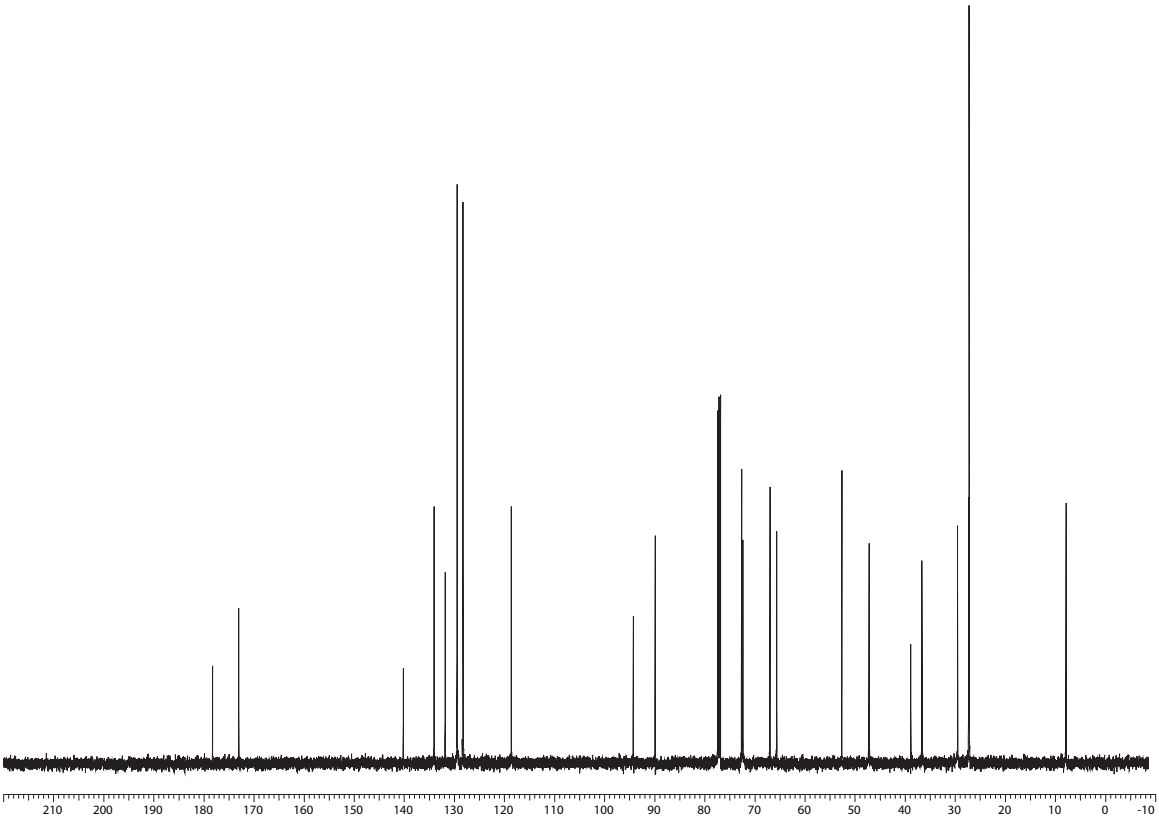
210 200 190 180 170 160 150 140 130 120 110 100 90 80 70 60 50 40 30 20 10 0 -10

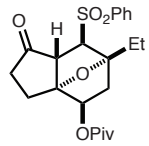
O
H
SO2Ph
Et
O
OPiv

2.41

10.5 10.0 9.5 9.0 8.5 8.0 7.5 7.0 6.5 6.0 5.5 5.0 4.5 4.0 3.5 3.0 2.5 2.0 1.5 1.0 0.5 0 -0.5

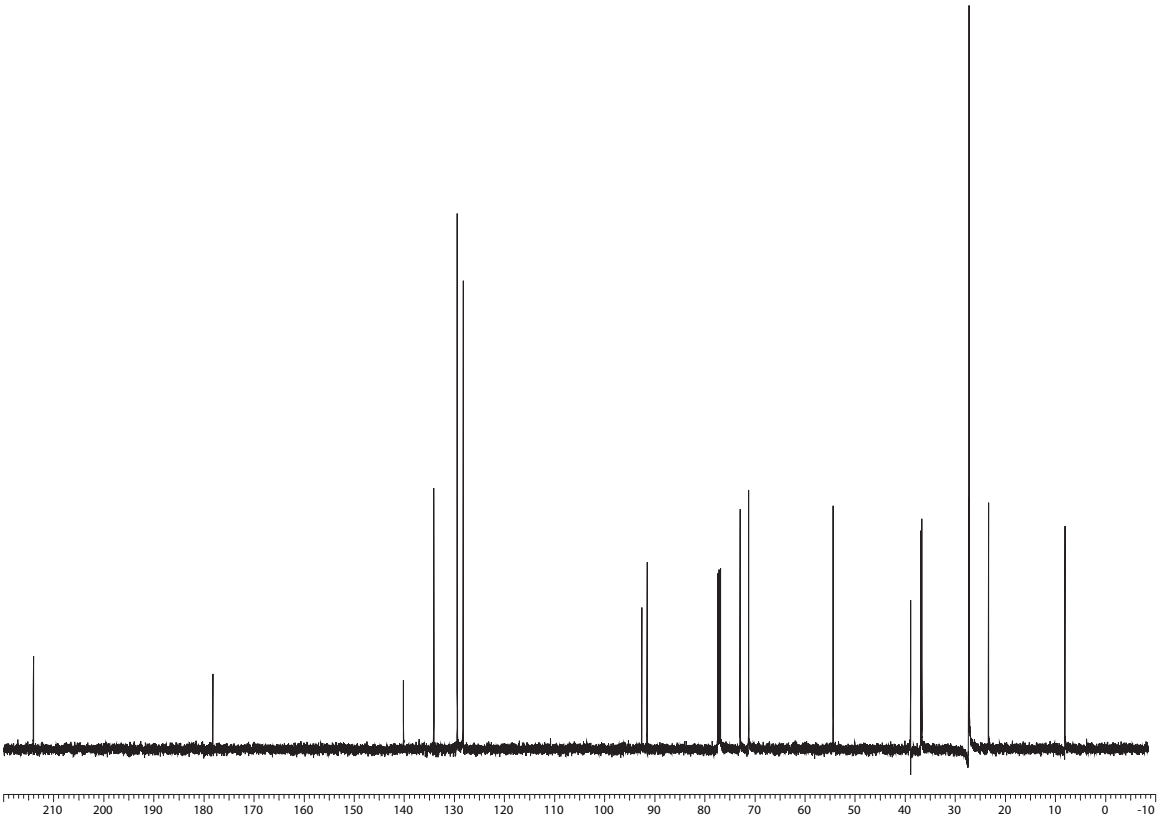
210 200 190 180 170 160 150 140 130 120 110 100 90 80 70 60 50 40 30 20 10 0 -10

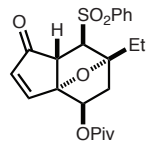
O
H
SO2Ph
Et
O
OPiv

2.42

10.5 10.0 9.5 9.0 8.5 8.0 7.5 7.0 6.5 6.0 5.5 5.0 4.5 4.0 3.5 3.0 2.5 2.0 1.5 1.0 0.5 0 -0.5

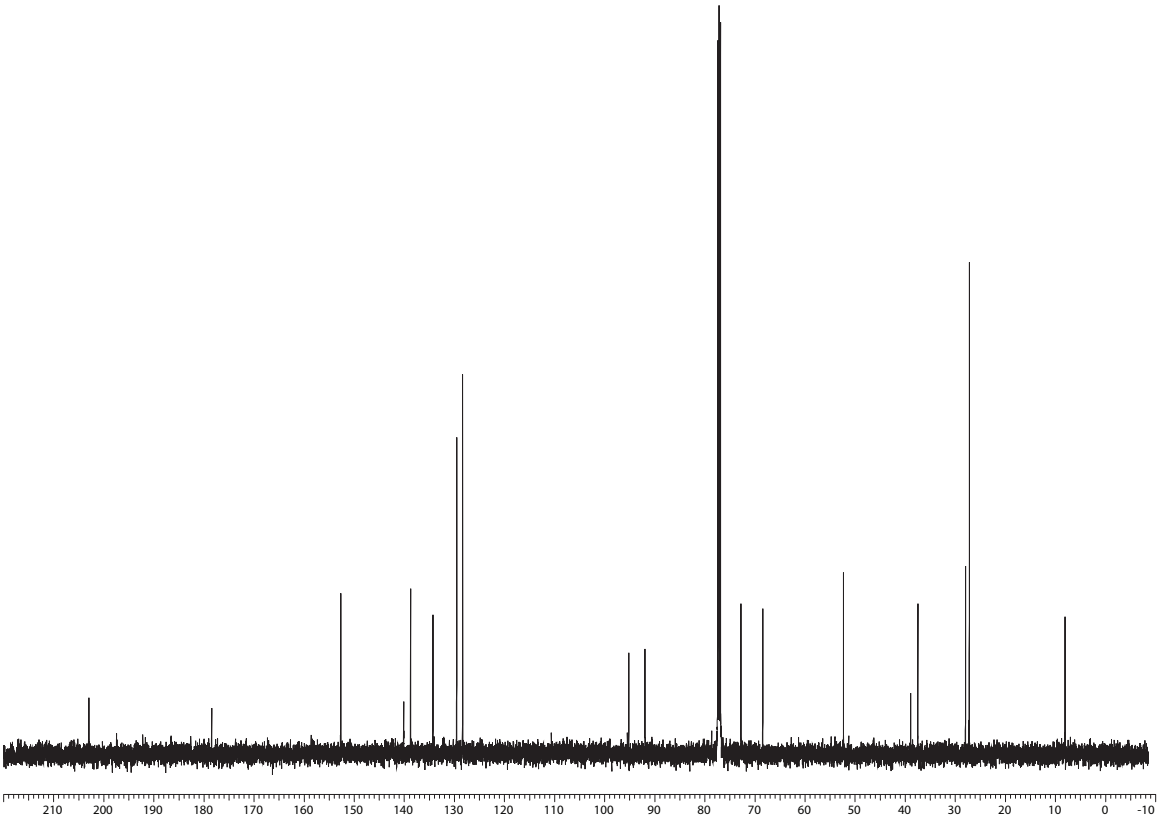
210 200 190 180 170 160 150 140 130 120 110 100 90 80 70 60 50 40 30 20 10 0 -10

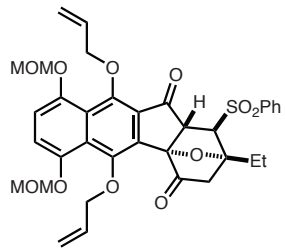
MOMO
O
O
H
SO2Ph
O
Et
MOMO
O
O

1.110

10.5 10.0 9.5 9.0 8.5 8.0 7.5 7.0 6.5 6.0 5.5 5.0 4.5 4.0 3.5 3.0 2.5 2.0 1.5 1.0 0.5 0 -0.5

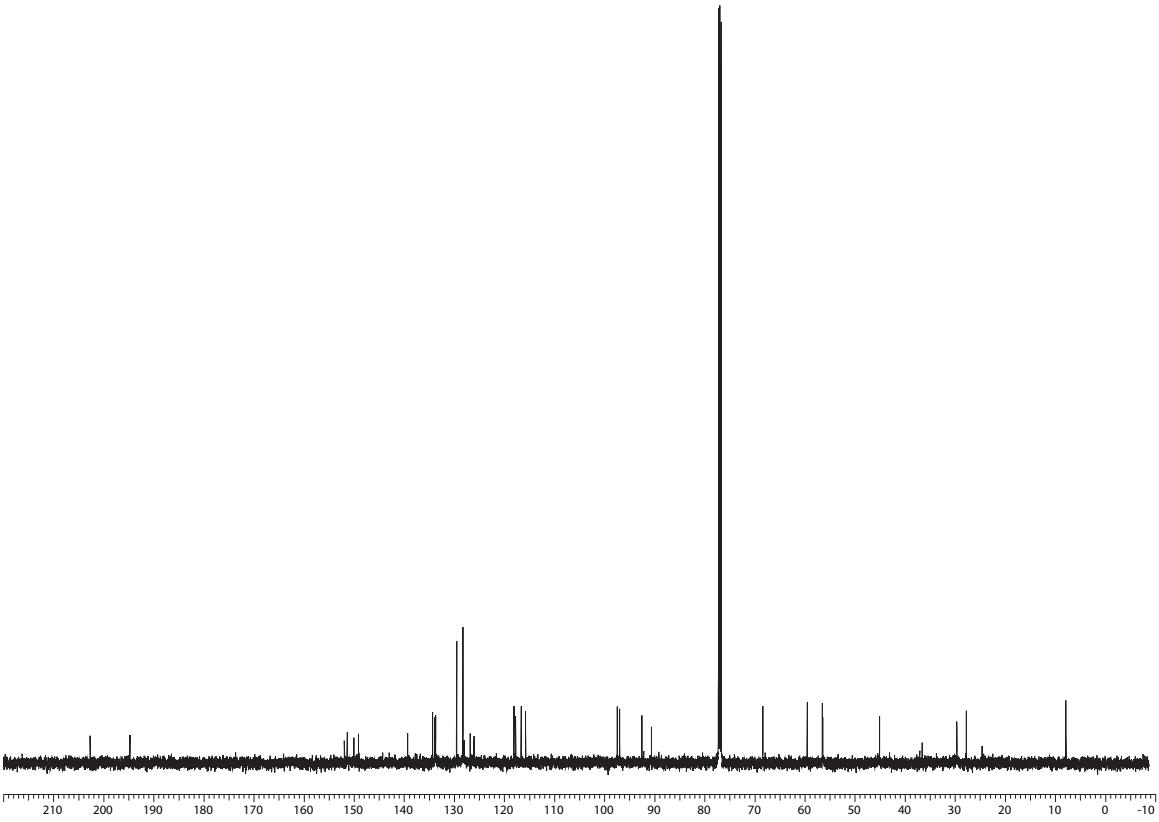
210 200 190 180 170 160 150 140 130 120 110 100 90 80 70 60 50 40 30 20 10 0 -10

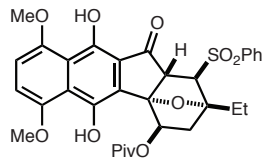
MeO
HO
O
H
SO2Ph
O
Et
MeO
HO
PivO

2.59

10.5 10.0 9.5 9.0 8.5 8.0 7.5 7.0 6.5 6.0 5.5 5.0 4.5 4.0 3.5 3.0 2.5 2.0 1.5 1.0 0.5 0 -0.5

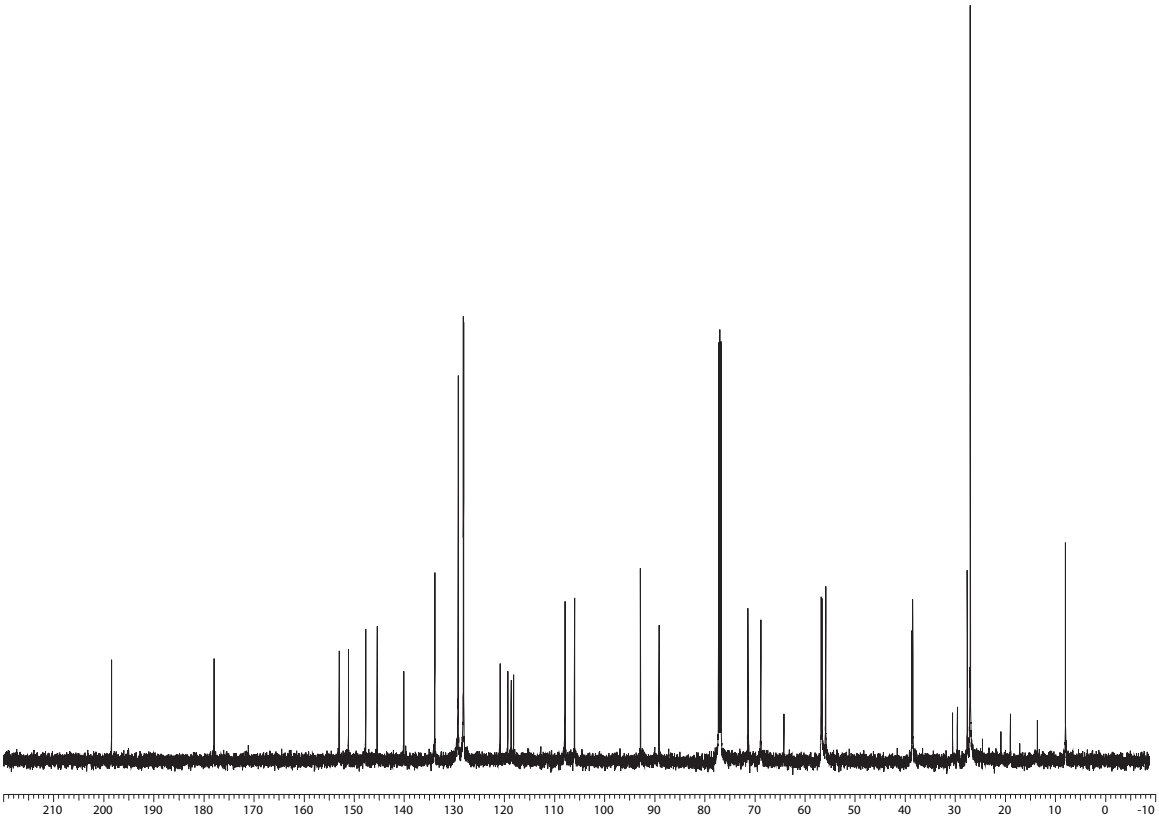
210 200 190 180 170 160 150 140 130 120 110 100 90 80 70 60 50 40 30 20 10 0 -10

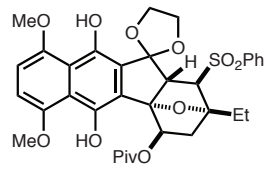
MeO
HO
O
O
H
SO2Ph
O
Et
MeO
HO
PivO

2.60

10.5 10.0 9.5 9.0 8.5 8.0 7.5 7.0 6.5 6.0 5.5 5.0 4.5 4.0 3.5 3.0 2.5 2.0 1.5 1.0 0.5 0 -0.5

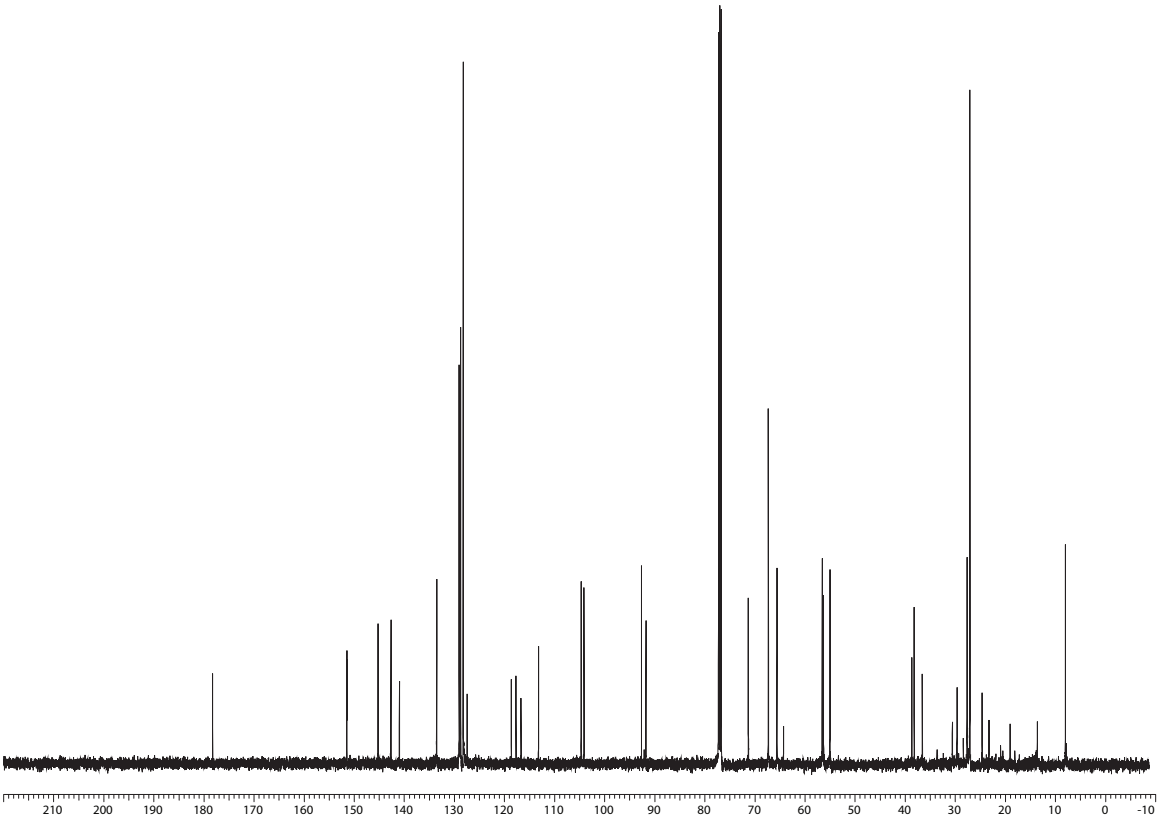
210 200 190 180 170 160 150 140 130 120 110 100 90 80 70 60 50 40 30 20 10 0 -10

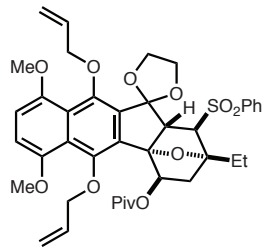
MeO
O
O
O
H
SO2Ph
O
Et
MeO
O
PivO

2.61

10.5 10.0 9.5 9.0 8.5 8.0 7.5 7.0 6.5 6.0 5.5 5.0 4.5 4.0 3.5 3.0 2.5 2.0 1.5 1.0 0.5 0 -0.5

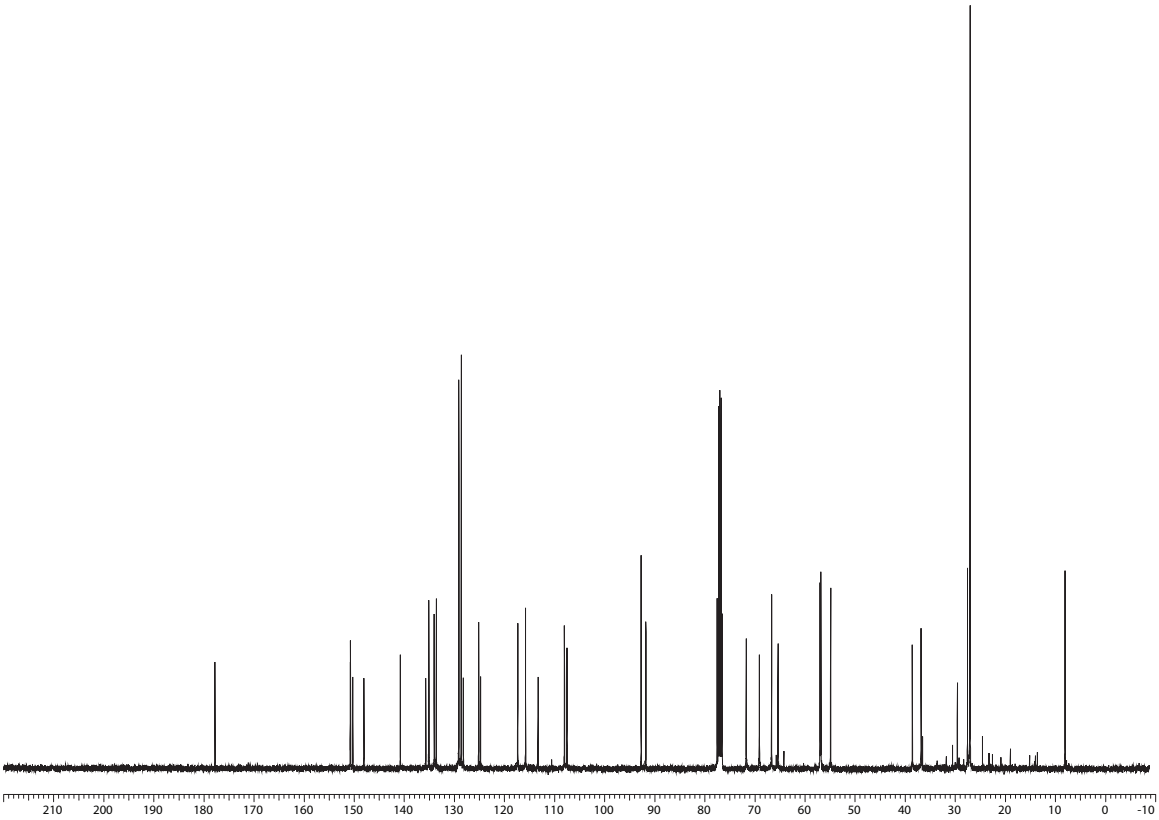
210 200 190 180 170 160 150 140 130 120 110 100 90 80 70 60 50 40 30 20 10 0 -10

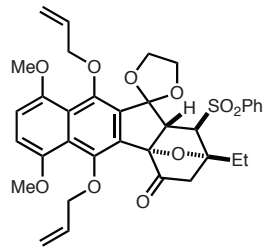
MeO
O
O
O
H
SO2Ph
O
Et
MeO
O
O

2.62

10.5 10.0 9.5 9.0 8.5 8.0 7.5 7.0 6.5 6.0 5.5 5.0 4.5 4.0 3.5 3.0 2.5 2.0 1.5 1.0 0.5 0 -0.5

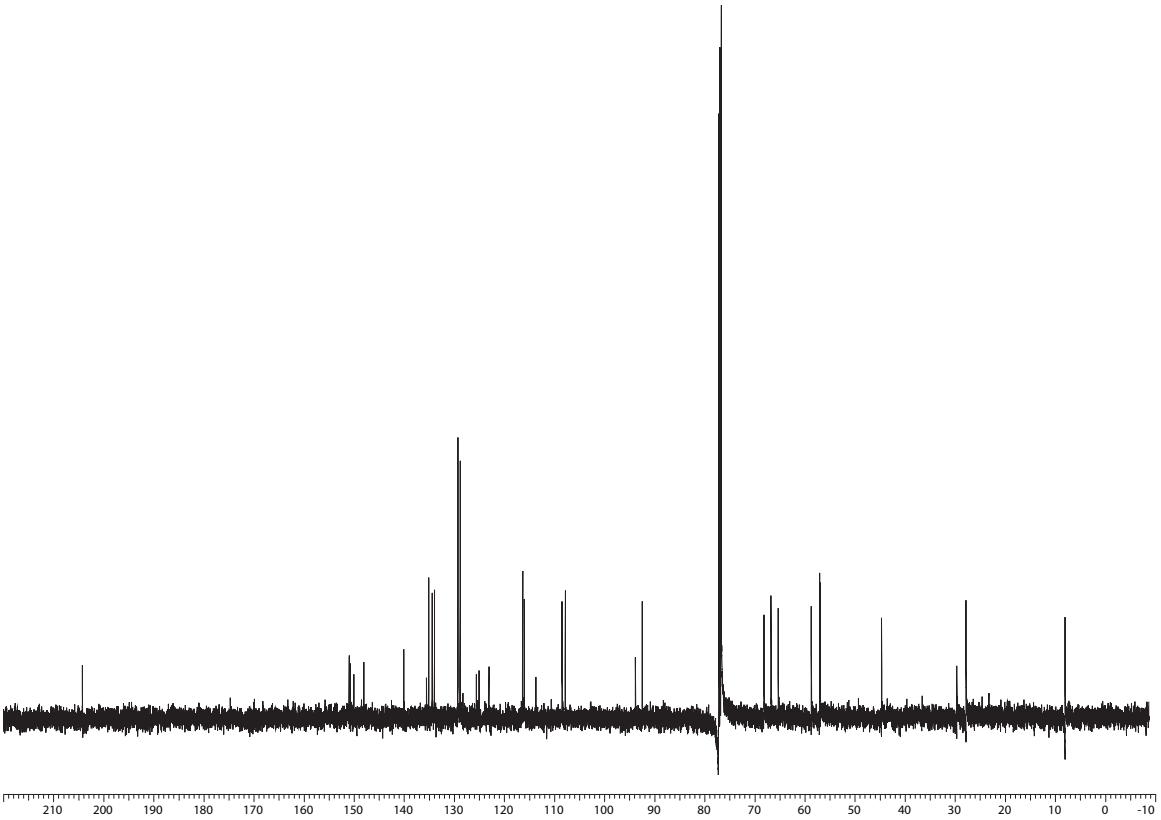
210 200 190 180 170 160 150 140 130 120 110 100 90 80 70 60 50 40 30 20 10 0 -10

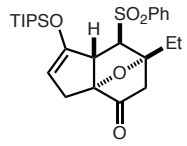
TIPSO
H
SO2Ph
Et
O
O

3.3

10.5 10.0 9.5 9.0 8.5 8.0 7.5 7.0 6.5 6.0 5.5 5.0 4.5 4.0 3.5 3.0 2.5 2.0 1.5 1.0 0.5 0 -0.5

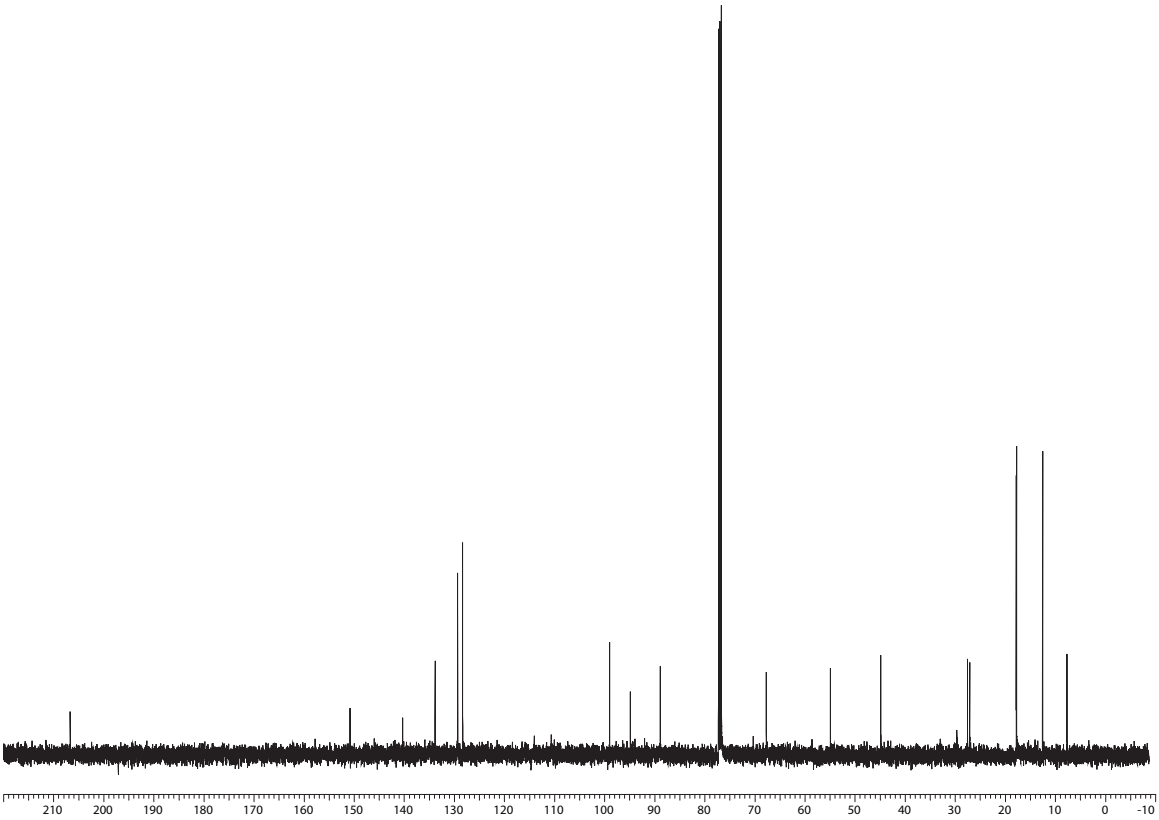
210 200 190 180 170 160 150 140 130 120 110 100 90 80 70 60 50 40 30 20 10 0 -10

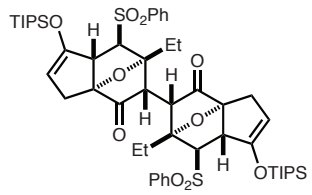
TIPSO
H
SO2Ph
Et
O
O
H
H
O
O
Et
H
PhO2S
OTIPS

3.5

10.5 10.0 9.5 9.0 8.5 8.0 7.5 7.0 6.5 6.0 5.5 5.0 4.5 4.0 3.5 3.0 2.5 2.0 1.5 1.0 0.5 0 -0.5

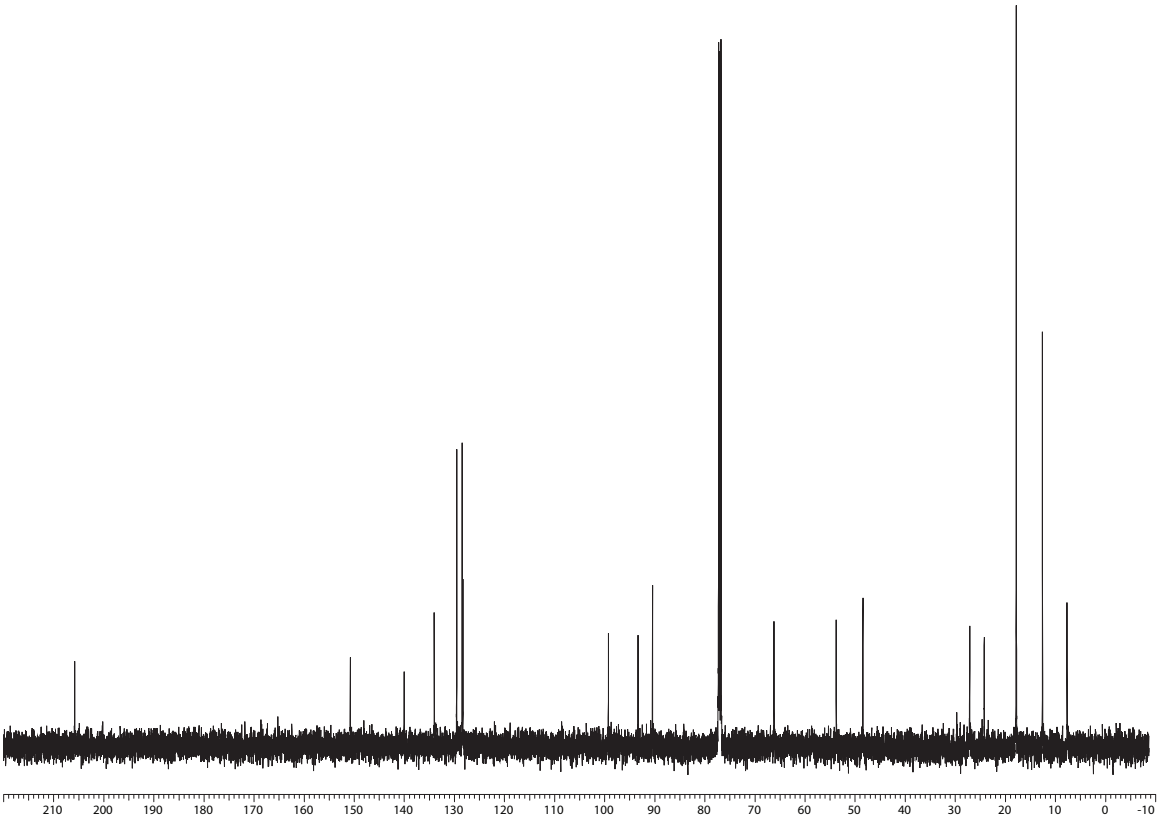
210 200 190 180 170 160 150 140 130 120 110 100 90 80 70 60 50 40 30 20 10 0 -10

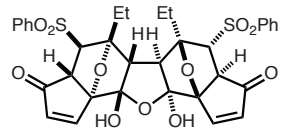
PhO2S
Et
Et
SO2Ph
H
H
H
O
O
O
O
O
HO
OH

3.8

10.5 10.0 9.5 9.0 8.5 8.0 7.5 7.0 6.5 6.0 5.5 5.0 4.5 4.0 3.5 3.0 2.5 2.0 1.5 1.0 0.5 0 -0.5

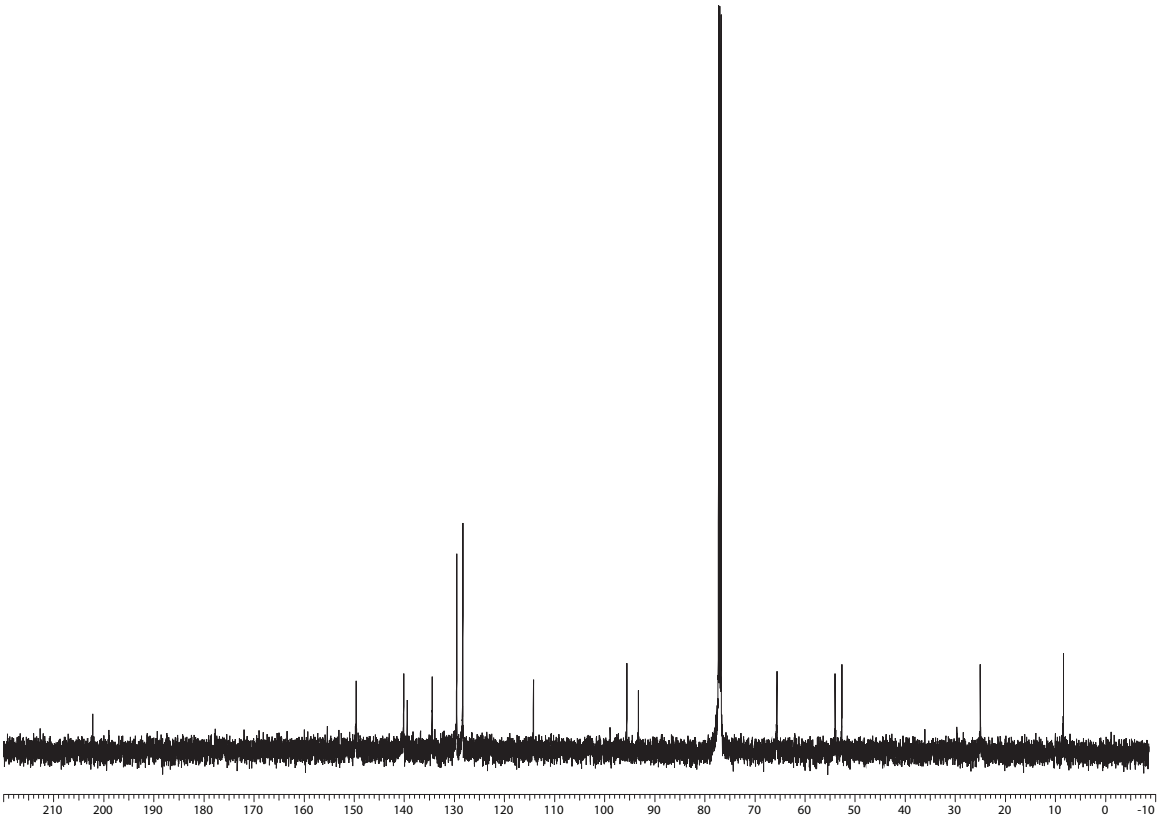
210 200 190 180 170 160 150 140 130 120 110 100 90 80 70 60 50 40 30 20 10 0 -10

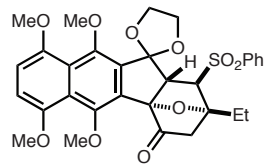
MeO
MeO
O
O
H
SO2Ph
O
Et
MeO
MeO
O

4.10

10.5 10.0 9.5 9.0 8.5 8.0 7.5 7.0 6.5 6.0 5.5 5.0 4.5 4.0 3.5 3.0 2.5 2.0 1.5 1.0 0.5 0 -0.5

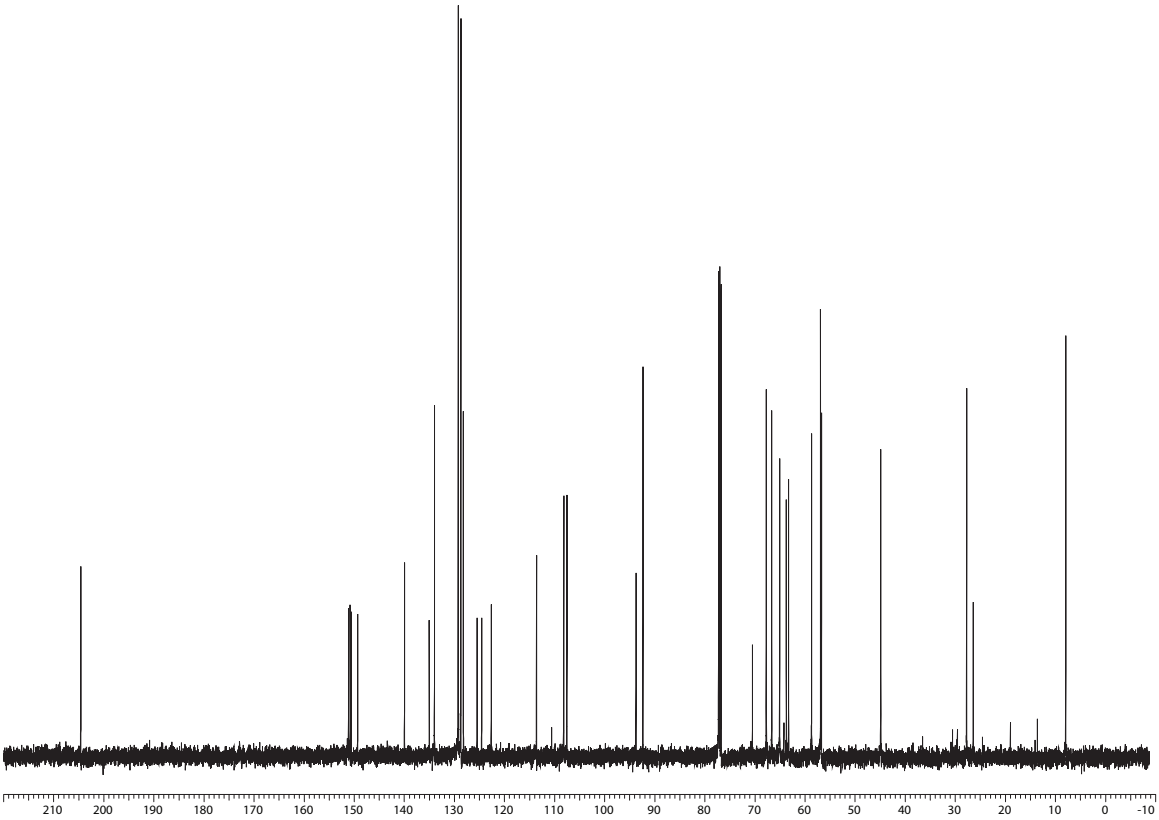
210 200 190 180 170 160 150 140 130 120 110 100 90 80 70 60 50 40 30 20 10 0 -10

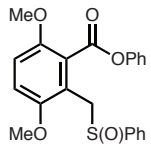
MeO
O
OPh
MeO
S(O)Ph

4.27

10.5 10.0 9.5 9.0 8.5 8.0 7.5 7.0 6.5 6.0 5.5 5.0 4.5 4.0 3.5 3.0 2.5 2.0 1.5 1.0 0.5 0 -0.5

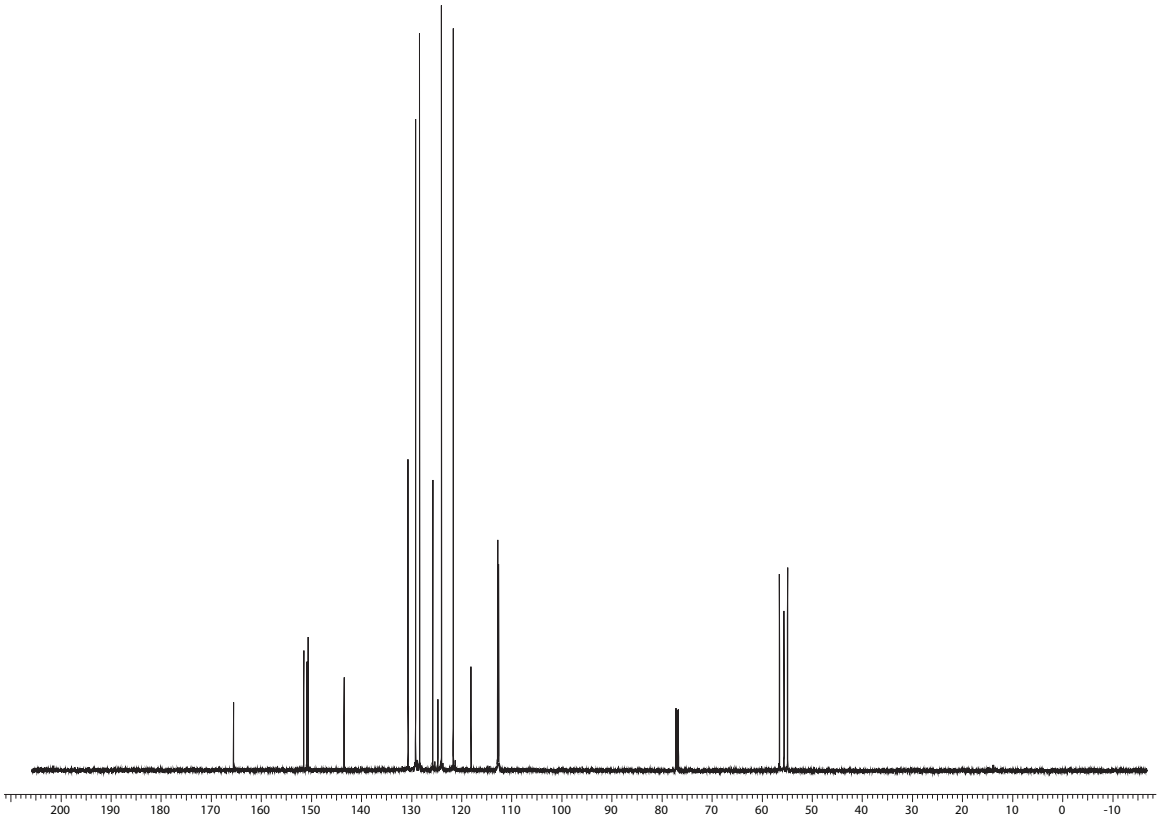
200 190 180 170 160 150 140 130 120 110 100 90 80 70 60 50 40 30 20 10 0 -10

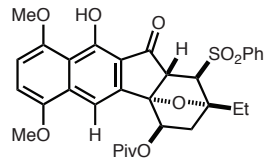
MeO
HO
O
H
SO2Ph
O
Et
MeO
H
PivO

4.28

10.5 10.0 9.5 9.0 8.5 8.0 7.5 7.0 6.5 6.0 5.5 5.0 4.5 4.0 3.5 3.0 2.5 2.0 1.5 1.0 0.5 0 -0.5

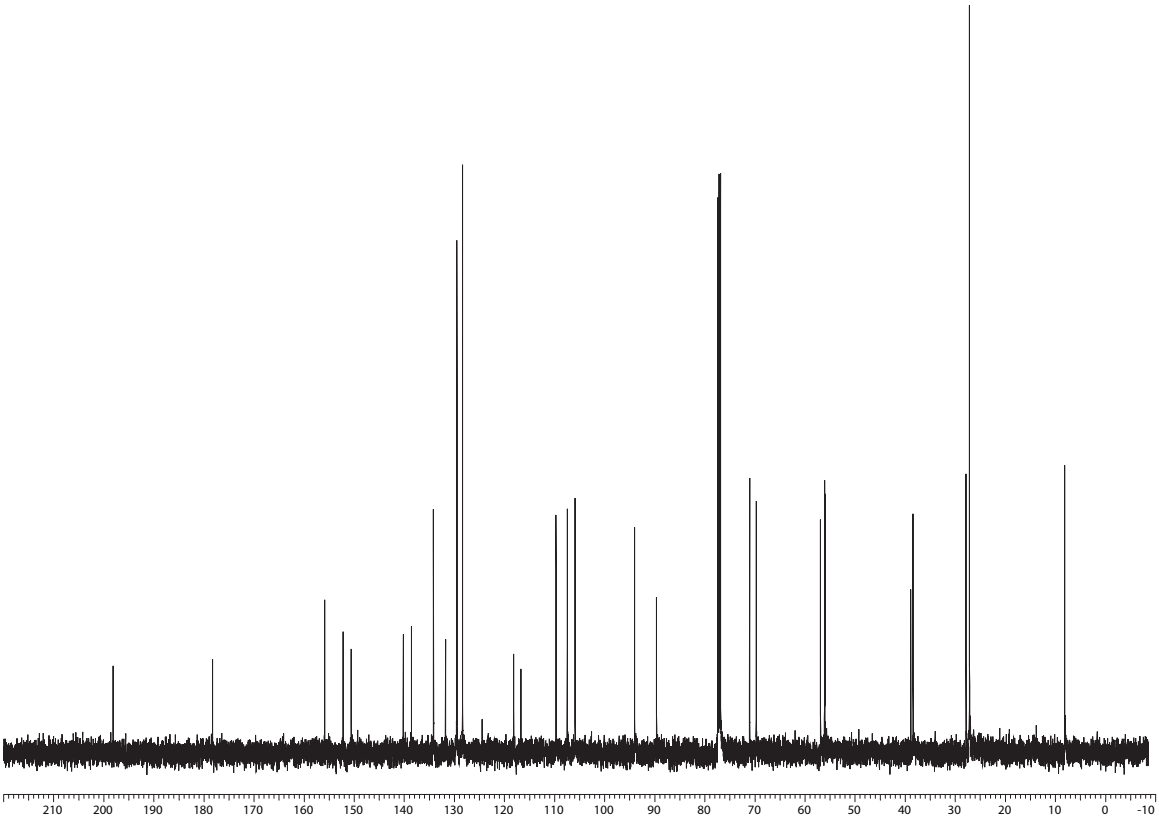
210 200 190 180 170 160 150 140 130 120 110 100 90 80 70 60 50 40 30 20 10 0 -10

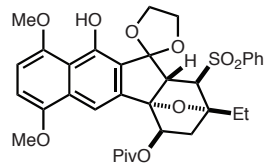
MeO
HO
O
O
H
SO2Ph
O
Et
MeO
PivO

4.29

10.5 10.0 9.5 9.0 8.5 8.0 7.5 7.0 6.5 6.0 5.5 5.0 4.5 4.0 3.5 3.0 2.5 2.0 1.5 1.0 0.5 0 -0.5

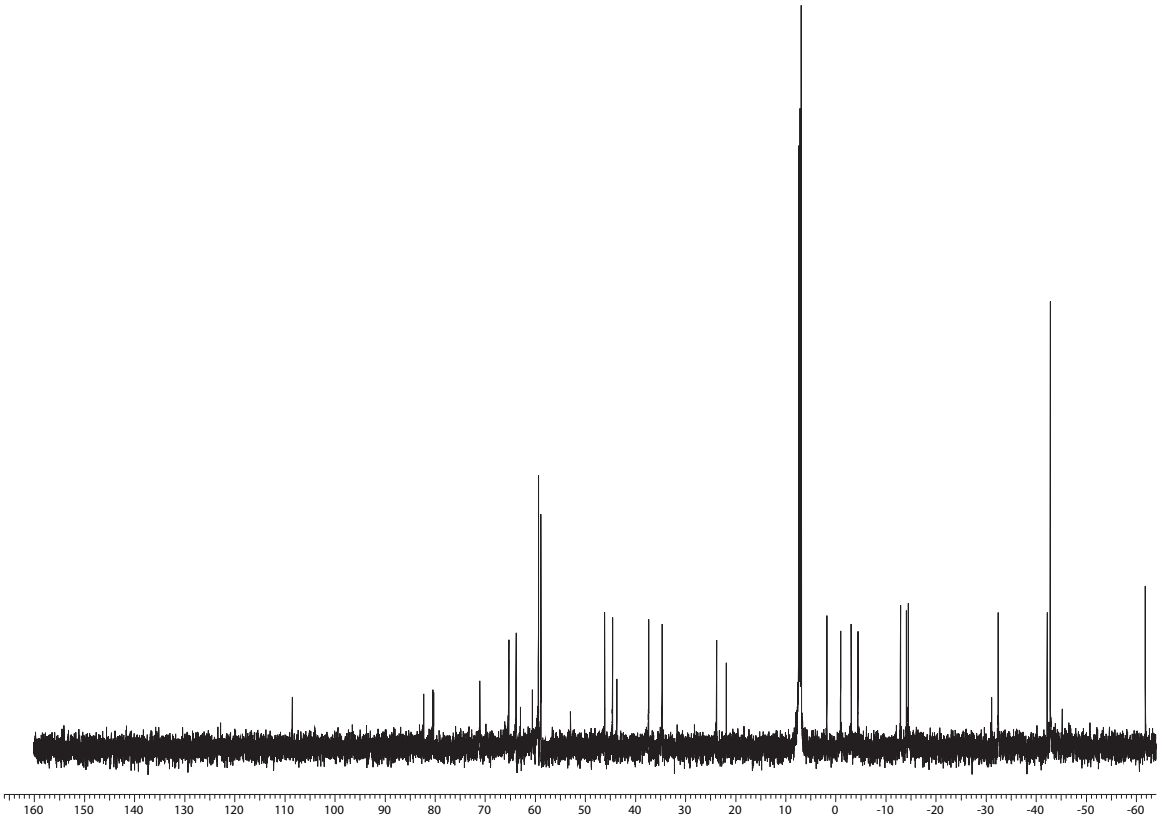
160 150 140 130 120 110 100 90 80 70 60 50 40 30 20 10 0 -10 -20 -30 -40 -50 -60

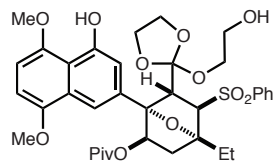
MeO
HO
OH
O
O
H
O
SO2Ph
O
MeO
PivO
Et

4.32

10.5 10.0 9.5 9.0 8.5 8.0 7.5 7.0 6.5 6.0 5.5 5.0 4.5 4.0 3.5 3.0 2.5 2.0 1.5 1.0 0.5 0 -0.5

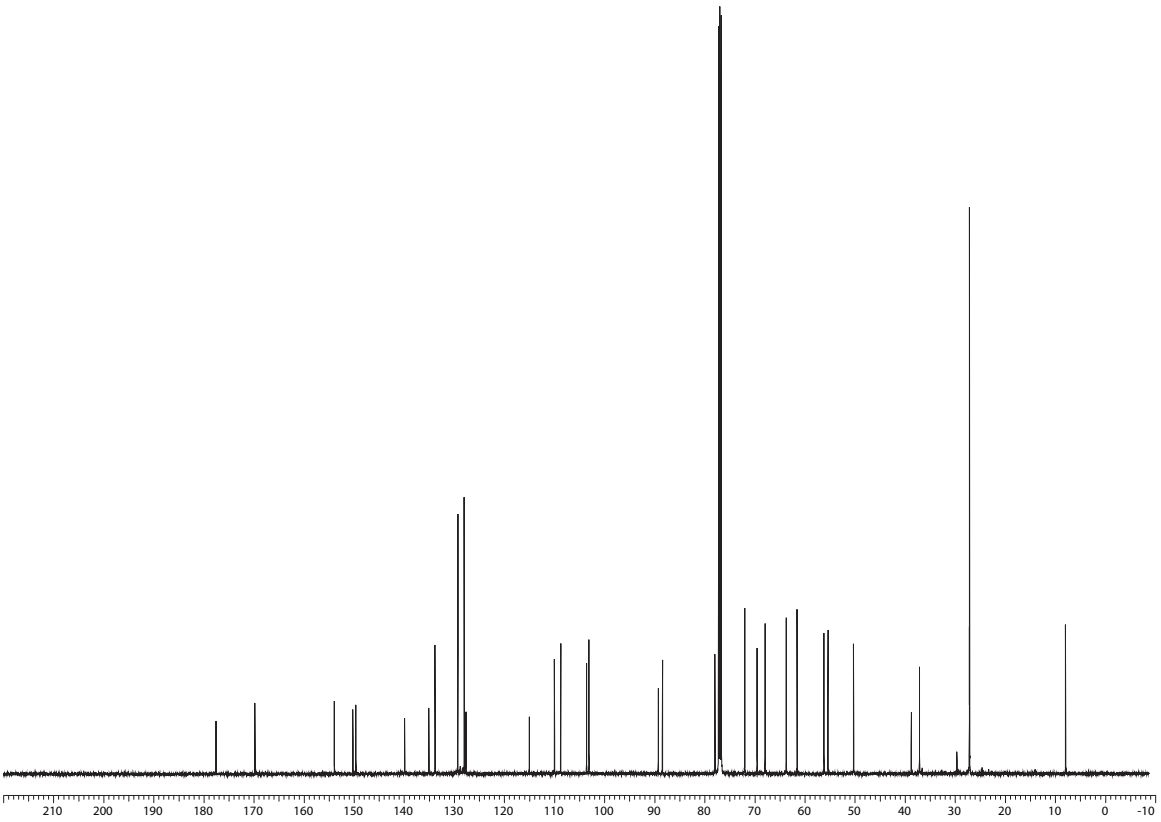
210 200 190 180 170 160 150 140 130 120 110 100 90 80 70 60 50 40 30 20 10 0 -10

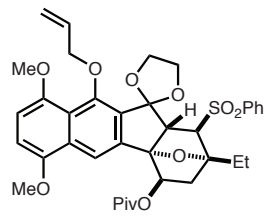
MeO
O
O
O
H
SO2Ph
O
Et
MeO
PivO

4.33

10.5 10.0 9.5 9.0 8.5 8.0 7.5 7.0 6.5 6.0 5.5 5.0 4.5 4.0 3.5 3.0 2.5 2.0 1.5 1.0 0.5 0 -0.5

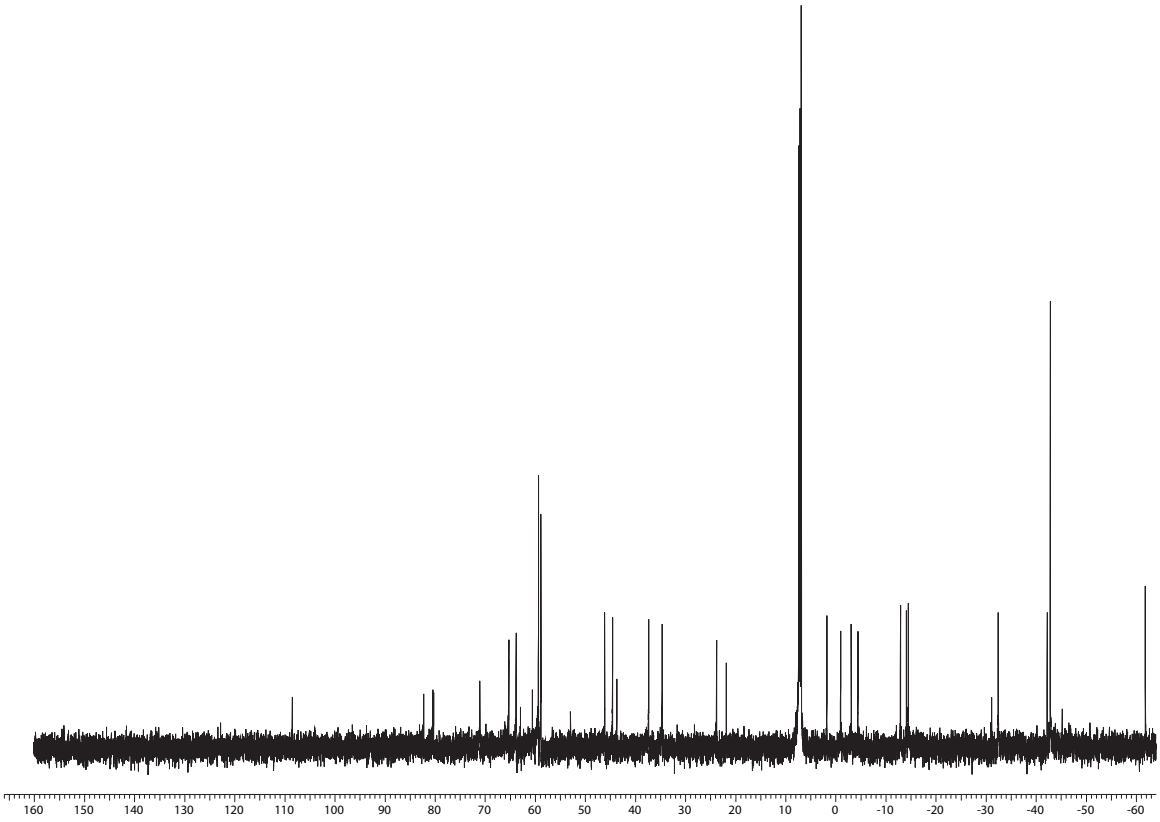
160 150 140 130 120 110 100 90 80 70 60 50 40 30 20 10 0 -10 -20 -30 -40 -50 -60

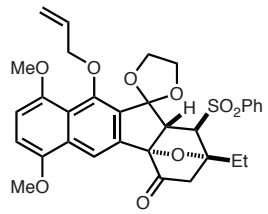
MeO
O
O
O
H
SO2Ph
O
Et
MeO
O

4.13

10.5 10.0 9.5 9.0 8.5 8.0 7.5 7.0 6.5 6.0 5.5 5.0 4.5 4.0 3.5 3.0 2.5 2.0 1.5 1.0 0.5 0 -0.5

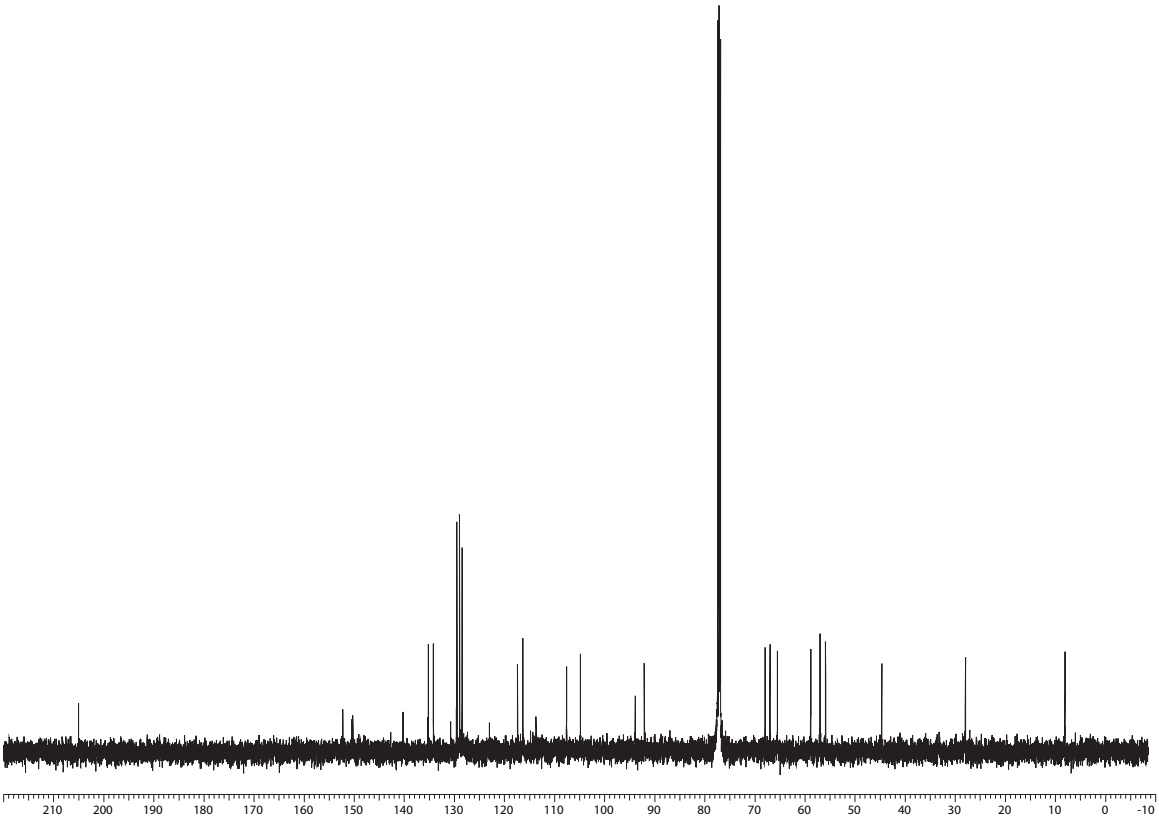
210 200 190 180 170 160 150 140 130 120 110 100 90 80 70 60 50 40 30 20 10 0 -10

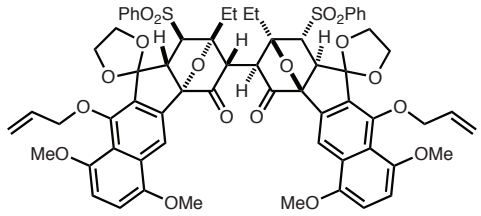
PhO2S
Et Et
SO2Ph
H
O
MeO
OMe

4.12

10.5 10.0 9.5 9.0 8.5 8.0 7.5 7.0 6.5 6.0 5.5 5.0 4.5 4.0 3.5 3.0 2.5 2.0 1.5 1.0 0.5 0 -0.5

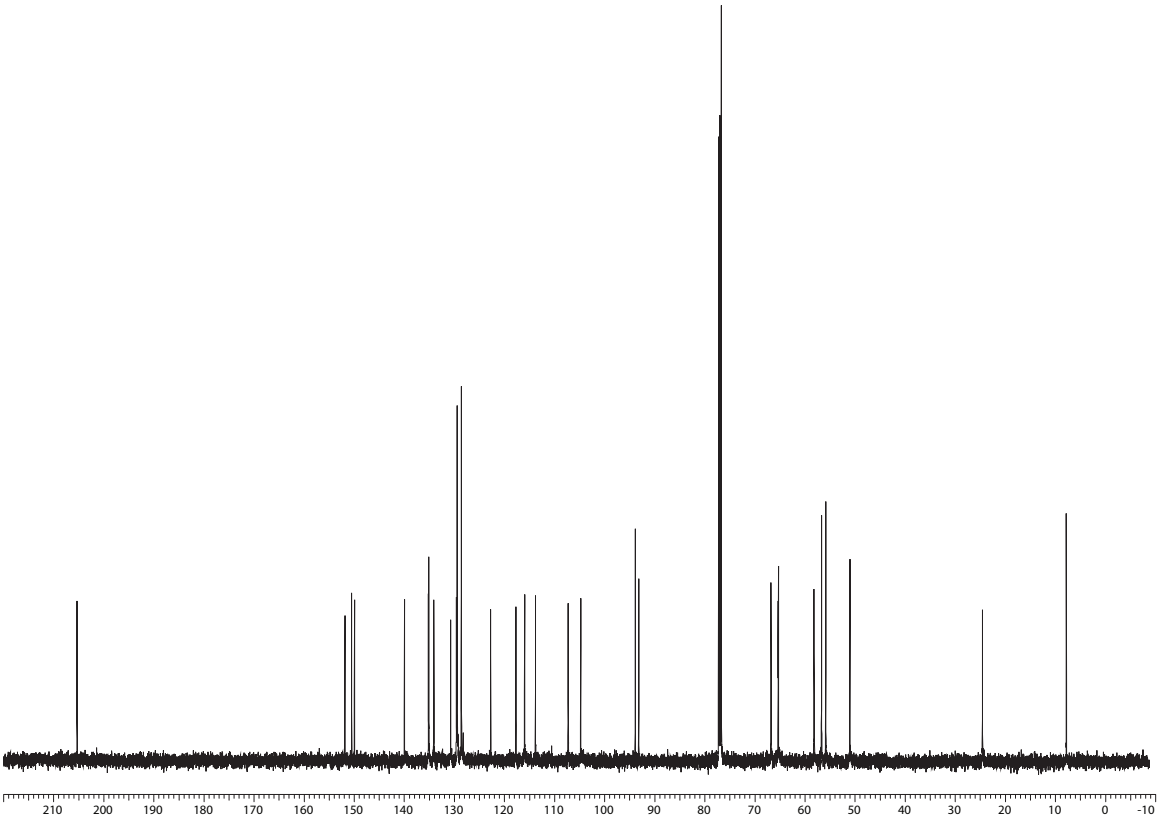
210 200 190 180 170 160 150 140 130 120 110 100 90 80 70 60 50 40 30 20 10 0 -10

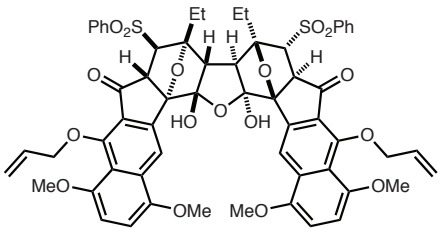
PhO2S
Et
Et
SO2Ph
H
H
H
H
O
O
O
O
O
HO
O
OH
O
O
MeO
OMe
MeO
OMe

5.7

10.5 10.0 9.5 9.0 8.5 8.0 7.5 7.0 6.5 6.0 5.5 5.0 4.5 4.0 3.5 3.0 2.5 2.0 1.5 1.0 0.5 0 -0.5

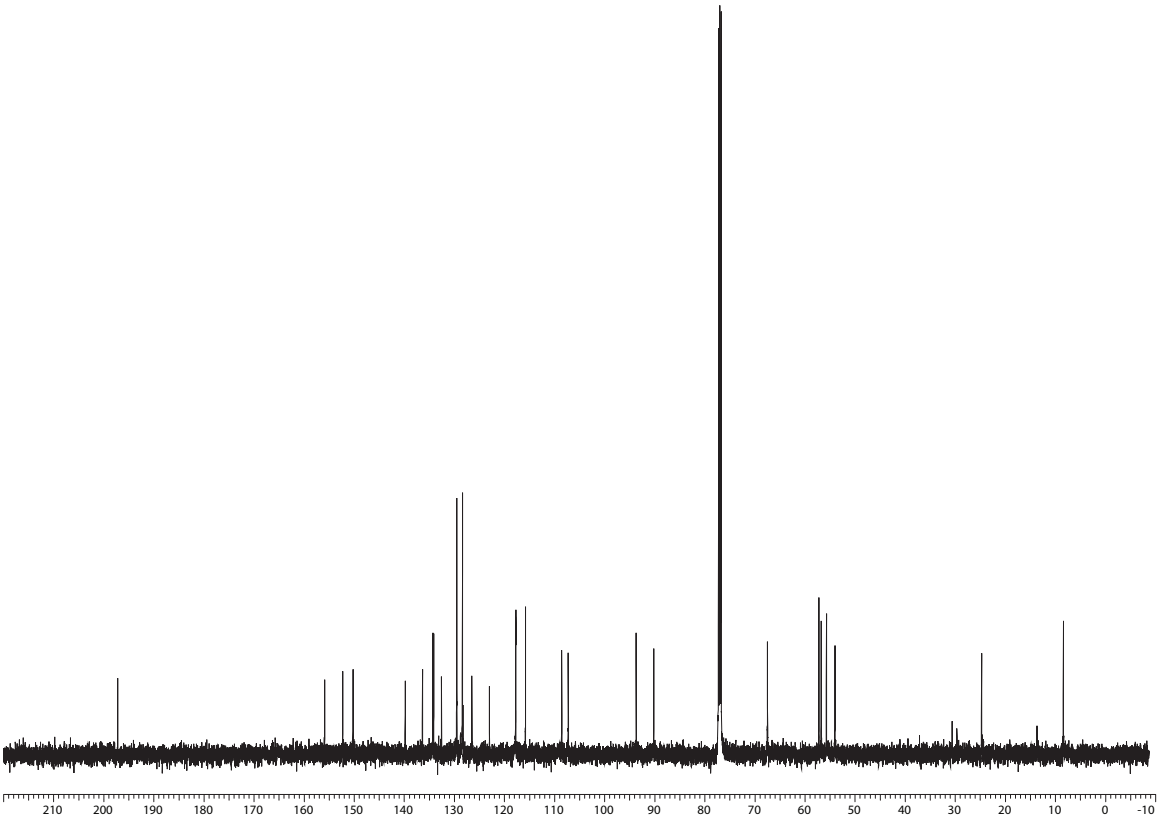
210 200 190 180 170 160 150 140 130 120 110 100 90 80 70 60 50 40 30 20 10 0 -10

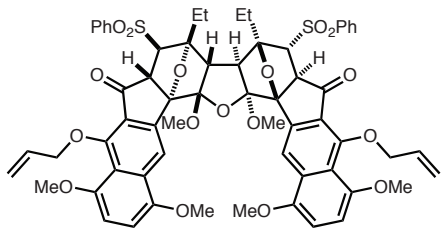
PhO2S
Et
Et
SO2Ph
H
H
H
H
O
O
O
O
O
MeO
OMe
O
O
MeO
OMe
MeO
OMe

5.16

10.5 10.0 9.5 9.0 8.5 8.0 7.5 7.0 6.5 6.0 5.5 5.0 4.5 4.0 3.5 3.0 2.5 2.0 1.5 1.0 0.5 0 -0.5

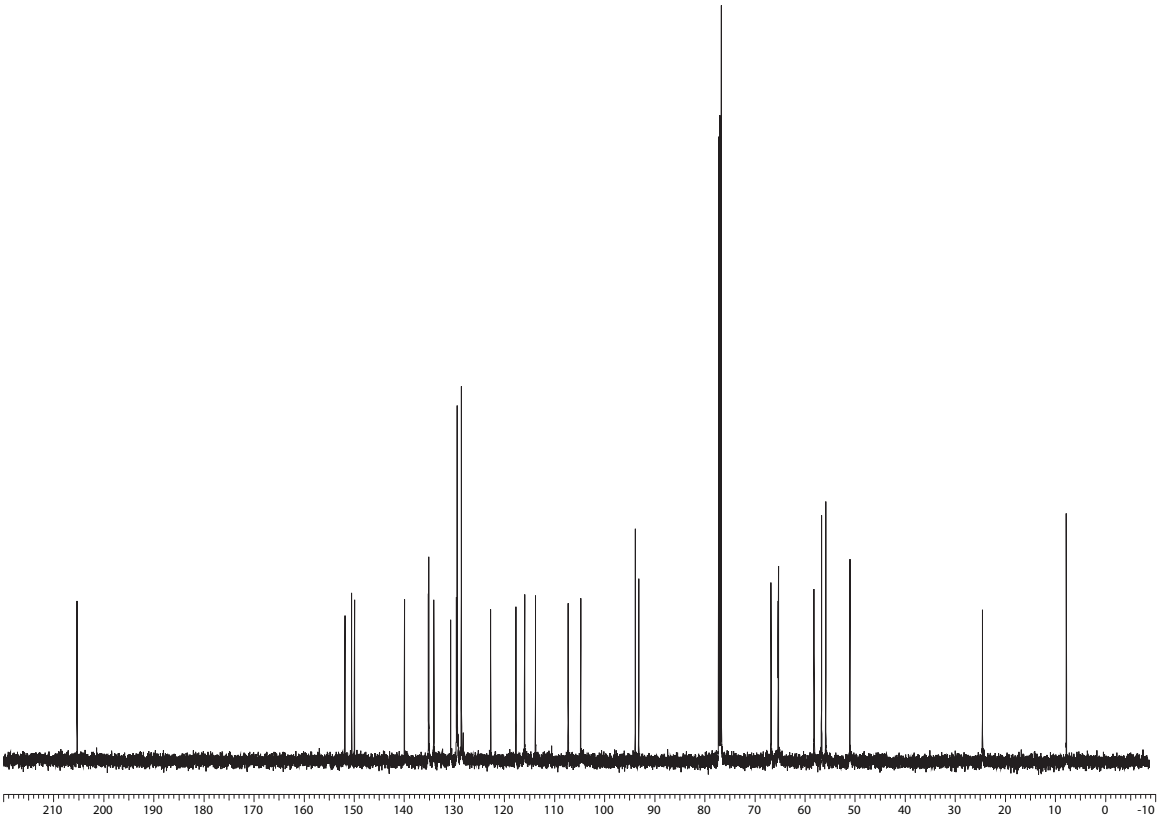
210 200 190 180 170 160 150 140 130 120 110 100 90 80 70 60 50 40 30 20 10 0 -10

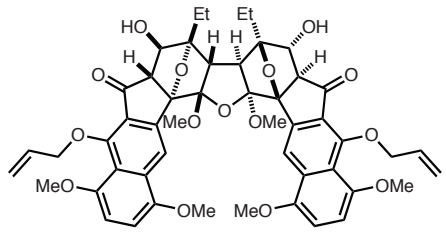
HO
Et
Et
OH
H
H
H
H
O
O
O
O
O
MeO
OMe
O
O
MeO
OMe
MeO
OMe

5.17

10.5 10.0 9.5 9.0 8.5 8.0 7.5 7.0 6.5 6.0 5.5 5.0 4.5 4.0 3.5 3.0 2.5 2.0 1.5 1.0 0.5 0 -0.5

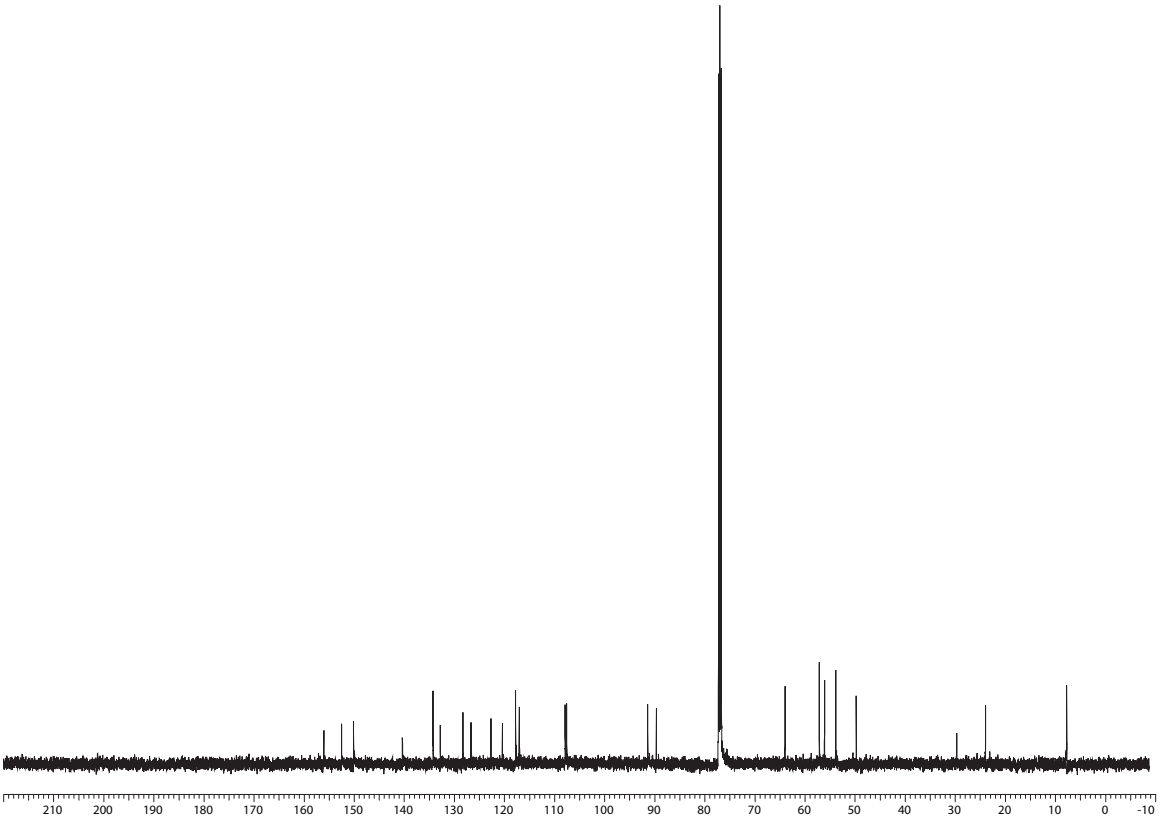
210 200 190 180 170 160 150 140 130 120 110 100 90 80 70 60 50 40 30 20 10 0 -10

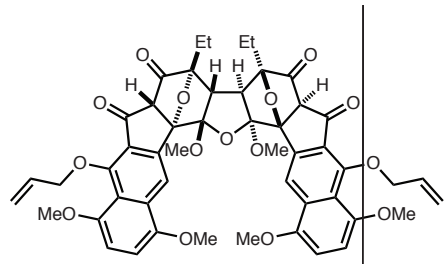
Et
Et
H
H
H
H
O
O
O
O
O
O
O
O
MeO
OMe
MeO
OMe
MeO
OMe
MeO
OMe

5.22

10.5
10.0
9.5
9.0
8.5
8.0
7.5
7.0
6.5
6.0
5.5
5.0
4.5
4.0
3.5
3.0
2.5
2.0
1.5
1.0
0.5
0
-0.5

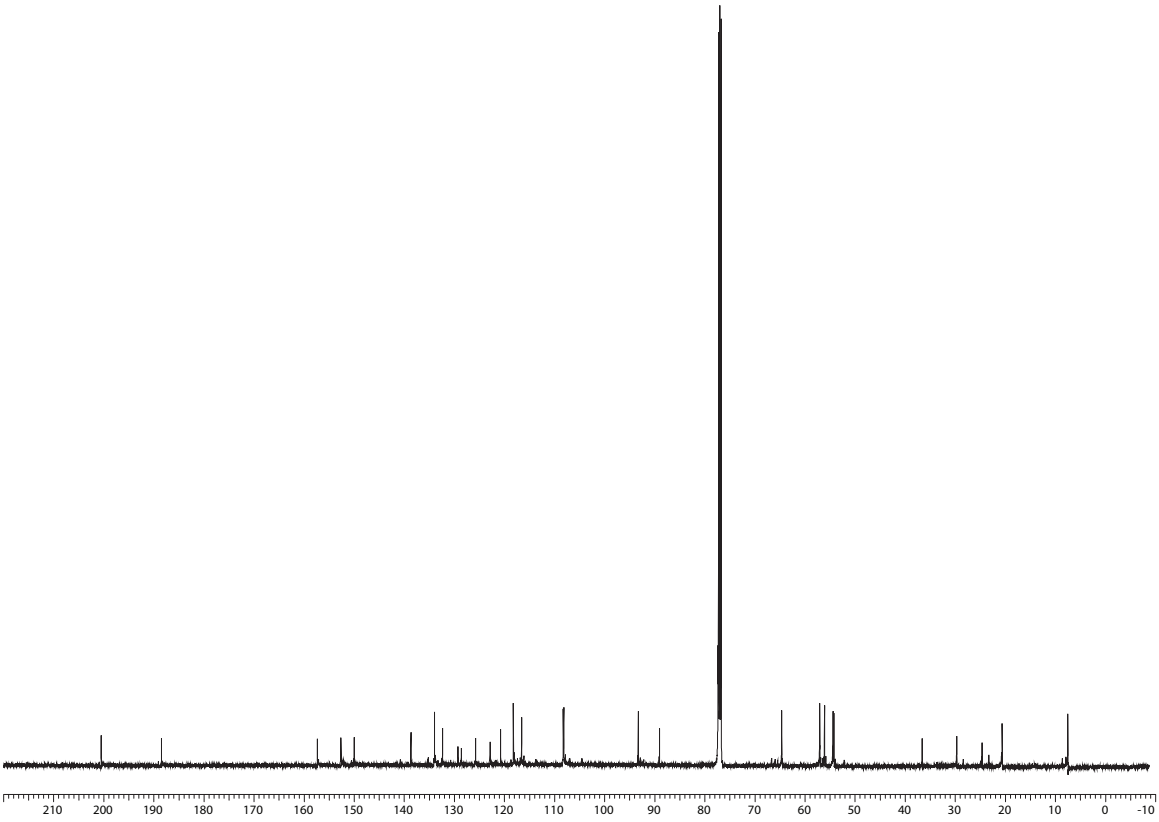
210
200
190
180
170
160
150
140
130
120
110
100
90
80
70
60
50
40
30
20
10
0
-10

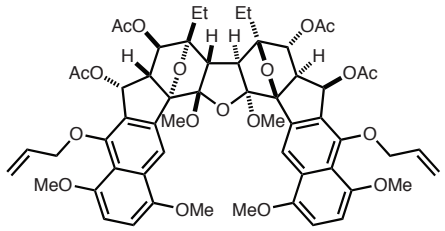
AcO
Et
Et
OAc
H
H
H
H
AcO
O
O
OAc
MeO
O
OMe
O
O
MeO
OMe
MeO
OMe

5.47

10.5 10.0 9.5 9.0 8.5 8.0 7.5 7.0 6.5 6.0 5.5 5.0 4.5 4.0 3.5 3.0 2.5 2.0 1.5 1.0 0.5 0 -0.5

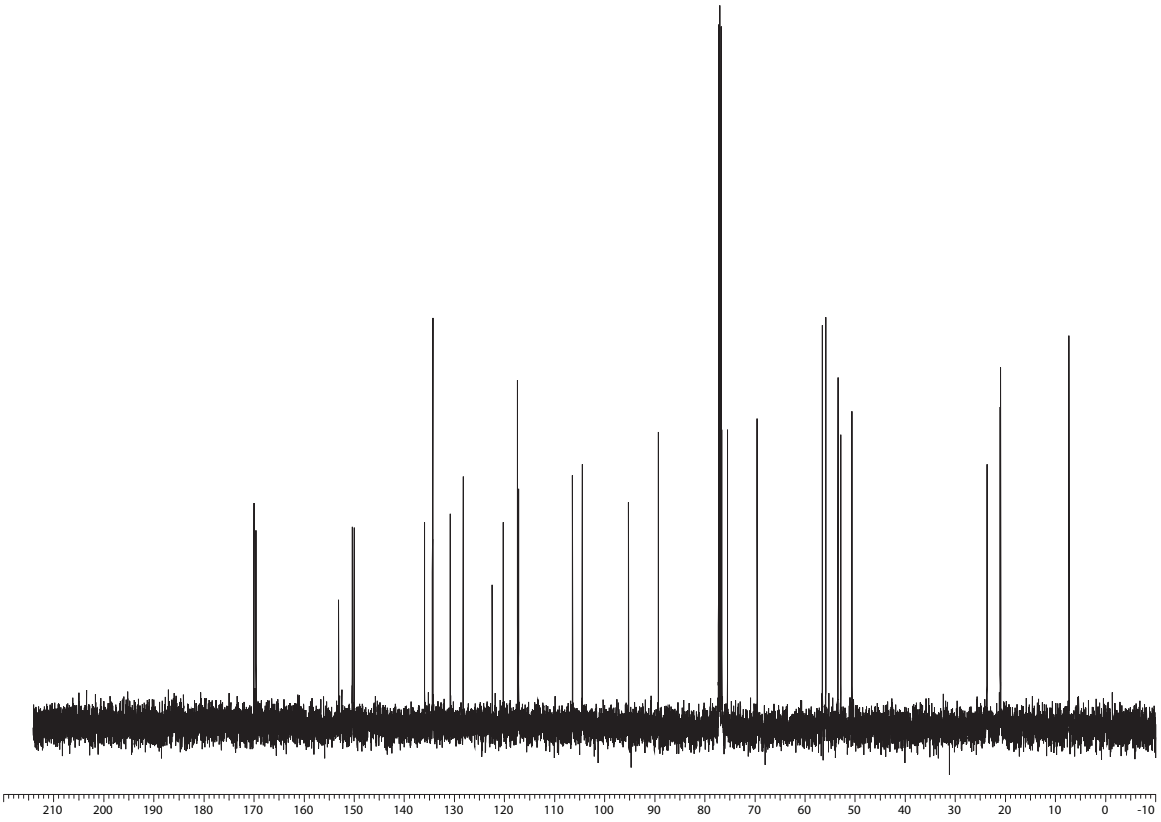
210 200 190 180 170 160 150 140 130 120 110 100 90 80 70 60 50 40 30 20 10 0 -10

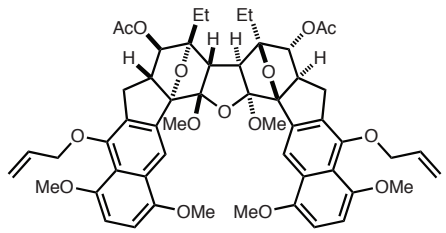
AcO
Et
Et
OAc
H
H
H
H
O
O
O
MeO
OMe
O
O
MeO
OMe
MeO
OMe

5.48

10.5 10.0 9.5 9.0 8.5 8.0 7.5 7.0 6.5 6.0 5.5 5.0 4.5 4.0 3.5 3.0 2.5 2.0 1.5 1.0 0.5 0 -0.5

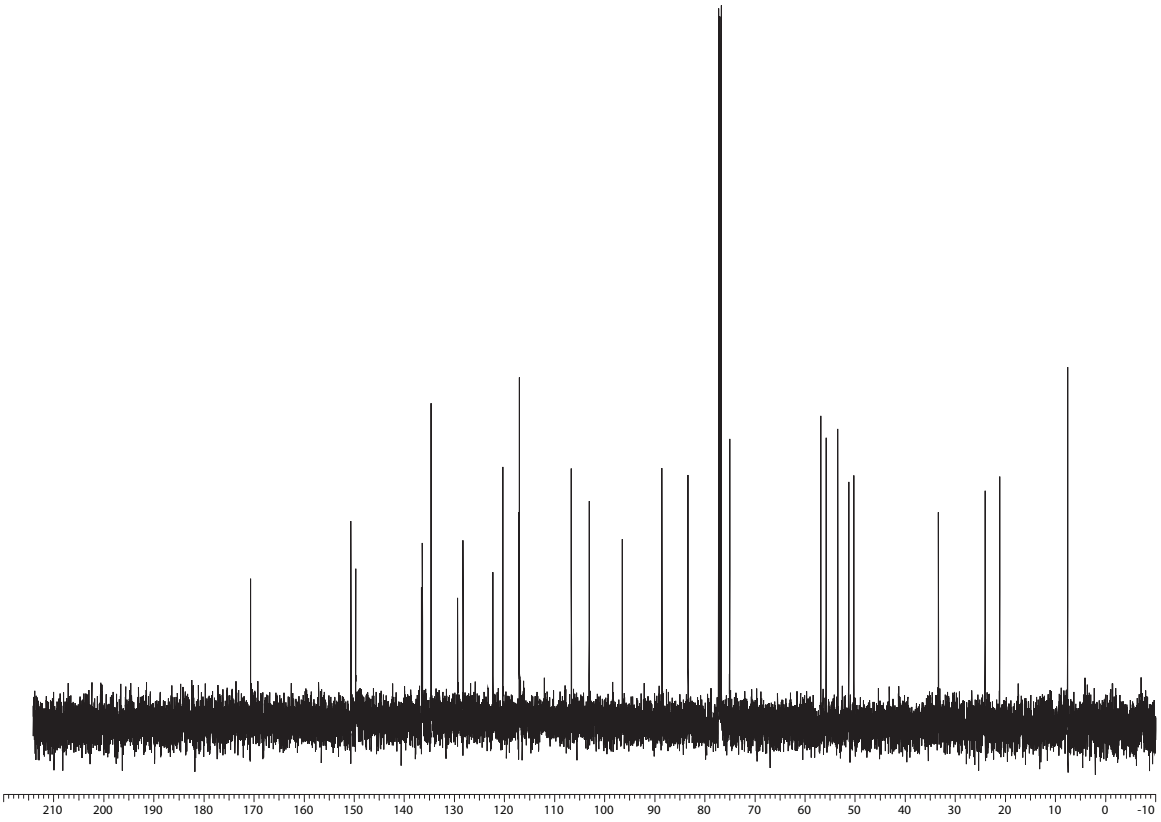
210 200 190 180 170 160 150 140 130 120 110 100 90 80 70 60 50 40 30 20 10 0 -10

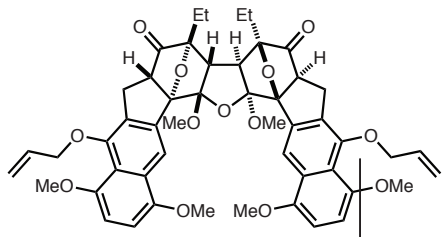
O
Et
Et
O
H
H
H
H
O
O
O
MeO
OMe
O
O
MeO
OMe
MeO
OMe

5.49

10.5 10.0 9.5 9.0 8.5 8.0 7.5 7.0 6.5 6.0 5.5 5.0 4.5 4.0 3.5 3.0 2.5 2.0 1.5 1.0 0.5 0 -0.5

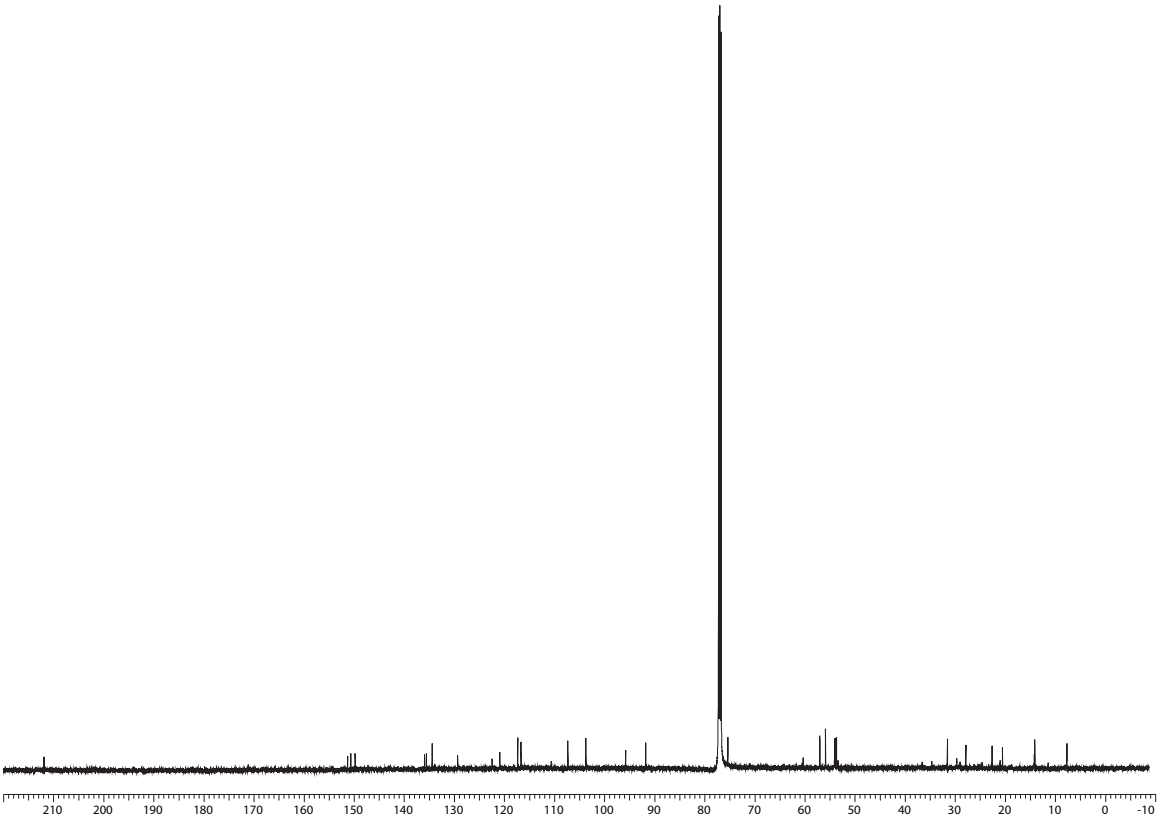
210 200 190 180 170 160 150 140 130 120 110 100 90 80 70 60 50 40 30 20 10 0 -10